Poster Abstract List

Poster sessions:

Poster Session 1 (P1) – Tuesday **Aug. 1st** 5:30 PM to 7:30 PM

- 2D Materials: Optics (2DO)
- 2D Materials: Transport (2DT)
- Interfaces, heterostructures, and Superlattices (IH)
- Nanowires, Nanotubes, Quantum Dots and Other Mesoscopic Systems (MS)
- Single Electron Transport (SE)
- Spintronics and Spin Phenomena in Low Dimensions (ST)

Poster Session 2 (P2) – Thursday **Aug. 3rd** 5:30 PM to 7:30 PM

- 2D Superconductivity, Majorana Modes (2DS)
- Edge Surface Channels in Quantum Hall Effect and Topological Insulators (ES)
- Quantum Hall Systems, Composite Fermions, Wigner Crystallization & Correlated Phases (QH)
- Quantum Information, Qubits Physics and Devices (QI)
- Topological Insulators: Magnetism & Quantum Anomalous Hall Effect (TI)

Poster Session 1

Resonance Contribution of Edge States in Absorption of Nanoperforated Graphene in Terahertz Range

V.V. Enaldiev and V.A. Volkov
V.A. Kotel'nikov Institute of Radio-engineering and Electronics of RAS, Moscow,125009,Russia
vova.enaldiev@gmail.com

Experiment [1,2] has revealed that edge states (ESs) exist around an each nanohole in nanoperforated graphene (NG). Neglecting intervalley interaction ESs spectra are determined by a single phenomenological boundary parameter $|a|<<1$ [1-3] (see Fig. 1a). In each valley the ES spectra form a quasi-equidistant ladder of quasi-stationary energy levels, indexed by total angular momentum, only in one band (conduction or valence) depending on the sign of parameter a. We calculate intraband optical absorption in NG and show that it is of resonance structure due to transitions between the ES levels related to an each nanohole [4] (see Fig. 1b,d). The resonance frequency equals energy difference between the neighboring ESs levels. In actual nanoperforated samples [1,2] the resonance corresponds to THz range. Peak value of absorption can reach about several percent for experimentally attainable concentration of nanoholes $n_a << 1/R^2$ [2] (R is a nanohole radius).

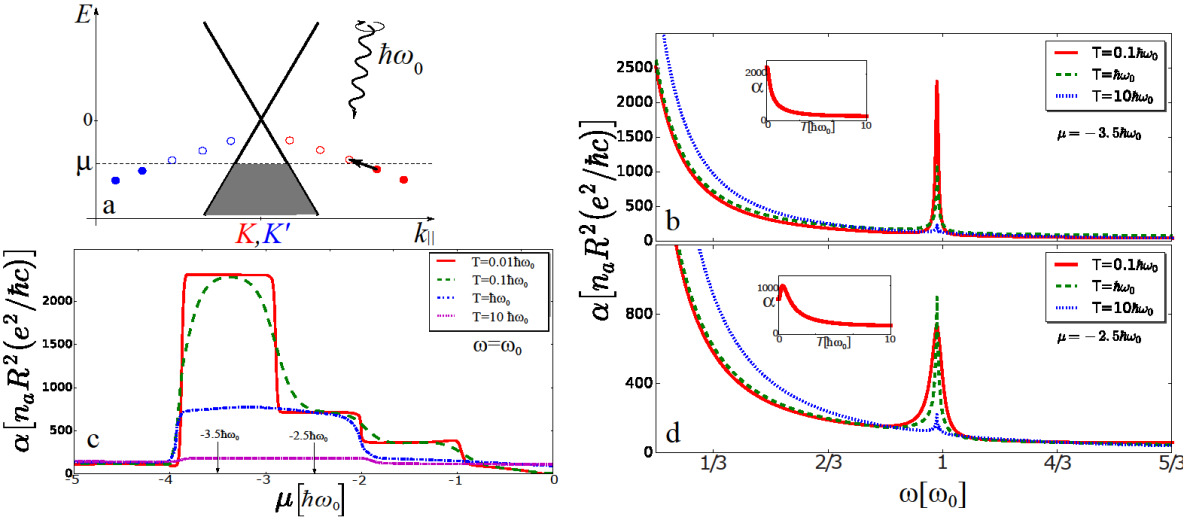

Fig. 1. (a) Semiclassical spectrum ($k_{||}=j/R$) of the ESs in graphene with a single nanohole in a reduced valley scheme at $a<0$. Arrow marks a transition which leads to the resonance. (b,d) Frequency dependence of absorption coefficient of NG at different temperatures and two Fermi levels: (b) $\mu=-3.5\hbar\omega_0$, (d) $\mu=-2.5\hbar\omega_0$. Resonance frequency $\omega_0= 2|a|\hbar v/R \approx 5$THz (for R=10 nm, a=-0.15, $v\approx10^6$ m/s) corresponds to the energy difference between the two neighboring edge states, circulated around an each nanohole. (c) Fermi energy dependence of absorption coefficient of NG at the resonance frequency ω_0. In Fig.1(b,c,d) the boundary parameter a=-0.15.

This work was supported by the Russian Science Foundation (project no.16-12-10411).

References

[1] Yu. I. Latyshev, et. al., Sci. Rep., **4**, 7578, (2014).
[2] Yu. I. Latyshev, et. al., JETP Lett., **98**, 214 (2013).
[3] I. V. Zagorodnev, Zh. A. Devizorova, V. V. Enaldiev, Phys. Rev. B, **92**, 195413 (2015).
[4] V. V. Enaldiev, V. A. Volkov, JETP Lett., **104**, 624 (2016).

Plasmon-Assisted Resonant Tunneling in Graphene-Insulator-Graphene Structures

D. Svintsov[1], V. Enaldiev[1], Zh. Devizorova[1] and V. Ryzhii[2]
[1]*Moscow Institute of Physics and Technology, Dolgoprudny 141700, Russia*
[2]*Research Institute of Electrical Communication, Tohoku University, Sendai, Japan*
svintcov.da@mipt.ru

Recent experiments have revealed the terahertz electroluminescence of graphene – insulator – graphene tunnel junctions [1]. The intensity of luminescence correlates with the presence of negative differential resistance in the static current-voltage curves, supporting the resonant-tunneling nature of emission. Its possible origin is plasmon-aided tunneling with the subsequent plasmon conversion into free-space radiation [2]. Motivated by this result, we develop a theory of plasmon-assisted tunneling in graphene tunnel junctions and find pronounced impact of conical band structure on inelastic tunneling [3].

The conductivity of tunnel-coupled graphene layers $\mathrm{Re}\,\sigma_{zz}(q,\omega)$ is negative at frequencies $\omega < eV/\hbar$, where V is the interlayer voltage. More surprisingly, the non-local tunnel conductivity exhibits square-root singularities for the frequencies ω and momenta q corresponding to the strong tunneling between chiral states with collinear momenta. Under conditions of negative resonant tunnel conductivity, the plasmons propagating along the double layer can rather gain energy from tunneling electrons than lose it for intra-layer interband excitation. The plasmon gain is manifested by the negative sign of the "effective conductivity" $\sigma_{xx} + \sigma_{zz}/(2qd)^2$ appearing in the plasmon dispersion law (Fig. 1).

Even if the tunnel transparency of the barrier layer is low so that the effective conductivity is positive, a significant fraction of tunnel current can be associated with the spontaneous emission of plasmons. We calculated the interlayer current associated with dynamically screened carrier-carrier scattering and extracted the plasmonic contribution. For voltages corresponding to the tangent of plasmon dispersion and a boundary of interlayer single-particle excitations, the plasmonic contribution to the current becomes resonantly large (see Fig. 2). These features are expected to appear as extra peaks in the static current-voltage curves, and enhanced electroluminescence is expected at these voltages as well.

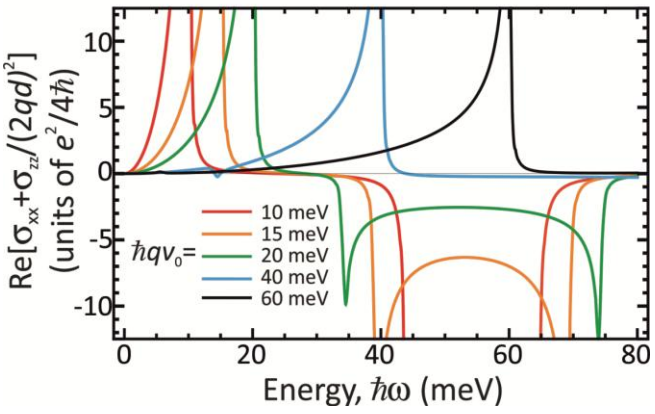

Fig. 1. Real part of effective conductivity (including in-plane σ_{xx} and tunnel σ_{zz} contributions) at different values of wave vector

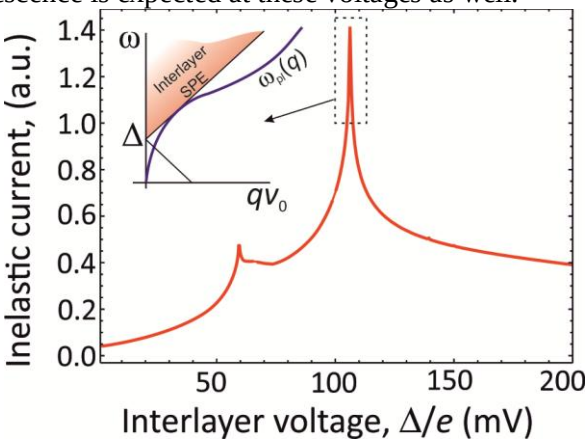

Fig. 2. Dependence of plasmon-assisted tunnel current accompanied on the shift Δ between Dirac points in the neighboring graphene layers.

References

[1] D. Yadav, S.B. Tombet, T. Watanabe, S. Arnold, V. Ryzhii, and T. Otsuji, 2D Mater. **3**, 45009 (2016).
[2] J. Lambe and S.L. McCarthy, Phys. Rev. Lett. **37**, 923 (1976).
[3] D. Svintsov, Z. Devizorova, T. Otsuji, and V. Ryzhii, Phys. Rev. B **94**, 115301 (2016).

Rhombohedral Multilayer Graphene : A Magneto-Raman Scattering Study

Y. Henni[1], H. P. Ojeda Collado[2, 3], K. Nogajewski[1], M. R. Molas[1], G. Usaj[2, 3], C. A. Balseiro[2, 3], M. Orlita[1], M. Potemski[1], C. Faugeras[1]
[1]*Laboratoire National des Champs Magnétiques Intenses, CNRS, (UGA, CNRS, UPS, INSA, EMFL), BP 166, 38042 Grenoble, Cedex 9, France*
[2]*Centro Atómico Bariloche and Instituto Balseiro, Comisión Nacional de Energía Atómica, 8400 S. C. de Bariloche, Argentina*
[3]*Consejo Nacional de Investigaciones Científicas y Técnicas (CONICET), Argentina*
clement.faugeras@lncmi.cnrs.fr

The electronic properties of ABC graphene trilayers has attracted lot of attention recently due to their potential applications in engineering carbon-based devices with gate tunable electrical conductivity. Morever,ABC-stacked thin layers of graphite are predicted to host peculiar surface electronic states, with a flat dispersion over most of the Brillouin zone [1]. The associated high density of states is likely to favor the emergence of exotic electronic phases, such as charge density waves, surface superconductivity, or magnetic ground state.

We present a micro-magneto-Raman scattering study of a thin graphite flake produced by exfoliation of natural graphite, composed of ~15 graphene layers, and including a large ABC-stacked domain. Exploring the low temperature Raman scattering spectrum of this domain up to B=29T [2], we identify inter Landau level electronic excitations within the surface flat bands, together with electronic excitations involving the gapped states in the bulk. This interband electronic excitation at B=0 can be observed, up to room temperature, directly in the Raman scattering spectrum as a broad (~180cm^{-1}) feature. Because the energy gap strongly depends on the number of layers, this electronic excitation can be used to identify and characterize ABC-stacked graphite thin layers.

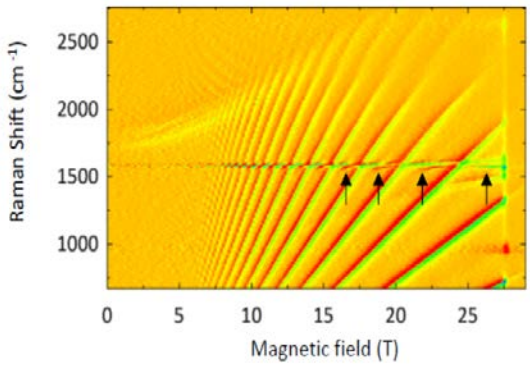

Fig. 1: False color map of the B-derivative of the Raman scattering response of a 15 ABC-stacked graphene sheets as a function of the magnetic field

References

[1] C-H. Ho et al., Phys. Rev. B 93, 075437 (2016)
[2] Y. Henni *et al.*, NanoLett. **16**, 3710, (2016)

Brightening of dark excitons in monolayers of semiconducting transition metal dichalcogenides

M. R. Molas[1], C. Faugeras[1], A. O. Slobodeniuk[1], K. Nogajewski[1], M. Bartos[1,2], D. M. Basko[3], M. Potemski[1]

[1]*Laboratoire National des Champs Magnétiques Intenses, CNRS, (UGA, CNRS, UPS, INSA, EMFL), BP 166, 38042 Grenoble, Cedex 9, France*

[2]*Central European Institute of Technology, CEITEC BUT, Brno University of Technology, Purkyňova 123, 612 00 Brno, Czech Republic*

[3]*Laboratoire de Physique et Modélisation des Milieux Condensés, Université de Grenoble-Alpes and CNRS, 25 rue des Martyrs, 38042 Grenoble*

clement.faugeras@lncmi.cnrs.fr

Monolayers (MLs) of semiconducting transition metal dichalcogenides (S-TMDs) are direct band gap semiconductors with the minima (maxima) of conduction (valence) bands located at the inequivalent $K^{\pm}$ points of their together hexagonal Brillouin zone. The lack of inversion symmetry with a strong spin-orbit interaction lead to well separated spin levels in the conduction (CB) and valence (VB) bands at the $K^{\pm}$ points. The spin-orbit splitting $\Delta_{so,vb}$ in the VB is as large as few hundreds of meV while the energy splitting in the CB, $\Delta_{so,cb}$, is predicted to be of the order of few tens of meV, and can also take negative values [1]. Because optical transitions in S-TMDs do conserve the spin, different ordering of electronic bands in the CB have profound consequences on their optical properties: depending on the sign of $\Delta_{so,cb}$, the excitonic ground state can be bright (parallel spin configuration for the top VB and the lowest CB subbands) or dark (anti-parallel spin configuration and optically forbidden ground state interband transition).

Here, we provide a direct measurement of the dark exciton emission in darkish MLs of S-TMDs by mixing the spin levels of both the bright and dark excitons by an in-plane magnetic field (B) [2]. Dark excitons appear in the low-temperature magneto-photoluminescence (PL) spectra as additional peaks growing with the magnetic field at energies lower than that of the bright exciton. For WSe_2 and WS_2 MLs, the dark exciton emission is observed at ∼50 meV below the bright exciton peak and displays a characteristic doublet structure. In the case of $MoSe_2$, no significant change in the emission spectrum is observed when applying a magnetic field, in agreement with the bright exciton ground state. MoS_2 is shown to belong to the family of darkish materials with a dark-bright splitting energy close to 100 meV. The emission intensity from dark excitons increases as B^2, in line with a perturbative activation by the in-plane magnetic field. Based on these results we classify the monolayers of WS_2, WSe_2, and MoS_2 as darkish materials, *i.e.*, the direct band gap systems but with a dark excitonic ground state, and the $MoSe_2$ ML as a bright material with a bright exciton ground state.

Moreover, we propose that different ordering of the spin-orbit split subbands in the CB for the bright and darkish S-TMD families is reflected in the zero-field low-temperature PL spectra: bright monolayers show a simple emission due to exciton and trions; the darkish ones display an additional broad/multipeak emission band due to localised/bound excitons.

References

[1] A. Kormányos *et al.*, 2D Materials. **2**, 022001 (2015).

[2] M. R. Molas *et al*., 2D Materials. **4**, 021003 (2017).

Infrared Magnetospectroscopy of High Mobility Graphene

B. Jordan Russell, Boyi Zhou, and E. A. Henriksen,
Department of Physics, Washington University in St. Louis,
St. Louis, MO 63130, USA
henriksen@wustl.edu

We present mid-infrared magnetospectroscopy measurements on boron-nitride encapsulated monolayer graphene samples at T = 6 K in magnetic fields up to 11 T. Focusing on one high-mobility device (μ~200,000 cm^2/Vs), several resonances can be resolved which correspond to both intra- and inter-band transitions. These show the expected $\sqrt{B}$ dependence on field [1,2], and typically have halfwidths of 3-4 meV reflecting the low levels of disorder in such samples. By gating the device we explore these transitions as a function of the filling factor, and find some of the interband Landau level transitions (e.g. N = -1 to +2, -2 to +3, &c.) to both decrease in energy and become significantly broadened. Meanwhile, the intraband N = -1 to 0 (and/or 0 to +1) transitions are observed to exhibit non-monotonic shifts and splittings as a function of varying the filling factor. The size of the splitting is not seen to change when the sample is tilted to ~20°.

Figure 1 shows normalized infrared transmission data for a monolayer graphene device with area < 200 μm^2. Several interband transitions are simultaneously visible. The intensities generally decrease with increasing transition energy, but also with increasing filling factor. In the case of the lowest interband transition, this is due to Pauli blocking; but for higher-level transitions is tentatively ascribed to the influence of many-particle interactions for the higher transitions. We will discuss these results in light of existing theory for the filling-factor dependence of magnetoexcitons in graphene [3-5]. We will also describe the experimental setup and its application to far-infrared measurements suitable for higher Landau level transitions, as well as magnetospectroscopy of high mobility bilayer graphene devices.

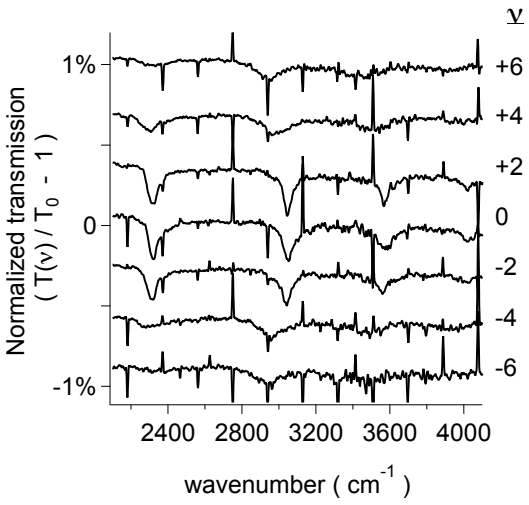

Fig. 1. Normalized infrared transmission of BN-encapsulated monolayer graphene device at B = 8 T, showing several interband transitions.

References

[1] V. Gusynin, S. Sharapov, & J. P. Carbotte, Phys. Rev. Lett. **98**, 157402 (2007)
[2] Z. Jiang *et al*., Phys. Rev. Lett. **98**, 197403 (2007).
[3] Y. Bychkov & G. Martinez, Phys. Rev. B **77**, 125417 (2008).
[4] K. Shizuya, Phys. Rev. B **81**, 075407 (2010).
[5] R. Roldán, J.-N. Fuchs, & M. O. Goerbig, Phys. Rev. B **82**, 205418 (2010).

Direct Growth of High Quality MoS_2-based Metal-Semiconductor-Metal Photodetectors.

Sudiksha Khadka, Thushan Wickramasinghe, Miles Lindquist, Ruhi Thorat, Shrouq Aleithan, Martin Kordesch and Eric Stinaff
Department of Physics and Astronomy, Nanoscale and Quantum Phenomena Institute, Ohio University, Athens, Ohio, OH 45701, USA
sk861011@ohio.edu

Scalable fabrication of two-dimensional materials-based devices with consistent characteristics remains a significant impediment in the field. Mono-to-few-layer MoS_2 metal-semiconductor-metal photodetectors (MSM PDs) have been reported with photo responsivities ranging from 1.1 mA/W to $1*10^3$ A/W, and response times from 10 s, to ~30 µs [1]. Here, we report on the characteristics of an as-grown ultra-thin MoS_2 metal-semiconductor-metal photodetector produced using a CVD process resulting in self-contacted, [2] two-dimensional materials-based devices. The photodetectors show high responsivity (~1 A/W) even at a low V_{DS} of 1.5 V and a maximum responsivity of up to 15 A/W when V_{DS} = 4 V and V_G = 8 V. The response time of the devices is found to be on the order of 1 µs, an order of magnitude faster than previous reports. These devices demonstrate the potential of this simple, scalable, and reproducible method for creating as-grown two-dimensional materials-based devices with broad implications for basic research and industrial applications.

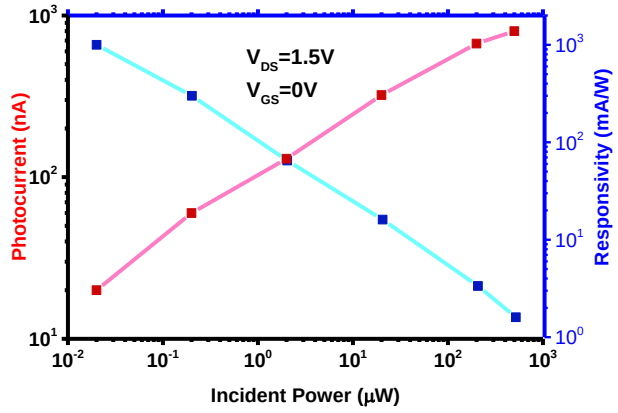

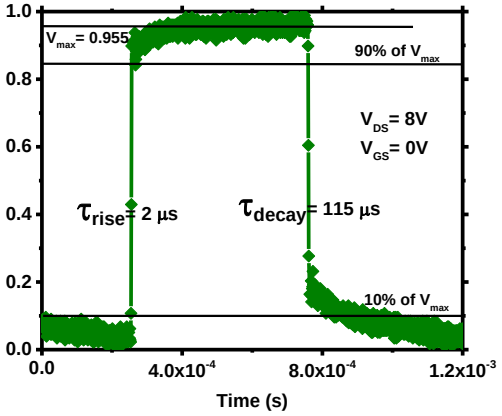

References:
[1] Buscema, Michele, Joshua O. Island, Dirk J. Groenendijk, Sofya I. Blanter, Gary A. Steele, Herre SJ van der Zant, and Andres Castellanos-Gomez. *Chem. Soc. Rev.* 44, 3691-3718 (2015)
[2] Khadka, Sudiksha, Miles Lindquist, Shrouq H. Aleithan, Ari N. Blumer, Thushan E. Wickramasinghe, Martin E. Kordesch, and Eric Stinaff. *Adv. Mater. Interf.* (2016).

Plasma excitations and Anomalous Plasmonic Retardation Effect in two-dimensional system of anisotropic fermions

A.R. Khisameeva[1,2], V.M. Muravev[1], I.V. Kukushkin[1]

[1]Institute of Solid State Physics RAS, 2 Academician Ossipyan str, Chernogolovka, Moscow Region 142432, Russian Federation

[2]Moscow Institute of Physics and Technology, 9 Institutskiy per., Dolgoprudny, Moscow Region, 141700, Russian Federation

phone: (496) 522-19-82, fax: (496) 522-81-60, e-mail: akhisameeva@issp.ac.ru

The spectra of plasma and magnetoplasma excitations in a two-dimensional system of anisotropic heavy fermions are investigated for the first time[1]. The spectrum of microwave absorption by disklike samples of stressed AlAs quantum wells at low electron densities shows two plasma resonances separated by a frequency gap [Fig.1]. These two plasma resonances correspond to electron mass principle values of (1.10 ± 0.05)m0 and (0.20 ± 0.01)m0 [2]. The observed results correspond to the case of a single valley strongly anisotropic Fermi surface. It is established that an increase in electron density results in the population of the second valley, manifesting itself as a drastic modification of the plasma spectrum. We directly determine the electron densities in each valley and the intervalley splitting energy from the ratio of the two plasma frequencies.

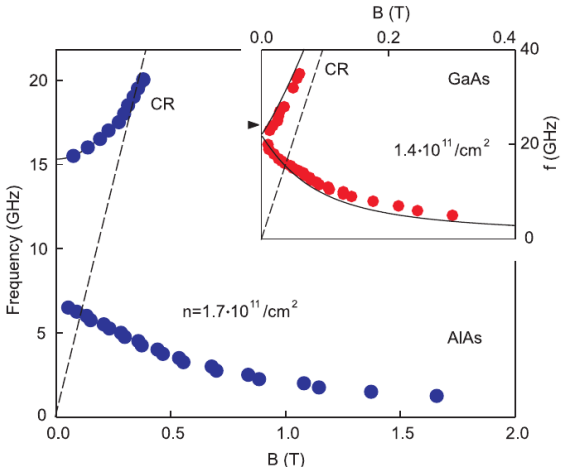

Figure 1: Magnetodispersion of two-dimensional plasma excitations in AlAs disks with anisotropic charge carriers. The inset shows the dispersion of magnetoplasmon waves in a GaAs quantum well for electrons with isotropic mass.

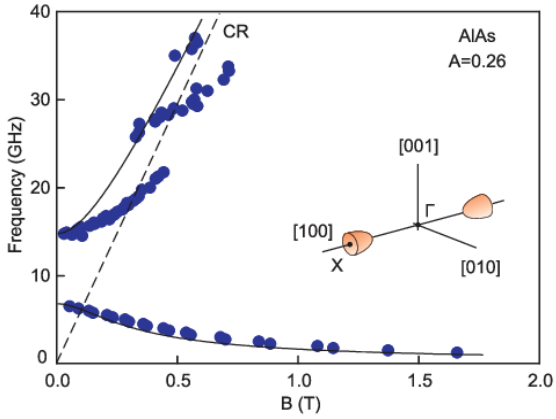

Figure 2: AlAs magnetoplasmon spectra for the sample with 2D electron density ns=1.70× 1011 cm-2(Retardation parameter A = 0.26).

The residual in-plane strain lifts the X and Y valley degeneracy, leading to an intervalley energy splitting E. For a 2DES where $n_s = 1.7 \times 10^{11}$ cm^{-2} , we find that all electrons occupy only the X valley, leaving the Y valley empty. As we increase the density, some of the electrons begin to fill the Y valley. The collective plasma excitations in such a system could be considered using a two-component anisotropic plasma model

Amazing feature is that reduction of the resonant plasma frequency and its flat magnetic field dependence. Observed strong hybridization of the plasma and light modes disappears whenever applied stress to the AlAs crystal makes 2D plasma spectrum in the system to be isotropic. Our experimental results demonstrate that coupling between light and 2D plasma, which is usually very weak, can be radically increased in the case of anisotropic solids [Fig.2]. To further prove the polaritonic nature of observed phenomenon we investigated density dependence of the 2D plasmon magnetodispersion.

Our results potentially pave a new way to increase efficiency of modern detectors and sources of terahertz and infrared radiation. As a system of choice for our experiments we choose 2DES in AlAs quantum well.

[1] V. M. Muravev, A. R. Khisameeva, V. N. Belyanin, V. Kukushkin, Phys.Rev. B 92, 041303(R) (2015)

[2] M.Shayegan, E.P. De Poortere, O.Gunawan, Y.P. Shkolnikov, E.Tutue, K.Vakili Phys.stat.sol.(b) 243, No. 14, 3629-3642(2006)

Ellipsometric Study on Temperature Dependence of Critical Points of 2-D $MoSe_2$

H. G. Park[1], T. J. Kim[1], V. L. Le[1], H. T. Nguyen[1], H. U. Kim[2], S.-K. Cha[2],
F. Ullah[3], Y. S. Kim[3], M.-J. Seong[4], and Y. D. Kim[1,*]
[1]*Department of Physics, Kyung Hee University, Seoul 02447, Republic of Korea*
[2]*KHU-KIST Department of Converging Science and Technology, Kyung Hee University, Seoul 02447, Republic of Korea*
[3]*Department of Physics and Energy Harvest Storage Research Center (EHSRC), University of Ulsan, Ulsan 44610, Republic of Korea*
[4]*Department of Physics, Chung-Ang University, Seoul 06794, Republic of Korea*
[*]ydkim@khu.ac.kr

Molybdenum diselenide ($MoSe_2$) is well known as one of transition metal dichalcogenides, which suggests promise as a potential substitute for silicon or organic semiconductors in state-of-the-art transistors, sensors, and photodetectors. In order to properly apply and correctly comprehend 2-D optoelectric device's function, the optical properties of monolayer $MoSe_2$ are needed. Although a few optical studies have been reported, no systematic study on temperature dependence of dielectric functions ε of 2-D $MoSe_2$ has been presented yet.

In this work, the 2-D $MoSe_2$ film was obtained by selenizing a pulsed-laser-deposited MoO_3 film on a sapphire substrate [1]. The dielectric function of 2-D $MoSe_2$ was measured in 0.74 - 6.42 eV energy range at temperatures from 31 to 300 K by spectroscopy ellipsometry. In Fig. 1(a), the existence of eight critical points (CPs) (*A*, *B*, *C*, and $E_{I\text{-}V}$) is clearly seen at 31 K some of which are new observations. Careful examination of the region near 1.7 eV in Fig. 1(b) on an expanded scale shows the existence of another new CP at the shoulder of the *A*-excitonic peak at 35 K, which is understood to be a combination of A^- trionic and A^0 excitonic CPs [2]. The CP energies are determined from standard lineshape analysis of numerically calculated second derivatives of ε with respect to energy. Blue shift and enhancement of most CP energies at low temperatures were observed and understood by the reduced lattice constant and electron-phonon interaction. These results will be useful for physical understanding and application of 2-D nano-optoelectronic devices based on $MoSe_2$.

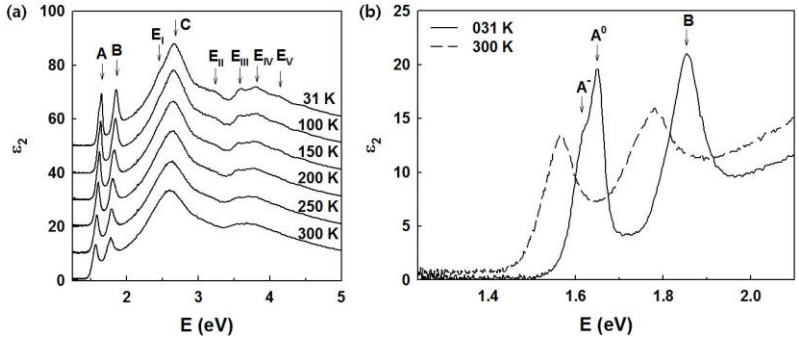

Fig. 1 Imaginary parts of ε of monolayer $MoSe_2$ (a) for temperatures from 31 to 300 K. (b) Spectra at 31 K and 300 K near regions of the *A*- and *B*-excitonic peaks.

References

[1] F. Ullah *et al*., CrystEngComm **18**, 6992 **(**2016).
[2] C. T. Le *et al*., Annal. Phys. **528**, 551 (2016).

Near-field nanoscopy of shot noise in bilayer graphene

K.-T. Lin[1], Q. Weng[1], H. Nema[1], S. Kim[1], K. Sugawara[2], T. Otsuji[2], S. Komiyama[3], and Y. Kajihara[1]
[1] Institute of Industrial Science, The University of Tokyo, Tokyo 153-8505, Japan
[2] Research Institute of Electrical Communication, Tohoku University, Sendai 980-8577, Japan
[3] Department of Basic Science, The University of Tokyo, Tokyo 153-8902, Japan
kuanting@iis.u-tokyo.ac.jp

Recently, there have been several advanced reports of graphene-based electronic device, like ultra-high frequency optoelectronic or electron devices [1]. The study of non-equilibrium electron dynamics (e.g. current fluctuation) in graphene devices, especially at the nanoscale, would be decisively important for understanding charge scattering mechanisms. So far the electrical noise has been studied by Ohmic contacts, which measure the noise integrated over the whole conductor. Local detection of the noise and its spatial imaging has remained to be a challenging task for decades

In this study, we report the first successful imaging of shot noise in bilayer graphene with nanometer resolution, observed with a passive THz scanning near-field optical microscope (s-SNOM) [2]. A sharp tungsten tip non-invasively probes shot noise by scattering fluctuating evanescent fields (~20 THz) generated on the surface of the graphene layer by the current fluctuation in the layer (Fig. 1(a)). The scattered waves are detected by a highly-sensitivity THz detector, based on quantum well (Fig. 1(b)) [3]. The graphene devices studied were patterned into a narrow, 1.4 μm-long and 0.7 μm-wide, constriction (Fig. 1(c)) by e-beam lithography and reactive ion etching in bilayer graphene epitaxially grown on a SiC substrate. The region of strong shot noise has been clearly imaged in the constricted region, where the current density is highest at a bias current of 1.77 mA. In the presentation, detailed characteristics of the shot noise, like the dependence on the bias-current amplitude and the tip height, will be discussed.

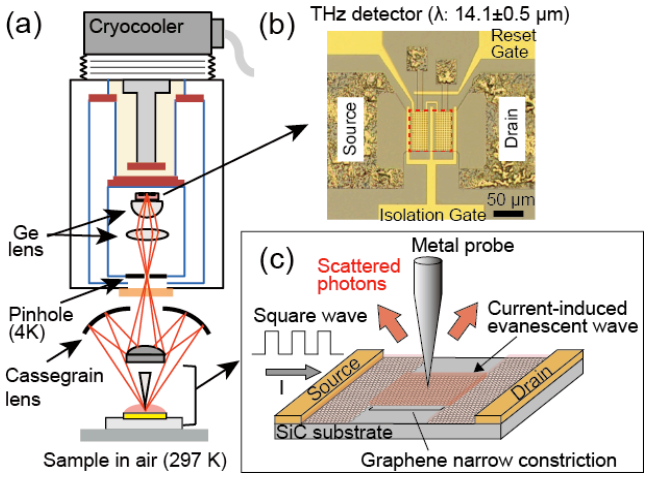

Fig.1 (a) Schematic diagram of the passive THz s-SNOM equipped with highly-sensitivity THz detector. (b) Photograph of the THz detector. (c) Schematic illustration of the experimental configuration used to detect current-driven evanescent wave in a graphene narrow constriction device.

References

[1] M. Ryzhii, V. Ryzhii, T. Otsuji, V. Mitin, and M.S. Shur, Phys. Rev. B **82**, 75419 (2010).
[2] K.-T. Lin et al., Rev. Sci. Instrum. **88**, 13706 (2017).
[3] S. Kim, S. Komiyama, T. Ueda, T. Satoh, and Y. Kajihara, Appl. Phys. Lett. **107**, 182106 (2015).

Linear polarized photoluminescence properties of few-layer ReS_2 and $ReSe_2$

Zhengguang Lu[1,2], Nihar Pradhan[1], Daniel Rhodes[1,2], Shahriar Memaran[1,2], Komalavalli Thirunavukkuarasu[3], Gregory T. McCandless[3], Zhigang Jiang[4], Luis Balicas[1], and Dmitry Smirnov[1,*]

[1]*National High Magnetic Field Laboratory, Tallahassee, FL 32310, USA*

[2]*Physics Department, Florida State University, Tallahassee, FL 32306, USA*

[3]*Physics Department, Florida A&M University, Tallahassee, FL 32310, USA*

[4]*School of Physics, Georgia Institute of Technology, Atlanta, GA 30332, USA*

*Zlu@magnet.fsu.edu

Rhenium disulfide (ReS_2) and rhenium diselenide ($ReSe_2$) are anisotropic group VII transition-metal dichalcogenide semiconductors, which have a distorted 1-T crystal structure with weak van der Waals interactions between layers. Though ReS_2 was reported to be a direct gap semiconductor [1], other recent studies have suggested that bulk ReS_2 is an indirect band gap material [2, 3]. Here, we report a detailed study of photoluminescence (PL) from linearly polarized excitons in ReS_2 and $ReSe_2$ as a function of the number of layers and temperature. The samples were prepared by mechanical exfoliation on to SiO_2/Si substrate. Two strong linearly polarized PL peaks at 1.541eV and 1.573eV dominate the low-temperature spectra (10K) of bulk ReS_2. As the number of layers decreases to 2 layers, two dominant PL peaks blueshift to 1.576eV and 1.655eV. $ReSe_2$ few-layer crystals exhibits qualitatively similar PL spectra with strongest linearly polarized peaks at 1.38eV and 1.40eV at 10K. The PL signal is several orders of magnitude lower compared to the group VI MX_2 direct bandgap monolayers ($MoSe_2$, WSe_2, MoS_2, WS_2). More importantly, thinner flakes show gradual decrease in PL intensity, which is consistent with the picture of the weakly coupled ReS_2 or $ReSe_2$ layers with an indirect gap bandstructure. As the temperature increases above about 50 K, the emission starts quickly decreasing. At 300K, the overall PL intensity decreases by approximately a factor of 1000 compared to that measured at 10K for all studied samples of ReS_2 and $ReSe_2$. Both materials exhibit similar anisotropy of PL emission. The angle between two dominant linearly polarized PL peaks varies with layer's thickness, which may be used for polarization control in optoelectronics.

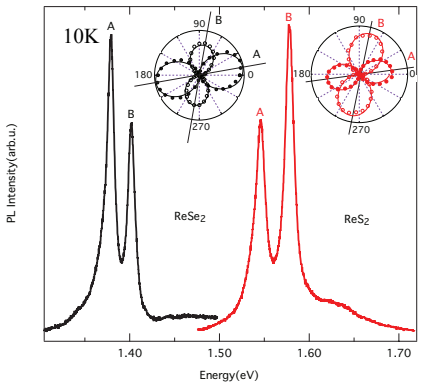

Fig.1 Unpolarized PL spectra of 8L $ReSe_2$ and 5L ReS_2. The insets summarize the angular polarization dependence for two strongest PL peaks.

References

[1] S.Tongay, et al., Nature Communications. **5**, 3252 (2014).

[2] O.B. Aslan, et al., ACS Photonics. **3**, 96 (2016)

[3] Gutierrez-Lezama, I., Reddy, B. A., Ubrig, N. & Morpurgo, A. F, 2D Materials. **3,** 045016 (2016)

Photocurrent in h-BN/MoS_2/h-BN Heterostructures

A. Saito, T. Ayano, and S. Nomura
Division of Physics, University of Tsukuba,
Tsukuba, 305-8571, Japan.
nomura.shintaro.ge@u.tsukuba.ac.jp

Atomically thin layered semiconductor transition metal dichalcogenides have attracted considerable attention recently as promising candidates for high sensitivity photodetectors at the low light regime. Molybdenum disulfide (MoS_2) is suitable to photodetectors because MoS_2 has the band gap in the visible and the near-infrared regimes [1]. High photosensitivity has been demonstrated in MoS_2 field effect transistors (FETs) on SiO_2. The photosensitivity, however, is suffered by the scatterings of the carriers by the oxide fixed charge, interface-trapped charge, and the surface roughness. Moreover, the MoS_2 channel exposed to the air is vulnerable to adsorbate that may degrade the performance of the detectors. Here, we report on photodetectors with encapsulated hexagonal boron nitride (h-BN)/MoS_2/h-BN heterostructure as a channel to reduce the extrinsic scatterings.

Polydimethly siloxane (PDMS)/polypropylene carbonate (PPC) dry transfer method [2] was employed to prepare h-BN/MoS_2/h-BN heterostructures on p-type silicon substrates with 270-nm-thick thermal SiO_2 layer. The thickness of MoS_2 thin films was characterized with atomic force microscopy. Cr/Au contacts were prepared for the source and drain electrodes and for the back gate. The samples were illuminated at the wavelength of 532 nm and the incident power between 1 nW and 2 μW using a continuous-wave laser and an optical microscope.

The h-BN/MoS_2/h-BN field-effect transistor with a 4.3 nm thick channel had a subthreshold swing of 208 mV/dec and a current on-off ratio of more than 10^5 at the drain voltage V_{DS} = 0.1 V at room temperature. The field-effect mobility was typically 25 cm^2/Vs. We measured photocurrent I_{ph} as defined by $I_{ph} = I_{DS}^{illum} - I_{DS}^{dark}$, where I_{DS}^{illum} and I_{DS}^{dark} are the drain current under illumination and at dark, respectively. The saturating behavior of the drain current was observed at $V_{DS} > 2$ V at dark at the back gate voltage V_g = 20 V. Under illumination, the saturation voltage was shifted to the higher voltage, and large photocurrent was observed at $V_{DS} > 2$ V. By contrast, the photocurrent was found to be small in the linear regime of $V_{DS} < 2$ V. With decrease in V_g, the onset of the photocurrent shifted to lower V_{DS}. This result indicates that the onset of the photocurrent is associated with the nonlinear screening in the electron gas near the drain contact. We obtained photoresponsivity I_{ph}/P exceeding 900 A/W at 0.82 mW/cm^2. Our results indicate that h-BN/MoS_2/h-BN FETs are promising for high photoresponsivity at low light regime.

References

[1] Kin Fai Mak and Jie Shan, Nature Photon. **10**, 216 (2016).
[2] L. Wang *et al.*, Science **342**, 614 (2013).

Selective Excitations of Two-dimensional Electron Systems by Arbitrary Vector Shaped Optical Pulse

H. Tanikawa,[1] T. Nakano, [1] H. Ito, [2] S. Nomura, [1] and K. Misawa[2]
[1]*Division of Physics, University of Tsukuba, Tsukuba, 305-8571, Japan.*
[2]*Department of Applied Physics, Tokyo University of A&T, Koganei, Tokyo 184-8588, Japan.*
nomura.shintaro.ge@u.tsukuba.ac.jp

The progress of arbitrary vector field shaping technique for ultrashort optical pulses has opened up new possibility to investigate the elementary excitations in two-dimensional electron systems (2DES). The temporal evolution of the amplitude and direction of the electric field of the optical pulses is programmed to any designed form [1]. This technique enables us to obtain, for example, optical pulses with prescribed bandwidth and pulse width, and polarization-twisted optical pulses where the direction of the electric field rotates with time at a prescribed frequency between 0 and 6 THz. This technique is a promising method to observe photoinduced Hall current in the absence of uniform magnetic fields [2]. In this paper, we present our results of the excitations of the two-dimensional electron systems by the vector field shaped optical pulses.

A 4*f* set-up was used for the arbitrary vector field shaping [1]. Femto-second optical pulses from a Ti:sapphire laser were diffracted by a volume-phase holographic grating. In the Fourier transformed space, the phases of the electric field vector of each frequency component of the optical pulse were controlled by a computer controlled spatial light modulator (SLM). The frequency components were recombined by the grating. The shaped pulses were calibrated by polarization-selective sum-frequency cross-correlation. The shaped pulses were incident on the surface of a Hall-bar structure of a GaAs single heterojunction or a GaAs/AlGaAs modulation-doped quantum well in a He cryostat. The photovoltage induced by the shaped pulses was detected by a lock-in amplifier.

The excitation photon energy dependence of the photovoltage showed a peak in the photovoltage near the band-gap of GaAs due to the heating of the electron temperature of the 2DES. In the lower energy side below the band-gap, we identified signals due to the impulsive stimulated Raman scattering, which increased linearly with the excitation power. The duration of the optical pulses was controlled by tuning the laser chirp parameter by the SLM. We have found that the photovoltage signal below the band-gap increases with increase in the duration of the pulse at a constant energy per pulse. This behavior is confirmed by changing the duration of the optical pulses by changing the bandwidth of the optical pulse. This demonstrates control of the excitation of the single particle excitations in 2DES around $\omega \sim 0$. Our arbitrary vector field shaping technique is expected to contribute to investigate circular polarization dependent excitations of the 2DES in the THz frequency regime.

References

[1] M. Sato *et al*., Nature Photon. **7**, 724 (2013).
[2] T. Oka and H. Aoki, Phys. Rev. B **79**, 081406 (2009).

Monolayered $MoSe_2$-WSe_2 lateral heterostructure growth and its potential use in valleytronics

Farman Ullah, [1] Chin Tam Le, [1] Yumin Sim, [2] Maeng-Je Seong, [2] Joon I. Jang, [3] and Yong Soo Kim [1],*

[1]*Physics Department, Penn State University, 1Department of Physics and Energy Harvest-Storage Research Center, University of Ulsan, Ulsan 44610, S. Korea*

[2]*Department of Physics, Chung-Ang University, Seoul 06794, S. Korea*

[3]*Department of Physics, Sogang University, Seoul 04107, S. Korea*

*yskim@ulsan.ac.kr (Y. S. Kim)

Monolayered in-plane heterostructure (HS) of semiconducting non-centrosymmetric transition metal dichalcogenides (TMDCs) are novel and of great interest due to their potential use in high-speed two-dimensional (2D) devices in terms of new emerging field of valleytronics.[1, 2]

Here, we present the synthesis of monolayer $MoSe_2$-WSe_2 in-plane HS by a novel pulsed-lased-deposition (PLD) assisted selenization method.[3] The grown HS with a sharp interface was verified by morphological and optical characterizations. Interestingly, the photoluminescence (PL) spectra acquired across the interface showed no signature of intermediate energy peak corresponding to $Mo_xW_{1-x}Se_2$ alloy or excitonic matter across the HS, thereby confirming the sharp interface. Furthermore, the two laterally attached monolayers of $MoSe_2$ and WSe_2, each with two degenerate energy valleys in *k*-space, were simultaneously polarized within a microscopic area of excitation across the interface by circularly polarized optical pumping. The $MoSe_2$ and WSe_2 showed relative degree of polarizations of 35% and 42%, respectively.

We believe that laterally grown TMDC HSs by our PLD-assisted method can be potentially important for advancing 2D valleytronics, especially when the photon excitation energy is actively tuned to the band edge of consisting TMDCs

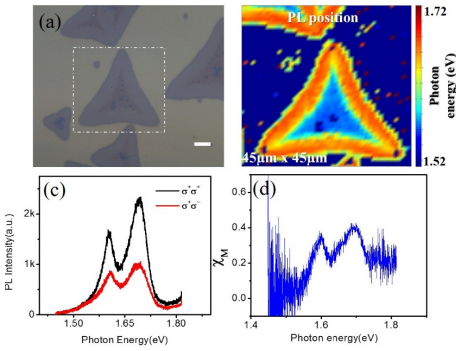

Fig.1 OM image of the in-plane heterostructure flake used for PL mapping. (b) PL peak position map (c) circular polarization resolved photoluminescence spectra across the interface for **σ**+ excitation and (d) the corresponding degree of valley polarization. The scale bar is 10 μm

References

[1] Y. Gong, J. Lin, X. Wang, G. Shi, S. Lei, Z. Lin, X. Zou, G. Ye, R. Vajtai and B. I. Yakobson, Nature Mater. **13**, 1135 (2014).

[2] P. Rivera, K. L. Seyler, H. Yu, J. R. Schaibley, J. Yan, D. G. Mandrus, W. Yao and X. Xu, Science **351**, 688 (2016).

[3] F. Ullah, T. K. Nguyen, C. T. Le and Y. S. Kim, CrystEngComm **18**, 6992 (2016).

Peculiarities of the photoluminescence line shape in Ga(N, As, P)/GaP. Experiment and Monte Carlo simulations.

V.V. Valkovskii[1], M.K. Shakfa[1], K. Jandieri[1], K. Volz[1], W. Stolz[1], M. Koch[1] and S.D. Baranovskii[1]
[1]*Department of Physics and Material Sciences Center, Phillips University Marburg, D-35032 Marburg, Germany*
vitalii.valkovskii@physik.uni-marburg.de

In the recent years much attention has been paid to the study of such semiconductor quantum well structures (QW) as GaInAs/InP, Ga(NAsP)/GaP, Ga(AsBi)/GaAs and number of other materials due to their unique physical properties and potential for applications in optoelectronic devices.

In many cases, optical spectra of QW are strongly influenced by disorder. In particular, energy relaxation of correlated electron-hole pairs through disorder-induced localized states determines the position and the shape of the photoluminescence (PL) lines. A lot of studies (both experimental and theoretical with numerical simulations) were conducted to find out the influence of disorder on QW optical properties. For many materials the dependences of PL lines on temperature and on the excitation power can be explained in the frame of Baranovskii-Eichmann model (BE) with exponential density of states (DOS) in the tail of localized states [1]. However, some materials, such as Ga(NAsP)/GaP, demonstrate unusual peculiarities in PL response, that cannot be explained in the frame of the standard BE model.

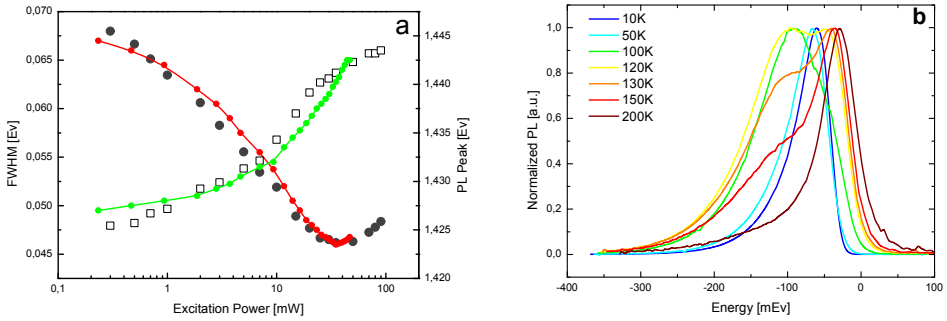

Fig. 1**.** (a) Typical dependence of Ga(N, As, P) PL line shape on excitation power at 10 K (rectangles) with Monte Carlo simulation results (colored lines with circles); (b) PL-lineshapes at different temperatures (energies below mobility edge are taken with minus).

In Fig.1 (a) one can see the typical dependence of the PL peak and linewidth (FWHM) on the excitation power. At low temperatures (10 K), a strong blue shift of PL line is observed, while the FWHM significantly reduces, when pump power is increased. The similar behavior was reported for GaAsBi/GaAs [2] and for InGaN/GaN [3]. Another interesting feature is presence of two peaks in PL spectra (Fig.1 (b)). When temperature is increased PL peak shifts from one to another. Such a behavior leads to sharp leap in PL Stocks Shift dependence on temperature, which is not expected in frame of conventional BE model.

To explain these features we introduce extended BE model with two types of localized states, distributed with the complex exponential-plus-Gaussian DOS. Kinetic Monte Carlo simulations has been performed to test the model and compare with experimentally observed results.

References

1. S.D. Baranovskii, R. Eichmann, and P. Thomas, Phys. Rev. B 58, 13081 (1998);
2. Yu. I. Mazur *et al* , J. Appl. Phys. 113, 144308 (2013);
3. Wang H, *et al* , Opt. Express 20 3932, (2012).

Magnetoplasmon-polaritons in lossy two-dimensional electron system

A.A. Zabolotnykh and V.A. Volkov
Kotelnikov Institute of Radio Engineering and Electronics of the RAS, Mokhovaya 11-7, Moscow 125009, Russia
zabolotnykh@phystech.edu

Plasma oscillations or plasmons in two-dimensional (2D) electron systems (ESs), in contrast to three-dimensional plasma oscillations, have no frequency gap at zero wave vector. Without dissipation in the long-wave limit and neglecting the retardation effects, frequency of plasmon-polariton depends on wave vector as a square root function. In 2D ES with dissipation, plasmons with frequencies below $1/\tau$ usually decay rapidly, and, in this sense, do not exist; here τ is the electron relaxation time.

However, the other situation occurs, when electrodynamic effects are taken into consideration (in this case plasmons are often called plasmon-polaritons). It was shown [1] that the plasmon-polaritons exist at all frequencies (even in a high-collision limit when the plasmon-polariton frequency is smaller than $1/\tau$) if the conductivity of 2D ES σ, which has velocity dimensionality in Gaussian units, exceeds $c/2\pi$, where c is the speed of light. Note, that condition $2\pi\sigma=c$ takes place if the resistivity $1/\sigma$ is 188 ohms/□ or less.

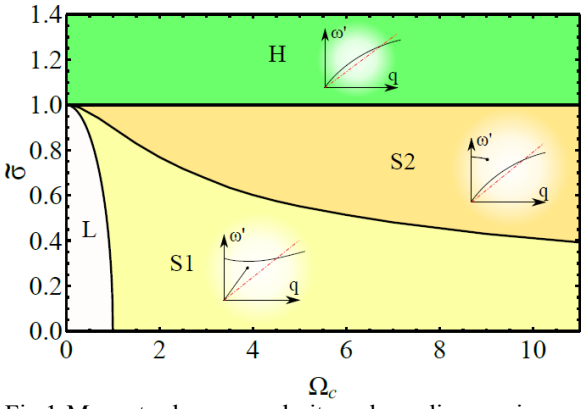

Fig.1 Magnetoplasmon-polariton phase diagram in space of dimensionless parameters: 2D dc conductivity $\tilde{\sigma} = 2\pi\sigma/c$ vs cyclotron frequency $\Omega_c = \omega_c\tau$. The characteristic plasmon-polaritons spectra $\omega(q)$ in each phase are presented schematically in the insets (dash-dotted line corresponds to the 2D light cone).

We generalize the results of paper [1] on 2D ESs placed in constant magnetic field which is perpendicular to 2D ES plane [2]. Note that plasmon-polaritons in magnetic field were considered by Chiu and Quinn [3] but only in the dissipationless ($\tau\to\infty$) 2D ES.

We find spectra of plasmon-polaritons in a lossy 2D ES in a perpendicular classical magnetic field B. It is convenient to classify the characteristic plasmon-polariton spectra using a phase diagram, see Fig. 1. We find that plasmon-polaritons in magnetic field exist at frequencies less than $1/\tau$ in phases S1, S2, and H, i.e. when the condition $(2\pi\sigma/c)^2+(\omega_c\tau)^2>1$ takes place, where σ is the static 2D conductivity in the absence of magnetic field and $\omega_c=eB/mc$ is the electron cyclotron frequency. Moreover, in phases S1 and S2 the spectra contain the termination point at which the damping of plasmon-polariton vanishes, i.e. plasmon-polariton propagates without any decay, in spite of the electron relaxation time is finite. This unexpected result is due to the plasmon-polariton becomes delocalized along the normal to the ES plane.

The work was financially supported by the Russian Science Foundation (Project No. 16-12-10411).

References

[1] V. I. Fal'ko and D. E. Khmel'nitskii, Sov. Phys. JETP **68**, 1150 (1989).
[2] V. A. Volkov and A. A. Zabolotnykh, Phys. Rev. B **94**, 165408 (2016).
[3] K. W. Chiu and J. J. Quinn, Phys. Rev. B **9**, 4724 (1974).

Interplay between the alignment of the dark and bright exciton states and the degree of circular polarization of the PL emission in monolayer transition metal dichalcogenides

M. Baranowski[1,2], A. Surrente[1], D. K. Maude[1], M. Ballottin[3], A. A. Mitioglu[3], P. C. M. Christianen[3], Y. C. Kung[4], D. Dumcenco[4], A. Kis[4] and P. Plochocka[1]

[1] *Laboratoire National des Champs Magnétiques Intenses, UPR 3228, CNRS-UGA-UPS-INSA, Grenoble and Toulouse, France*

[2] *Department of Experimental Physics, Faculty of Fundamental Problems of Technology, Wroclaw University of Science and Technology, Wroclaw, Poland*

[3] *High Field Magnet Laboratory (HFML—EMFL), Radboud University, 6525 ED Nijmegen, Netherlands*

[4] *Electrical Engineering Institute and Interdisciplinary Center for Electron Microscopy (CIME), École Polytechnique Fédérale de Lausanne (EPFL), CH-1015 Lausanne, Switzerland*

paulina.plochocka@lncmi.cnrs.fr

The unique band structure of transition metal dichalcogenides (TMDs) monolayers makes these materials very attractive for valleytronic applications. The valley spin-locking, together with the large valence band splitting, suppresses exciton inter valley scattering. Using circular polarized optical excitation a significant degree of circular polarization degree of the photoluminescence (PL) can be achieved in MoS_2, WS_2 and WSe_2 monolayers. However, there remain some puzzling aspects of the achievable degree of circular polarization of the PL emission in TMDs. Despite the very similar band structure of tungsten and molybdenum based monolayers, it is much easier to achieve polarized emission in the tungsten based TMDs [1]. One thing that distinguishes the Mo and W based TMDs is the bright and dark exciton alignment.

Here we show that the robustness of circular polarization in PL correlates with the sign of the dark-bright exciton splitting. The importance of the alignment of the bright and dark exciton states results from the competition between intravalley bright-dark exciton scattering and intervalley scattering. We propose a simple model for the excitons kinetics, which explains in a consistent way differences in the observed degree of circular polarization of the PL emission in different TMDs monolayers. Our studies suggests that the intravalley scattering between dark and bright exciton states play an important role in the observed degree of PL circular polarization and can enhance polarization in tungsten based materials. A crucial point of the model is that the intervalley scattering, related to the electron–hole exchange interaction, is effective *only for bright exciton states*. Therefore, the dark exciton ground state provides a robust reservoir for valley polarization which tries to maintain a Boltzmann distribution of the bright exciton states in the same valley via intravalley bright dark exciton scattering. Our model correctly explains the literature data together with our own detailed excitation energy dependent study of the degree of circular polarization of the PL emission in an $MoSe_2$ monolayer. Finally, we are able to conclude from our results, that phonon mediated intervalley scattering is not the main mechanism responsible for valley depolarization in TMDs [2].

References

[1] M. Baranowski, A. Surrente, D. K. Maude, M. Ballottin, A. A. Mitioglu, P. C. M. Christianen, Y. C. Kung, D. Dumcenco, A. Kis and P. Plochocka , 2D Mater. **4**, 025016, (2017)

[2] G. Kioseoglou, A. T. Hanbicki, M. Currie, A. L. Friedman, B. T. Jonker *Scientific Reports* **6**, 25041, (2016)

Manifold coupling between transition metal dichalcogenides and plasmonic gold nanoparticle arrays

S. Diefenbach, E. Parzinger, J. Kiemle, S. Funke, B. Miller, R. Csiki, P. Thiesen, A. Cattani-Scholz, M. Stutzmann, U. Wurstbauer, and A.W. Holleitner
Walter Schottky Institute and Physics Department, TU Munich, Munich, Germany
wurstbauer@wsi.tum.de

We investigate the coupling between the optically active semiconducting transition metal dichalcogenide MoS_2 and WSe_2 and plasmonic active octanethiole stabilized gold nanoparticle (Au-NP) arrays. This hybrid system is expected to increase the already strong light-matter interaction [1] in these materials via plasmonic enhancement of the light field for optical, optoelectronic as well as solar harvesting applications.

Monolayers of pristine and Au-NP covered MoS_2 and WSe_2 crystals as well as Au-NP on the bare substrate have been studied in a comprehensive approach combining µ-photoluminescence (PL), µ-Raman, spectroscopic imaging ellipsometry (SIE) [2] as well as Kelvin force probe microscopy (KPFM). We find for both materials a 20-fold PL enhancement for the hybrid structure compared to the pristine layers almost independent for resonant and non-resonant excitation [3]. SIE proves that the surface plasmon polariton (SPP) of the Au-NP array spectrally overlaps with the A and B excitons of MoS_2 and the B exciton in WSe_2 and it clearly indicates the coupling between the layers. KPFM and µ-Raman studies [2], however, enclose that the charge carrier densities in the hybrid structures are depleted compared to the pristine flakes. Altogether, we do not find evidence for plasomic enhancement of the light field. This can be explained by the fact, that the SPPs are oriented parallel to the 2D crystals and therefore does not couple to the dipolar transitions in the TMDs. Instead, the enhanced PL signal is assigned to the altered dielectric environment and the reduced charge carrier density in the TMD materials.

We acknowledge financial support by the ERC project NanoREAL, the Deutsche Forschungsgemeinschaft (DFG) via excellence cluster ‘Nanosystems Initiative Munich’ as well as DFG projects WU 637/4-1 and HO3324/9-1 and the TUM international graduate school of science and engineering (IGSSE).

References

[1] U. Wurstbauer *et al.*, J. Phys. D, in press (2017).
[2] S. Funke *et al.* J. Phys.: Condens. Matter **28**, 385301 (2016).
[3] S. Diefenbach *et al.* (2017).
[3] B. Miller *et al.* Appl. Phys. Lett. **106**, 122103 (2015).

Strained InSe monolayer for optoelectronic

Imen Ben Amara[1,*], Aida Hichri[2], and Sihem Jaziri[1, 2]

[1] *Faculté des Sciences de Tunis, Laboratoire de Physique de la Matière Condensée, Université Tunis El Manar Campus Universitaire, 2092, Tunis, Tunisia*

[2]*Faculté des Sciences de Bizerte, Laboratoire de Physique des Matériaux, Université de Carthage, 7021, Bizerte, Tunisia.*

Sihem.jaziri@fsb.rnu.tn

Tuning band energies of 2D semiconductors through strain engineering can significantly boost their electronic and optical performances[1]. Based on first principle calculations, lattice in-plane compressive strain effect on bands structure of InSe monolayer (ML) induces an indirect-direct gap transition with enlargement bandgap size. The origin and mechanism of this crossover is explained by the momentum angular contribution and In-Se strength interaction. Strain impact deals to a new unexplored strained ML InSe with high charges carriers's mobility overcoming some limitations of unstrained InSe[2]. Owing to its excellent optoelectronic and electronic merits, the optical response versus energy is evaluated within dielectric theory and infers the allowed optical transitions, dielectric constants and refractive index .The birefringence, transparency, semiconductor-metal nature transition and strong absorption properties are either demonstrated. From a theoretical point of view, we consider how the exciton behavior in the direct gap strained ML InSe evolves under environmental dielectrics.

References

[1] Yeung Yu Hui et al, ACNNANO, **7**, 7126 (2013).

[2] A. Politano, D. Campi , M. Cattelan, I. Ben Amara , S. Jaziri , A. Mazzotti, A. Barinov, B. Gürbulak , S. Duman , S. Agnoli, L. S. Caputi , G. Granozzi , and A. Cupolillo,* "Indium selenide: an insight into electronic band structure and surface excitations" accepted for publication in Scientific Reports (2017).

Uniform wafer-scale growth of stencil templated, high-quality monolayer MoS_2

Justin R. Young, Michael Chilcote, Matthew Barone, Sara Mueller, Roland Kawakami and Ezekiel Johnston-Halperin
Department of Physics, The Ohio State University
Columbus, OH, 43210, USA
Johnston-Halperin.1@osu.edu

With the widespread interest in transition metal dichalcogenides and the recent focus on two-dimensional (2D) vertically stacked heterostructures, a need for an inexpensive and reliable method of producing clean, high-quality, patterned 2D materials has emerged. Here, we report on a templated MoS_2 growth technique by metal sulfurization where Mo is deposited through a SiN stencil onto highly-crystalline sapphire substrates. After sulfurization, the resulting MoS_2 films are shown to be high-quality with thicknesses that can be tuned layer-by-layer—down to a single layer—through manipulation of the initial Mo deposition time. The quality of these films is confirmed through scanning electron and atomic force microscopies as well as Raman and photoluminescence spectroscopy. This facile growth technique results in templated, high-quality MoS_2 films with centimeter-scale uniformity, feature sizes down to 100 nm, and offers both a means to easily probe MoS_2 growth dynamics and a route to 2D stacked heterostructures with arbitrary geometry and pristine interfaces. We will discuss potential applications of this novel growth technique for the development of TMD heterostructures and alloys.

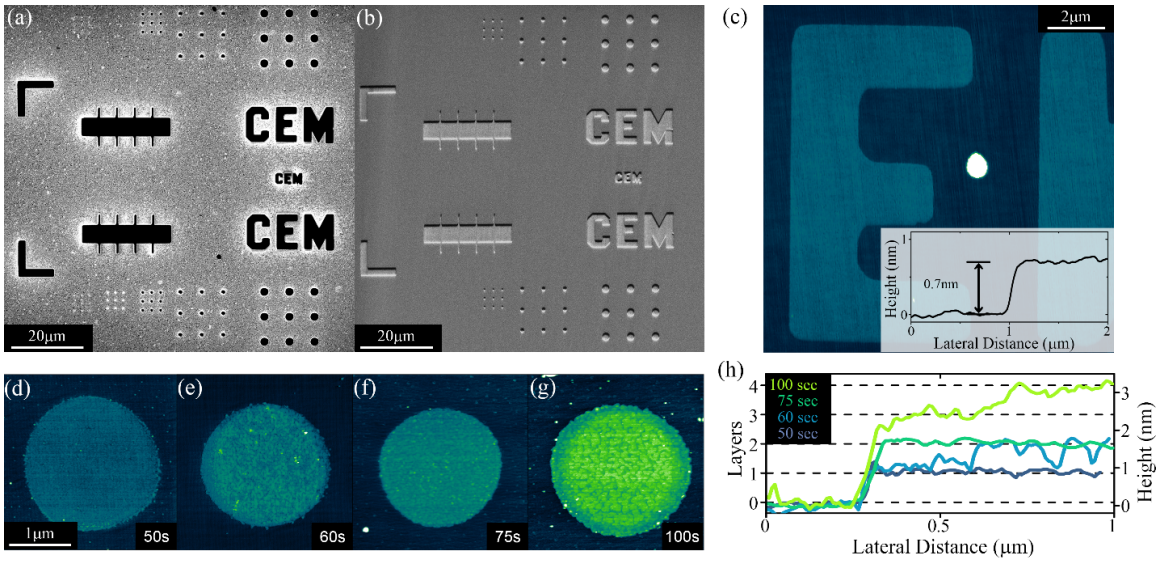

Figure 1. Physical characterization of MoS_2 films. (a) FIB image of a completed SiN mask. Dark areas are patterned holes in the SiN. (b) SEM image of a completed MoS_2 growth. Light areas are single-layer MoS_2. (c) AFM image of the "E" corresponding to a single-layer MoS_2 growth. Visible vertical striations are the atomic plateaus present on the sapphire substrate. The inset shows an AFM line scan of the "E" edge with a step height of 0.7 nm, corresponding to a single-layer film. (d)-(g) AFM images of 2 μm wide MoS_2 dots on sapphire at initial Mo film deposition times of 50, 60, 75, and 100 seconds. (h) AFM line cuts across the edges of the dots shown in (d)-(g) demonstrating the layer-by-layer growth of MoS_2.

Magneto-optical investigation of strained 2D WSe_2 monolayers

A. Mitioglu[1,2 *], M. Ballottin[1], J. Buhot[1], S. Anghel[2], L. Kulyuk[2], P. C. M. Christianen[1]
[1]*High Field Magnet Laboratory (HFML - EMFL), Radboud University, NIJMEGEN, The Netherlands;*
[2]*Institute of Applied Physics, Academiei Str. 5, Chisinau, MD-2028, Republic of Moldova.*
*E-mail: a.mitioglu@science.ru.nl

Monolayer transition metal dichalcogenides (TMDCs), such as MoS_2, $MoSe_2$, WS_2 and WSe_2, are novel two dimensional materials with a direct bandgap located at two degenerate valleys (K+ and K-) at the corners of the hexagonal Brillouin zone. The energy bandgap lies in the visible spectral range, which gives rise to efficient light emission and absorption. The optical spectra in monolayer TMDCs are dominated by excitonic effects due to strong 2D confinement and electron-hole (e-h) exchange [1]. Strong spin-orbit interaction and optical selection rules enable the creation of excitons in a specific valley using circularly polarized light. In addition, linearly polarized illumination leads to excitons, whose states are a superposition of those of K+ and K- valleys, which also emit linearly polarized light due to valley coherence.

The micro-photoluminescence (PL) spectra of TMDCs are dominated by sharp neutral and charged exciton (trions) lines. Recently, we reported that under an applied magnetic field both exciton and trion emission lines of WSe_2 shift in position with magnetic field and split up into two lines of opposite circular polarization (Valley splitting). This behavior was explained using a single-electron picture and a massive Dirac model [2]. As a result, we found an effective valley *g*-factor of 4 and a Fermi velocity of 0.51×10^6 cm^2/s. However, also significantly different *g*-factor values have been reported [3]. Possible origins for the spread in *g*-factors are the effects of doping or strain, although Li and co-workers [4] claimed that doping does not influence the effective *g*-factor. Recent theoretical work confirmed that moderate strain together with e-h exchange leads to a splitting of the exciton peak [5].

High resolution micro-PL reveals that some WSe_2 flakes exhibit a PL spectrum with a splitted exciton peak (see Fig. 1). The splitting is due to a moderate intrinsic strain, as evidenced by concomitant Raman measurements. We have performed detailed polarized-resolved PL measurements on a set of strained WSe_2 flakes, in magnetic fields up to 30 T. Our results elucidate the influence of the combined effect of strain and e-h exchange on the exciton energy structure and the resulting effective *g*-factors.

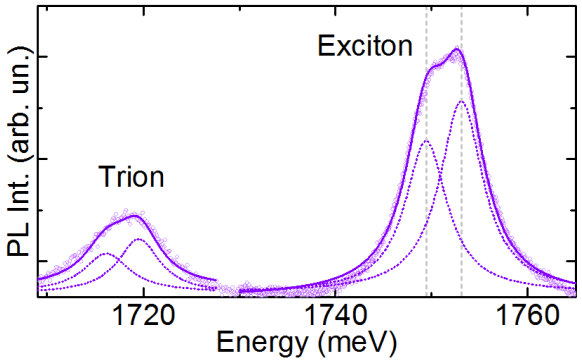

Fig.1. Typical high resolution micro-PL spectrum of monolayer WSe_2

References

[1] For a review see *e.g.* (a) X. Xu, W. Yao, D. Xiao, T. F. Heinz, *Nature Phys.* **10(5)**, 343 (2014); (b) K. F. Mak and J. Shan, *Nature Photonics* **10**, 216 (2016); (c) J. R. Schaibley, H. Yu, G. Clark, P. Rivera, J. S. Ross, K. L. Seyler, W. Yao, and X. Xu, *Nat. Rev. Mat.* **1**, 16055 (2016).

[2] A. Mitioglu, P. Plochocka, Á. Granados del Aguila, P. C. M. Christianen, G. Deligeorgis, S. Anghel, L. Kulyuk, and D. K. Maude, *Nano Lett.* **15**, 4387 (2015)

[3] G. Aivazian, Z. Gong, A. M. Jones, R-L Chu, J. Yan, D. G. Mandrus, C. Zhang, D. Cobden, W. Yao, and X. Xu, *Nature Phys.* **11**, 148 (2015)

[4] Y. Li, J. Ludwig, T. Low, A. Chernikov, X. Cui, G. Arefe, Y. D. Kim, A. M. van der Zande, A. Rigosi, H. M. Hill, S. H. Kim, J. Hone, Z. Li, D. Smirnov, and T. F. Heinz, *Phys. Rev. Lett.* **113,** 266804 (2014)

[5] (a) H. Yu et al., *Nat. Comm.* **5**, 3876 (2014); (b) H. Yu, et al., *National Sci. Rev.*, **2**, 57 (2015).

Optical Nonlinearity of Layer-dependent TMDC Atomic Layer

Tikaram Neupane, Quinton Rice, Sheng Yu, Bagher Tabibi, and Felix Jaetae Seo*

Advanced Center for Laser Science and Spectroscopy, Department of Physics, Hampton University, Hampton, Virginia 23668, USA. *jaetae.seo@hamptonu.edu

The electronic bandgap of transition metal dichalcogenides (TMDCs) depends on the number of layers. The monolayer has a direct band gap which is wider than the indirect bandgap present in bilayers or multilayers. Therefore, the TMDCs show characteristic nonlinear optical properties depending on the number of atomic layers for the given excitation energy. The bandgap changes due to the number of atomic layers in TMDCs for the given excitation energy provide the resonant and nonresonant optical susceptibilities [1, 2]. The possible nonlinear optical processes include the nonresonant transition through one photon or two photons; and the resonance transition through two photon absorption. The resonant optical nonlinearity is relatively slow and large, but the nonresonant optical nonlinearity is relatively fast and weak. The nonlinear figure of merit (FOM) of resonant excitation is relatively small due to large nonlinear absorption susceptibility, but the nonlinear FOM of nonresonant excitation is relatively large due to high nonlinear refraction susceptibility. The nonlinear characterization with Z-scan technique resolves the nonlinear absorption, nonlinear refraction, and their polarities. The polarities of nonlinear absorption include positive and negative nonlinear absorptions of reverse saturable absorption (RSA) and saturable absorption (SA), respectively. The RSA is possibly due to the higher excited state absorption (ESA) cross-section than the ground state absorption (GSA) cross-section. In contrast, the SA is attributable to the higher GSA than the ESA. The nonlinear optical materials with RSA can be utilized for optical power limiting, but it is not recommended due to low nonlinear figure of merit. The nonlinear optical materials with SA can be used for Q-switching and mode-locking. The polarities of nonlinear refraction include positive and negative nonlinearities of self-focusing and defocusing, respectively. The optical materials with nonlinear refraction can be utilized for optical power limiting and modulation. Therefore, the bandgap changes due to number of layers in the TMDCs significantly changes the nonlinear optical properties. Acknowledgement: This work at HU is supported by ARO W911NF-15-1-0535, NSF HRD-1137747, and NASA NNX15AQ03A.

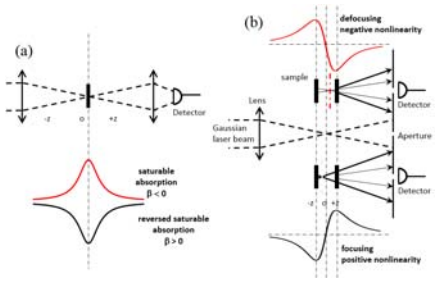

Fig.1 Schematic description of (a) open Z-scan and (b) close Z-scan

References

[1] T. Neupane, Q. Rice, B Tabibi, and F. Seo, Transition of Saturable and Reverse Saturable Absorptions between Monolayer and Bilayer/Multilayer, (Preparing for J. of Applied Physics).

[2] Y. Li, N. Dong, S. Zhang, X. Zhang, Y. Feng, K. Wang, L. Zhang, and J. Wang, Laser Photon. Rev. **9** 427 (2015).

Excition Polarizaton Coherence in Tungsten Diselenide Atomic Layer

Tikaram Neupane, Quinton Rice, Sheng Yu, Bagher Tabibi, and Felix Jaetae Seo*

Advanced Center for Laser Science and Spectroscopy, Department of Physics, Hampton University, Hampton, Virginia 23668, USA. * jaetae.seo@hamptonu.edu

The coherence loss of exciton polarization [1, 2] in tungsten diselenide (WSe_2) atomic layer is of great interest for optoelectronic applications including ultrafast modulation, switching, and information processing. The total exciton dephasing time, T_2, characterizes the coherence loss of exciton polarizations which are related to the pure dephasing time T_2^* and population relaxation time T_1. The coherency of exciton polarization is also dependent on the exciton-exciton and exciton-phonon coupling strengths. The exciton-phonon coupling is dominant at higher temperatures, while the exciton-exciton coupling is stronger at higher excitation intensity. At higher temperatures, the exciton-phonon coupling contribution to the total exciton dephasing time may be more dominant than the exciton-exciton coupling contribution. At higher excitation intensities, the exciton-exciton coupling contribution to the total exciton dephasing time may be much stronger than the exciton-phonon coupling contribution. Therefore, the contributions of exciton-exciton and exciton-phonon couplings to the total dephasing time are negligible at lower temperature and weaker excitation intensity. However, the phonon density increases at higher temperature, and the exciton density increases at higher excitation intensity. The larger scattering at higher phonon density and the larger elastic collision at higher excitation intensity reduce the total dephasing time. The characteristic total dephasing time of WSe_2 monolayer was analyzed as functions of excitation intensity and exciton-exciton coupling; and temperature and exciton-phonon coupling. The dephasing time of WSe_2 atomic layer in the range from a few ps to sub ps may be utilized for optoelectronic modulator or switching. The longer dephasing time of exciton or electron in the WSe_2 atomic layer with valley photonic chirality could be utilized for information processing. Acknowledgement: This work at HU is supported by ARO W911NF-15-1-0535, NSF HRD-1137747, and NASA NNX15AQ03A.

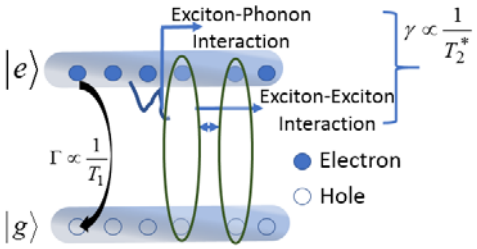

Fig.1 Dynamics of exciton dephasing and the recombination process

References

[1] T. Neupane, Q. Rice, B. Tabibi, and J. T. Seo, Exciton Dephasing of Two-dimensional Atomic Layers (preparing for Optics communications).

[2] G. Moody, C. K. Dass, K. Hao, C-H Chen, L-J Li, A. Singh, K. Tran, G. Clark, X. Xu, G. Berghauser, E. Malic, A. Knorr, and X. Li, Nat. Commun. **6**, 8315 (2015).

Quantum Dot – 2D Conductor Phototransistors: Graphene versus Semiconductor Materials

Kimberly Sablon and Andrei Sergeev
Sensors and Electron Devices Directorate, U.S. Army Research Laboratory,
2800 Powder Mill Rd, Adelphi, Maryland USA
podolsk37@gmail.com

Recent intensive investigations have demonstrated exceptional properties of hybrid quantum dot – 2D conductor nanomaterials, which open wide perspectives for development of low-cost phototransistors with high gain, selective photoresponse, MHz electronic bandwidth, and high sensitivity in the visible and short-wave infrared ranges. Experimental research of hybrid structures includes a variety of quantum dot media (PbS, PbSe, ZnO, etc) and a number of 2D materials (graphene, WS_2, MoS_2, etc). In this presentation we describe mechanisms of photoresponse, basic characteristics of photodetectors and their dependence on material parameters, and detector limiting performance.

The main subject of this work is the comparative analysis of hybrid phototransistors with graphene and semiconductor 2D materials used for the emitter – collector channel. The key difference between graphene and 2D semiconductors is a continuous density of electron states (DOS) in graphene in the semiconductor bandgap energy range. The optoelectronic QD – graphene nanostructures do not require fine electron level alignment to provide effective photocarrier transfer from QDs to the graphene emitter – collector channel. Efficient electron coupling between QD medium and graphene improves the operating rate of the detector. Thus, graphene is a universal material, which may be combined with practically any QD absorber. At the same time, due to filling by carriers from the micrometer-size QD medium (unintentional doping), the graphene in hybrid structures is always a weakly degenerate conductor. Therefore, the graphene photoresponse per an additional photocarrier is smaller than that in a semiconductor by the factor of kT/ε_F, where ε_F is the Fermi energy in graphene. However, the high mobility of graphene strongly increases the photoconductive gain, which more than compensates the effect of degenerate statistics. As a result, the graphene-based hybrid transistors substantially surpass 2D semiconductor devices in responsivity, sensitivity, and operating rate.

The presented model well describes the dependence of the responsivity on the electromagnetic power for a graphene transistor and determined the characteristic saturation power. As the characteristic power is proportional to the DOS in graphene and the noise current is proportional to $DOS^{1/2}$, the detector dynamic range is proportional to $DOS^{1/2}$ and it may be effectively controlled by the gate voltage. The gate control of operating regimes opens intriguing possibilities for adaptive sensing. Finally, we calculated the limiting sensitivity of hybrid phototransistors and demonstrate that the sensitivity close to the limiting value has been achieved in the recent work [2] due to electric field enhanced coupling between QDs and graphene. Thus, the hybrid phototransistors have already reached some level of maturity, but there is still significant room for further optimization of trade-off detector characteristics.

References

[1] K. Sablon et al., High-Response Hybrid Quantum Dots - 2D Conductor Phototransistors: Recent Progress and Perspectives, Nanophotonics (2017), accepted.
[2] I. Nikitskiy et al., Integrating an electrically active colloidal quantum dot photodiode with a graphene phototransistor. Nature Communications, **7**, 11954 (2016).

Interference effects in magnetic focusing with strong spin-orbit interactions

S. Bladwell and O. P. Sushkov
School of Physics, UNSW
Kensington, 2052, NSW, Australia

Transverse magnetic focusing is a versatile experimental technique where charge carriers are focused from a source to a detector using a weak transverse magnetic field; it is the direct propagation of charge mass spectroscopy to the solid state. When used in systems with large spin-orbit interactions the strong spin-orbit interaction results in a real space separation between the spin states, and a resulting 'double' focusing peak.

Two additional features make the physics of this particular system exceptionally rich; firstly a Fermi wavelength that is comparable to the feature size [1], and secondly, the presence of additional spin orbit interactions related to in-plane magnetic fields [2]. In this work we theoretically investigate these interference effects, focusing on Quantum interference of the first focusing peak. Due to large pre-factors relatively weak secondary spin orbit interactions can have a significant effect on the magnetic focusing peak, suppressing one spin-split peak, while enhancing the other. From our theoretical analysis, we present some detailed experimental predictions.

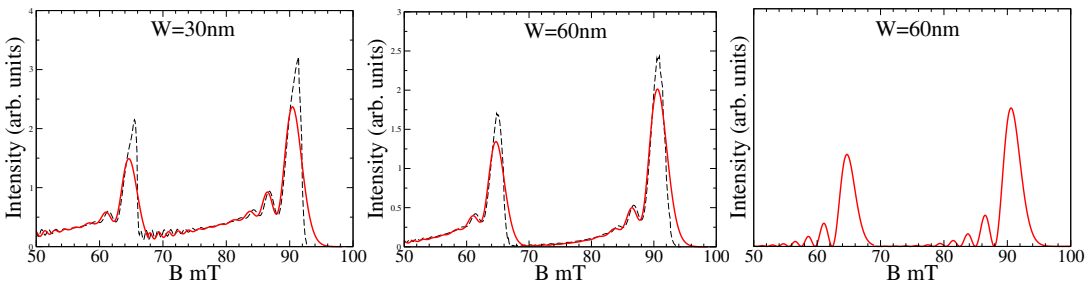

Figure 1: From left to right, interference patterns with quantum point contact (QPC) widths of 30nm, 60nm, and 60nm with fully polarized spin states. The accumulated Berry phase smears the interference pattern for un-polarized QPCs [3].

[1] H. Van Houten, C. W. J. Beenakker, J. G. Williamson, M. E I Broekaart, P. H. M. Van Loosdrecht, B. J. Van Wees, J. E. Mooij, C. T. Foxon, and J. J. Harris, Phys. Rev. B. **39**, 8556 (1989).

[2] S. Bladwell, O.P. Sushkov, Phys. Rev. B. Phys. Rev. B **92**, 235416 (2015)

[3] S. Bladwell, O.P. Sushkov, arxiv:1702.04425, (2017)

Electron correlation effects on bound electron-pair state and screening of a donor impurity center in a two-dimensional electron system

L. Cândido[1], B. G. A. Brito[2], and G.-Q. Hai[3]
[1]*Instituto de Física, Universidade Federal de Goiás, Brazil*
[2]*Departamento de Física, Universidade Federal do Triângulo Mineiro, Brazil*
[3]*Instituto de Física de São Carlos, Universidade de São Paulo, Brazil*

We study the bound state and screening of a donor impurity center of charge $+Ze$ in a two-dimensional (2D) electron layer using the fixed-node diffusion quantum Monte Carlo (DMC) method. The DMC method is quite advantageous than the mean field theory because it is able to present the bound electron states together with the extended free electron states simultaneously.

For Z=1 case at low-electron-density limit, the system reduces to an isolated D^- center with a positive charge center binding two electrons, or equivalently an H^- ion with effective Bohr radius and effective Rydberg. In 3D, the problem of two-electron atom with variable Z has been extensively studied and it can bind two electrons for $Z > Z_c = 0.9110\ldots$. This is a model system to investigate the electron correlations to learn about correlation effects in real physical system. In 2D, the electron correlation is enhanced considerably. This is evident by the binding energy of a 2D H^- which is almost nine times larger than that of 3D. It is no doubt that an impurity center with variable charge Z immersed in a 2D electron gas is an interesting system to investigate strong electron correlation effects as well as correlation induced electron (de)localization in two dimensions. On the other hand, recent progress in dopant engineering and coherent control of dopant states have stimulated theoretical studies on the quantum states of donors localized near a semiconductor interface. In this case, the distance d between the impurity center and the 2D electron layer plays a role in determining the bound electron states.

In our DMC simulations, the electron-impurity and electron-electron pair-correlation functions and the ground-state energy of the system are obtained in a wide range of electron densities (r_s = 1 to 20). For the impurity in the same layer of the electrons, we show that the impurity center with Z=1 can bind two electrons even at high electron density though the binding energy decreases with increasing the electron density in the layer. When the charge Z is reduced, the impurity center losses one of the two bound electrons at about Z=0.7. The electron distribution function around the impurity shows such an electron delocalization process. With decreasing the impurity charge Z, one of the electrons from the strongly correlated electron pair loses to the electron gas around it and leaves behind a one-electron impurity center. We have also simulated the system with the impurity center staying out of the 2D electron layer with a distance d. We show effects of interplay of the charge Z and distance d on the bound states and their delocalization processes.

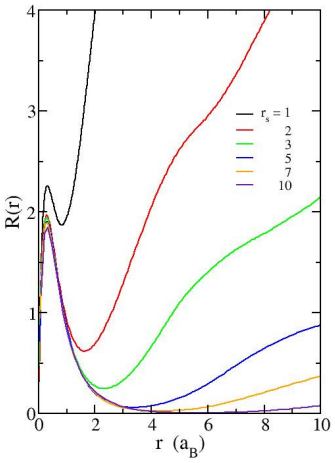

In the figure we show the radial distribution function R(r) of electrons around the impurity center of Z=1 for different r_s values. A well-defined sharp peak at $r \approx 0.2\ a_B$ is found for the two bound electrons. This peak is practically independent of the electron density. The very broadened distribution for larger distance is due to the 2D electron gas around the impurity center.

This work was supported by FAPESP, FAPEG and CNPq.

Magnetotransport in Narrow-Gap Semiconductor Nanostructures

O. Chiatti and J. Boy
Novel Materials Group, Humboldt-Universität zu Berlin, Newtonstr. 15, 12489 Berlin, Germany

C. Heyn and W. Hansen
Epitaxial Nanostructures, Universität Hamburg, 20355 Hamburg, Germany

S. F. Fischer
Novel Materials Group, Humboldt-Universität zu Berlin, Newtonstr. 15, 12489 Berlin, Germany
sfischer@physik.hu-berlin.de

The Shubnikov de-Haas effect and the Quantum Hall effect (QHE) are a powerful tools to investigate the electric transport properties of a two-dimensional electron gas (2DEG). Our experimental work has been directed at the magnetotransport under the influence of in-plane electric fields. We have combined quantum point contacts (QPCs) with in-plane gates and Hall-bars in a narrow-gap semiconductor heterostructure with strong spin-orbit interaction. The investigated structures were fabricated by micro-laser photolithography and wet-chemical etching from an InGaAs/InAlAs quantum well with an InAs-inserted channel [1].

The 2DEG has carrier densities of about $6.7 \cdot 10^{11}$ cm^{-2} and mobilities of $(0.8-1.8) \cdot 10^5$ cm^2/Vs after illumination. We have performed magnetotransport measurements at temperatures down to 250 mK. Hall-bar structures were investigated in tilted magnetic fields up to 10 T. Combined QPC and Hall-bar structures were studied using various symmetric and asymmetric in-plane gate voltages in perpendicular magnetic fields up to 10 T. We examined the effective Lande-factor g^* and the Landau-level broadening Γ. By varying the in-plane gate voltage, we observed the transition from reflection of the quantum Hall edge channels at the constriction to transmission.

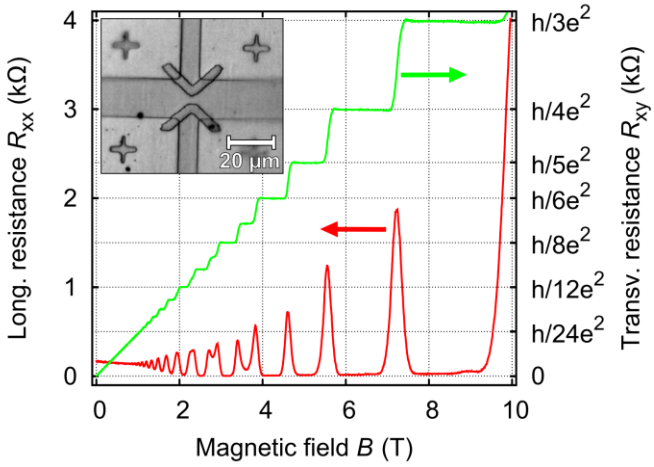

Fig.1 Low-temperature magnetotransport measurements of a Hall-bar, after illumination with an infrared light-emitting diode. The longitudinal resistance R_{xx} and the transversal resistance R_{xy} were measured simultaneously as a function of perpendicular magnetic field B at a bath temperature of 0.3 K. The inset shows a confocal microscopy image of a Hall-bar with constriction. The dark grey areas are the mesa; the two V-shaped marks are the etched trenches that form the constriction of the QPC. From [1].

References

[1] Chiatti *et al.*, Appl. Phys. Lett. **106**, 052102 (2015).

Hybrid superconductor-semiconductor atomic-scale layered $(PbSe)_{1.14}(NbSe_2)_n$ thin films

C. Grosse, M. Trahms, O. Chiatti and S.F. Fischer
Novel Materials Group, Humboldt-Universität zu Berlin, Newtonstr. 15, 12489 Berlin, Germany

A. Mogilatenko
Ferdinand-Braun-Institut, Leibniz-Institut fürHöchstfrequenztechnik, 12489 Berlin, Germany

M. B. Alemayehu, M. Falmbigl, D. C. Johnson,
Dept. of Chemistry,
University of Oregon, Eugene, Oregon 97403, United States

sfischer@physik.hu-berlin.de

Hybrid electronic heterostructure films of semi- and superconducting layers possess very different properties from their bulk counterparts. Here, we investigate the normal-to-superconducting transition in ferecrystals: atomic-scale layered structures of single-, bi- and trilayers of $NbSe_2$ separated by PbSe layers. We have synthesized 2D layered materials of $(PbSe)_{1.14}(NbSe_2)_n$ as turbostratically disordered ferecrystal crystal thin films with n = 1, 2 and 3 using the MER method. The structural (see Fig. 1) and electrical properties have been investigated.

We demonstrate that, despite the structural orientation disorder, superconductivity occurs in these ferecrystals. In general, this opens the possibility of studying emergent phenomena, such as the two-dimensional superconductivity of individual $NbSe_2$ layers, embedded in hybrid heterostructures of specifically designed stacking sequences. The observation of systematic variations in superconductivity in these compounds along with the ability to vary the nanoarchitecture using the MER approach, provides an avenue to further our understanding of the interplay between neighbours in 2D heterostructures.

For example, the use of three component heterostructures of the form ABCB would enable the properties of the C layer to be probed as a function of carrier concentration via modulation doping from A. This type of investigation might also increase our understanding of the effect of substrates on the properties of 2D layers.

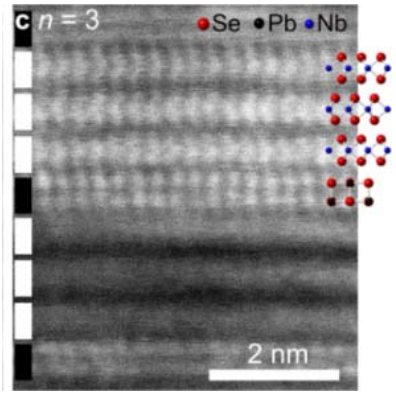

Fig.1 High-resolution cross-sectional HAADF-STEM images of (PbSe)1.14(NbSe2)n with marked NbSe2 monolayer (white bar), PbSe atomic bilayer (black bar) and indication of the atomic columns.. From [1].

References

[1] Grosse *et al.*, Sci. Rep. **6**, 33457 (2016).

Nanoscale thermal imaging of dissipation in quantum systems and graphene

D. Halbertal[1], J. Cuppens[1,2], M. Ben Shalom[3], L. Embon[1], N. Shadmi[4], Y. Anahory[1], HR Naren[1], J. Sarkar[1], A. Uri[1], Y. Ronen[1], Y. Myasoedov[1], L. S. Levitov[5], E. Joselevich[4], A. K. Geim[3] and E. Zeldov[1]

[1]*Department of Condensed Matter Physics, Weizmann Institute of Science, Rehovot, Israel.*
[2]*Catalan Institute of Nanoscience and Nanotechnology (ICN2), CSIC and the Barcelona Institute of Science and Technology, Campus UAB, Bellaterra, 08193 Barcelona, Spain.*
[3]*National Graphene Institute, The University of Manchester, Booth St. E, Manchester M13 9PL, UK and the School of Physics and Astronomy, The University of Manchester, Manchester M13 9PL, UK.*
[4]*Department of Materials and Interfaces, Weizmann Institute of Science, Rehovot 7610001, Israel.*
[5]*Department of Physics, Massachusetts Institute of Technology, Cambridge, Massachusetts, USA.*
dorri.halbertal@weizmann.ac.il

Energy dissipation is a fundamental process governing the dynamics of physical systems. In condensed matter physics, in particular, many processes of interest are deeply rooted in the intricate details of how and where the dissipation occurs. Despite its vital importance, direct imaging of dissipation in quantum systems is currently impossible because the existing thermal imaging methods lack the necessary sensitivity and are unsuitable for low temperature operation.

We developed a nanoSQUID with sub 50 nm diameter that resides at the apex of a sharp pipette [1] that acts as scanning nano-thermometer providing cryogenic thermal imaging with four orders of magnitude improved thermal sensitivity of below 1 μK/Hz$^{1/2}$ [2]. The device scans out of contact and its unique thermal properties allow a non-invasive thermal imaging of very low nanoscale energy dissipation down to the fundamental Landauer limit of 40 fW for continuous readout of a single qubit at 1 GHz at 4.2 K. These advances enable observation of changes in dissipation due to single electron charging of individual quantum dots in carbon nanotubes. We utilized the technique to study dissipation in hBN encapsulated graphene and revealed a fascinating dissipation mechanism due to resonant localized states at the edges of graphene providing the first visualization of inelastic electron scattering mechanism on the nanoscale, opening the door to direct imaging of microscopic dissipation processes in quantum matter.

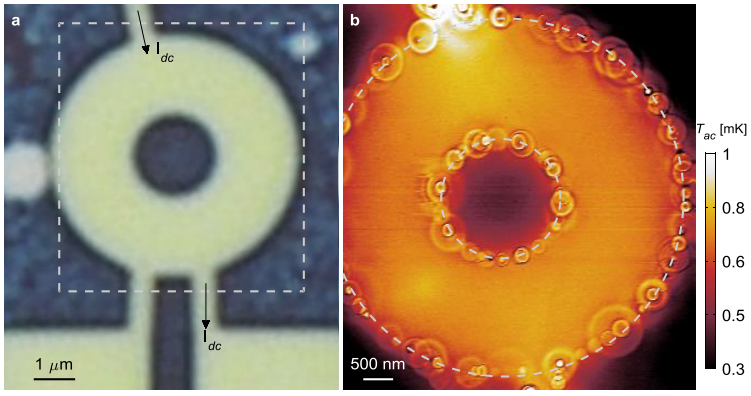

(a) Optical image of hBN/graphene/hBN structure patterned into a washer shape (bright). (b) Thermal image of the outlined area in (a) in presence of $I_{dc} = 6$ μA at 4.2 K. The necklace of rings reveals the presence of resonant states along the edges of graphene that serve as local centers of energy dissipation.

References

[1] D. Vasyukov, Y. Anahory, L. Embon, D. Halbertal, J. Cuppens, L. Neeman, A. Finkler, Y. Segev, Y. Myasoedov, M. L. Rappaport, M. E. Huber, and E. Zeldov, Nature Nanotech. **8**, 639 (2013).
[2] D. Halbertal, J. Cuppens, M. Ben Shalom, L. Embon, N. Shadmi, Y. Anahory, H. R. Naren, J. Sarkar, A. Uri, Y. Ronen, Y. Myasoedov, L. S. Levitov, E. Joselevich, A. K. Geim, and E. Zeldov, Nature **539**, 407 (2016).

Electrostatically Induced Quantum Point Contact in Bilayer Graphene

Hiske Overweg[1], Hannah Eggimann[1], Marius Eich[1], Pauline Simonet[1], Riccardo Pisoni[1], Yongjin Lee[1], Kenji Watanabe[2], Takashi Taniguchi[2], Thomas Ihn[1], Klaus Ensslin[1]

[1]*Laboratory for Solid State Physics, ETH Zürich,*
Otto-Stern-Weg 1, 8093 Zürich, Switzerland
[2]*National Institute for Material Science*
1-1 Namiki, Tsukuba 305-0044, Japan
overwegh@phys.ethz.ch

We report on the observation of six quantized conductance plateaus in a one-dimensional channel induced in bilayer graphene. The employed device geometry allows for a complete pinch-off of the one-dimensional channel. Whereas previous works [1,2,3] show a maximal resistance on the order of the resistance quantum, we can achieve a resistance of R ~ 10 MΩ at T = 1.7 K, and even R ~ 10 GΩ at T = 0.13 K. Tunnel barriers with resistances of this order of magnitude are a promising step towards the realization of electrostatically defined quantum dots in bilayer graphene.

The device, shown in Fig. 1a, consists of a bilayer graphene flake encapsulated in hexagonal boron nitride by the van der Waals stacking technique. A graphite flake serves as a global back gate and two metal split gates (SG) are positioned on top of the device. To tune the electron density in the channel defined by the split gates an extra gate (CH) is situated on top of the split gates, with a dielectric layer of Al_2O_3 in between.

Temperature dependent measurements of the resistance show that by carefully tuning all gate voltages, a band gap of 47 meV can be induced underneath the split gates and the channel gate. By varying the channel gate voltage and keeping the other gate voltages unchanged, a finite charge carrier density can be induced in the 100 nm wide channel between the split gates. The conductance as a function of the channel gate voltage is shown in Figure 1b and is consistent with transport of quantized modes through a one-dimensional channel. Unexpectedly, we find a step size of 2 e^2/h and we do not observe any quantization below G = 8 e^2/h.

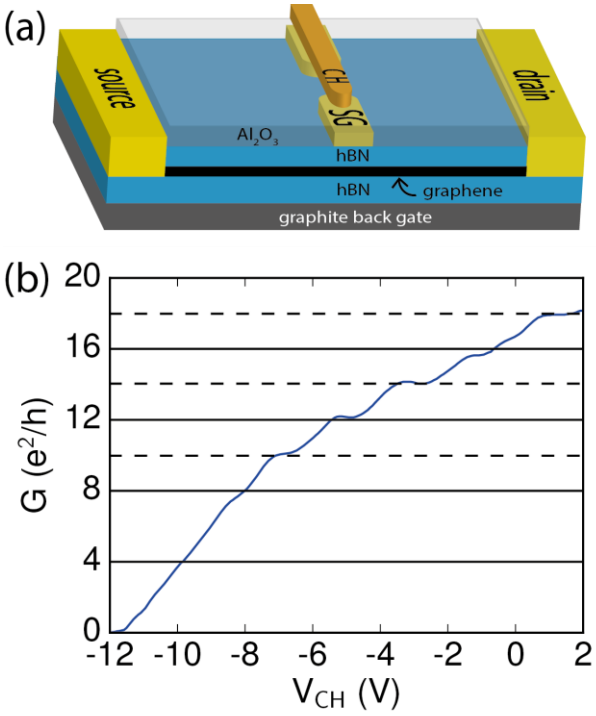

Fig.1 (a) Device layout of the bilayer graphene quantum point contact. (b) Conductance as a function of the channel gate voltage

References

[1] M. T. Allen et al., Nature Communications **3**, 934 (2012)

[2] A. S. M. Goossens et al., Nano Letters **12**, 4656–60 (2012)

[3] S. Dröscher et al., New Journal of Physics **14**, 103007 (2012)

Large contact noise in graphene field-effect transistors

Paritosh Karnatak[1], T. Phanindra Sai[1], Srijit Goswami[1], Subhamoy Ghatak[1], Sanjeev Kaushal[2] and Arindam Ghosh[1]

[1]*Department of Physics, Indian Institute of Science, Bangalore 560 012, India.*
[2]*Tokyo Electron Ltd., Akasaka Biz Tower, 3-1 Akasaka 5-Chome, Minato-ku, Tokyo 107-6325, Japan.*
paritosh@physics.iisc.ernet.in

Intrinsic time-dependent fluctuation in the electrical resistance at the graphene-metal interface, or the contact noise, adversely affects the performance of graphene field effect transistors but remains largely unexplored.

We have investigated contact noise in graphene field effect transistors of varying device geometry and contact configuration, with channel carrier mobility ranging from 5,000 $cm^2V^{-1}s^{-1}$ to 80,000 $cm^2V^{-1}s^{-1}$. Using a phenomenological model for contact noise due to current crowding for two dimensional conductors, we show that the contacts dominate the measured resistance noise in all graphene field effect transistors when measured in the two-probe or invasive four probe configurations, and surprisingly, also in nearly noninvasive four probe (Hall bar) configuration in the high mobility devices. We identify the fluctuating electrostatic environment of the metal-channel interface as the major source of contact noise, which could be generic to two dimensional material-based electronic devices.

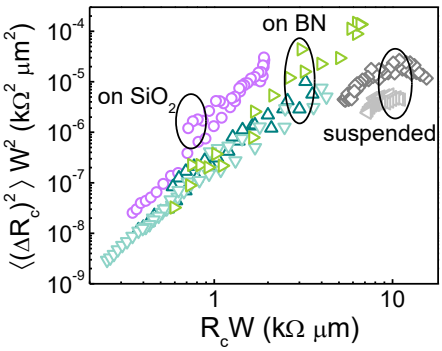

Fig.1 Contact noise follows a universal scaling with the contact resistance and the magnitude depends only on the substrate.

References

[1] Karnatak, P., Sai, T.P., Goswami, S., Ghatak, S., Kaushal, S. and Ghosh, A., Nat. Commun. **7,** 13703 (2016).

Performance Oriented Graphene Nanoribbon Tunnel Field Effect Transistor Design Strategy

Yawei Lv, Qijun Huang, Sheng Chang, Hao Wang and Jin He
School of Physics and Technology, Wuhan University,
Wuhan, 430072, China
changsheng@whu.edu.cn

Graphene nanoribbon (GNR) is suitable for tunnel field effect transistor (TFET) application because of its small carrier effective mass [1] and tunable energy gap (E_g) [2]. Due to the uniqueness of GNR, TFET design based on it can be varied according to different application requirements such as on state current (I_{on}), off state current (I_{off}) and supply voltage. For examples, if a large I_{on} is required, a small E_g GNR can be used, whereas a large E_g GNR is suitable for small I_{off} requirement. For stricter TFET performance indexes, GNR heterojunction structures can afford. In this paper, the GNR TFET design strategy shown in Fig. 1 is discussed. The investigations are based on tight binding (TB) Hamiltonian and nonequilibrium Green's function (NEGF) method. Energy band structure construction and modulation is the key factor between performance index and TFET structure as shown in Fig. 2. The essence of performance oriented GNR TFET design is the transport mechanism analyses, which can be revealed by local density of states (LDOS), energy band diagrams and current spectrums. Based on the mechanisms, the design strategy can be obtained.

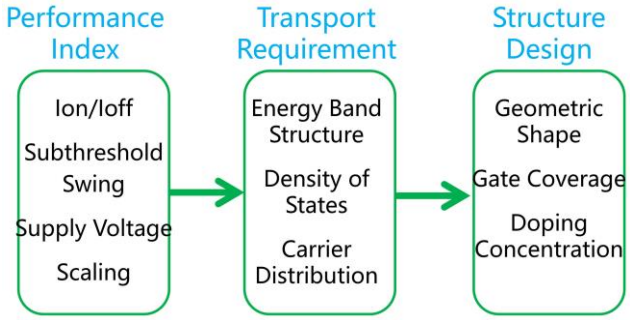

Fig.1 Section scheme of the GNR TFET design.

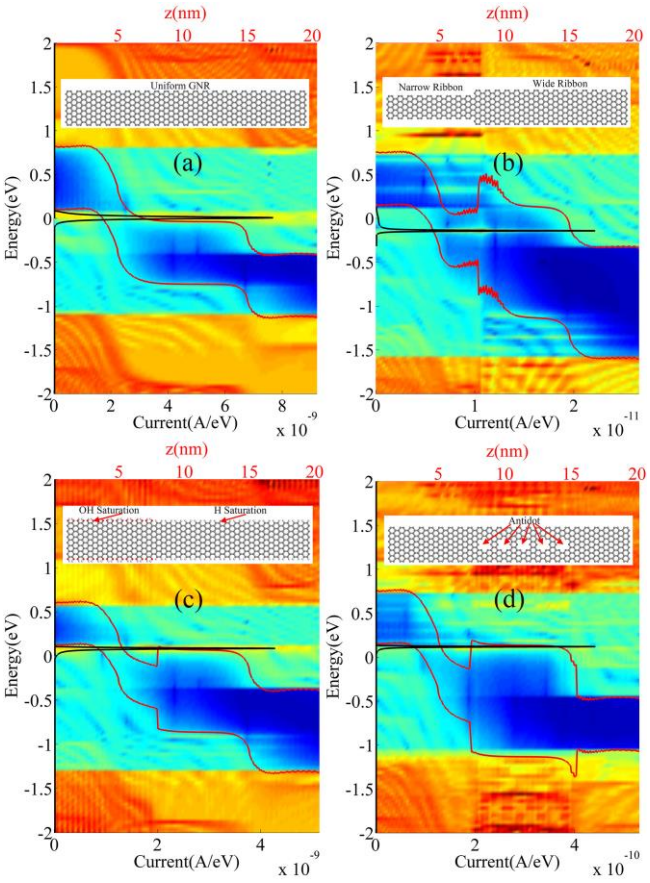

Fig.2 GNR structures and TFET transport mechanism analyses.

References

[1] Y. Lv, S. Chang, Q. Huang, H. Wang, and J. He, Sci. Rep. **6**, 38009 (2016).

[2] Y. Lv, Q. Huang, S. Chang, H. Wang, and J. He, IEEE Trans. Electron Devices **63**, 4514 (2016).

Electronic Transport in Macroscopic-length Nanoribbons with Fano Defects

Carlos Ramírez
Departamento de Física, Facultad de Ciencias, Universidad Nacional Autónoma de México, Apartado Postal 70-542, 04510 Ciudad de México, México
carlos@ciencias.unam.mx

The conductance is one of the most important properties of a material, which is also very susceptible to quantum effects caused by miniaturization. Theoretically, it can be studied by means of its transmission function, according to the Landauer formalism [1,2]. Recently, we have developed a new efficient method to calculate the scattering matrix of arbitrary systems modeled by tight-binding Hamiltonians [3], which determine such transmission function. This method allows iterative calculation of the scattering matrix of a system in terms of the scattering matrices of their components. In this work, we use this method to study the electronic transport of macroscopic-length nanoribbons with Fano defects. These defects are structures attached to sites in the Nanorribon, such as atomic chains. Cases with defects located in periodic and aperiodic sequences in square-lattice and graphene-like nanoribbons are considered. Finally, transport properties in nanoribbons with variations in its transversal-width are analyzed.

This work has been supported by UNAM-DGAPA-PAPIIT IA106617. Computations were performed at Miztli under project LANCAD-UNAM-DGTIC-329.

References

[1] Y. Imry and R. Landauer, Rev. Mod. Phys. **71**, S306 (1999).
[2] D.A. Ryndyk, Theory of Quantum Transport at Nanoscale, Springer, New York (2016).
[3] C. Ramírez and L.A. Medina-Amayo, Ann. Phys. (2017). DOI: 10.1016/j.aop.2017.01.015

Tunable pseudo-Zeeman effect in graphene

A. Georgi[1], P. Nemes-Incze[1, †], R. Carrillo-Bastos[2, 8], D. Faria[5, 9], S. Viola Kusminskiy[3, 6], D. Zhai[8], M. Schneider[3], D. Subramaniam[1], T. Mashoff[4], N. M. Freitag[1], M. Liebmann[1], M. Pratzer[1], L. Wirtz[7], C. R. Woods[10], R. V. Gorbachev[10], Y. C.[10], K. S. Novoselov[10], N. Sandler[8], and M. Morgenstern[1]

[1]II.Institute of Physics B and JARA-FIT, RWTH Aachen University, Aachen, Germany. [2]Facultad de Ciencias, UABC, Ensenada, Baja California, Mexico. [3]Dahlem Center for Complex Quantum Systems and Institut fur Theoretische Physik, Freie Universitat, Berlin, Germany. [4]Institut fur Physik, Johannes Gutenberg-Universitat, Mainz, Germany. [5]Instituto de Fisica, Universidade Federal Fluminense, Niteroi, Rio de Janeiro, Brazil. [6] Institute for Theoretical Physics II, University of Erlangen-Nuremberg, Erlangen, Germany. [7]Physics and Materials Science Research Unit, University of Luxembourg, Luxembourg. [8]Dept. of Physics and Astronomy, and NQPI, Ohio University, Athens, Ohio, USA. [9]Instituto Politecnico, UERJ, Manchester United Kingdom. [†] on leave from MFA-EK, Centre for Energy Research, Budapest, Hungary.

Mechanical strain influences dramatically the distribution and dynamics of charge carriers in graphene, as elegantly described by the concept of a pseudo-magnetic field. In addition to the Landau quantization, already observed experimentally[1], the pseudofield introduces a Zeeman term, breaking the underlying chiral symmetry of the honeycomb lattice. In analogy with the spin alignment of an electron in a magnetic field, the pseudo-spin of graphene, can be oriented by a pseudo-magnetic field through this Zeeman term. The pseudo-spin polarization can be revealed as a sublattice symmetry breaking that can be tuned by appropriate straining of the membrane. Using the tip of a scanning tunneling microscope to produce controlled deformations, we demonstrate that it is possible to achieve redistributions of the local density of states of up to 30% between the two sublattices [1]. The observed pseudo-spin polarization scales with the lifting height of the strained deformation and is quantitatively reproduced by analytic models in the lattice (tight-binding) and the continuum (Dirac equation). These results add a key ingredient to the celebrated analogy of graphene charge carriers to ultra-relativistic Dirac fermions. Furthermore, the deduced fields of about 1000T could provide an effective THz valley filter, a basic element of valleytronic devices.

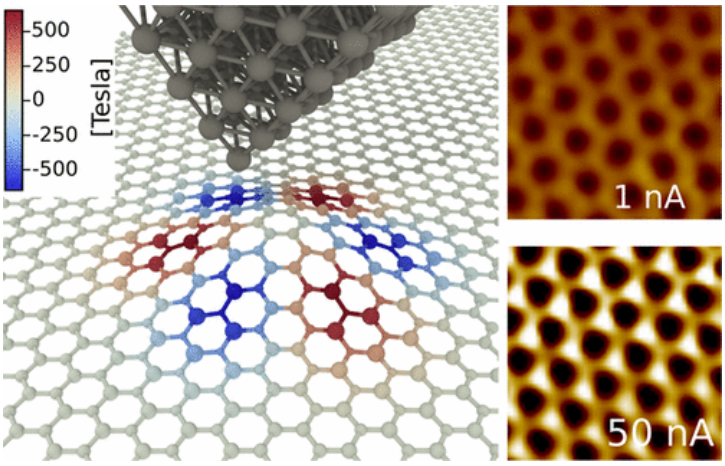

Fig. 1 Mechanical deformation induced by the STM tip on a graphene membrane on SiO_2. The pseudomagnetic field induced by the deformation becomes visible as a sublattice symmetry breaking on the STM images.

References

[1] Levy, N. et al. Science 329 (2010).

[2] Georgi at al. Nano Letters Article ASAP Feb 17, 2017 (Web)

Electrical and Scanning Photocurrent Studies on Multilayer $MoTe_2/SnS_2$ Heterostructure Tunnel Field Effect Transistors

K. C. Lee[1], Z. W. Lin[2], Y. S. Lu[1], L. C. Li[3], Y. F. Lin[1], T. S. Lim[4], and Y. W. Suen*[1,2]

[1]*Department of Physics, National Chung Hsing University, Taichung, Taiwan*

[2]*Institute of Nanoscience and Nanotechnology, National Chung Hsing University, Taichung, Taiwan*

[3]*Center for Nano Science and Technology, National Chiao Tung University, Hsinchu, Taiwan*

[4]*Department of Applied Physics, Tunghai University, Taichung, Taiwan.*

*ysuen@phys.nchu.edu.tw

We report the fabrication and electrical properties of tunnel field effect transistors (TFETs) based on multilayer Van der Waals $MoTe_2/SnS_2$ heterojunctions proposed by Szabó et al [1]. The dry transfer method was used to stack a $MoTe_2$ flake picked up by a PDMS stamp onto a SnS_2 flake placed on a Si substrate covered by a 285 nm thick SiO_2 film. Both layered materials were obtained by mechanical exfoliation method. The 20/80 nm Ti/Au electrodes were defined by e-beam lithography. The multilayer SnS_2 is n type for most of the back gate biases, while $MoTe_2$ is bipolar [2].

The TFET device exhibits an ON/OFF ratio over 10^4 at V_{DS} ~ 1V. The subthreshold swing (SS) obtained from the I_{DS}-V_{GS} transfer curve at V_{DS} ~ 0.5V is about 1.25 V/dec, which is equivalent to about 44 mV/dec if the dielectric is scaled down to 10 nm EOT from 285 nm. This equivalent SS is smaller than the 60 mV/dec limit for conventional thermionic devices and manifests the onset of the tunnelling current. The temperature (T) dependence of log(I_{DS}) vs V_{DS} curve in the tunnelling current dominant regime does not exhibit a diffusion transport like behaviour; instead, its linear part gives a less T sensitive slope.

We investigate the photocurrent distribution near the heterojunction by scanning a focused 1-uW 633-nm laser beam with a spot size of about 1.5 μm. The induced photocurrent is most pronounced near the boundary between $MoTe_2/SnS_2$ heterojunction and $MoTe_2$ with the direction towards SnS_2 (drain). This result is consistent with a type II or type III band alignment of $MoTe_2/SnS_2$, which can be controlled by the back gate. The band diagram will be further discussed in our report.

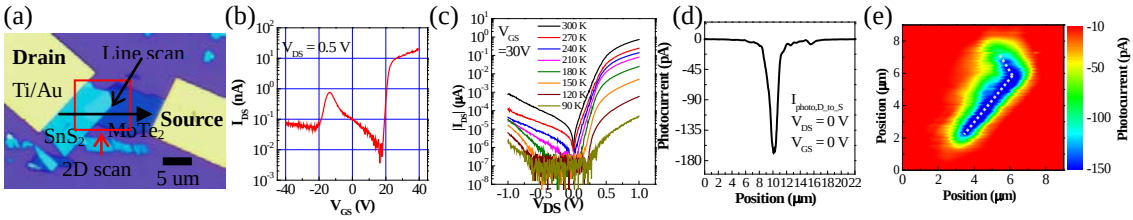

Fig. 1 (a) OM micrograph of the TFET device; (b) I_{DS} vs V_{GS} at V_{DS}=0.5V; (c) I_{DS} vs V_{DS} at V_{GS}=30V at various Temperatures; (d)(e) line scan and 2D mapping of scanning photocurrent microscopy data at V_{GS} = V_{DS}=0V.

[1] Á. Szabó, S. J. Koester, and M. Luisier, IEEE Electron Device Lett. **36** (5), 514 (2015)

[2] Y.F. Lin, Y. Xu, C. Y. Lin, Y.W. Suen, M. Yamamoto, S. Nakaharai, K. Ueno, and K. Tsukagoshi, *Advanced Materials* **27** (42), 6612 (2015).

Strain engineering in InAs/GaSa double quantum well systems

Lars Tiemann[1,*], Susanne Mueller[1], Quansheng Wu[2], Thomas Tschirky[1], Klaus Ensslin[1], Werner Wegscheider[1], Matthias Troyer[2], Alexey A. Soluyanov[2,3], Thomas Ihn[1]
[1]*Solid State Physics Laboratory, ETH Zurich, 8093 Zurich, Switzerland*
[2]*Theoretical Physics and Station Q Zurich, ETH Zurich, 8093 Zurich, Switzerland*
[3]*Department of Physics, St. Petersburg University, St. Petersburg, 199034, Russia*
*Lars.Tiemann@physik.uni-hamburg.de

A heterojunction consisting of an InAs quantum well that confines 2D electrons and a GaSb quantum well that confines 2D holes can show a variety of fascinating quantum effects, such as quantum Hall effects, electron-hole correlations and a quantum spin Hall insulator (QSHI) phase [1]. For the QSHI phase to emerge in InAs/GaSb systems, the corresponding quantum well widths need to be fine-tuned, in such a manner that the lowest electron energy subband in the InAs quantum well energetically drops below the lowest hole subband in the GaSb quantum well. The electronic band structure in *k*-space will then exhibit a mini band gap so that topological spin-resolved channels can form near the sample boundaries. Experimentally, however, it is often found that the mini band gap is not well-developed, which is signaled by semimetallicity around the charge neutrality point [2], i.e., where the system crosses over between electron and hole conduction.

We will present an experimental and theoretical study that outlines the impact of strain on the electronic properties of the InAs/GaSb material system [5]. In contrast to related recent works [3,4], which studied the impact of *constant* strain resulting from the pseudomorphic growth on a series of samples, we utilize samples mounted to piezoelectric elements to study *strain as a variable parameter*. We observe two distinct effects: (1) a susceptibility of the resistance around the charge neutrality point to strain, and (2) a dependence on the charge carrier density on the (crystal) direction of the strain. Both effects are indicative of modulations of the electronic band structure. To understand the details of these band structure modulations, we have performed complementary numerical band structure simulations for strained and unstrained quantum wells using symmetrized Wannier-based tight-binding (TB) models. Comparing the theoretical results with our experimental data allows us to present a consistent picture of the impact of strain and how strain engineering can be exploited in this material system.

References

[1] C. Liu, T. L. Hughes, X.-L. Qi, K. Wang, and S.-C. Zhang, Phys. Rev. Lett. **100**, 236601 (2008)
[2] for example: I. Knez *et al.*, Phys. Rev. B **81**, 201301 (2010); K. Suzuki *et al.*, Phys. Rev. B **87**, 235311 (2013); C. Charpentier *at al.*, Appl. Phys. Lett. **103,** 112102 (2013)
[3] T. Akihoa, F. Couëdoa, H. Irie, K. Suzuki, K. Onomitsu, and K. Muraki, Appl. Phys. Lett. **109**, 192105 (2016).
[4] L. Du, T. Li, W. Lou, X. Wu, X. Liu, Z. Han, C. Zhang, G. Sullivan, A. Ikhlassi, K. Chang, R.-R. Du, arXiv:1608.06588 (2016).
[5] L. Tiemann, S. Mueller, Q. Wu, T. Tschirky, K. Ensslin, W. Wegscheider, M. Troyer, A. A. Soluyanov, T. Ihn, arXiv:1610.06776 (2016).

Visualize hot electrons in two-dimensional devices at steady state

Qianchun Weng[1,2], Susumu Komiyama[3], Le Yang[4], Zhenghua An[4], Yusuke Kajihara[1], and Wei Lu[2]

[1]*Institute of Industrial Science, The University of Tokyo, Komaba 4-6-1, Meguro-ku, Tokyo, 153-8505, Japan*

[2]*National Laboratory for Infrared Physics, Shanghai Institute of Technical Physics, the Chinese Academy of Sciences, Shanghai 200083, PR China*

[3]*Department of Basic Science, The University of Tokyo, Komaba 3-8-1, Meguro-ku, Tokyo, 153-8902, Japan*

[4]*Department of Physics, Fudan University, Shanghai 200433, PR China*

qcweng@iis.u-tokyo.ac.jp

Hot electrons can be easily generated in two-dimensional systems when driven out of equilibrium. To understand the hot electron transport and related energy flow in operating devices are of fundamental importance. However, to experimentally study the nanoscale hot electron distribution is not an easy task, especially when the device is operated in steady-state. Current induced excess noise has been demonstrated to be a unique probe for hot electron kinetics, but existing studies are limited to time-resolved noise measurement and no spatial information can be obtained.

Here, we demonstrate a new experimental technique which can directly visualize hot electron distributions in real-space when the device is steadily operated. It is a home-made terahertz near-field microscope, [1] which is so sensitive to detect fluctuating evanescent fields generated by local current fluctuations (Fig. 1). A sharp tungsten tip is used to locally scatter the evanescent fields into terahertz radiation, which can be detected by an ultra-highly sensitive detector, called charge sensitive infrared phototransistor (CSIP), [2] placed in the far-field.

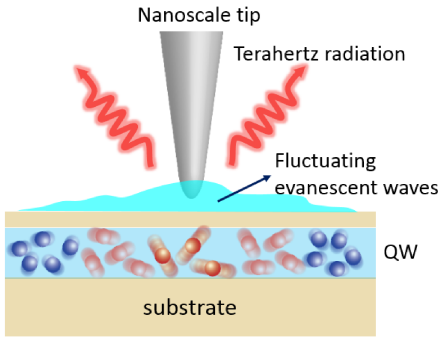

Fig.1. Terahertz nanoscopy for local hot electron dynamics.

We perform the study on a GaAs/AlGaAs quantum well (QW) device with the two-dimensional electron gas (2 DEG) buried 13 nm below the surface. The device was fabricated to the nanoscale by electron-beam lithography and wet-etching. High electric-field is therefore generated in the nano-constriction under constant applied voltage, where hot electrons can be excited. For the first time, we directly imaged the hot electron generation and nanoscale energy dissipation within the device. Our experimental technique should be a powerful tool for studying nonequilibrium dynamics down to the nanoscale.

References

[1] Y. Kajihara, *et al*. *Rev. Sci. Instrum*. **81**, 033706 (2010).

[2] S. Komiyama. *IEEE J. Sel. Top. Quantum Electron*. **17**, 54-66 (2011).

Puddle-Induced Resistance Oscillations in the Breakdown of the Graphene Quantum Hall Effect

M. Yang,[1] O. Couturaud,[2] W. Desrat,[2] C. Consejo,[2] D. Kazazis,[3,4] R. Yakimova,[5] M. Syväjärvi,[5] M. Goiran,[1] J. Béard,[1] P. Frings,[1] M. Pierre,[1] A. Cresti,[6,7] W. Escoffier,[1] and B. Jouault[2]

[1]*Laboratoire National des Champs Magnétiques Intenses, EMFL-LNCMI, INSA, UPS, CNRS UPR 3228, Université de Toulouse, 143 avenue de Rangueil, 31400 Toulouse, France*

[2]*Laboratoire Charles Coulomb (L2C), UMR 5221 CNRS-Université de Montpellier, 34095 Montpellier, France*

[3]*Centre de Nanosciences et de Nanotechnologies, CNRS, Université Paris-Sud, Université Paris-Saclay, C2N Marcoussis, 91460 Marcoussis, France*

[4]*Laboratory for Micro and Nanotechnology, Paul Scherrer Institute, 5232 Villigen-PSI, Switzerland*

[5]*Department of Physics, Chemistry and Biology, Linköping University, SE-58183 Linköping, Sweden*

[6]*Université Grenoble Alpes, IMEP-LAHC, F-38000 Grenoble, France*

[7]*CNRS, IMEP-LAHC, F-38000 Grenoble, France*

ming.yang@lncmi.cnrs.fr

We report on the stability of the quantum Hall plateau in very large Hall bars (100 μm width) made from a chemically gated graphene film grown on SiC substrate [1]. In the Quantum Hall regime, the quantized plateau of the Hall resistance at h/2e ²appears from B≃ 5T and persists up to B≃ 80 T (figure a). At high current density, the longitudinal resistance displays small and periodic oscillations (figure 1-b) when plotted versus 1/B, with zero phase extrapolation for infinite magnetic field. The extracted carrier density is consistent with as-grown graphene on SiC, e.g. without the chemical gate. We relate the longitudinal resistance oscillations to the presence of inhomogeneous doping across the sample where patches of pristine (e.g. non-gate) graphene are present. Numerical simulations, based on a charge transfer between the SiC substrate[2, 3], the gated graphene layer and the patches of ungated graphene, reproduce well the experimental data and indicate that the patches covers up to 30% of the total sample's surface. These in-plane inhomogeneities, in the form of high carrier density graphene pockets, modulate the quantum Hall effect breakdown and decrease the breakdown current. The model also suggests a linear evolution of the carrier density as the magnetic field is increased, thus stabilizing the quantum Hall regime at filling factor of 2 for a broad magnetic field range.

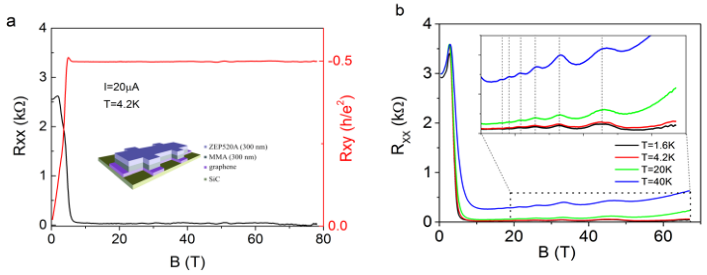

Fig. (a) Simultaneous measurement of $R_{xx}(B)$ and $R_{xy}(B)$ under high magnetic field up to 80T. (b) Clear additional 1/B-periodic SdH oscillations can be seen in $R_{xx}(B)$ in the quantum Hall regime.

References

[1] M. Yang et al. Phys. Rev. Lett. **117,** 237702 (2016).

[2] S. Kopylov et al. Appl. Phys. Lett. **97,** 112109 (2010).

[3] T. J. B. M. Janssen et al. Phys. Rev. B **83,** 233402 (2011).

Confinement and Transmission in Graphene Quantum Wires Formed by Strain

D. Zhai,[1] Y. Wu,[2] C. Pan,[2] B. Cheng,[2] T. Taniguchi,[3] K. Watanabe,[3] N. Sandler,[1,†] and M. Bockrath[2,‡]
[1]*Department of Physics and Astronomy, Ohio University, Athens, Ohio 45701, USA*
[2]*Department of Physics and Astronomy, University of California, Riverside, California 92521, USA*
[3]*Advanced Materials Laboratory, National Institute for Materials Science, Tsukuba, Ibaraki 305-0044, Japan*
[†]sandler@ohio.edu; [‡]marcbock@ucr.edu

The effects of strain on the electronic and transport properties of graphene have triggered intensive theoretical investigations, which showed that graphene valley filters might be achieved by strain engineering. However, little experimental progress has been made in implementing these ideas. Here, we report transport studies of graphene on top of hexagonal boron nitride, with out-of-plane strained folds. Differential conductance measurements across the linear strained region reveal distinct transport regimes as the gate voltage is changed. In some samples, Coulomb blockade diamonds -characteristic of quantum dot behavior- are observed, while others show Fabry-Perot interferences with higher transmission. The data is consistent with results from a Dirac model including pseudo-magnetic fields produced by a strained Gaussian fold. Theoretical results for the dependence of transport properties on the geometric parameters of the fold, as well as on the incident energy and angle of carriers, for both types of samples are presented. These devices constitute the first step towards a practical realization of valley filters with graphene. Further implications for valley polarization properties of transmitted currents are discussed.

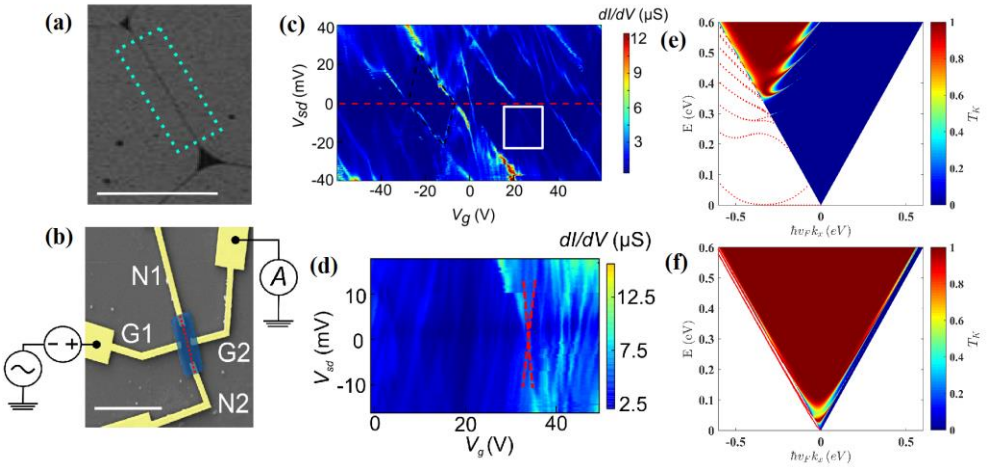

Fig. 1 SEM images of (a) linear strained region and (b) transport measurement setup with the red dotted line denoting the strained region. Transport measurement of dI/dV vs source-drain voltage (V_{sd}) and gate voltage (V_g) shows either (c) Coulomb blockade diamonds or (d) Fabry-Perot interferences. Theoretical results for a Gaussian fold deformation along (e) zigzag direction or (f) 1º away from armchair direction. The contour plots show the transmission spectra, while the red dots represent the quantum wire bound states.

Molecular Attachment to MoS_2 is Facilitated by Nb Doping

Boyang Zheng, Youjian Tang, and Vincent H. Crespi
Physics Department, Penn State University,
University Park, PA 16803, USA
boyang@psu.edu yzt102@psu.edu vhc2@psu.edu

Moderate band gaps and inversion symmetry breaking make transition metal dichalcogenides (TMD) promising materials for spintronics and valleytronics [1,2]. We explore the possibility to further engineer the electronic band structure of TMDs through the rational design of molecules with desired electronic structure that are then covalently attached to a TMD layer to yield strongly hybridized joint molecule/layer bands. The doping of Nb into MoS_2 single layer can effectively stabilize the functionalized layer by compensating for the band filling associated with the extra covalent bond from the attached molecule, even for attachment sites several lattice constants away from the location of the Nb. By tuning the molecular orbitals of the attached molecule, we find systems in which the first and/or second conduction bands of the combined system strongly hybridize the molecular and layer states. The resulting strong energy dependence to the character of these conduction band states could have substantial impact on the electronic, optical, and transport properties of the combined system.

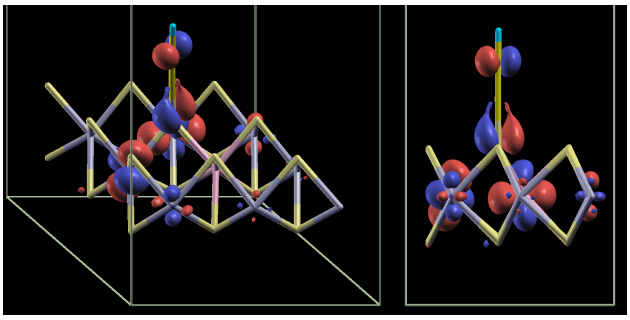

Fig. 1: A conduction band state which strongly couples the layer and the attached molecule.

References

[1] J. R. Schaibley, H. Yu, G. Clark, P. Rivera, J. S. Ross, K. L. Seyler, W. Yao, and X. Xu, Nat. Rev. Mater. **1**, 16055 (2016).

[2] D. Xiao, G.-B. Liu, W. Feng, X. Xu, and W. Yao, Phys. Rev. Lett. **108**, 196802 (2012).

Strained fold-assisted transport in graphene systems

R. Carrillo-Bastos[‡], C. León[§], D. Faria[*], A. Latge[§], E. Y. Andrei[**] and N. Sandler[***]

[‡]*Fac. de Ciencias, Univ. Autónoma de Baja California, Ensenada, Baja California, México*

[§]*Instituto de Física, Universidade Federal Fluminense, Niteroi, Rio de Janeiro, Brazil.*

[*]*Inst. Politécnico do Rio de Janeiro, Univ. do Estado de R. de Janeiro, Nova Friburgo, Brazil.*

[**]*Department of Physics and Astronomy, Rutgers University, Piscataway, New Jersey, USA*

[***]*Department of Physics and Astronomy and Nanoscale and Quantum Phenomena Institute, Ohio University, Athens, Ohio, USA*

Deformations in graphene systems are central elements in the field of *straintronics*. Various geometries have been proposed [1], but there have been limited successes in their experimental realization. Because folds occur naturally in graphene samples, or could be engineered with appropriate substrates, we study their effects on transport properties. Using a combination of tight-binding, Green's function and band structure calculations we characterize the effects of a Gaussian fold (amplitude A and width b) that extends along the zigzag direction of a graphene ribbon. The deformation, introduced within elasticity theory, is described in terms of the strain ε and the corresponding pseudo-magnetic fields B_{pm}. We show that the local density of states (LDOS) exhibits enhanced values along the fold region due to the localization of higher energy states. These states exhibit sublattice symmetry breaking, as expected [2], and are valley polarized resulting in extra ballistic channels at lower energies. The local valley polarization at zero magnetic field results from the breaking of inversion symmetry, and gives a topological protection to the newly formed channels. These properties persist for other fold orientations with those along the zigzag direction providing optimal valley filtering properties. We confirm that these results persist in the presence of strong edge disorder, showing that folds are ideal candidates for electronic waveguides [3]. These findings may provide an explanation for experimental reports on ballistic transport in graphene ribbons [4].

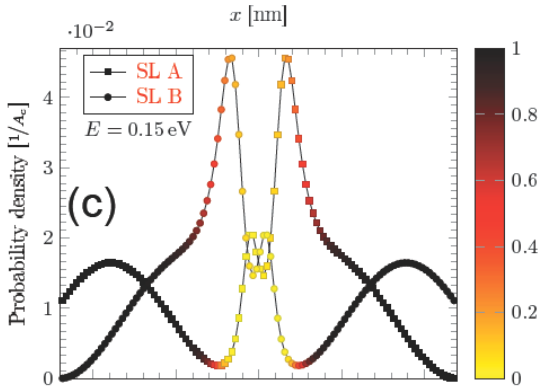

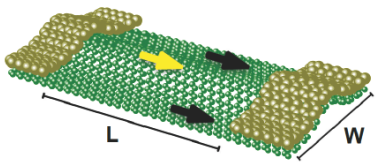

Fig. 1. DOS (left) for graphene with a with Gaussian fold (right), for states with same velocity. Color scale refers to the location of states in band structure: yellow refers to states near Dirac point K and black to states near K'.

References

[1] F. Guinea, M. Katsnelson and A. Geim, Nature Physics **6**, 30 (2009).

[2] R. Carrillo-Bastos, et al, Phys. Rev. B **90**, 041411(R) (2014).

[3] R. Carrillo-Bastos, et al, Phys. Rev. B **94**, 125422 (2016).

[4] J. Baringhaus, et al. Nature **506**, 349 (2014).

Atomic Layers for Piezoelectric Biosensing

Ananda Ewing-Boyd,[1)] Albert Seo,[2)] Sheng Yu,[1)] Quinton Rice,[1)] Tikaram Neupane,[1)]
Qiliang Li,[3)] Felix Seo,[1),*] and Bagher Tabibi,[1),*]

[1)] *Advanced Center for Laser Science and Spectroscopy, Center for Atmospheric Research and Education, Department of Physics, Hampton University, Hampton Virginia 23668*

[2)] *Department of Biomedical Engineering, Virginia Commonwealth University, Richmond, VA 23284*

[3)] *Department of Electrical and Computer Engineering, George Mason University, Fairfax, VA 22030*

*jaetae.seo@hamptonu.edu, bagher.tabibi@hamptonu.edu

Piezoelectricity is a mechano-electric effect which produces electricity in response to mechanical compression, tensile stress, shear, etc. The origin of piezoelectricity is due to the polarization change at the ground electronic state which includes ionic, electronic, dipole, space charge, or interfacial polarizations. Recently, two-dimensional atomic layers are of great interest for piezoelectricity due to their extreme sensitivity to atomic shift or strain, reduced number of neighboring ions, and large surface-to-volume ratio. Piezoelectricity comes with crystal inversion asymmetry, for example, along the armchair direction of transition metal dichalcogenides (TMDCs, TM: Mo or W, DC: Te, Se, S) or boron nitride (BN). In this presentation, Yu's recent article (Scientific Report, 5, 12854 (2015) [1]) has been revisited for the undergraduate research and education and application development.

Fig.1 Schematic of Piezoelectric Biosensor with PN-junction in doped-MoS_2 monolayer and WSe_2-MoS_2

In Yu's article, for the PN-junction, a sulfur ion of MoS_2 was replaced by a phosphorous ion for the P-junction, and by a chlorine ion for the N-junction to form surface charge polarization in addition to other polarizations. The output voltage, electrostatic energy over total charge, of MoS_2 PN-junction with 1% and 8% tensile strain gives 0.036 V and 0.31 V, respectively. For the MoS_2/WSe_2 hetero-junction, single arrays of hexagonal honeycombs in the zigzag direction for both MoS_2 and WSe_2 are stacked on top of each other to generate interfacial polarization in addition to other polarization effects. The output voltages of MoS_2/WSe_2 nano-ribbon hetero-junction with 1% and 8% tensile strain gives 0.04 V and 0.185 V, respectively. From the undergraduate research and education, the applications of PN- and hetero-junction with TMDCs were found to be a self-powered adhesive biosensor for life-support heart-rate monitoring for patients suffering from heart-related problems, as well as real-time muscle dynamics for athletes looking to improve their performance. Acknowledgement: This work at HU is supported by ARO W911NF-15-1-0535, NSF HRD-1137747, and NASA NNX15AQ03A.

References

[1] S. Yu, K. Eshun, H. Zhu and Q. Li, *Sci Rep*., 5, 12854 (2015).

Photophysics of Single Nano-scale Metal-halide Cluster: an Optical Indicator for Molecular Oxygen

Ruby N. Ghosh and Reza Loloee
Physics Department, Michigan State University,
East Lansing, MI 48814, USA, PA 16803, USA
ghosh@pa.msu.edu

Measurements of the phosphorescent emission from a single metal-halide cluster provides a window into the photo-physics of these unique nano-scale optical indicators. Absorption of a UV photon by the family of molybdenum chloride clusters results in the emission of bright red emission with a long phosphorescent lifetime (~180us).[1] As the phosphorescent emission arises from spin forbidden transitions between the excited triplet and singlet ground state of the Mo-cluster, collisions with ground state molecular oxygen, $^3O_2$, provides an efficient pathway to quench both the intensity and lifetime of the phosphorescence.[2] Photo-bleaching, following repeated excitation of the metal-halide indicator is not observed. These optical properties are specific to *single* isolated Mo-clusters, in the as synthesized crystalline material there are strong interactions between the Mo-clusters which significantly alter their optical characteristics.[1]

We report on lifetime measurements from isolated $K_2Mo_6Cl_{14}$ clusters as a function of oxygen quencher concentration. A linear fit to the Stern-Volmer equation with an intercept of one, demonstrates that the observed phosphorescence quenching is due to bi-molecular collisional quenching between isolated Mo-clusters and molecular oxygen. The quenching of the emission from a luminnophore by simple bi-molecular collisional processes can be modeled with the Stern-Volmer equation:

$$\tau_o/\tau = 1 + K_{SV}\,[\text{quencher}]$$

where τ_o and τ are the emission lifetimes in the absence and presence of quencher respectively and K_{SV} is the overall dynamic quenching constant. The figure shows the least squares fit (solid lines) to the lifetime data (markers) at three different temperatures.

We discuss how our data demonstrates that the measured phosphorescence emission arises from single, isolated nano-scale Mo-clusters in the absence of cluster-cluster interactions that would be observed in a crystalline solid material.

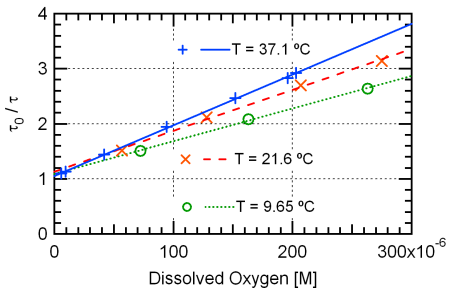

Fig.1 Normalized phosphorescence lifetime (τ_0/τ) as a function of quencher concentration, demonstrating that the emission arises from bio-molecular interactions between of an isolated nano-scale cluster and $^3O_2$.

References

[1] T. C. Zietelow, M. D. Hopkins, H. D. Gray, *J. Sol. St. Chem*. **57**, p. 112 (1985).
[2] R.N. Ghosh, P.A. Askeland, S. Kramer, R. Loloee, *Appl. Phys. Lett*. **98**, 221103 (2011).

Pulsed laser deposited two-dimensional semiconductor materials for electronic and optical device applications

Jianhua Hao*
Department of Applied Physics, The Hong Kong Polytechnic University, Hong Kong, P. R. China
The Hong Kong Polytechnic University Shenzhen Research Institute, Shenzhen, P.R. China
****Email: jh.hao@polyu.edu.hk; Tel: (852)2766 4098***

Abstract:

Two-dimensional (2D) materials have aroused great interest. The technique of pulsed laser deposition (PLD) is appealing for the growth of 2D materials as an alternative to conventional chemical vapour deposition (CVD).[1] In our recent works, we have deposited wafer-scale amorphous black (a-BP) ultrathin films at 150 °C by PLD.[2] As proof-of-concept devices, field-effect transistors (FETs) based on a-BP ultrathin films have been demonstrated. Field-effect mobility up is superior to those found in conventional elemental amorphous materials. Furthermore, we have made lanthanide doped 2D layered semiconductor such as MoS_2:Er and realize near-infrared (NIR)-to-NIR down- and up-conversion luminescence[3], which can be extended to a wide range of spectrum, including telecommunication range at 1.55 μm. The results will benefit for not only investigating many appealing fundamental issues, but also developing novel nanophotonic devices. Most recently, we demonstrate the directly growth of wafer-scale 2D layered InSe nanosheets by PLD.[4] The InSe layers exhibit high crystallinity, good uniformity, stoichiometric growth by *in situ* precise control as well as thickness dependent electrical and optical properties. The 2D InSe layer can be designed into high performance electronic and optoelectronic devices, and also favorable to be a platform for the synthesis of novel heterostructures. Our works imply that that PLD will play an important role in making various 2D materials and heterostructures for electronic and optical device applications.[1]
The works are supported by the grants from NSFC (No. 11474241) and Hong Kong RGC GRF (PolyU 153281/16P).

References:
1. Z. Yang and J. Hao*, *J. Mater. Chem. C* 4, 8859 (Invited Review) (2016).
2. Z. Yang, J. Hao*, S. Yuan, S. Lin, H. M. Yau, J. Dai, and S. P. Lau*, *Adv. Mater.* 27, 3748 (2015).
3. G. Bai, S. Yuan, Y. Zhao, Z. Yang, S. Y. Choi, Y. Chai, S. F. Yu, S. P. Lau, and J. Hao*, *Adv. Mater.*, 28, 7472 (2016).
4. Z. Yang, W. Jie, C.-H. Mak, S. Lin, H. Lin, X. Yang, F. Yan, S. P. Lau, and J. Hao*, *ACS Nano* 11, 4225 (2017).

Biography

Jianhua Hao is a Full Professor and Associate Head of Department of Applied Physics in the Hong Kong Polytechnic University (PolyU). He received his BSc, MSc and PhD at Huazhong University of Science and Technology. After working at Penn State University, University of Guelph and University of Hong Kong, Jianhua Hao joined the faculty in PolyU in 2006. He has published more than 210 SCI papers, including Chem. Soc. Rev., Adv. Mater., Angew. Chem. Int. Ed., Adv. Funct. Mater., ACS Nano as corresponding author. He was also invited to give a number of keynote/invited lectures in various international conferences. He is the first inventor of several US patents. He serves as Editorial Board Member/Senior Editor for several international journals, such as Scientific Reports and Advanced Optical Materials. (http://ap.polyu.edu.hk/apjhhao/).

Effect of Rashba spin-orbit coupling in the Radiation-Induced Resistance Oscillations in 2D electron systems.

Jesus Inarrea.
Physics Department, Universidad Carlos III de Madrid,
Avenida de la Universidad 25, Leganes, 28911, Madrid.
jinarrea@fis.uc3m.es

In this contribution we present a theoretical study on the effect of radiation on the mangetoresistance of two-dimensional electron systems with strong Rashba spint-orbit coupling. We want to study the interplay between two well-known effects in these electron systems: the radiation-induced resistance oscillations and the typical beating pattern of systems with intense Rashba interaction. Based on the radiation-driven electron orbit model [1] previously developed by the authors, we analytically derive an exact solution for the electron wave function corresponding to a total Hamiltonian with Rashba and radiation terms. We consider a perturbation treatment for elastic scattering due to charged impurities to finally obtain the magnetoresistance of the system. Without radiation we recover a beating pattern in the amplitude of the Shubnikov de Hass oscillations: a set of nodes and antinodes in the magnetoresistance. In the presence of radiation this beating pattern is strongly modified following the profile of radiation-induced magnetoresistance oscillations (see Fig.). We study their dependence on intensity and frequency of radiation, including the teraherzt regime. The obtained results could be of interest for magnetotransport of non-ideal (massive) Dirac fermions in 3D topological insulators subjected to radiation.

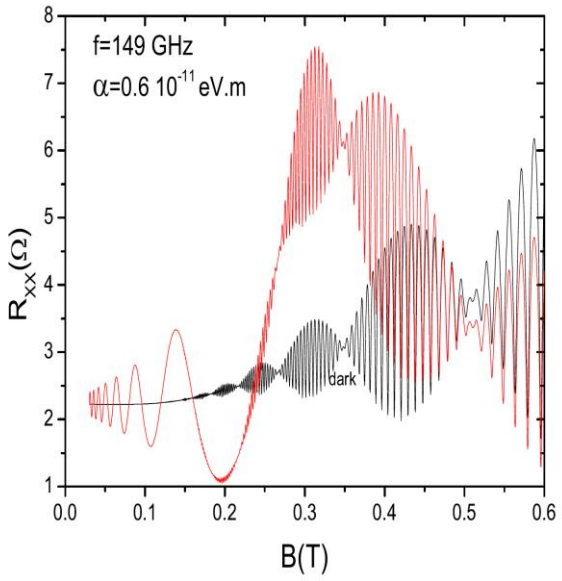

References

[1] J. Inarrea and G. Platero, Phys. Rev. Lett. 94, 016806, (2005)

Franck-Condon blockade approach to Radiation-Induced Zero-Resistance States

Jesus Inarrea.
Physics Department, Universidad Carlos III de Madrid,
Avenida de la Universidad 25, Leganes, 28911, Madrid.
jinarrea@fis.uc3m.es

In this contribution we examine by a novel theoretical approach a topic that has seen much contemporary experimental and theoretical activity – Radiation-Induced Zero-Resistance States in the two-dimensional electron system. We study the microscopic origin of such a remarkable effect starting from the concept of Franck-Condon blockade. Thus, the wave functions of the states involved in scattering must overlap, otherwise the scattering turns out to be negligible and current and magnetoresistance dramatically drop. As a result electrons remain in their initial states and zero-resistance states rise up. This new theoretical approach stems from a previous model, "the radiation-driven electron orbit model", developed also by the authors of the present manuscript to study another intriguing effect: the radiation-driven resistance oscillations [1]. This model, in turn, is based on the exact solution of the electronic wave function in the presence of a static magnetic field interacting with radiation and a perturbation treatment for elastic scattering due to randomly distributed charged impurities. This scattering between Landau states, (vibrational states) is successfully completed when there is a net overlap between the initial and final wave functions (see Fig. 1). In this model the Landau states semiclassically describe orbits driven by radiation, "driven LS", whose center positions oscillate according to the radiation frequency. These radiation-driven oscillations alter dramatically the scattering conditions. In some cases the Landau states advance during the scattering jump and on average the advanced distance by electrons is going to be bigger than in the dark giving rise to peaks in RIRO. In others the LS go backward during the jump and the net distance is smaller obtaining valleys. But in all of them there must be a net overlap of wave functions in order to have important and valuable contributions to the magnetoresistance. This idea is similar to the one in Franck-Condon physics and extensively used in vibrational spectroscopy and molecular quantum mechanics.

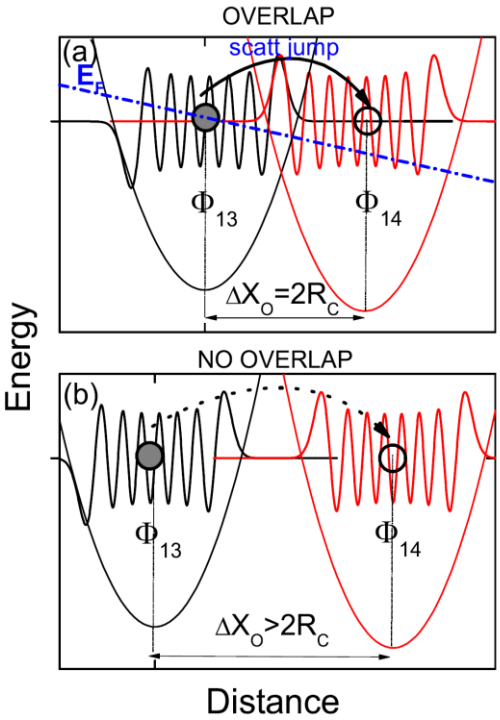

The radiation-induced resistance oscillations and zero-resistance states are still open and controversial issues after more than a decade of their discovery. No consensus among the people devoted to this field has been reached on their physical origin to date yet. We think that the present contribution will shed some light on the physics of both effects, especially on zero resistance states. We also think that the present model being based on the Franck-Condon physics could be of interest to a broad audience, including physicists of different areas.

References [1] J. Inarrea and G. Platero, Phys. Rev. Lett. 94, 016806, (2005)

Microwave Reflection from a High Mobility GaAs/AlGaAs 2DES at large filling factors

Annika Kriisa,[a+] H-C. Liu,[a] R. L. Samarweera,[a] M. S. Heimbeck,[b] H. O. Everitt,[b,c] W. Wegscheider,[d] and R. G. Mani[a]

[a] *Dept. of Physics and Astronomy, Georgia State University, Atlanta, GA 30303*

[b] *Army Aviation & Missile RD&E Center, Redstone Arsenal, Huntsville, Alabama, 35898*

[c] *Dept. of Physics, Duke University, Durham, NC 27708*

[d] *Laboratorium für Festkörperphysik, ETH-Zürich, 8093 Zürich, Switzerland*

+ Author for correspondence: annikakriisa@gmail.com

Microwave-induced zero-resistance-states in the photo-excited high quality GaAs/AlGaAs system evolve from the minima of microwave photo-excited "¼-cycle shifted" magnetoresistance oscillations.[1] Such magnetoresistance oscillations are known to exhibit nodes at cyclotron resonance ($hf = \hbar\omega_c$) and cyclotron resonance harmonics ($hf = n\hbar\omega_c$). Here f is the microwave frequency, ω_c is the cyclotron frequency, n is an integer, and $\hbar=h/2\pi$ is the reduced Planck's constant. Further, the effective mass extracted from the radiation-induced magnetoresistance oscillations is known to differ from the canonical effective mass ratio for electrons in the GaAs/AlGaAs system.[1] In an effort to reconcile this difference, we have looked for cyclotron resonance (CR) in the microwave reflection from the high mobility 2DES and attempted to correlate the observations with observed oscillatory magnetoresistance over the $30 < f < 330$ GHz band.

Experiments indicate strong reflection resonance on both sides of the magnetic field axis for linearly polarized microwave/terahertz photo-excitation over the examined frequency band. In addition, there is evidence for electronic heating in the vicinity of CR, which is indicated by a reduced amplitude of the Shubnikov-de Haas oscillations. Such results are correlated here to extract the cyclotron effective mass, which is then compared with the effective mass obtained from the microwave radiation-induced magnetoresistance oscillations.

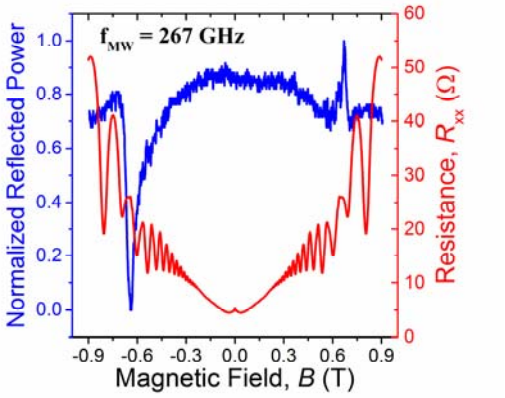

Fig. 1 Diagonal resistance, $R_{xx,}$ (red) and the reflected microwave power (blue) as a function of magnetic field for samples of high mobility GaAs/AlGaAs at T = 1.7 K and f = 267 GHz.

References

[1] R. G. Mani, J. H. Smet, K. von Klitzing, V. Narayanamurti, W. B. Johnson, V. Umansky, Phys. Rev. Lett. **92**, 146801(2004).

Angular Phase Shift in Polarization-Angle Dependence of Microwave-Induced Magnetoresistance Oscillations

Han-Chun Liu, R. L. Samaraweera, and R. G. Mani
Department of Physics and Astronomy, Georgia State University, Atlanta, Georgia 30303, USA
C. Reichl and W. Wegscheider
Laboratorium für Festkörperphysik, ETH Zürich, CH-8903 Zürich, Switzerland
hliu20@student.gsu.edu

High-mobility GaAs/AlGaAs heterojunctions subjected to microwave photoexcitation in the perpendicular magnetic field configuration exhibit ¼-cycle phase-shifted oscillatory magnetoresistance and zero-resistance states at low magnetic fields or high filling factors [1]. Associated studies have shown that the amplitude of oscillatory magnetoresistance is polarization-angle sensitive for linearly polarized radiation and can be described by an empirical cosine square law, $R_{xx}(\theta)=A \pm C\cos^2(\theta-\theta_0)$ to extract the phase shift, θ_0, where R_{xx} is diagonal resistance, θ is polarization angle [2].

Previous studies have shown that after averaging over small contributions less than the uncertainty of measurement, there remained nontrivial microwave frequency (f)-dependence of θ_0 and a small influence of the magnetic field magnitude upon θ_0 at a given f [3]. However, with this approach, the evolution between discrete f remained unknown. Thus, here, we examine the f-variation of the θ_0 with small increments, Δf, over a wide microwave band for Hall bar sections with two length-to-width (L/W) ratios. Fig.1 (a) and (d) show color plots of the normalized resistance f vs. θ for the *L/W=1* and the *L/W=2* sections, respectively. Panel (b) and (e) illustrate the sinusoidal variation of the resistance vs. the polarization angle, θ, at the indicated f. Panel (c) and (f) display the θ_0 evolution over $36 \le f \le 40$ *GHz* with the average θ_0 indicated by the dotted line. The results, panels (c) and (d), suggest that the overall average of θ_0 extracted from Hall bar device sections with $L/W = 1$ and $L/W = 2$ is the same. We compare these observations with expectations arising from the "pondermotive force" theory for the microwave radiation-induced transport phenomena [4].

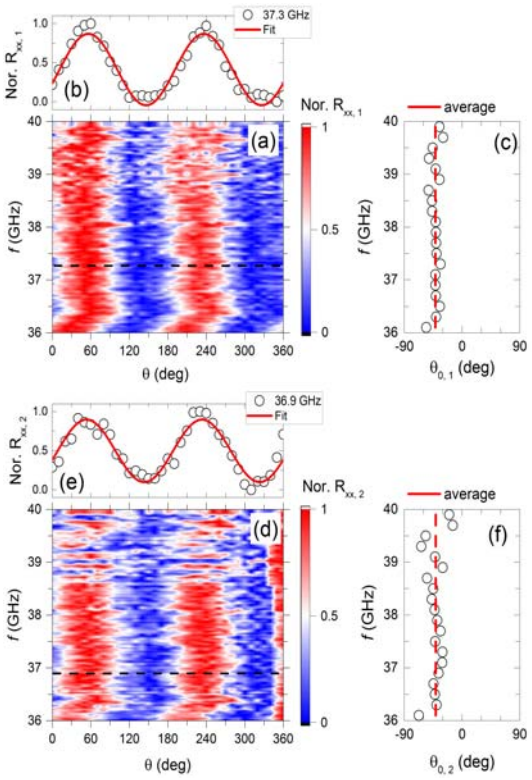

Fig.1 The normalized resistance at θ vs. f for the *L/W=1* (panel: a) and the *L/W=2* (panel: d). Panel (b) and (e) illustrate the sinusoidal variation in normalized resistance. Panel (c) and (f) show the θ_0 evolution with f.

References

[1] R. G. Mani *et al.,* Nature 420, **646** (2002).
[2] A. N. Ramanayaka *et al.,* Phys. Rev. B **85**, 205315 (2012).
[3] H.-C. Liu *et al.,* J. Appl. Phys. **117**, 064306 (2015).
[4] H.-C. Liu *et al*., Phys. Rev. B **94**, 245312 (2016).

Optoelectronic properties of graphene enhanced by colloidal quantum dots

Oleg Makarovsky[1], Lyudmila Turyanska[1,2], Mark Greenaway[1,3], Laurence Eaves[1], Amalia Patané[1], Mark Fromhold[1], Samuel Lara-Avila[4], Sergey Kubatkin[4], Nobuya Mori[5]
[1]School of Physics and Astronomy, The University of Nottingham, NG7 2RD, UK; [2]School of Chemistry, University of Lincoln, LN6 7DL, UK; [3]Department of Physics, Loughborough University, Loughborough, LE11 3TU, UK; [4]Chalmers University of Technology, Göteborg, S-41296, Sweden; [5]Division of Electrical, Electronic and Information Engineering, Osaka University, Japan
oleg.makarovsky@nottingham.ac.uk

The exploitation of graphene in electronics and optoelectonics[1] requires the availability of large-scale graphene layers with high carrier mobility and tailored optoelectronic properties. Here we describe a method for enhancing these properties in single layer graphene (SLG) grown by different techniques: n-type SiC-grown SLG and p-type CVD SLG. We demonstrate that decorating SLG with a surface layer of colloidal PbS quantum dots (QDs) (Fig. 1a) enhances the photoresponse[2] up to 10^9A/W and leads to a significant increase the carrier concentration and a 3-fold increase of the low temperature mobility[3-4] (Fig. 1b). Our Monte Carlo simulations and numerical modeling show that these effects arise from the spatial correlation of electrically charged scattering centers close to the graphene layer and charges localised in the QDs (Fig.1c). This correlation smooths out fluctuations in the electrostatic potential landscape (δU), thus reducing elastic scattering and enhancing the carrier mobility.

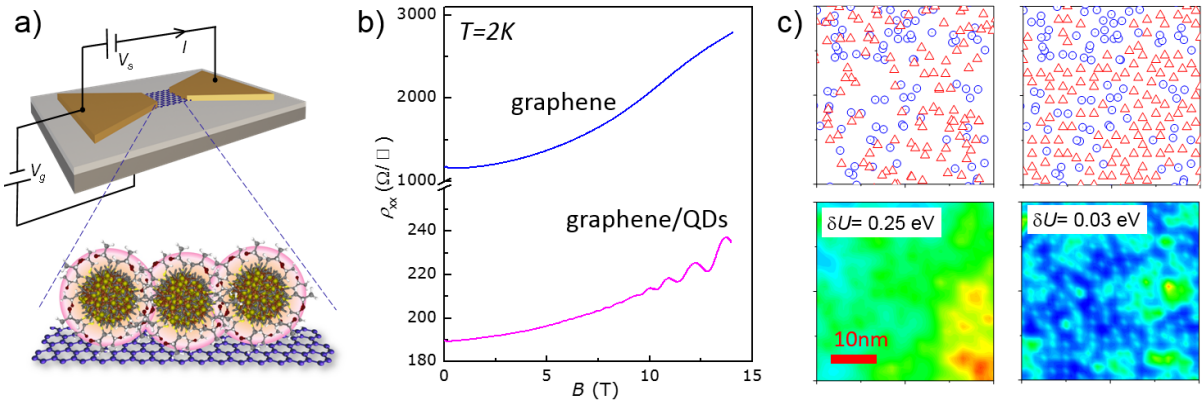

Figure 1 (a) Cartoon of a 2-terminal CVD-graphene device decorated with colloidal PbS QDs. (b) Magnetoresistance of SiC-graphene device before (blue) and after (magenta) deposition of QDs. (c) Numerical modelling of uncorrelated (left) and correlated (right) distributions of charged defects (circles) and charged QDs (triangles) and corresponding maps of local electrostatic potential landscape.

[1] F. Bonaccorso, Z. Sun, T. Hasan and A. C. Ferrari, *Nat. Photonics* **4**, 611 (2010).
[2] L. Turyanska, O. Makarovsky et al. Adv. Electron. Mater. **1**, 1500062 (2015).
[3] L. Turyanska, O. Makarovsky, L. Eaves, A. Patanè, and N. Mori, *2D Materials* **4**, 025026 (2017).
[4] O. Makarovsky et al. *submitted for publication*

Quantum Hall Effects in Hybrid Graphene

Paul Cadden-Zimansky
Physics Program, Bard College,
Annandale-on-Hudson, NY, 12504, USA
paulcz@bard.edu

The directly accessible surface and linear band structure of graphene have provided a physical system to both revisit fundamental questions concerning transport in 2-dimensions and produce new ordered states not possible in conventional 2DEGs. In particular, the differing Berry phases in monolayer, bilayer, and trilayer graphene each lead to distinct versions of the quantum Hall effect, with distinct Landau level spacing and degeneracies. While each of these systems has been studied individually, less work has been done examining the electronic states that arise in clean-interface hybrid graphene consisting of lateral combinations of different graphene thicknesses. In this work, I'll present results from transport experiments on quantum Hall effects in mono-bilayer graphene, a system which reveals phenomena distinct from what is found in each of its homogenous components. In particular the onset of formation of graphene's unusual zero-energy Landau level in hybrid graphene may provide insight into the many-body ordering of this quantum state.

Gate-Defined Nanostructures in MoS_2 van der Waals Heterostructures

R. Pisoni, Y. Lee, H. Overweg, M. Eich, P. Simonet, T. Ihn and K. Ensslin
Solid State Physics Laboratory, ETH Zürich, CH-8093 Zürich, Switzerland
K. Watanabe and Takashi Taniguchi
Advanced Materials Laboratory, National Institute for Material Science, 1-1 Namiki, Tsukuba 305-0044, Japan
R. Gorbachev
National Graphene Institute, University of Manchester, Manchester M13 9PL, UK
pisonir@phys.ethz.ch

We have realized ultra-high quality MoS_2-based van der Waals heterostructures with gated graphene contacts (Figure 1a).

Shubnikov-de Haas oscillations (SdHO) occurring at magnetic fields as low as 1T document the electronic quality of our devices (Figure 1b,c). We observe a 3-fold degeneracy of the Landau levels shifted in magnetic field by the valley Zeeman effect.

Negatively biased split gate electrodes allow us to form a channel which can be completely pinched off for sufficiently large gate voltages (Figure 1d). Plateau-like features occur at conductance values consistent with the expected degeneracies at zero and finite magnetic fields [1].

Laterally confined two-dimensional (2D) materials offer the opportunity to engineer quantum states with tunable spin, charge and even valley degrees of freedom. The pure thinness of these materials in combination with 2D insulators such as boron nitride pave the way for ultra-small strongly coupled gate-defined quantum devices.

We are confident that our observation of quantized conductance is the first step towards gate-defined quantum dots in 2D semiconducting transition metal dichalcogenides in order to control and manipulate the spin and valley states of single confined electrons.

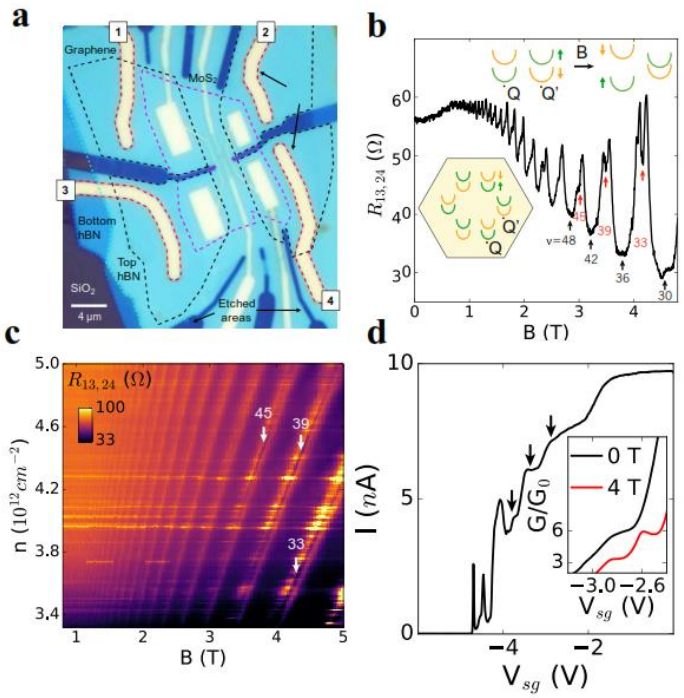

Figure 1: **a**, Optical micrograph of the device. **b**, Two-terminal pinch off curve. Inset: Four-terminal conductance. **c**, Four-terminal resistance as a function of magnetic field. **d**, Landau level fan diagram.

References

[1] R. Pisoni, Y. Lee, H. Overweg, M. Eich, P. Simonet, K. Watanabe, T. Taniguchi, R. Gorbachev, T. Ihn and K. Ensslin, *arXiv:1701.08619* (2017).

Dirac Fermions Density of States in HgTe Quantum Well

M. L. Savchenko[1,2], D. A. Kozlov[1,2], J. Ziegler[3], Z. D. Kvon[1,2], N. N. Mikhailov[2], and D.Weiss[3]
[1] *Novosibirsk State University, Novosibirsk 630090, Russia*
[2]*Rzhanov Institute of Semiconductor Physics, Novosibirsk 630090, Russia*
[3]*Experimental and Applied Physics, University of Regensburg, D-93040 Regensburg, Germany*
SavchenkoMaximL@gmail.com

Since the discovery of the massless Dirac electrons in graphene systems with linear dispersion of carriers have been under intensive study. HgTe quantum wells with thickness of about 6.3–6.6 nm are the examples of such systems that have gapless single-valley two-dimensional Dirac fermions, high quality with mobility more than 10^5 cm^2/Vs and have all advantages of quantum well structures [1].

There have been done many experiments on HgTe structures that show the absence of any energy gap in the spectrum of Dirac fermions and demonstrate a number of features indicating both the linearity of the spectrum of Dirac electrons in a wide energy range and a strong effect of valleys of heavy holes, which are 10–20 meV below the Dirac point. However, the density of states, which is the most important characteristic directly related to the energy spectrum of the system, has not yet been systematically studied. In this work, we present the Fermi energy dependences of the density of states of the system of Dirac fermions obtained by means of capacitance measurements and analyze factors affecting the density of states at the Dirac point.

It is found that the density of states of Dirac electrons is a linear function of the Fermi energy at $E_F > 30$ meV with the corresponding velocity $v = 8.2\times10^5$ m/s. At lower energies this dependence deviates from the linear law, indicating a strong effect of disorder, which is associated with fluctuations of a built-in charge, on the density of states of the studied system near the Dirac point. At negative energies, a sharp increase in the density of states is observed, which is associated with the tail of the density of states of valleys of heavy holes. The described behavior is in agreement with the proposed model, which includes both the features of the real spectrum of Dirac fermions and the effect of the fluctuation potential.

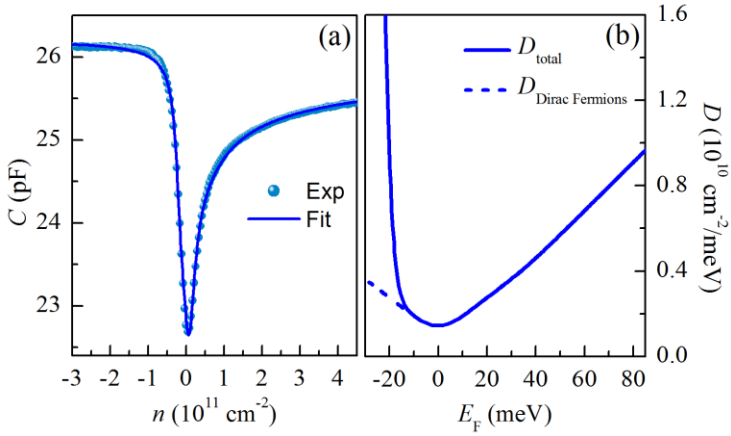

Fig. 1. (a) Experimental data and fitting curve of $C(n)$. (b) Density of states versus the Fermi energy, which is obtained with the parameters extracted from the fit in panel (a).

References

[1] B. Buttner, C. X. Liu, G. Tkachov, E. G. Novik, C. Brune, H. Buhmann, E. M. Hankiewicz, P. Recher, B. Trauzettel, S. C. Zhang, and L. W. Molenkamp, Nat. Phys. **7**, 418 (2011).

Effects of dynamic nuclear polarization in transition metal dichalcogenides

Girish Sharma, Edwin Barnes, Sophia Economou
Department of Physics, Virginia Tech,
Blacksburg, VA 24061, USA
girish9@vt.edu

The interplay of Ising spin-orbit coupling and Berry curvature effects in transition metal dichalcogenides (TMDs) results in anomalous transport properties. For example, when a single valley is polarized using a circularly polarized laser light, spin-polarized carriers are produced, and an external electric field generates an anomalous Hall current. These electrons (holes) however interact with the underlying nuclear spins via the hyperfine interaction, which has a flip-flop term of considerable magnitude in the conduction band. This interaction dynamically polarizes the nuclei, which in turn alters the steady state population of the electrons (and hence the associated transport responses), via a feedback mechanism. An experimental detection of this signal can thus be a signature of nuclear spins in TMDs.

Dephasing in Strongly Anisotropic Black Phosphorus

F. Telesio[1], N. Hemsworth[2], V. Tayari[2], S. Xiang[1], S. Roddaro[1], M. Caporali[3],
A. Ienco[3], M. Serrano-Ruiz[3], M. Peruzzini[3], G. Gervais[4], T. Szkopek[2], and S. Heun[1]
1NEST, Istituto Nanoscienze-CNR and Scuola Normale Superiore, Pisa, Italy
2Dept. of Electrical and Computer Engineering, McGill University, Montréal, Québec, H3A 2A7, Canada
3Istituto Chimica dei Composti OrganoMetallici-CNR, Sesto Fiorentino, Italy
4Physics Dept., McGill University, Montréal, Québec, H3A 2T8, Canada
francesca.telesio@nano.cnr.it

Black phosphorus (bP) is a direct band gap semiconductor, which, thanks to its layered structure, can be exfoliated down to the monolayer. It attracted great interest for various properties, among which anisotropic transport, optical, and thermoelectric properties have been recently observed and related to the puckered structure of bP layers [1]. Here we present recent results on bP devices, in particular experimental observation of weak localization in a 65 nm-thick black phosphorus field effect transistor [2]. Weak localization (WL) is a quantum effect, related to coherent scattering at low temperatures. Using the Hikami-Larkin-Nagaoka model [3], the dephasing length L_φ (or inelastic scattering length) can be inferred from weak localization. Our study is performed for various gate voltages (V_g), in the hole-doped regime, at temperatures down to 250mK. L_φ is found to increase with increasing hole density, attaining a maximum value of 55 nm at a hole density of approximately 10^{13}cm^{-2}. The temperature dependence of L_φ was also investigated. Above 1K it decreases, with a weaker temperature dependence than $T^{-1/2}$, the one expected for electron-electron interaction in two dimensions. Rather, the observed power law was found to be close to that observed previously in quasi-one-dimensional systems such as metallic nanowires and carbon nanotubes. We attribute this result to the puckered structure of bP which forms a strongly anisotropic medium for localization. Therefore, the anisotropic structure of black phosphorus plays a crucial role also for quantum interference effects such as WL.

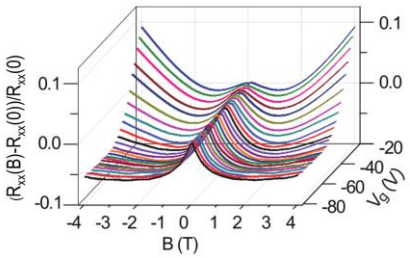

Fig.1 Weak localization peak: plot of the normalized longitudinal resistance $(R_{xx}(B)-R_{xx}(0))/R_{xx}(0)$ versus magnetic field B and V_g at T = 0.26 K.

References:

[1] F. Xia, H. Wang, and Y. Jia, Nat. Commun. 5, 4458 (2014).
[2] N. Hemsworth, V. Tayari, F. Telesio, S. Xiang, S. Roddaro, M. Caporali, A. Ienco, M. Serrano-Ruiz, M. Peruzzini, G. Gervais, T. Szkopek, and S. Heun, Phys. Rev. B 94, 245404 (2016).
[3] G. Bergmann, Phys. Rep. 107, 99 (1984)

Split-gated Point-Contact for Electrostatic Confinement of Transport in MoS_2/h-BN Hybrid Structures

Madhu Thalakulam and Chithra H Sharma
School of Physics, Indian Institute of Science Education and Research Thiruvananthapuram, 695016, Kerala, India
madhu@iisertvm.ac.in

Electrostatically gated nanoscale devices on two dimensional electron systems such as Quantum point contacts (QPC) [1,2] and quantum dots [3] are the basic building blocks of potential devices for quantum information, [4] quantum metrology [5] and charge sensing applications. [6–8] Owing to its atomically flat interfaces and the inherent two-dimensional nature, van der Waals heterostructures hold the advantage of large-scale uniformity, flexibility and portability over the conventional bulk semiconductor heterostructures. Gate defined nanoscale devices explored on graphene have met with limited success due to the lack of band gap. Here we present a split-gate defined point contact device on MoS_2/h-BN heterostructure, the first step towards realizing electrostatically gated quantum circuits on van der Waals semiconductors. The electron flow in the device is controlled and confined by varying the voltage on the split-gate. The formation of the point contact in our device is elucidated by the three characteristic regimes observed in the pinch-off curve; transport similar to the conventional FET, electrostatically confined transport and the tunneling dominated transport. We are able to seamlessly tune the transport across these regimes by tuning the split-gate voltage. The heavily doped silicon back-gate is used for tuning the carrier concentration in the MoS_2 layer. We also explore the role of the carrier concentration and the drain-source voltages on the pinch-off characteristics. Our devices exhibit the point contact behaviour at all temperatures ranging from 4 K to 300 K, making them potential candidates for the implementation of quantum electrical metrology and other charge detection applications at higher temperatures.

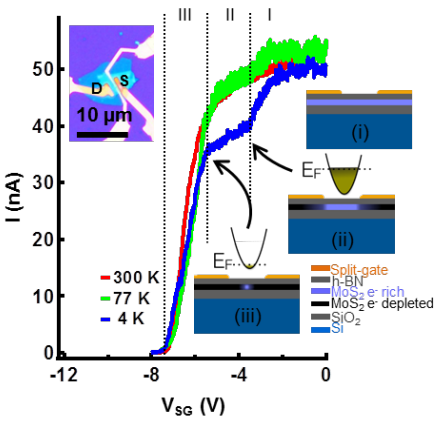

Fig.1 Pinch-off characteristics at 4 K (blue), 77 K (green) and 300 K (red) with illustration (i), (ii) and (iii) explaining the different regimes in the transport. The parabolas represent the electrostatic confinement of charge carriers in the point-contact. The inset shows the optical image of the device.

References

[1] D. A. Wharam et al., J. Phys. C Solid State Phys. **21**, L209 (1988).
[2] B. J. van Wees et al., Phys. Rev. Lett. **60**, 848 (1988).
[3] M. A. Kastner, Phys. Today **46**, 24 (1993).
[4] D. Loss and D. P. DiVincenzo, Phys. Rev. A **57**, 12 (1997).
[5] S. P. Giblin t al., Appl. Phys. Lett. **108**, 023502 (2016).
[6] J. M. Elzerman et a., Nature **430**, 431 (2004).
[7] M. Field et al., Phys. Rev. Lett. **70**, 1311 (1993).
[8] M. Thalakulam et al., Appl. Phys. Lett. **96**, 183104 (2010).

Double Carrier Transport in Electron-Doped Region in Black Phosphorus FET

K. Hirose[1], T. Osada[1], K. Uchida[1], T. Taen[1], K. Watanabe[2], T. Taniguchi[2], and Y. Akahama[3]
[1]*Institute for Solid State Physics, University of Tokyo, Kashiwa, Chiba 277-8581, Japan.*
[2]*National Institute for Materials Science, Tsukuba, Ibaraki 305-0044, Japan.*
[3]*Graduate School of Material Science, University of Hyogo, Kamigori, Hyogo 678-1297, Japan.*
osada@issp.u-tokyo.ac.jp

The advancement of carrier mobility in thin-film black phosphorus (BP) field effect transistor (FET) has made it possible to observe the quantum oscillation and the quantum Hall effect of two dimensional (2D) carriers. They have been studied mainly in negatively gated (hole-doped) region. In this paper, we report the newly found double carrier transport in positively gated (electron-doped) region.

The samples were prepared by the mechanical exfoliation and dry transfer techniques in the grove box to avoid degradation by oxygen and water. First, a thin-film BP flake with the thickness of 15-20 nm is fixed on an atomically-flat hexagonal boron nitride (h-BN) flake on the SiO_2/n^+-Si substrate. Next, it is partially covered by a smaller h-BN flake. Electrodes are formed on the edge of this top h-BN flake by the lithography process in the atmosphere. Since the measured region in BP layer is sandwiched by two h-BN layers, we can avoid the degradation and improve carrier mobility. Using this simple method, we have achieved the Hall mobility of 6,000 cm^2/Vs and 5,800 cm^2/Vs at 4.2K for holes and electrons, respectively. These values are comparable to the reported highest mobility.

In the negatively-gated (hole-doped) side, we have observed negative magnetoresistance (MR) due to weak localization and Shubnikov-de Haas (SdH) oscillations with clear spin splitting. The carrier density estimated from the SdH period is well proportional to the gate voltage with small correction of charge neutrality. This fact indicates that a single 2D hole gas is formed in the inversion layer.

In contrast, anomalous transport behaviors have been observed in the positively gated (electron-doped) side. The gate voltage dependence of conductance showed an anomalous shoulder structure. In the gate voltages below it, normal behaviors, the negative MR and single SdH oscillation, were observed like the hole-doped side. In the gate voltages above it, the MR turned to positive and saturated accompanied by slow and fast SdH oscillations. The summation of carrier densities estimated from two SdH periods coincides with the density expected from the gate voltage. This fact suggests the existence of two closed Fermi surfaces. In addition, the overall shape of MR can be qualitatively explained by the two carrier model.

The appearance of the second Fermi surface in high positive gate voltages is explained by the carrier population onto the second subband. In thin-film BP FETs, the 3D conduction band splits into 2D subbands due to finite thickness and strong gate electric field. Since the present BP sample is rather thick (15-20 nm), the subband separation is considered to be small, so that electrons easily populate on the second subband. The present result demonstrates to control the subband configuration by the gate voltage in BP FETs.

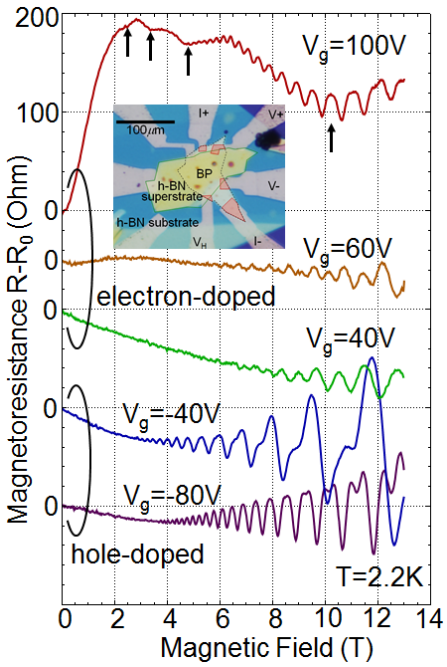

Fig.1 Magnetoresistance of thin-film BP FET under several gate voltages. Inset: microscope image of the device.

Interfacial Strain Engineering between α-Al_2O_3 and MoS_2 Monolayer

Sheng Yu,[a] Quinton Rice,[a] Tikaram Neupane,[a] Bagher Tabibi, [a] Qiliang Li, [b] Felix Jaetae Seo [a,*]

[a] *Advanced Center for Laser Science and Spectroscopy, Department of Physics, Hampton University, Hampton, Virginia 23668, US,* *jaetae.seo@hamptonu.edu

[b] *Department of Electrical and Computer Engineering, George Mason University, Fairfax, VA 22030, USA*

The interfacial strain between semiconductor and metal gate is of great interest for the metal–oxide–semiconductor field-effect transistor (MOSFET) because the interfacial strain characterizes the morphology and charge transport in the semiconductor. The interfacial interaction between a crystalline α-Al_2O_3 (0001) and MoS_2 monolayer provides the tensile strain on MoS_2, and the compressive strain on α-Al_2O_3. The strains change the morphologies of both materials improves carrier density. According to the first principle calculations [1], Al_2O_3 with thickness of 1.3 nm induces a 0.3% tensile strain on the MoS_2 monolayer. The tensile strain on MoS_2 monotonically increases for the thicker dielectric layers of α-Al_2O_3 which modifies the electronic and optical properties of the atomic monolayer. The dielectric layers of α-Al_2O_3 with thickness from 1.3 nm to 5.2 nm monotonically increased the tensile strain on the MoS_2 from 0.30% to 0.62%.

The indirect gap of MoS_2/ α-Al_2O_3 was reduced as the dielectric thickness of Al_2O_3 was increased from 1.3 nm, 2.6 nm, 3.9 nm to 5.2 nm. The bandgap of the MoS_2 monolayer was ~0.36 eV with the Al_2O_3 of 5.2 nm. The lattice parameter of MoS_2/α-Al_2O_3 was increased monotonically as the temperature was increased due to thermal expansion. The lattice parameter of the interfacial structure between MoS_2 and α-Al_2O_3 was much more sensitive for the thinner Al_2O_3 at higher temperatures.

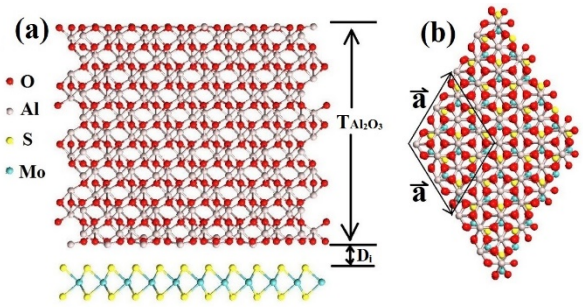

Fig 1. Schematic diagram of interfacial interaction between Al_2O_3 (0001) and MoS_2 monolayer, where *T* represents the thickness (~1.3 nm) of the dielectric layer, and D_i represents the distance between Al_2O_3 and MoS_2 monolayer.

Acknowledgement: This work at HU is supported by ARO W911NF-15-1-0535, NSF HRD-1137747, and NASA NNX15AQ03A.

References

[1] S. Yu, S. Ran, H. Zhu, K. Eshun, C. Shi, K. Jiang, F. J. Seo and Q. Li, Appl. Surf. Sci. (2017). (under revision).

Piezoelectricity from Atomic defect-mediated MoS_2 Monolayer

Sheng Yu,[a,b] Quinton Rice,[a] Tikaram Neupane,[a] Bagher Tabibi,[a] Qiliang Li, [b] Felix Jaetae Seo [a,*]

[a] *Advanced Center for Laser Science and Spectroscopy, Department of Physics, Hampton University, Hampton, Virginia 23668, USA.* * jaetae.seo@hamptonu.edu

[b] *Department of Electrical and Computer Engineering, George Mason University, Fairfax, VA 22030, USA*

The MoS_2 monolayer is inversion symmetric along the zigzag direction, and inversion asymmetric along the armchair direction. The MoS_2 monolayer at the atomic defect region has inversion asymmetry along both zigzag and armchair directions. The atomic defect in the 5x5 unit cells also modifies the electronic band structure. Piezoelectricity appears in the inversion asymmetric crystal and converts mechanical deformational force to electricity. The intrinsic piezoelectric coefficient (e_{11}) of the MoS_2 monolayer is ~290 pC/m. According to the first principle calculation, the piezoelectric coefficient (e_{11}) of MoS_2 monolayer was enhanced up to 18% when a single Mo atom was shifted ~20% along the armchair direction within the 5x5 unit cell. The piezoelectric coefficients (e_{11}) of the MoS_2 monolayer were ~323 pC/m and ~331 pC/m when a single S atom and a single Mo atom were shifted 20% along zigzag direction ($0.2\vec{L}_Y$), respectively. The piezoelectricity enhancement is attributable to the atomic defect-induced electronic and ionic polarizations.

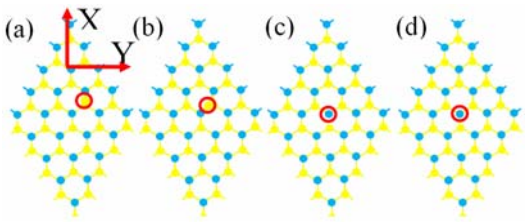

Fig. 1 Schematic sketch of atomic shift in the MoS_2 monolayer.

The electronic bandstructure was also modified by the defects with various lengths and directions of atomic shift. The relative position of conduction band minimum (CBM) and valence band maximum (VBM) to the Fermi level were also modified. The atomic shift created the defect-related energy levels within the forbidden band. The defect energy levels by the Mo shift with large displacement of $0.2\vec{L}_X$ and $0.2\vec{L}_Y$ were exhibited within the forbidden band. Both Mo-shift and S-shift along the armchair direction with a large displacement of $0.2\vec{L}_X$ induced the deeper gap energy levels compared to those induced by an atomic shift along the zigzag direction with $0.2\vec{L}_Y$. Therefore, the enhancement of piezoelectricity and the modification of the electronic band structure induced by single atomic shift in MoS_2 monolayer are promising for tnano mechno-electric system (NMES) application.

Acknowledgement: This work at HU is supported by ARO W911NF-15-1-0535, NSF HRD-1137747, and NASA NNX15AQ03A.

Effects of interlayer twists in proximitized graphene-dichalcogenide layers

Abdulrhman Alsharari[1], Mahmoud Asmar[2] and Sergio Ulloa[1]
[1]*Department of Physics and Astronomy, Ohio University*
Athens, OH 45701-2979, USA
[2]*Department of Physics and Astronomy, Louisiana State University*
210-G Nicholson Hall, *Baton Rouge, LA, USA.*
aalsharari@ut.edu.sa

Proximity effects on deposited graphene on a TMD substrate are expected to change the dynamics of the electronic states in graphene, inducing spin orbit coupling (SOC) and staggered potential effects. An effective Hamiltonian that describes different symmetry breaking terms in graphene, while preserving time reversal invariance, shows that an inverted mass regime is possible. A transition from an inverted mass phase to a staggered gap is possible in real materials, as a relative gate voltage between the layers is applied. Berry curvature and valley Chern numbers demonstrate that the system may exhibit quantum spin Hall and valley Hall effects [1].
We further study relative rotation angles of the layers as they may give rise to interesting physical behavior not present in commensurate structures. We use a continuum model capable of describing the commensurate as well as the incommensurate systems with relative rotation angle and anisotropic expansion, and examine the topological characteristics of the resulting electronic states. Contrasting with tight binding results when appropriate, we explore the behavior of gaps and proximitized spin-orbit couplings in the system as function of twist angle and other structure characteristics.

References

[1] A. Alsharari, M. Asmar and S. Ulloa, *Phys. Rev. B* **94**, 241106(R) (2016).

Long-Range Magnetic Interactions and Helical Order in Transition Metal Dichalcogenide Lateral Heterostructures

O. Ávalos-Ovando[1], D. Mastrogiuseppe[2], and S. E. Ulloa[1]
[1]*Department of Physics & Astronomy, and Nanoscale and Quantum Phenomena Institute, Ohio University, Athens, OH 45701, USA*
[2]*Instituto de Física Rosario (CONICET), 2000 Rosario, Argentina*
oa237913@ohio.edu

Heterostructures created between different 2D materials such as graphene, transition metal dichalcogenides (TMD), silicine and germanene, are now being explored for their distinct properties [1]. In-plane or lateral heterostructures (LHS) are unique and most promising in the design of materials with different electronic characteristics. Among these, LHS formed from different TMDs provide carriers with strong spin-orbit coupling and interfacial states with unique topological properties. These may allow interesting exchange effects between magnetic impurities (MIs).

When MIs are embedded in a metal, they are known to interact indirectly through the host conduction electrons, a mechanism known as the RKKY interaction. A sizable non-collinear Dzyaloshinskii-Moriya (DM) interaction between MIs has been shown to exist [2], which is long ranged when the MIs lie on/near the edges of TMD nanoflakes [3].

We present here a study of the formation of states at the 1D interface of LHS of different TMDs, as shown in Fig. 1(a). We model the LHS via a tight-binding approach with experimental and DFT parameters. We study the properties of zigzag and armchair boundaries and analyze the formation of interface states for different gap-nesting conditions. We find strongly localized midgap states hybridized across the interface. These are further shown to serve as an effective 1D host for MI arrays that interact at long range and with sizeable DM interaction, opening the possibility of interesting magnetic phases. The combination of long-range interactions and DM terms leads to helical and strongly frustrated impurity interactions in these chains, as shown in Fig. 1(b). We present results for 1D MI chains built at LHS interfaces, considering all RKKY and DM interactions. The low-energy configurations are shown to depend strongly on impurity concentration and doping levels in the host, providing the possibility of exploring phase space and the ultimate control of MI chains for various spintronics applications.

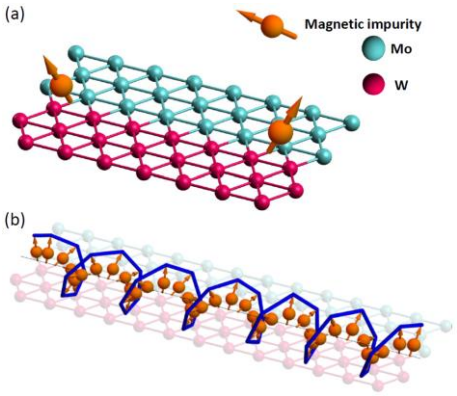

Fig.1: (a) MoS_2-WS_2 HS, with two magnetic impurities connected to the zigzag interface. Sulfur atoms are not shown.
(b) Helical order (blue line), when a chain of impurities sets at the interface.

References

[1] K. S. Novoselov *et al.*, Science **353**, aac9439 (2016).
[2] F. Parhizgar *et al.*, PRB **87**, 125401 (2013); D. Mastrogiuseppe *et al.*, PRB **90**, 161403(R) (2014).
[3] O. Ávalos-Ovando *et al.*, PRB **93**, 161404(R) (2016); *Ibid.* **94**, 245429 (2016); arXiv:1607.08553.

Spin-orbit interactions in inversion-asymmetric two-dimensional hole systems: A variational analysis

E. Marcellina,[1] A. R. Hamilton,[1] R. Winkler,[2,3] and Dimitrie Culcer[1]
[1]*School of Physics, The University of New South Wales, Sydney 2052, Australia*
[2]*Department of Physics, Northern Illinois University, DeKalb, Illinois 60115, USA*
[3]*Materials Science Division, Argonne National Laboratory, Argonne, Illinois 60439, USA*
e.marcellina@unsw.edu.au

Two-dimensional semiconductor heterojunctions are the building block of numerous nanostructures. Semiconductor holes, especially, have attracted growing attention owing to the exceptionally strong spin-orbit interaction. A thorough understanding of the latter is key to achieving all-electrical spin control required in semiconductor spintronics [1], quantum computing [2], as well as realizing the long-awaited exotic Majorana fermions [3].

While hole-based Majorana fermions have yet to materialize, rapid progress has been made in achieving electrical spin control in various low-dimensonal hole systems. However, a comprehensive theoretical understanding of spin-orbit interactions two-dimensional holes is still incomplete. In particular, calculations of spin-orbit interaction in most two-dimensional holes have been numerical, which is thus material-specific and difficult to generalize to other material systems.

To overcome these shortcomings, here we devise a general, transparent framework to quantify the strength of spin-orbit interactions in various holes heterojunctions [4]. Specifically, we integrate the variational method with **k.p** perturbation theory and the theory of invariants to evaluate the dependence of Rashba and Dresselhaus spin-orbit interactions on experimental parameters such as material, hole density, and background dopant type. We demonstrate that this semianalytical approach is readily generalizable to various materials, and show results for common semiconductors GaAs, Ge, InSb, InAs, and Si. We recover the established trend that the spin-orbit induced splitting increases with hole density and molecular weight (Fig. 1). We also find that even in zincblende materials with finite Dresselhaus spin-orbit interactions, the leading contribution to the spin splitting is the Rashba spin-orbit interaction naturally present in heterojunctions.

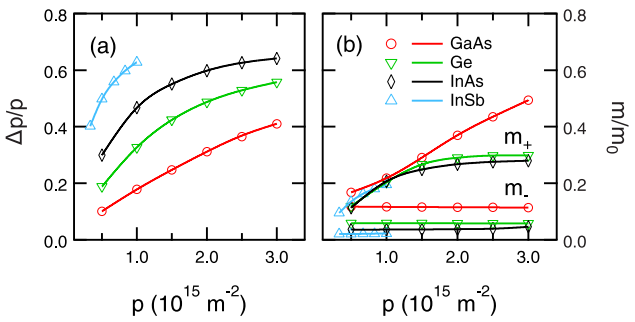

Fig. 1 Semianalytical results for the (a) Rashba spin splitting Δp and (b) spin-dependent effective masses $m_{\pm}$ for GaAs, Ge, InAs, and InSb inversion layers with a background dopant concentration of 3×10^{20} m^{-3}.

References

[1] I. Žutić, J. Fabian, and S. Das Sarma, Rev. Mod. Phys. 76, 323 (2004).

[2] D. D. Awschalom, L. C. Bassett, S. D. Dzurak, E. L. Hu, and J. R. Petta, Science 339, 1174 (2013).

[3] L. Mao, J. Shi, Q. Niu, C. Zhang, Phys. Rev. Lett. 106, 157003 (2011).

[4] E. Marcellina, A. R. Hamilton, R. Winkler, and D. Culcer, Phys. Rev. B 95, 075305 (2017).

Time-Resolved Oscillations of Exciton-Polariton Condensates in an Etched 1-D Ring Trap

D. Myers[1], B. Ozden[1], S. Mukherjee[1], D. Snoke[1], L. Pfeiffer[2], K. West[2]
[1]*Department of Physics and Astronomy, University of Pittsburgh*
Pittsburgh, PA 15260, USA
[2]*Department of Electrical Engineering, Princeton University*
Princeton, New Jersey 08544, USA
dmm154@pitt.edu

We present a study of exciton-polaritons trapped in 1-D etch-defined rings. The rings, with a radius of ~100 μm, are formed using photolithography of an MBE-grown structure and a BCL3/Cl2 reactive ion etch, with thicknesses (difference between inner and outer radius) of ≈15 μm. The etching process results in a parabolic trapping potential in the middle of the ring between the inner and outer edges. The polaritons were excited non-resonantly using a mode-locked Ti:sapphire laser with a pulse width of ~2 ps. We observed energy level splitting due to the radial confinement, as well as long-range propagation along the ring. A polariton condensate was observed far from the pump location in a region of lower energy caused by the cavity gradient. Time-resolved measurements at high pump power revealed oscillations of polariton emission intensity throughout the ring (Fig. 1). These oscillations showed a correlation between depletion of the low-energy side of the ring with an increase in density nearer to the high-energy side, and vice versa. This "breathing" state of the polariton condensate continued long after the excitation time (~1 ns), and fit with the expected oscillation frequency from the constant force due to the approximately linear cavity gradient.

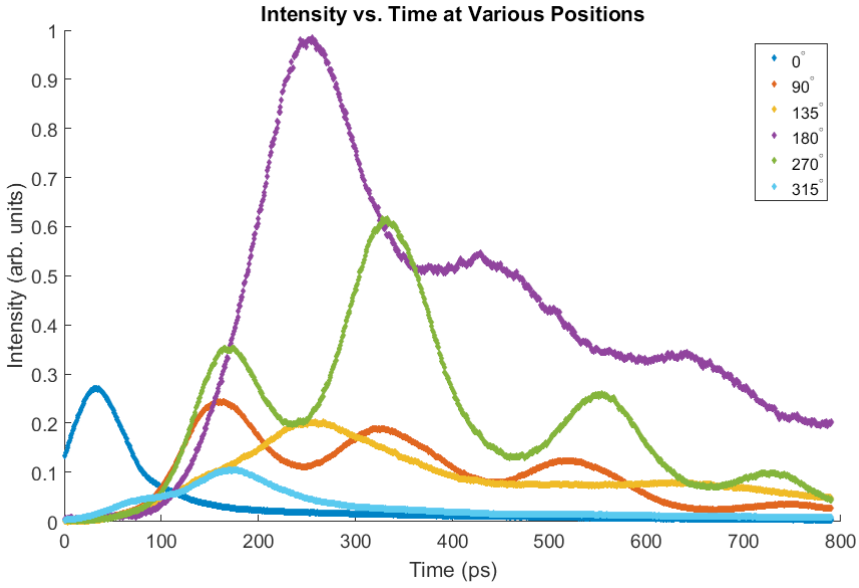

Fig. 1: Plot of the polariton luminescence intensity vs. time at various positions around the ring near $k_{||} = 0$. The angle is defined from the positive x-axis, which is aligned with the cavity gradient. The pump is at 0°, while the lowest energy location is at 180°.

Interaction of current and exciton-polariton condensate in AlGaAS/GaAs microcavities

B. Ozden,[1] D. Myers[1], D. Snoke[1], L. Pfeiffer[2], and K. West[2]

[1)] *Department of Physics & Astronomy, University of Pittsburgh, Allen Hall, 3941 O'Hara Street, Pittsburgh, Pennsylvania 15260, USA*

[2)] *Department of Electrical Engineering, School of Engineering and Applied Sciences, Princeton University, Engineering Quadrangle, Olden Street, Princeton, New Jersey 08544, USA*

Burcu2@pitt.edu

Cavity exciton-polaritons in semiconductor microcavities have become a unique solid-state system for investigating polariton condensates. In the past few decades there has been an enormous research for the study of optical properties of exciton polariton condensates in semiconductor microcavities. However, there has been no effort by many group to study the effects of polariton condensation on in-plane transport which is important criteria for optical devices to be used in circuits. Therefore, the influence of external electric fields on the energy of the polariton condensate is explored in this study.

Our results are obtained from optical cavities at cryogenic temperatures, which contain twelve quantum wells (QWs) and are processed into contacted mesas, allowing application of the electric fields parallel to the plane of the quantum wells. In this study we have investigated pillars in two different geometries, rectangular and ring shape. A continuous wave Ti:Sappire pump laser was used for the non-resonant pumping of the pillar. Both the pump power and the bias was varied at constant temperature to be able to observe threshold effects. In order to obtain energy-resolved imaging a CCD camera on the output of a spectrometer was used. A Keithley 2600B system source meter was used to sweep the applied voltage between reverse and forward bias.

We investigated both the influence of current on the condensate and the effect of the condensate on the current. We didn't observe a detectable threshold in the current with the formation of the condensate. On the other hand, a noticeable blueshift in the energy of the condensate is observed as the in-plane current increases. (see Figure 1)

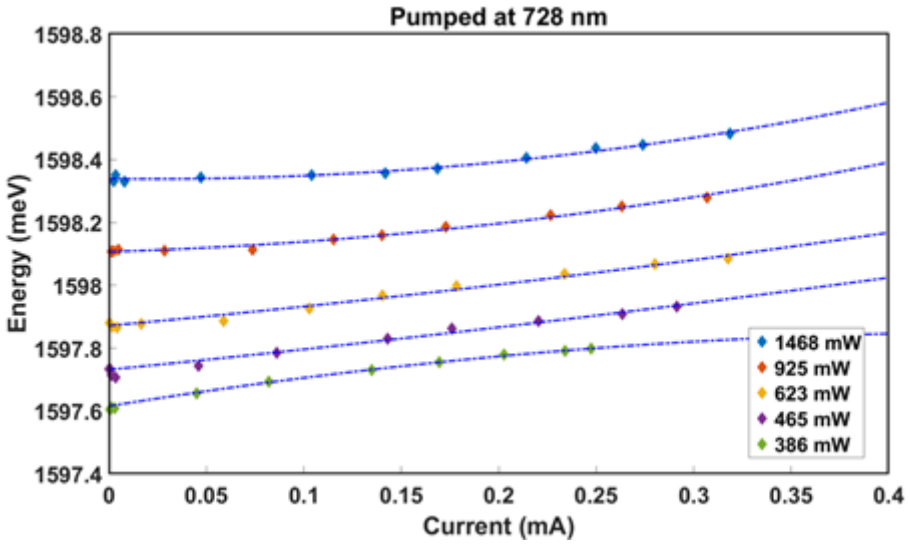

Fig.1 This figure shows energy vs. current at different pump powers indicating blueshift in the energy of the condensate as the in-plane current increases.

Epitaxy of Hexagonal Boron Nitride on Silicon Carbide Substrates

D. Pennachio[1], N.S. Wilson[1], T. Brown-Heft[1], K.M. Daniels[2], R.L. Myers-Ward[2], D.K. Gaskill[2], C.R. Eddy, Jr.[2], and C. Palmstrøm[1]
Materials Department, University of California, Santa Barbara, CA 93106, USA
[2]U.S. Naval Research Laboratory, Washington, DC 20375, USA
[3]Electrical and Computer Engineering, University of California, Santa Barbara, CA 93106, USA
dpennachio@umail.ucsb.edu

Hexagonal boron nitride (h-BN) thin film growth methods have predominantly leveraged the catalytic breakdown of precursors on transition metal substrates for self-limiting depositions [1,2]. Unfortunately, as metals are not available in single crystals of sufficient size or quality, a replacement is required to produce suitable epitaxial films. Our lab explores h-BN growth on conventional, non-metallic substrates with surfaces or buffer layers to promote large area epitaxy. We utilize chemical beam epitaxy (CBE) in an ultra-high vacuum (UHV) environment for deposition, as it allows *in-situ* monitoring for feedback of growth conditions; precise growth control, with the potential for monolayer precision; and compatibility with UHV characterization techniques to provide insight into the nucleation process.

In this experiment, 6H-SiC(0001) was chosen as a candidate substrate due to its crystalline quality, temperature stability, and potential coincident lattice match. CBE depositions of h-BN were achieved on SiC substrates through thermal decomposition of borazine at high temperatures, independent of surface catalysis. Utilizing a UHV-interconnected characterization suite, film stoichiometry and surface chemistry were measured by *in-situ* x-ray photoemission spectroscopy (XPS). Near stoichiometric depositions of single-to few-monolayer films have been achieved, as determined by B1s:N1s XPS peak area ratios and substrate peak attenuation (Fig. 1E).

Different SiC surface terminations were examined for their viability as an epitaxial surface. Progression of *in-situ* reflection high-energy electron diffraction (RHEED) during h-BN deposition provides evidence of a difference in film nucleation between the Si-rich (3x3) and the C-rich $(6\sqrt{3}\times6\sqrt{3})\,R30°$ SiC surface reconstructions: while the (3x3) reconstruction quickly transitioned to a (1x1) reconstruction upon precursor dosing, the C-rich reconstruction persisted despite thicker depositions (Fig. 1). XPS of the C-rich surface showed a higher binding energy shoulder of the C1s peak, indicative of sp^2-bonding in a graphene-like layer at the surface [3]. Triangular nuclei seen by scanning electron microscopy after deposition on the C-rich SiC surface suggests epitaxial arrangement to this buffer layer. Along with reconstructions available through UHV annealing, CVD-grown epitaxial graphene on 4H-SiC was investigated. *In-situ* scanning probe microscopy and *ex-situ* transmission electron microscopy were performed to acquire additional information on film morphology.

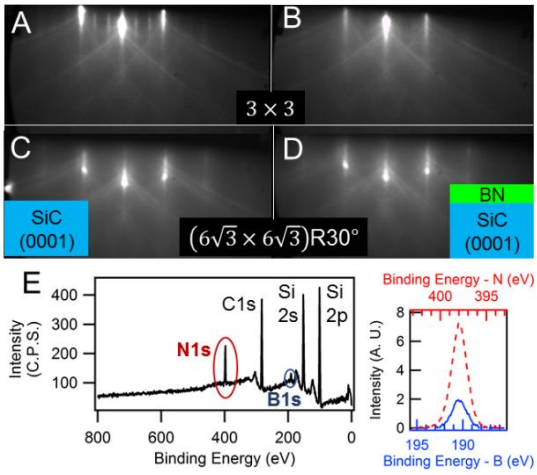

Fig 1: A-D) RHEED of the (3x3) (A, B) and $(6\sqrt{3}\times6\sqrt{3})R30°$ (C, D) reconstructed SiC surfaces before (A, C) and after (B, D) exposure to borazine. E) XPS of the h-BN/SiC surface in (D), showing stoichiometric B1s:N1s with no impurity peaks.

References:

[1] M. Paffett, R. Simonson, P. Papin, and R. Paine, Surf. Sci. **232**, 286 (1990).
[2] L. Song *et al.*, Nano Lett. **10**, 3209 (2010).
[3] F. Varchon *et al.*, Phys. Rev. Lett. **99**, 3 (2007).

Tunable Electronic Properties in Molecular Graphene

E. Räsänen, S. Paavilainen, M. Ropo, J. Nieminen, and J. Akola
Laboratory of Physics, Tampere University of Technology,
P.O. Box 662, FI-33101 Tampere, Finland
esa.rasanen@tut.fi

In recent years, research on graphene has extended to other honeycomb structures. Some of those systems are called as “artificial graphene” as they provide controllability in terms of, e.g., the lattice constant [1]. High-precision tunability of a graphene-like band structure has been demonstrated for molecular graphene [2]. In this system, adsorbate CO molecules are positioned in a triangular configuration on a copper (111) surface to confine the conduction electrons in a honeycomb geometry. Remarkably, the system also allows opening of a gap at the Dirac point through Kekulé distortion, which can be induced by modifying the CO adsorption pattern.

Here, we uncover the electronic structure of molecular graphene produced by adsorbed CO molecules on a copper (111) surface by means of first-principles calculations [3]. Our results show that the band structure is fundamentally different from that of conventional graphene, and the unique features of the electronic states arise from *co-existing honeycomb and Kagome symmetries*. Furthermore, the Dirac cone does not appear at the K-point but at the Γ-point in the reciprocal space and is accompanied by a third, almost flat band. Calculations of the surface structure with Kekulé distortion show a gap opening at the Dirac point in agreement with experiments. Finally, we use our computational approach to assess the feasibility of the system as an *electronic Lieb lattice* according to recent experiments [4].

References

[1] M. Polini *et al*., Nat. Nanotechnology **8**, 625 (2013).
[2] K. K. Gomes *et al*., Nature **483**, 306 (2012).
[3] S. Paavilainen, M. Ropo, J. Nieminen, J. Akola, and E. Räsänen, Nano Lett. **16**, 3519 (2016).
[4] M. R. Slot *et al.*, arXiv: 1611.04641.

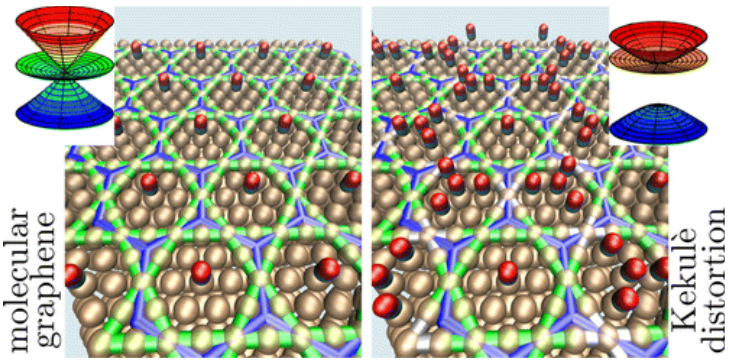

Fig. 1 Visualization of molecular graphene (left) and Kekulé distortion (right) constructed with CO molecules (red) on copper (brown). Blue and green lines show the honeycomb and Kagome structures, respectively. The insets show the corresponding bands close to the G-point.

Energetic Balance in the Morphology of Folded Graphene Ribbons

J. C. Rode, C. Belke, H. Schmidt and R. J. Haug
Institute for Solid State Physics, Leibniz Universitaet Hannover,
Appelstraße 2, 30167 Hannover, Germany
rode@nano.uni-hannover.de

Stacking of van der Waals bound 2D materials is consistently gaining importance in electronic as well as optical and mechanical research[1]. In this, twisted bilayer graphene (TBG) may be seen as a model system: It consists of two sheets from the same material with interlayer rotation as decisive degree of freedom. In recent years, TBG samples created by folding of a monolayer have already revealed a variety of interesting electronic spectra[2,3] and mechanical traits[4]. We here expand on the mechanical aspects of such structures and find an energetic balance in the system, interconnecting many of its morphological parameters.

TBG are prepared by nanomachining via Atomic Force Microscope (AFM), giving rise to ribbons tearing out of monolayer sheets (see figure). Characteristic AFM-measured quantities like interlayer distance as well as length and bulge of the folded edge are found to be interrelated, the former two showing a pronounced twist-angle dependence. These findings are understood in the recently proposed picture of a thermally activated growth process[5], and appear suited to furthering our general understanding about interaction in van der Waals bound materials.

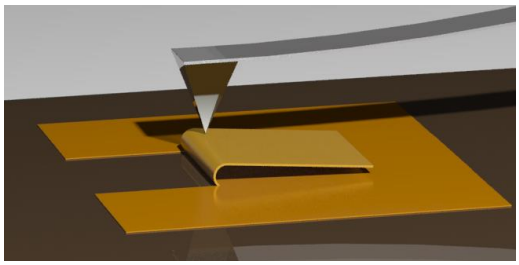

Fig. 1: Schematic of a graphene flake lying on a substrate. A ribbon has been folded out of the plane via Atomic Force Microscope, forming a strip of twisted bilayer graphene.

References

[1] A.K. Geim, and I.V. Grigorieva, Nature **499**, 419 (2013).
[2] H. Schmidt, J.C. Rode, D. Smirnov, R.J. Haug, Nat. Comm. **5**, 5742 (2014).
[3] J.C. Rode, D. Smirnov, H. Schmidt, R.J. Haug, 2D Materials **3**, 035005 (2016).
[4] J.C. Rode, C. Belke, H. Schmidt, R.J. Haug, arXiv:1608.08133 [cond-mat.mtrl-sci] (2016).
[5] J. Annett, and G. L.W. Cross, Nature **535**, 271 (2016).

Optimization of Ti/Al/Ti/TiN based Au-Free Ohmic Contact to AlGaN/GaN HEMTs and SBDs for Mass Productions and Applications

Hui Sun[1,2], Jianguo Chen[2], Peng Liu[1], and Dongmin Chen[1]
[1] *Academy for Advanced Interdisciplinary Studies, Peking University, Beijing 100871, PR China*
[2]*Founder Microelectronics International Co., Ltd., Shenzhen 518116, PR China*
shui@pku.edu.cn

AlGaN/GaN based material and devices have caught great attentions because of the superior intrinsic properties of GaN and the spontaneous formation of high density two-dimensional electron gas (2DEG) at the AlGaN/GaN interface. Au-free ohmic contacts to GaN-HEMTs are compatible with standard Si CMOS technologies which are meaningful to developed to satisfy the need of industry production. Ti/Al/Ti/TiN based Au-free ohmic contact metal stacks is the most widely accepted metal system worldwide because it can fabricate together with Si CMOS products.

In this presentation, we first improved the Ti/Al/Ti/TiN based ohmic contact resistance to 0.58Ω·mm, which is lower than 1Ω·mm reported before[1] and comparable with Ti/Al/W/(Metal)[2] and Ti/Al/Ni/Pt(Metal)[3] based ohmic contact. The AlGaN/GaN heterostructure layers were grown on 150-mm silicon wafers by metalorganic chemical vapor deposition (MOCVD). The epi-stack consists of a 25-nm $Al_{0.25}Ga_{0.75}N$ barrier layer, a 150-nm GaN Channel layer, a 2.8-μm GaN buffer layer, and a 200-nm AlN nucleation layer on p-type Si (111) substrate. The passivation cap layer of the wafers is 2 nm GaN. After ohmic contact patterned, we etched the cap layer and AlGaN barrier layer using BCl_3/Cl_2 based ICP etcher leaving 4nm AlGaN barrier. Before metal deposition, we treated the surface using buffered HF, H_2O_2 and HCl solution sequentially. The Ti/Al/Ti/TiN metal stacks were deposited by PVD without any interruption avoiding pollution at metal interface. Followed metal patterned, the wafer was annealed at 850℃ for 45s.

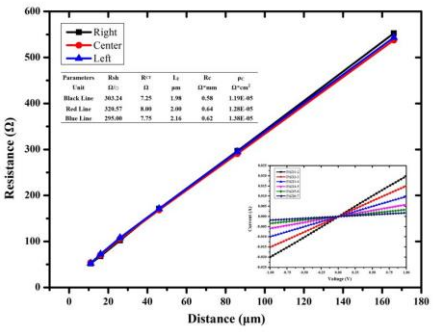

Fig.1 TLM curve of ohmic contact (Insert: I-V information between each two pad of the "Right" TLM structure).

Fig.1 show the ohmic performances at different position of the wafer. The fitted curves are very straight which mean great ohmic contact performance we have. And the values we measured are 0.58Ω·mm, 0.64Ω·mm and 0.62Ω·mm, respectively. Fig.2 is the ohmic contact resistance mapping on 150mm wafer. From which we can see that 59% of the resistance are lower than 1Ω·mm, 68% of the resistance are lower than 2Ω·mm and 88% of the resistance are lower than 3Ω·mm, indicating outstanding process technologies we have in ohmic contact. More modification processes such as anneal conditions control, contact etch speed optimization, interface morphology and interface treatment we have studied in details, of which the data is not shown here.

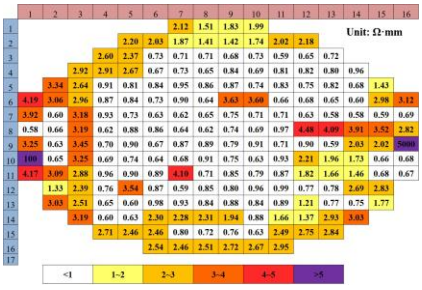

Fig.2 Ohmic contact resistance map of 150mm wafer

References

[1] H. S. Lee, D. S. Lee, and P. Tomas, IEEE Electron Device Lett. 32, 623 (2011).
[2] Z. Liu, M. Sun, H. S. Lee, M. Heuken, and T. Palacios, Appl. Phys. Express 6, 096502 (2013).
[3] B. D. Jaeger, M. V. Hove, D. Wellekens, X. Kang, H. Liang, G. Mannaert, K. Geens, and S. Decoutere, in 2012 IEEE International Symposium on Power Semiconductor Devices and ICs, 3–7(ISPSD, 2012)

Threshold Voltage and Drain Current Instabilities in GaN MIS-HEMTs

Hui Sun[1,2], Peng Liu[1], Jianguo Chen[2], and Dongmin Chen[1]
[1] *Academy for Advanced Interdisciplinary Studies, Peking University, Beijing 100871, PR China*
[2]*Founder Microelectronics International Co., Ltd., Shenzhen 518116, PR China*
shui@pku.edu.cn

GaN based metal-insulator-semiconductor high electron mobility transistors (MIS-HEMTs) have attracted a lot of attentions in the field of high power applications. The gate dielectric layer with good insulating property may effectively suppress the parasitic gate leakage currents, and eliminate the current collapse as commonly encountered in GaN based transistors [1]. However, due to the presence of the dielectric-GaN interface traps, a relating phenomenon of positive threshold drift is usually observed after the gate is forward stressed [2]. Such threshold voltage instability will limit the reliability of GaN high power devices. In previous reports, people have investigated the threshold instability by different means. The investigated emission time has extended to μs regime [3].

In this presentation, we report the investigation of threshold voltage and drain current instabilities of a GaN-MISHEMT by means of DC current-voltage measurements. By applying a reverse gate stress, the gate dielectric-GaN interface traps are filled, resulting in positive threshold shift and drain current degradation. The number of the occupied interface traps increases with the gate stress magnitudes. From the recovering processes, the emission characteristic time constants of the deep level traps are extracted as 310 s and 2170 s in our device structure and operation condition, and the corresponding trap energy levels are calculated. Our results suggest that in the use of a depletion-mode GaN device, the gate terminal has to be carefully protected to prevent the instabilities problems.

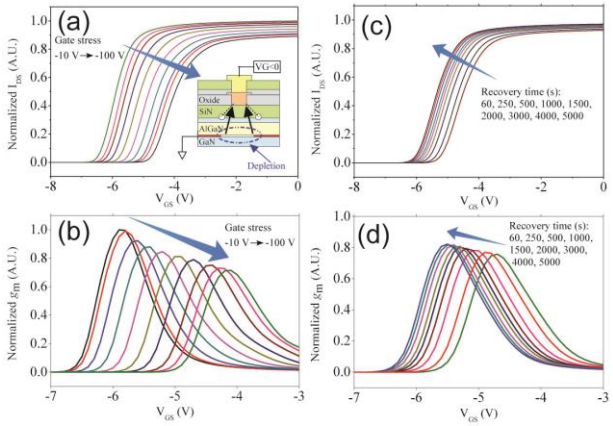

Fig.1 The transfer characteristics (a) and the trans-conductance (b) measured after applying the gate stress from -10 V to -100 V with -10 V step, showing both the V_{TH} positive shift and I_{DS} degradation. The transfer characteristics (c) and trans-conductance (d) recovery properties after the -100 V gate stress is applied.

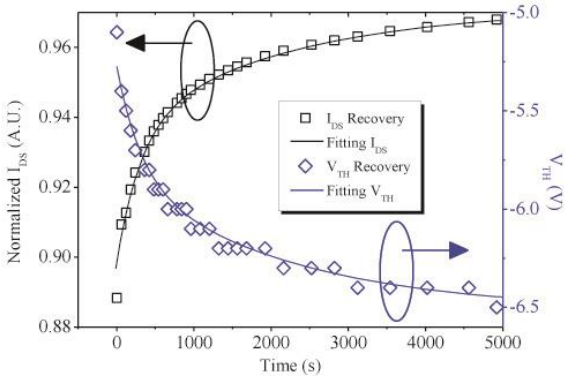

Fig.2 The recoveries of both V_{TH} and I_{DS} and the fittings by two-exponential functions, yielding the emission characteristic time310 ± 30s and 2170 ± 100s. The fittings start from the second data point at t = 60s, because between the first and second data points, the recoveries are mainly governed by the fast emission process.

References

[1] M. Ochiai,M. Akita, Y. Ohno, S. Kishimoto, K.Maezawa and T. Mizutani: Jpn. J. Appl. Phys. **42**, 2278(2003).
[2] P. Lagger, C. Ostermaier, G. Pobegen and D. Pogany: Electron Devices Meeting (IEDM), IEEE International (2012).
[3] P. Lagger, A. Schiffmann, G. Pobegen, D. Pogany and C. Ostermaier: IEEE Electron Device Lett. **34**, 1112(2013).

Inter-valley Auger recombination in InGaAs/InP quantum wells

M. A. Tito[1], Yu. A. Pusep[1], A. Gold[2], M. D. Teodoro[3], G. E. Marques[3], and R. R. LaPierre[4]
[1]*São Carlos Institute of Physics, University of São Paulo, 13560-970 São Carlos, SP, Brazil*
[2]*Université de Toulouse (UPS), CEMES-CNRS, 118 Route de Narbonne, 31062 Toulouse, France*
[3] *Universidade Federal de São Carlos, 13565-905, São Carlos, SP, Brazil*
[4]*Centre for Emerging Device Technologies, Department of Engineering Physics, McMaster University, Hamilton, Ontario L8S 4L7, Canada*
Marcoatp@ifsc.usp.br

Auger recombination is one of the most important non-radiative processes which affects the efficiency of optoelectronic devices particularly at high excitation power or high injection, when a high density of carriers is generated. In the presented work the electron transport and recombination processes of photoexcited electron-hole pairs were studied in InGaAs/InP single quantum wells. Comprehensive transport data analysis reveals asymmetric shape of the quantum well potential where the electron mobility was found to be dominated by interface-roughness scattering. The low-temperature time-resolved photoluminescence was employed to investigate recombination kinetics of photogenerated electrons. Remarkable modification of Auger recombination shown in Fig.1 was observed with variation of the electron mobility.

In high mobility quantum wells the increasing pump power resulted in a new and unexpected phenomenon: a considerably enhanced Auger non-radiative recombination time. We propose that the distribution of the photoexcited electrons over different conduction band valleys might account for this effect. Such phonon-assisted inter-valley Auger recombination process is important in direct band gap semiconductors when the difference between the energies of the Γ conduction band minimum and a lateral (X or L) conduction band minimum is close to the gap between the conduction band and valence band extrema. This condition favors transference of the energy of recombining electron-hole pair to a third electron excited into the lateral conduction band valley. In low mobility quantum wells, disorder-induced relaxation of the momentum conservation rule causes inter-valley transitions to be insignificant, resulting in decreasing of non-radiative recombination time with the increasing pump power. Thus, we propose that the disorder driven transition between two types of Auger processes (intra and inter-valley) was observed.

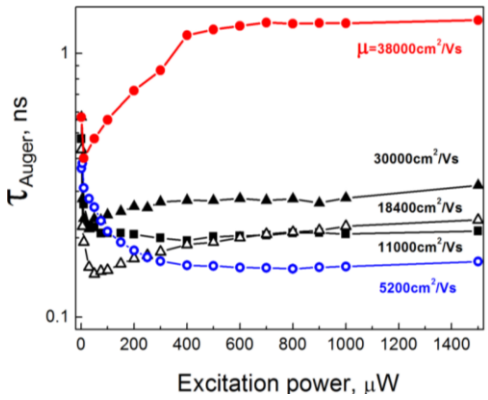

Fig.1 Auger recombination time measured as a function of the pump power at T=7 K in InGaAs/InP QWs with different electron mobility.

References

[1] M. A. Tito, Yu. A. Pusep, A. Gold, M. D. Teodoro, G. E. Marques, and R. R. LaPierre, J. Appl. Phys. **119**, 094301 (2016).

Lateral composition modulation in $W_xMo_{1-x}S_2$ monolayers

Yuanxi Wang[1], Amin Azizi[1,2], Zhong Lin[3], Ke Wang[1], Ana Laura Elias[3], Mauricio Terrones[1,2,3], Vincent H. Crespi[1,2,3], and Nasim Alem[1,2]

[1]*Materials Research Institute, Penn State University, University Park, PA 16802, USA*

[2]*Department of Materials Science and Engineering, Penn State University, University Park, PA 16802, USA*

[3]*Department of Physics, Penn State University, University Park, PA 16802, USA*

yow5110@psu.edu

The close similarity in structural and electronic properties of monolayer MoS_2 and WS_2 has led to the expectation that they will form a random alloy when mixed into $W_xMo_{1-x}S_2$. Here we report the recent observation of atomically thin W and Mo stripes in triangular monolayer flakes of $W_xMo_{1-x}S_2$ produced by sulfurization of MoO_3/WO_3. Aberration-corrected annular dark field (ADF) scanning transmission electron microscopy (STEM)reveals that the lateral stripes are oriented parallel to the edges of the triangles.

First-principles density functional theory was used to investigate the mechanism of stripe formation by comparing the formation energies of the striped alloy structure and random alloy structures, showing nearly identical stabilities. However, phase segregation at the growth edge favors one metal over the other depending on the local sulfur availability and edge geometry, insensitive to the composition deeper into the monolayer. Stripe formation is thus driven by kinetics and modulated by fluctuations that couple the local chemical potentials of metals and chalcogenide, a mechanism that can also be potentially exploited to produce superlattices in other $A_xB_{1-x}C$ alloys where formation of alternating layers (stripes) of A and B atoms are modulated in a 3D (2D) structure by the third species C.

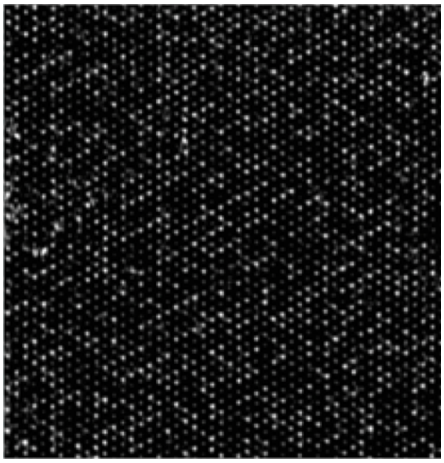

Fig.1 Scanning transmission electron microscopy image of a $W_xMo_{1-x}S_2$ monolayer showing atomically thin stripes of alternating Mo (dark) and W (bright) atoms.

The resulting striped alloy is electronically isotropic, but vibrationally anisotropic, due to the very different atomic masses of Mo and W: first-principles calculations predict that phonon anomalies associated with stripe formation lead to an anisotropic thermal conductivity.

References

[1] Y. Wang, A. Azizi, Z. Lin, K. Wang, A. L. Elias, M. Terrones, V. H. Crespi and N. Alem, Nano Lett. **16**, 6982 (2016)

High field mangeto-transport in two-dimensional electron gas $LaAlO_3/SrTiO_3$

Ming Yang,[1] Kun Han,[2] Olivier Torresin,[1] Mathieu Pierre,[1] Shengwei Zeng,[2] Zhen Huang,[2] T. V. Venkatesan,[2] Michel Goiran,[1] J. M. D. Coey,[2,3] Ariando,[2] and Walter Escoffier[1]

[1]*Laboratoire National des Champs Magnétiques Intenses (LNCMI-EMFL), CNRS-UGA-UPS-INSA, 143 Avenue de Rangueil, 31400 Toulouse, France*

[2]*Department of Physics and NUSNNI-Nanocore, National University of Singapore, 117411 Singapore*

[3]*School of Physics and CRANN, Trinity College, Dublin 2, Ireland*

ming.yang@lncmi.cnrs.fr

The transport properties of complex oxide $LaAlO_3/SrTiO_3$ interface, with 10 unit cells of $LaAlO_3$, are investigated under high magnetic field (55T) [1]. After back-ground substraction, we observe small oscillations of the magneto-resistance with altered periodicity when plotted versus inverse magnetic field. We assume that this effect is linked to the Rashba spin-orbit coupling which fits reasonably well the experimental data [2] and remains consistent with large negative magneto-resistance when the field is parallel to the sample's plane [3]. Moreover, we observe a large inconsistency between the carrier density extracted from the pseudo-period of the Shubnikov-de Haas oscillations and from the Hall Effect. This discrepancy is explained by the contribution of at least two bands with different characteristics. On one hand, 2D electrons originating from the Ti2g (dxy orbitals) – derived orbitals of Ti and lying close the interface are sensitive to interface disorder and display low electronic mobility together with high carrier density. On the other hand, 2D electrons occupying the dxz and dyz orbitals are located deeper in the STO side of the interface and display low carrier concentration and high mobility. The interplay between these two types of charge carriers and their contribution to magneto-transport is discussed.

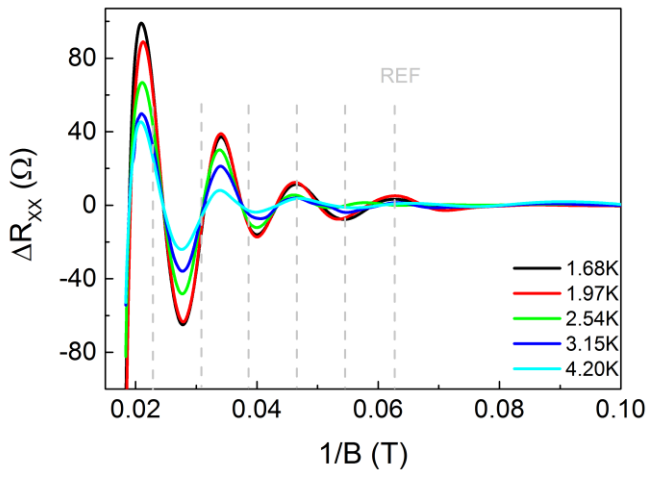

Fig. 1: Temperature dependence of oscillating part of the longitudinal resistance after subtraction of a smoothed background. The non-perfect periodicity of the SdH oscillations when plotted versus 1/B is related to the presence of strong Rashba spin-orbit coupling in $LaAlO_3/SrTiO_3$

References

[1] M. Yang *et al.* Appl. Phys. Lett. **109,** 122106 (2016).

[2] A. Fête et al. New J. Phys.**16**, 112002 (2014).

[3] M. Diez et al. Phys. Rev. Lett. **115**, 016803 (2015).

[4] M. Shalom et al. Phys. Rev. Lett. **105,** (2010).

Fermi arcs formation in Weyl semimetals: the key role of intervalley interaction

Zh.A. Devizorova[1,2] and V.A. Volkov[2,1]
[1]*Moscow Institute of Physics and Technology, 141700 Dolgoprudny, Russia*
[2]*Kotelnikov Institute of Radio-engineering and Electronics RAS, 125009 Moscow, Russia*
DevizorovaZhanna@gmail.com

We propose an analytical model [1] describing the surface states (including the Fermi arcs) observed in the recent investigations of Weyl semimetals [2]. The effective two-valley (two-cone) Hamiltonian is supplemented by the boundary conditions taking into account both the intravalley and intervalley interfacial interaction. We demonstrate that the latter is crucial for the formation of the surface states having the form consistent with the experimental data. The boundary condition contains two real phenomenological parameters. One describes the intravalley and the other one describes the intervalley interfacial interaction. We show that the shape and connectivity of the surface states are determined by the interplay between these parameters. In the case of noninteracting valleys, the Fermi contours take the form of rays which can either intersect or not. In the latter case, the presence of the intervalley interaction above some threshold value leads to the linking of the rays with the Fermi arcs formation, as shown in Fig. a. In the former case, the rays repel at the crossing point due to the intervalley interaction also forming the Fermi arcs (see Fig. b). The Fermi contours which do not form arcs in the two-valley approximation can nevertheless connect two remote valleys. We consider this possibility qualitatively in the four-valley approximation Comparing our results with the experimental data we obtain the values of the phenomenological boundary parameters.

The work was financially supported by the Russian Science Foundation (Project No. 16-12-10411).

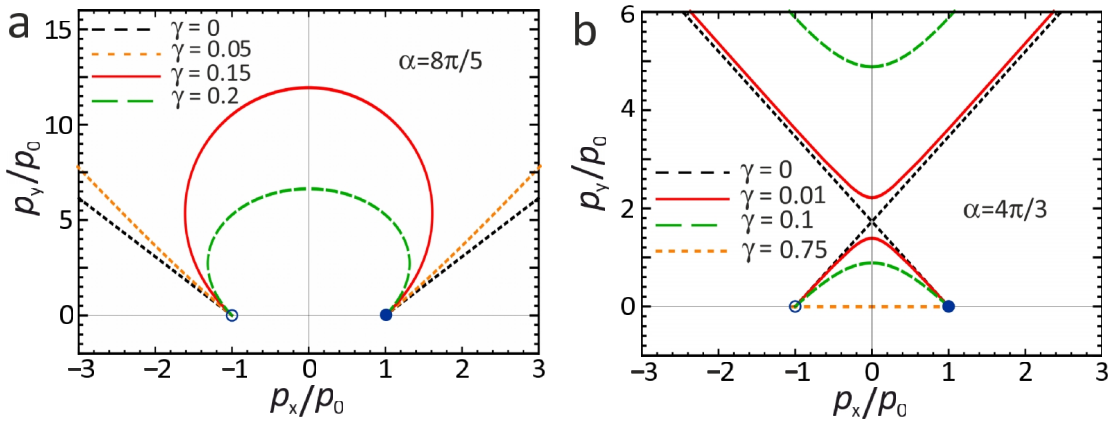

(a)The evolution of the (001) surface states' Fermi contours $E(p_x, p_y)=0$ as a function of the intervalley interaction γ for the fixed intravalley parameter α corresponding to not intersecting rays in the absence of the intervalley interaction (γ=0). The empty and solid blue circles show the projections of the bulk Weyl points with the opposite chiral charges. (b)The (001) surface states Fermi contours depending on the intervalley interaction γ at fixed α, for which the Fermi rays have the crossing point in the limit γ=0.

References

[1] Zh. A. Devizorova and V. A. Volkov, Phys. Rev. B **95**, 081302(R) (2017).
[2] S.-Y. Xu, I. Belopolski, N. Alidoust, et al., Science **349**, 613 (2015).

Correction ofPbSnTefilmsconductivity by the local doping with indium

D.V. Ishchenko, A.E. Klimov, S.P. Suprun
Institute of Semiconductor Physics Siberian Branch Russian Academy of Science
630090, 13 Lavrent'eva str., Novosibirsk, Russia
miracle4348@gmail.com

Currently, there is considerable interest in solid solutions of lead-tin-tellurium (LTT)for the following reasons: it is the perspectivematerial for far IR and THz rangephotodetectors [1], as a topological insulator [2] and for the exchange environment for a quantum computer [3]. In all these cases, it is required to have the high-resistancebulk of film which can be obtained by doping of LTT with indium [4]. However, up to the present time there is no any technique that allows to carry outthemodification of conductivity in the required areas of LTT epitaxial layers.

At the same time in the problems mentioned above for LTT use is requiredto have somehigh-resistance field of films.Sothe method of local diffusion of indium in the LTTfilms from 10 nm thickness layer deposited on a filmsurface by MBE has been developed.

It is known that LTT native oxide is predominantly consisting of the tellurium oxide. To remove it the undoped films were processed by oxide etchesbefore the indium deposition.

The polycrystalline samples with high mobility were used for measurement of the electrical properties. Temperature dependences of hole concentration in p-type conductivity LTT film with tin content of about 26 % and 1.9 microns thickness are shown in figure. The conductivity of $A^{IV}B^{VI}$-semiconductors is determined by intrinsic defects, which concentration does not decrease with temperature (curve 1). Undoped film was divided into several parts, each of which was doped with certain concentration. It is seen that increasing indium concentration measured without illumination leads to the hole concentration decrease from$2\cdot10^{18}cm^{-3}$ (without indium) to $5\cdot10^{12}cm^{-3}$ (with 1 % of indium) at 10 K.

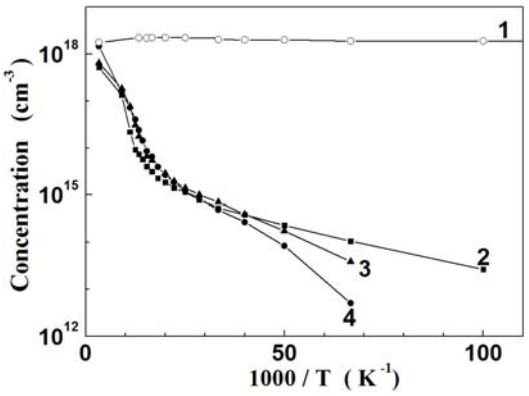

Fig.Temperaturedependencesofholeconcentrationin: 1 – virginsample, 2 –with 0.3 at.%of indium, 3 – 0.5 at.%, 4 – 1 at.%.

The film composition was measured in several points of the surface by EDX. It was shown that film had high homogeneity of indium content within the measurement accuracy.

So the technique of local diffusion of indium into LTT films from limit source was developed and offered. Such technique allows to obtain high resistivity areas of films and to correct conductivity of epitaxial LTT layers and can be used for creation of the planar transistor structures.

References

[1] D.R. Khokhlov, Phys. Usp.**49**, 955 (2006)
[2] S. Safaei, P. Kacman, and R. Buczko, Phys. Rev. **B 88**, 045305 (2013).
[3] A. E. Klimovet. al., Russian Microelectronics.**35**. 5. 277 (2006).
[4] B.A. Volkovet. al., Phys. Usp.**45**, 819 (2002)

Single domain high-quality Bi_2Se_3 epitaxial films grown on BaF_2

A.Yu. Kuntsevich[1,2,+], V.P. Martovitskii[2] and Yu.G. Selivanov[2]

[1]*National Research University Higher School of Economics, Moscow, 101000,Russia*

[2]*P.N.Lebedev Physical Institute, Moscow, 119991, Russia*

[+]alexkun@lebedev.ru

Bismuth diselenide is one of the most studied time-reversal-symmetry protected 3D topological insulators (TI) with the largest band gap (0.3 eV) among the family. Possible TI applications require growth of high structural quality thin films with a surface dominated transport. Single domain Bi_2Se_3 films were obtained on a lattice matched (111) InP substrates [1, 2], while a record surface state mobility was achieved using virtual substrate [3]. Almost in all reported communications growth is performed from elements with Se/Bi flux ratio being well above 10.

In our work we demonstrate modified two-step MBE growth of high-quality single domain Bi_2Se_3 films on lattice mismatched (5.6%) (111) BaF_2 substrate. Elemental Se and binary Bi_2Se_3 are evaporated from standard effusion cells. Before and during first-step low temperature deposition of 2QL film we do not supply Se flux trying to avoid ill controlled substrate Se termination. Subsequent heating of the initial Bi_2Se_3 layer under Se flux results in relaxed single domain template film grown in Van-der Waals epitaxy mode. Employment of binary Bi_2Se_3 charge allows us both to increase the second step growth temperature to 350 C and simultaneously to maintain stoichiometry of the layer with only 1:1 ratio between Se and Bi_2Se_3 fluxes. Growth of the body of the layer proceeds in a step-flow mode.

Resultant films are single crystalline with regular triangular domains as large as a few um (Fig1). XRD polar scans support single domain character of the films. Another figure of merit is high mobility of the surface carriers. From magnetoresistance and Hall resistance in a Se-capped sample 2-liquid model estimates for high mobility carriers $n=3\ 10^{12}$ cm^{-2} and $\mu=0.8$ m^2/Vs. This is comparable with the record parameters achieved so far. Period of the Shubnikov-de Haas oscillations gives almost the same density, and tilted magnetic field experiments signify 2D nature of the high mobility carriers.

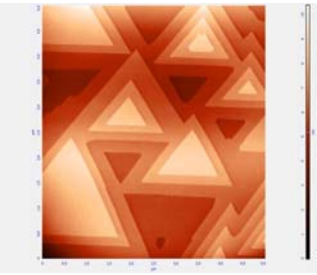

Fig.1 :5umx5um AFM image of 20 nm thick Bi_2Se_3 film

Our results thus suggest an alternative route towards high-quality single domain Bi_2Se_3 thin films.

References

[1] X. Guo et al, Appl. Phys. Lett, 102, 151604 (2013)

[2] N.V. Tarakina et al, Adv. Mater. Interfaces, 1, 1400134 (2014)

[3] N. Koirala et al, Nano Lett., 15, 8245 (2015)

Dimensionality Control of a Novel 2D Electron Gas Based on $KTaO_3$ (001) Interface

Ludi Miao, Jing Wang, Renzhong Du, Bailey Bedford, Nathan Huber, Ke Wang, and Qi Li
Physics Department, Penn State University,
University Park, PA 16803, USA
qil1@psu.edu

The discovery of two-dimensional electron gases (2DEGs) at transition metal oxide (TMO) surfaces and interfaces has opened up broad interest due to their exotic properties such as quantum Hall effect, 2D superconductivity and gate controlled ground states. Recently, 5*d* TMOs are hotly investigated due to their strong spin-orbit coupling (SOC), a key element of topological materials. Among them, $KTaO_3$ (KTO) not only hosts 2DEGs but also involves strong SOC. Here we report the discovery of 2DEG based on KTO oxide interface, with low temperature mobility as large as $8000 cm^2V^{-1}s^{-1}$. Strong Shubnikov-de Haas (SdH) oscillation in magnetoresistance is observed at low temperatures. Based on this playground we demonstrate a novel technique to perform quantum confinement. Indeed, we observed a drastic change in SdH oscillation from 3D-like behavior to 2D-like behavior. In addition, Fermi surface reconstruction due to the quantum confinement is also observed from SdH oscillation. Our results not only provide a novel playground for condensed matter physics and all-oxide device applications, but also open a promising new route in tailoring the dimensionality of electron gas systems.

Short Wavelength Infrared Detection Using Type II InAs/GaSb superlattice structure

Wenquan Ma, Jianliang Huang, Yanhua Zhang, and Yulian Cao
Key Laboratory of Semiconductor Materials Sciences, Institute of Semiconductors, Chinese Academy of Sciences, Qinghua East A35, Beijing 100083, China
wqma@semi.ac.cn

Type II InAs/GaSb superlattice (SL) structure has many advantages for infrared photodetector applications and its detection wavelength is proved to be able to cover the range of about 3 to 30 μm by tuning the constituent layer thickness and the thickness ratio of InAs to GaSb. However, it is important to explore the possibility to further extend the detection wavelength as far as possible to cover the whole range of the short wavelength (SW) infrared window by using type II InAs/GaSb SLs.

We reveal that a strong In intermixing occurs during the growth of SW InAs/GaSb SL structure. The In intermixing is strongly related to the growth temperature and can have a very big impact on the SL band structure. To reduce the influence of the In intermixing on the SL band structure, besides lowering the growth temperature, another effective scheme is to increase the GaSb layer thickness in the SL structure. Experimentally, we demonstrate that a *p-i-n* type of detector reaches 2.56 μm (50% cutoff wavelength) at 77 K [1]. We also demonstrate that type II SL structure can reach the detection wavelength very close to 1 μm by inserting thin AlSb barriers and the detector exhibits a narrow-band photoresponse feature [2,3].

References

[1], J.L. Huang, W.Q. Ma, Y. Wei, Y.H. Zhang, K. Cui, Y.L. Cao, X.L. Guo, and J. Shao, IEEE J. Quantum Electron. **48**, 1322 (2012).
[2], J.L. Huang, W.Q. Ma, Y.H. Zhang, Y.L. Cao, K. Liu, W.J. Huang, and S.L. Lu, IEEE Photo. Technol. Lett., **27**, 2276 (2015).
[3], Y.H. Zhang, W.Q. Ma, J.L. Huang, Y.L. Cao, K. Liu, W.J. Huang, C.C. Zhao, H.M. Ji, and T. Yang, IEEE Electron Device Lett. **37**, 1166 (2016).

.

Fast and Highly Sensitive Ionic Polymer Gated WS_2-Graphene Photodetectors

Jake Mehew,[1,2] Selim Unal,[2] Elias Torres Alonso,[2] Gareth F. Jones,[2] Saad Fadhil Ramadhan,[2,3] Monica F. Craciun,[2] and Saverio Russo.[2]

[1]*EPSRC Centre for Doctoral Training in Metamaterials, University of Exeter, Exeter, EX4 4QL*

[2]*Centre for Graphene Science, University of Exeter, Exeter, EX4 4QL, UK*

[3]*Department of Physics, College of Science, University of Duhok, Duhok, Iraq*

j.mehew@exeter.ac.uk

The combination of graphene with semiconductor materials in heterostructure photodetectors, has enabled amplified detection of femtowatt light signals using micron-scale electronic devices. Presently, the speed of such detectors is limited by long-lived charge traps and impractical strategies, e.g. the use of large gate voltage pulses, have been employed to achieve bandwidths suitable for applications, such as video-frame-rate imaging. [1-4]

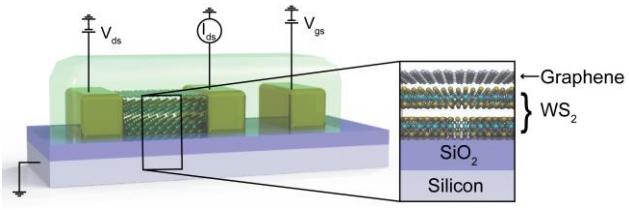

Fig.1 Device schematic with electrical connections included. A voltage (V_{gs}) is applied to the transparent polymer (PEO + $LiCl0_4$) using a gate electrode in close vicinity to the WS_2-graphene photodetector.

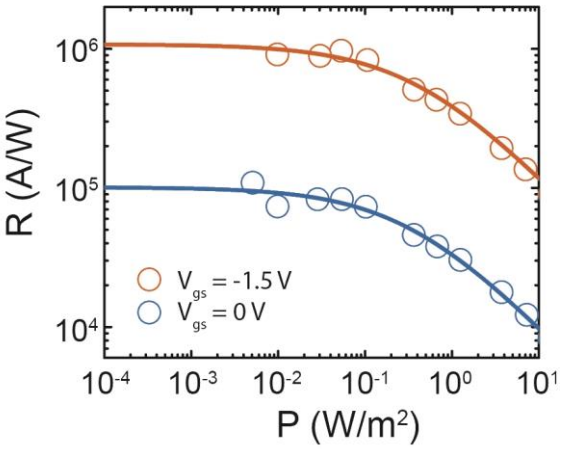

Fig.2 Responsivity as a function of incident optical power with and without a finite bias applied to the polymer gate.

Here, we report graphene-few layer WS_2 heterostructure photodetectors encapsulated in an ionic polymer (Fig. 1), which are uniquely able to operate at bandwidths up to 1.5 kHz, whilst maintaining internal gain as large as 10^6. Highly mobile ions and a nanometre scale Debye length of the ionic polymer are used to screen charge traps and tune the Fermi level of graphene over an unprecedented range at the interface with WS_2. We observe a responsivity R = 10^6 A/W (Fig. 2) and detectivity D* = $3.8x10^{11}$ Jones, approaching that of single photon counters.

The combination of both high responsivity and fast response times makes these photodetectors suitable for video-frame-rate imaging applications.

References

[1] Konstantatos G., Nat. Nano., 7 (2012) 363
[2] Sun Z., Adv. Mat., 24 (2012) 5878
[3] Roy K., Nat. Nano., 8 (2013) 826
[4] Zhang W., Sci. Rep., 4 (2014) 3826

Electronic and structural characterization of a graphene-MoS_2 van der Waals heterostructure.

Karen Muñoz[1] and Camilo Espejo[2]

[1]*Maestría en modelado y simulación. Universidad de Bogotá Jorge Tadeo Lozano, Bogotá, Colombia.*

[2] *Grupo de modelado y simulación de sistemas, Universidad de Bogotá Jorge Tadeo Lozano, Bogotá, Colombia.*

karena.munozp@utadeo.edu.co

camilo.espejo@utadeo.edu.co

Keywords. Heterostructure, Density Functional Theory, van der Waals interactions, abinit.

In recent years it has arisen great interest in the study and applications of graphene like materials [1,2] such as MoS_2 [3] and other so called 2D materials [4]. Due to the weak van der Waals forces which held the layers of these materials together, it is possible to build a new kind of heterostructures by stacking the monolayers of different materials one on top of each other [1,5]. Thanks to both nowadays computational power and efficient algorithms it is possible to study this type of heterostructures [6] using theoretical approaches such as density functional theory (DFT). In this work it was conducted a study of the structural and electronic properties of a van der Waals heterostructure composed of graphene and MoS_2. Its initial structural parameters were taken as the magnitude of the primitive vectors of each material ($2.47\,\mathring{A}$ for graphene [7] and $3.167\,\mathring{A}$ for MoS_2 [8]) and with them we built a supercell consisting of five cells of graphene and four cells of MoS_2 which guarantee in plane periodicity with a margin of error of 2.5%, similar result to that obtained reported in [9]. In Figure 1 the heterostructure is displayed using the Avogadro program.

Using the DFT code ABINIT [10] convergence studies were performed, geometry optimization and band structure of each component to find the appropriate parameters for calculations of the heterostructure. Dispersion energy was calculated with DFT-D3 method [11]. Our results show that the optimum distance between the layers is $3.3\,\mathring{A}$ without vdW and $3.1\,\mathring{A}$ with vdW. The binding energy is of $-30.2\,meV/atom$ without vdW and $-70.81\,meV/atom$ with vdW and band structure graphene-MoS_2 bulk it was observed and band gap of 0.04 eV at K point and 0.02 eV at H point.

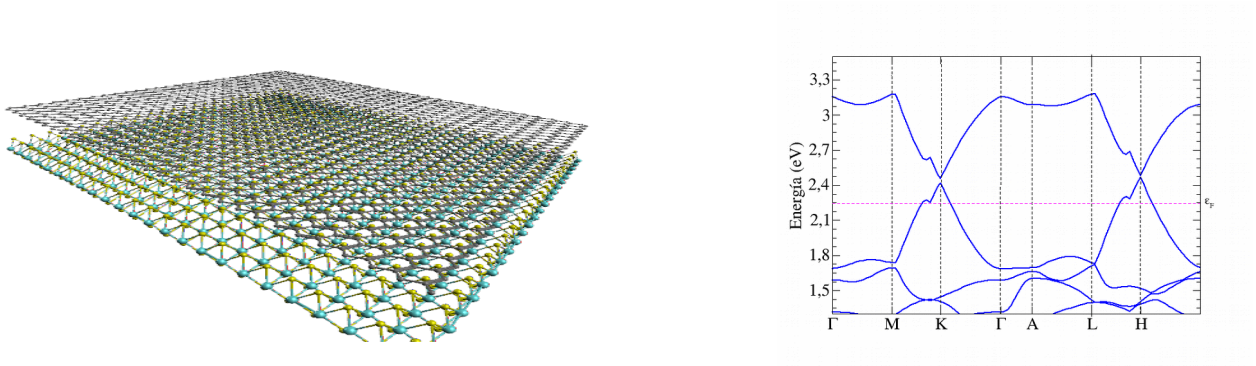

Figure 1: Bilayer of graphene/MoS_2 and band structure of graphene/MoS_2 bulk.

References

[1] Geim, Grigorieva A. K., and I. V. Van der waals heterostructures. *Nature*, 499:419–425, 2013.

[2] K. S. Novoselov, A. K. Geim, S. V. Morozov, D. Jiang, Y. Zhang, S. V. Dubonos, I. V. Grigorieva, and A. A. Firsov. Electric field effect in atomically thin carbon films. *Science*, 306(5696):666–669, 2004.

[3] C. Espejo, T. Rangel, A. H. Romero, X. Gonze, and G.-M. Rignanese. Band structure tunability in MoS_2 under interlayer compression: A DFT and GW study. *Phys. Rev. B*, 87:245114, Jun 2013.

[4]Li Tao, Eugenio Cinquanta, Daniele Chiappe, Carlo Grazianetti, Marco Fanciulli, Madan Dubey, Alessandro Molle, and Deji Akinwande. Silicene field-effect transistors operating at room temperature. Nature Nanotechnology, 10(3):227–231, March 2015.

[5] Xiaomu Wang and Fengnian Xia. Van der Waals heterostructures: Stacked 2D materials shed light. *Nature Materials*, 14(3):264–265, March 2015.

[6] Jerzy Bernholc. Computational Materials Science: The Era of Applied Quantum Mechanics. Physics Today, 52(9):30–35, January 2008.

[7] Towfiq Ahmed, N. A. Modine, and Jian-Xin Zhu. Graphene/MoS2 van der Waals Bilayer as the Anode Material for Next Generation Li-ion Battery: A First-Principles Investigation. arXiv:1502.07398 [cond-mat], February 2015. arXiv: 1502.07398.

[8] Mos2: crystal structure, physical properties: Datasheet from landolt-b¨ornstein - group iii condensed matter · volume 41d: “non-tetrahedrally bonded binary compounds ii” in springermaterials (http://dx.doi.org/10.1007/10681735 690). Copyright 2000 Springer-Verlag Berlin Heidelberg.

[9] Jin-Wu Jiang and Harold S. Park. Mechanical properties of MoS_2 /graphene heterostructures. Applied Physics Letters, 105(3), 2014.

[10] X. Gonze, *et. al*. Recent developments in the ABINIT software package. Computer Physics Communications, 205:106-131, August 2016.

[11] Stefan Grimme, Jens Antony, Stephan Ehrlich, and Helge Krieg. A consistent and accurate ab initio parametrization of density functional dispersion correction (DFT-D) for the 94 elements H-Pu. J. Chem. Phys., 132(15):154104, 2010.

A Universal Large Scale Layer Engineering and Patterning Scheme for van der Waals Materials

Chithra H. Sharma, Abin Varghese and Madhu Thalakulam
School of Physics, Indian Institute of Science Education and Research Thiruvananthapuram, 695016, Kerala, India
madhu@iisertvm.ac.in

All-two-dimensional devices consisting of semiconducting, metallic and insulating van der Waals (vW) materials offer a comprehensive solution to overcome the current scaling limit of the microelectronics industry. Devising methods for layer engineering, patterning and improving the contacts in these materials are of paramount importance in realizing all-two-dimensional logic circuits. All-two-dimensional technology could greatly benefit from a universal layer-engineering scheme for the vW materials irrespective of their material or electrical properties. Various schemes have been explored for controlled etching of vW materials which involves chemical treatment, thermal processing or RF plasma, most of which damage the material. We present here a microwave plasma based layer engineering and patterning strategy for MoS2 and other vW materials. The layer removal does not involve any reactive gasses or chemical reactions and relies on breaking the weak inter-layer vW interaction making it a generic technique for a wide spectrum of layered materials and heterostructures. Compatibility of the microwave process with the standard device fabrication schemes and the capability to etch large area bulk samples down to the few layer regime retaining the material and electrical qualities make this technique a viable processing tool for the integration of vW materials into the semiconductor industry. The process preserves the pre-etch layer topography and yields a smooth and pristine-like surface. From Raman spectroscopy, atomic force microscopy, photoluminescence spectroscopy, scanning electron microscopy and transmission electron microscopy, we confirm that the structural and morphological properties of the material have been retained. The devices made from the plasma etched samples showed similar mobility to that of pristine sample and improved contacts were observed in plasma treated samples, suggesting that the process has not compromised on the electrical properties as in the case of other etching and patterning techniques. [1] Additionally, we demonstrate that our plasma etching strategy can be extended for device patterning using a lithography defined metal mask, making this a versatile process suitable for large scale layer engineering and patterning vW material systems.

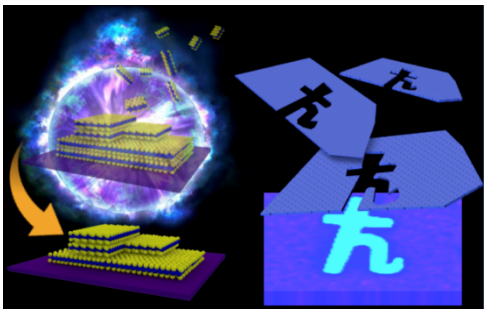

Fig.1 Schematic showing the topography preserved layer engineering and pattering.

References

[1] J. Wu, H. Li, Z. Yin, H. Li, J. Liu, X. Cao, Q. Zhang, and H. Zhang, Small **9**, 3314 (2013).

Observation of Topological Hall Effect in $SrCoO_3$ Thin Films

Ding Zhang[1,2], Nianpeng Lu[1], Yujia Wang[1], Zheng Duan[1], Pu Yu[1,2,3], and Qi-Kun Xue[1,2]
[1]*State Key Laboratory of Low Dimensional Quantum Physics and Department of Physics, Tsinghua University, Beijing, 100084, China*
[2]*Collaborative Innovation Center of Quantum Matter, Beijing, China*
[3]*RIKEN Center for Emergent Matter Science (CEMS), Saitama, Japan*
dingzhang@tsinghua.edu.cn

Topologically nontrivial spin textures formed in a ferromagnetic material, such as skyrmions, constitute a fictitious magnetic field on the charge carriers. This emergent field therefore may produce an additional Hall signal—the so-called topological Hall effect (THE) [1,2]—on top of the ordinary and anomalous Hall effects. Here we artificially realize THE by straining a ferromagnetic metal via interface engineering, a strategy different from the established approach of merging a ferromagnet with a strongly spin-orbit coupled film [3]. We observe THE and anomalous magnetization in strained $SrCoO_3$ thin films on $(LaAlO_3)_{0.3}$-$(SrAl_{0.5}Ta_{0.5}O_3)_{0.7}$(001) (LSAT) substrates at low temperatures and in the magnetic field window of ±4 Tesla. Both features strongly indicate the formation of a skyrmion lattice. Our high quality $SrCoO_3$ thin films grown by pulsed laser deposition and subsequent annealing in ozone atmosphere show fully metallic behavior with record-low residual resistivity values (Fig. 1 (a)). Magnetotransport measurements unveil the archetypical characteristics of THE (Fig. 1 (b)): at 25K, where the anomalous Hall signal vanishes, a triangular shaped hump (dip) emerges from 0 to 4 T (0 to -4 T). This anomaly can be readily attributed to the THE after excluding the possible multi-band Hall effect. Fig. 1 (c) further highlights the twisted magnetization curves when applying a perpendicular magnetic field, confirming the existence of spin textures.

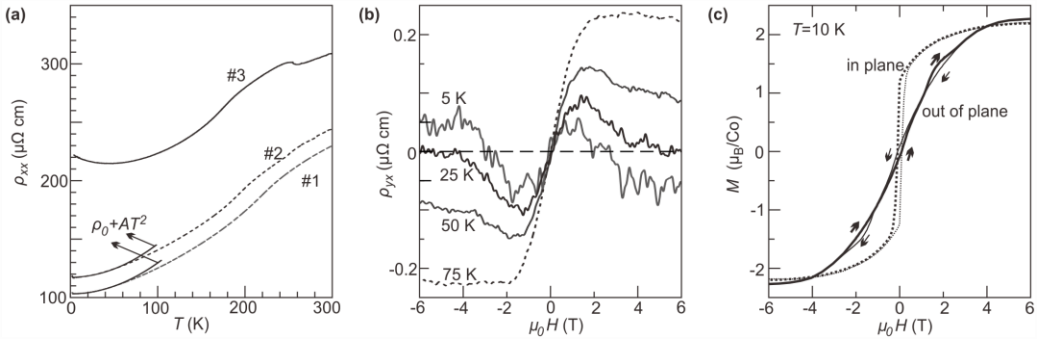

Figure 1 (a) Resistivity as a function of temperature for three $SrCoO_3$ thin films. (b) Hall resistivity of sample #1 at different temperatures. (c) Magnetization curves obtained at 10 K.

References

[1] M. Lee, W. Kang, Y. Onose, Y. Tokura, and N. P. Ong, *Phys. Rev. Lett*. **102**, 186601 (2009).

[2] A. Neubauer, C. Pfleiderer, B. Binz. A. Rosch, R. Ritz, P. G. Niklowitz, and P. Boni, *Phys. Rev. Lett*. **102**, 186602 (2009).

[3] J. Matsuno, N. Ogawa, K. Yasuda, F. Kagawa, W. Koshibae, N. Nagaosa, Y. Tokura, and M. Kawasaki, *Sci. Adv.* **2**, e1600304 (2016).

Thermal Energy and Charge Currents in Multi-Terminal Nanorings

Christian Riha[1] , Tobias Kramer[1,2], Christoph Kreisbeck[1], Olivio Chiatti[1] , Sven S. Buchholz[1] , Dirk Reuter[2] , Andreas D. Wieck[3] and Saskia F. Fischer[1]

[1]*Novel Materials Group, Humboldt-Universität zu Berlin, 12489 Berlin, Germany*
[2]*Konrad-Zuse-Zentrum für Informationstechnik Berlin, Takustraße 7, 14195 Berlin, Germany*
[3]*Optoel. Materialien und Bauelemente, Univ. Paderborn, 33098 Paderborn, Germany*
[4]*Angewandte Festkörperphysik, Ruhr-Universität Bochum, 44780 Bochum, Germany*

sfischer@physik.hu-berlin.de

Heat flow, transport and fluctuations in quantum wire structures are of interest in semiconductor nanostructures with potential applications for quantum devices. In the limit of non-interacting charge carriers the heat and charge transfer processes are coupled, as given by the Wiedemann-Franz relation between the electrical and thermal conductivity.
Here, we present combined experimental and computational investigations [1-4] of thermal non-equilibrium in low-dimensional (non-interacting) electron systems. We study the thermal energy and charge transfer close to the quantum limit in a ballistic nanoscale device (Fig. 1) consisting of multiply connected one-dimensional waveguides. The fabricated device is based on an AlGaAs/GaAs heterostructure and is covered by a global top-gate to steer the energy and charge transfer in the presence of a temperature gradient, which is established by a heating current. The evaluation of the heat transfer using thermal noise measurements shows the device acting as a switch for charge and energy transfer. A mode-dependent redistribution of the energy current was also found if a scatterer breaks the device symmetry.

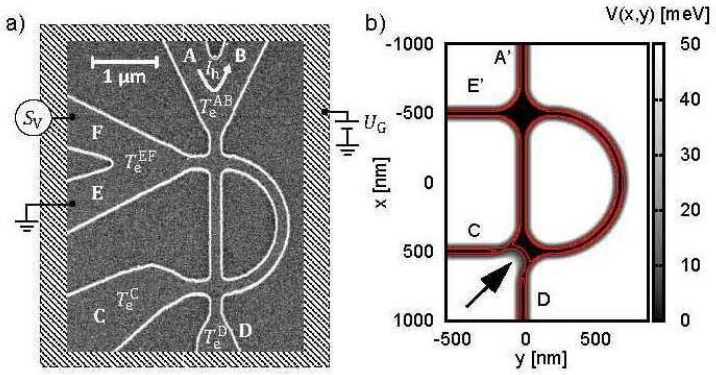

Fig. 1 Device geometry. (a) Scanning electron micrograph of an identically processed sample. The 1D waveguides with a lithographical width of 170 nm form a half-ring connected to reservoirs A-F. (b) Device potential for the ballistic transport model.

Acknowledgements: This work has been financially supported by the German Science Foundation within the priority programme SPP1386 "Nanostructured Thermoelectrics".

References

[1] T. Kramer, *et al.* , AIP Advances **6**, 065306 (2016).
[2] C. Riha, *et al*. Phys. Status Solidi **213**, 571-581 (2016). (*Feature article*)
[3] C. Riha, *et al*. Appl. Phys. Lett. **106**, 083102 (2015).
[4] S. S. Buchholz, *et al.* Phys. Rev. B **85**, 225301 (2012).

Polarization Rotation via Phonon Coherence in Coupled Quantum Dots

Andrew R. Jacobs, Joshua Casara, Cameron Jennings, Parveen Kumar, and Michael Scheibner
Department of Physics, University of California, Merced
Merced, CA 95348, USA
ajacobs@ucmerced.edu

The ability to generate and use coherent lattice vibrations in solid-state materials is crucial to the nascent field of phononics. In fact, such functionality could prove invaluable in preexisting electronic and optical devices to increase efficiency by taking advantage of mechanical or thermal vibrations. A convenient aspect of phononics is the ability to draw parallels to well-established areas of study, such as circuit electronics and photonics. In this sense, one can envision single-phonon control as analogous to single-electron control in circuit-operated devices and single-photon control in photonic studies. Indeed, lattice vibrations are being discussed as candidates for qubits in future quantum information schemes, much like electronic spins or polarized photons.

One promising system for coherent phonon production is quantum dots. In particular, quantum dots offer a considerable amount of tunability with regard to their material properties and size during fabrication. Past studies have proposed quantum dots for use in coherent polaron generation [1] and phonon lasing [2]. Here, we theoretically study the use of pairs of coupled quantum dots to promote coherent behavior in phonons. This is accomplished by mixing a single-dot, bound exciton—phonon state with a longer lived, spatially indirect exciton [3].

The scheme we study here relies on coupling between a continuum single-dot state and a discrete indirect state via phonon-mediated hole tunneling. As a result, Fano-type interference occurs, giving rise to asymmetric optical spectra from the coupled dots. Because hole tunneling only occurs for a particular spin state of the exciton, optical selection rules dictate that only certain polarizations of light will encounter the asymmetric spectrum. All other polarizations will observe a standard Lorentzian spectral peak from the coupled dots. These two spectral configurations have different refractive indices, so we theoretically demonstrate an optophononic polarization rotation due to the Fano-like spectrum induced by the coherent phonon behavior.

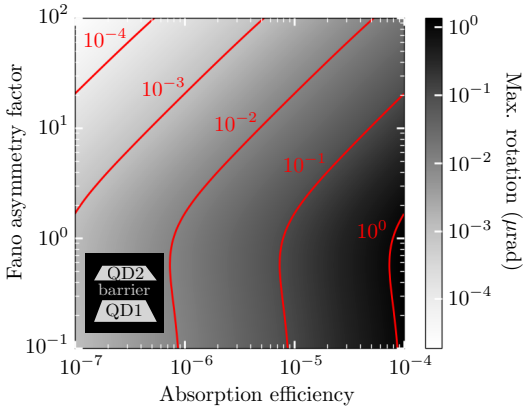

Fig. 1 Map of maximal polarization rotation as a function of optical efficiency and Fano asymmetry; red contours indicate constant polarization angle. Inset: schematic of two coupled quantum dots separated by a tunnel barrier.

Using the original Fano model and assuming an optically active region of size 10 nm, composed of the two dots and a tunnel barrier, we calculate a polarization rotation greater than 20 microradians in ideal circumstances. We also demonstrate the robustness of the rotation to imperfect absorption efficiency, as well as varying indirect exciton linewidth, spectral fluctuations, and Fano asymmetry. Lastly, we extend the scope of the treatment to a larger range of Fano asymmetries. We calculate the asymmetric spectrum using a fully quantum mechanical, master equation formalism that accounts for both weak- and strong-coupling regimes of the exciton with the lattice vibrations of the dots.

[1] S. Sauvage et al., Phys. Status Solidi B **243**, 3895 (2006).
[2] A. Khaetskii, V. N. Golovach, X. Hu, and I. Zutic, Phys. Rev. Lett. **111**, 186601 (2013).
[3] M. L. Kerfoot et al., Nat. Commun. **5**, 3299 (2014).

Coordination Defects: a Novel Type of Grain Boundary-Producing Defect

B. Katz and V. Crespi
Physics Department, Penn State University,
University Park, PA 16803, USA
bnk120@psu.edu

A novel defect type in two-dimensional systems is presented, which involves the local coordination number of atoms in an otherwise regular structure. While point-like by itself, such a 'coordination defect' is shown to have a dramatic influence on the growth of the system following its formation due to its introduction of a mismatch in bond network topology and physical ring size. The potential growth pathways of an example graphene system are followed after the occurrence of such a defect using molecular dynamics [1] and first-principles calculations [3]; the unavoidable overcorrections that occur as the system grows past the defect may possibly cause a runaway feedback resulting in the spawning of one or more grain boundaries. These defects can be of varying size, producing predictable changes in the growth of the system after the defect. The appearance of this defect type is predicted to have similar ramifications across a broad array of two-dimensional systems, potentially providing a new method of controlling grain boundary behavior and location.

References

[1] S. G. Srinivasan, A. C. T. van Duin, and P. Ganesh, J. Phys. Chem. A, **119**, 4 (2015).
[2] Stuart, Tutein, Harrison, J Chem. Phys., **112**, 6472-6486 (2000).
[3] M. Dion, H. Rydberg, E. Schröder, D. C. Langreth, and B. I. Lundqvist, Phys. Rev. Lett. **92**, 246401 (2004).

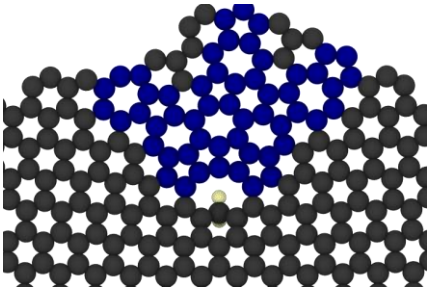

Fig.1 A pointlike coordination defect (in yellow) can result in a cascade of additional defects (in blue) as the system attempts to simultaneously correct mismatches in ring size and topology, potentially spawning grain boundaries.

Kondo effect in self-assembled SiGe quantum dot

R. Shikishima[1], H. Kiyama[1], K. Kawaguchi[1], M. Bamesreiter[2], D. Bougeard[2], and A. Oiwa[1,3]
Physics Department, Penn State University, [1]*Institute of Scientific and Industrial Research, Osaka University, 8-1 Mihogaoka, Ibaraki, Osaka 567-0047, Japan*
[2]*Institut für Experimentelle und Angewandte Physik, Universität Regensburg, D-93040 Regensburg, Germany*
[3]*Center for Spintronics Research Network, Graduate School of Engineering Science, Osaka University, 1-3 Machikaneyama, Toyonaka, Osaka, Japan*
kiyama@sanken.osaka-u.ac.jp

Spins in semiconductor quantum dots (QDs) are a promising candidate for qubits because of their long coherence time, electrical controllability, and scalability. Studies for electron spins in GaAs QDs have shown that the contact hyperfine interaction with nuclear spins in host materials is the dominant mechanism of the loss of spin coherence. For longer spin coherence time, QDs made of group IV semiconductor has been extensively studied because of its low natural abundance of nuclear spins. Recently, SiGe self-assembled QDs and nanowires are gaining interest because of the p-type structures [1,2]. The contact hyperfine interaction will be absent for holes because of the p-orbital-like symmetry, therefore the spin coherence time may be further improved. In addition, strong spin-orbit interaction is expected in the SiGe QD systems, which is useful for electrical coherent manipulation of spins [3].
In this work, we investigate the transport properties of single hole transistors using self-assembled SiGe QD at low temperatures. SiGe QDs are grown by molecular beam epitaxy in Stranski-Krastanow mode. We choose QDs with a diameter of approximately 80 nm, and fabricate source and drain electrodes by depositing aluminum [Fig. 1(a)]. Figure 1(b) shows the differential conductance measured at a temperature of 2 K as a function of the source-drain voltage and the voltage applied to the P-doped Si back-gate layer. Coulomb diamond structures are observed, though the boundaries of the diamonds are indistinct because of the large tunnel coupling to leads. At the back-gate voltage around −4 V, we observe zero-bias peaks, which may be attributed to Kondo effect. We investigate the temperature [Fig. 1(c)] and magnetic field dependences of the zero-bias peaks, and find that both dependences are consistent with Kondo effect in QDs.

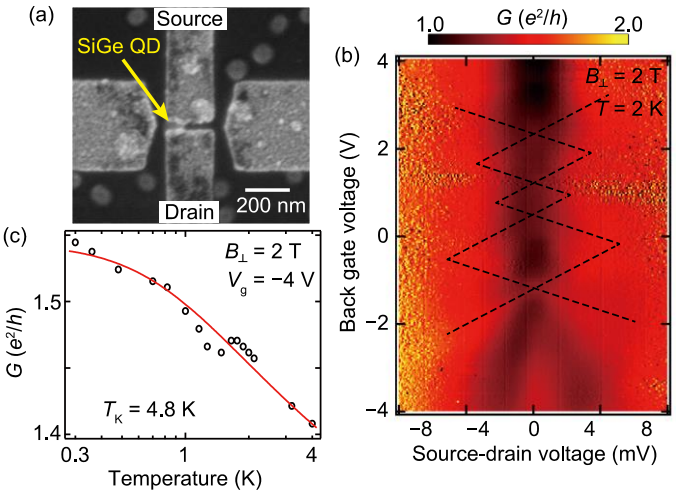

Fig.1 (a) Scanning electron micrograph of the device. (b) Differential conductance as a function of the source-drain voltage and the back-gate voltage. (c) Temperature dependence of the zero-bias peak conductance.

References

[1] G. Katsaros *et al*., Nature Nanotech. **5**, 458 (2010).
[2] A. P. Higginbotham *et al*., Nano Lett. **14**, 3582 (2014).
[3] S. Nadj-Perge *et al.*, Nature **468**, 1084 (2010).

Coupling of Spin States in Quantum Dots to a Magnetic Field Resilient Resonator

A. J. Landig, J. V. Koski, P. Scarlino, C. Reichl, W. Wegscheider, A. Wallraff, T. Ihn, and K. Ensslin,
Laboratory for Solid State Physics, ETH Zurich,
CH- 8093 Zurich, Switzerland
alandig@phys.ethz.ch

We investigate spin physics of a double quantum dot (DQD) coupled to a magnetic field resilient resonator. In-plane magnetic field resilience is achieved by fabricating the resonator out of a thin film of NbTiN [1]. The DQD is operated in a two-electron configuration near the (1,1) –> (0,2) charge transition, where the singlet (1,1)S and the singlet (0,2)S states hybridize and couple via dipole interaction with the cavity field in the resonator, observed on resonance as a change in its transmission amplitude. As the sample is subjected to an external magnetic field of up to 2 T, spin blockade [2] is observed in resonator response. Furthermore, we observe how applying a voltage bias across the DQD can either lift or induce a spin blockade, depending on the direction of the bias applied.

Our experimental configuration allows us to directly probe the occupation of the singlet states. In contrast to a related experiment [3], the minimum energy determined by the experimentally controllable interdot tunnel coupling can be either above or below the energy of the resonator mode. This allows us to independently address the two cases where either (1,1)S or (0,2)S has lower energy. Our setup allows us to determine the g-factor of the substrate, the energy difference between the singlet and triplet states, and the interdot tunnel coupling of the DQD by measuring the resonator response.

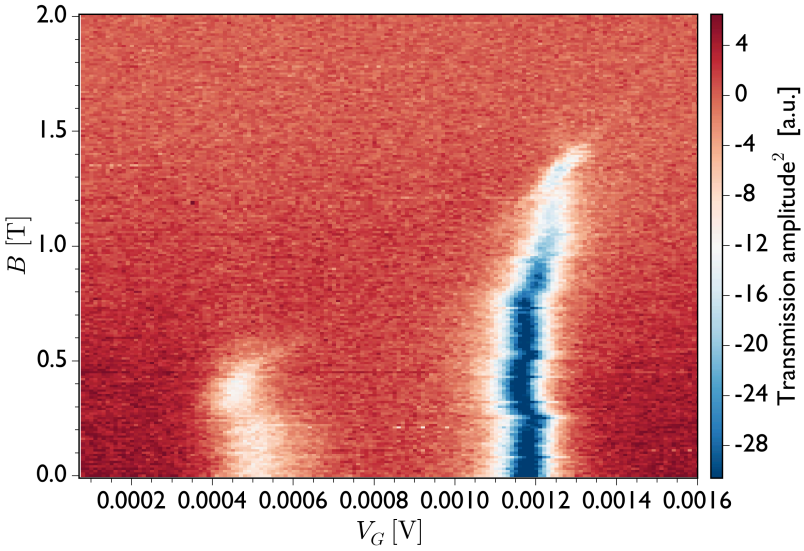

References

[1] N. Samkharadze, A. Bruno, P. Scarlino, G. Zheng, D. P. DiVincenzo, L. DiCarlo, and L. M. K. Vandersypen, Phys. Rev. Applied **5**, 044004 (2015).
[2] K. Ono, D. G. Austing, Y. Tokura, and S. Tarucha, Science **297**, 1313-1317 (2002).
[3] M. D. Schroer, M. Jung, K. D. Petersson, and J. R. Petta, Phys. Rev. Lett. **109**, 166804 (2012).

Selective-area growth of GaAs nanowires on Ge(111) substrates

Yusuke Minami, Akinobu Yoshida, Katsuhiro Tomioka, Junichi Motohisa

Graduate School of Information Science and Technology and Research Center for Integrated Quantum Electronics(RCIQE), Hokkaido University, North 14 West 9, Sapporo 060-0814 Japan.

e-mail:minami@rciqe.hokudai.ac.jp

III-V compound semiconductor nanowires (NWs) are expected to be used as future high-efficiency photovoltaic devices with various multi-junction cell structures consisting of highly lattice-mismatched system because nanometer-scaled footprints of the NWs suppress formation of misfit dislocations due to lattice mismatch [1]. Also, periodic array of NWs exhibits more efficient light absorption due to strong light-trapping effect [2] than planar structures. In addition, the NWs array saves material resource and cost. In this study, we characterized selective-area growth of GaAs NWs on Ge(111) toward GaAs NWs/Ge two-junction solar cells [3].

In the experiment, p-Ge(111) substrates with a 20 nm-thick SiN film was used as mask template. Since GaAs NWs preferentially grow along the <111>B direction, formation of (111)B-polar surface is important for aligning vertical GaAs NWs on non-polar Ge(111) substrates [4]. Thus, AsH_3 was supplied prior to the growth for the replacement of outermost Ge with As in order to from (111)B-polar surface. After that, low-temperature buffer GaAs was grown to prevent desorption of As atoms from the (111) polar surface. We found that the uniformity of NWs with lateral {-110} facets was improved by introducing the low-temperature buffer growth. We also grew GaAs NWs with V/III ratio of 62.5 - 250. Fig. 1(a) shows a representative SEM image of GaAs NWs on Ge(111) with V/III ratio of 62.5. The aspect ratio (average height/average diameter) of GaAs NWs increased as V/III ratio decreased because formation of As-trimer was decreased while suppressing lateral over growth. Fig. 1(b) shows a transmission electron microscope (TEM) image at the GaAs NW/Ge heterointerface. The TEM revealed no misfit dislocations were formed at the GaAs/Ge heterointerface. Optical properties of the grown GaAs NWs will be discussed.

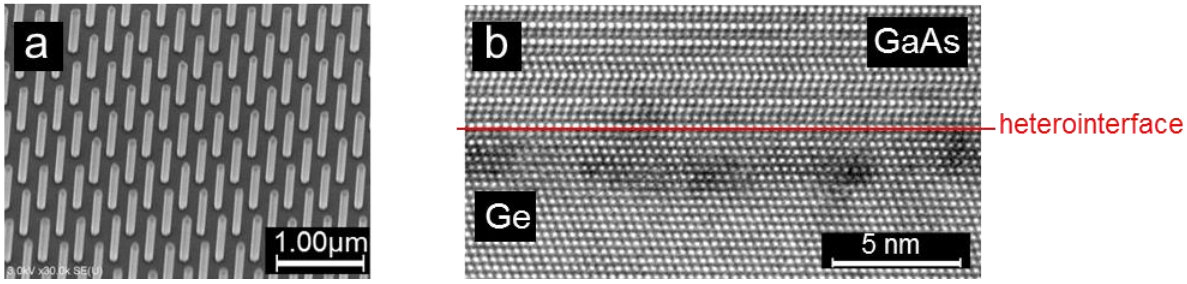

Fig. 1. (a) SEM images showing GaAs NWs on Ge(111) with low-temperature buffer growth. (b) TEM images showing crystal structures and heterointerface of GaAs NW/Ge

Reference

[1] F. Glas, *Phys. Rev. B* **74**, 121302(R) (2006)

[2] O. L. Muskens *et al*., *Nano Lett.* **8,** 2638 (2008)

[3] J. Motohisa and K. Hiruma, *Jpn. J. Appl. Phys*. **51,** 11PE07 (2012)

[4] K. Tomioka *et al*., *Nano Lett*. **15**, 7253 (2015)

Electrical characterization/magneto-transport of few-electron quantum dots formed by crystal phase engineering in InAs Nanowires

Malin Nilsson[1], Sebastian Lehmann[1], Kimberly A. Dick[1,2] and Claes Thelander[1]
[1] *Solid State Physics and NanoLund, Lund University, Box 118, S-221 00 Lund, Sweden*
[2] *Center for Analysis and Synthesis, Lund University, Box 124, S-221 00 Lund, Sweden*

We have studied electronic properties of quantum dots (QDs) epitaxially formed in InAs nanowires (NWs) by inserting thin segments of wurtzite (WZ) in otherwise zinc blende (ZB) crystal structure. These WZ segments act as tunnel barriers for electron transport and define the QD in the axial dimension [1]. The axial extension of the QD is less than 10 nm, [Fig. 1(a)], which leads to a strong quantum confinement and enables the QD to be fully depleted of electrons [Fig. 1(b)]. An important motivation for studying this system is that the InAs QD can be used as an epitaxial template for realizing coupled InAs-GaSb core-shell QDs [2], suitable for investigations of electron and hole interactions [3].

The magneto-transport in the system has been studied for the lowest electron orbitals (n). $|g|$*-factors have been extracted from the magnetic-field dependent split of the spin states ($\Delta E = |g|^*\mu_B B$), visible as an on-set of inelastic co-tunneling during Coulomb blockade when the QD is an odd-N state [Fig. 1(c)]. For a B-field perpendicular to the substrate plane, we found nearly similar $|g|$*-factors for the three lowest orbitals (in one device $|g|^*$= 8.7, 8.4, 8.8 for n =1-3, respectively). In angle-dependent in-plane measurements, we find an oscillating behavior of the $|g|$*-factor with a maximum when the B-field is aligned with the axis of the NW. The radial confinement in the QD is essentially determined by global back gate. The corresponding extracted single particle level spacing (E_Δ) for the three orbitals discussed above is in the order of 17-6 meV which make the measured $|g|$*-factors large compared to previously reported values.

In addition to the magneto-transport measurements, we have also used local side-gates to efficiently control the spatial distribution of the electron wave function [4]. The long-term goal is to be able to tune electron-hole interactions in self-assembled InAs-GaSb core-shell QDs.

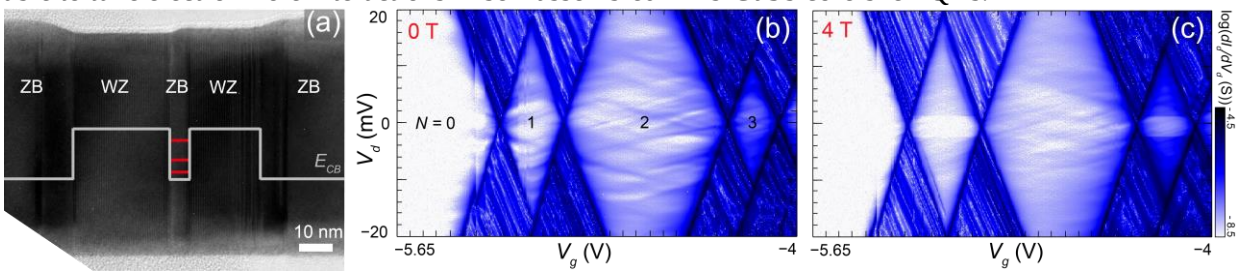

Fig. 1 (a) Transmission electron microscope (TEM) image of a quantum dot (QD) formed between two wurtzite (WZ) segments in an otherwise zinc blende (ZB) nanowire. A simple estimation of the conduction-band edge (E_{CB}) alignment is illustrated where the red lines symbolize quantized energy levels. (b) Charge stability diagram recorded at B = 0 T, where the electron occupation (N) of the QD is indicated. V_d and V_g are the drain bias and the back gate, respectively. (c) Charge stability diagram recorded at B = 4 T, where the spin-splitting of the electron state is visible inside the odd-N diamonds. The electron temperature is approximately 150 mK.

References

[1] M. Nilsson *et al*., Phys. Rev. B **93**, 195422, (2016).
[2] L. Namazi *et al*., Nanoscale **7**, 10472-10481, (2015).
[3] M. Nilsson *et al*., Phys. Rev. B **94**, 115313, (2016).
[4] S.Roddaro *et al*., Nano Lett. **11**, 1695–1699, (2011).

Observation of Crossed Andreev Reflection on superconductor-InAs double nanowire junction device

S. Baba[1], C. Juenger[2], Y. Sato[1], S. Matsuo[1], A. Baumgatner[2], H. Kamata[3], K. Li[4], H.Q. Xu[4,5], C. Schonenberger[2], S. Tarucha[1,3]

[1]*Department of Applied Physics, The University of Tokyo, Hongo, Bunkyo-ku, Tokyo, Japan*

[2]*Department of Physics, University of Basel, Klingelbergstrasse 82, CH-4056 Basel, Switzerland*

[3]*Center for Emergent Matter Science, RIKEN, Wako, Saitama, Japan*

[4]*Key Lab for the Physics and Chemistry of Nanodevices, Peking University, Peking, China*

[5]*Division of Solid State Physics, Lund University, Lund, Sweden*

sato@meso.t.u-tokyo.ac.jp

Recent development of superconductor (SC)-semiconductor nanostructure junctions has provided a new topic of crossed Andreev reflection (CAR), offering a promising way to generate entangled electron spin pairs [1,2] between the split electrons. Furthermore, CAR onto separated two quantum wires gives parafermions, which are generalized Majorana Fermions and an important ingredient for future topological quantum computation, according to a theoretical prediction [3]. CAR has been studied on a single nanowire (NW) [1] or a single carbon-nanotube [2], and preservation of spin correlation has recently been demonstrated with a double quantum dot (QD) Josephson junctions [4]. However, the microscopic mechanism of the CAR, for example the determining factors of the efficiency [5] and contribution of SC proximity region are not yet clear, and there are few experiments about CAR onto separated two nanostructures with a SC.

Here, to gain a new perspective of this mechanism, we carry out measurements of CAR on a device with larger overlap of SC and semiconductor than previous works [1,2] to form a larger SC proximity region. Figure 1 shows a double NW device with one SC contact made of Ti/Al on both wires (blue) and two Ti/Au contacts which are on each wire (yellow) [6]. Gate voltages V_{SG1} and V_{SG2} applied to Ti/Au sidegates (SG1, SG2) enable us to modulate QDs formed on NWs independently. Then, differential conductance on both wires are measured at the same time. Figure 2 shows the conductance on the upper wire as a function of V_{SG2} (V_{SG1} was also modulated linearly), and magnification of conductance on the other wire (i.e. average is subtracted from the raw value and multiplied by 10). It can be clearly seen that there are positive correlations between the conductance peak of the upper wire and of the other, indicating CAR.

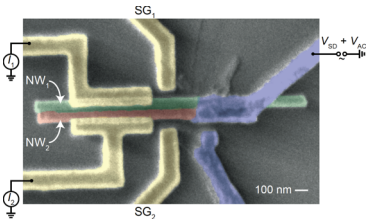

Fig.1 SEM image of the device. Contacts and Gates of Ti/Al (blue) and Ti/Au (yellow) were deposited on two InAs NWs (green and red).

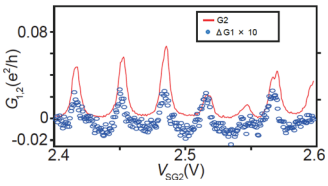

Fig.2 Measured conductance from SC contact to the upper gate (GR), and magnified conductance of the other wire (blue dots).

Moreover, small conductance peaks between the main peaks (secondary peaks) was observed. We interpret this as a contribution of SC proximity region, and this will be discussed in this talk.

References

[1] L. Hofstetter *et.al.*, Nature **461**, 960 (2009).
[2] J. Schindele *et.al.*, Phys. Rev. Lett. **109**, 157002 (2012).
[3] J. Klinovaja and D. Loss, Phys. Rev. B **90**, 045118 (2014).
[4] R.S. Deacon *et.al.*, Nature Commu. **6**, 7446 (2015).
[5] P. Recher *et.al.*, Phys. Rev. B **63**, 165314 (2001).
[6] S. Baba *et.al.*, in preparation (2017).

Hole transport properties in physically defined silicon quantum dots operating at 25 K

N. Shimatani[1], Y. Yamaoka[1], R. Ishihara[2], A. Andreev[3], D. A. Williams[3], S. Oda[1], T. Kodera[1]

Department of Electrical and Electronic Engineering, Tokyo Tech[1],

IIR, Tokyo Tech and Qutech/Kavli Nanoscience Institute[2], Hitachi Cambridge Laboratory[3]

2-12-1 Ookayama Meguro Tokyo[1],

shimatani.n.aa@m.titech.ac.jp

Spins in silicon quantum dots are expected as qubits with long coherence time. However, operation temperature in many reports on silicon quantum dots is below hundred mK [1]. Figure 1 shows cooling power of the state-of-the-art dilution refrigerators as a function of temperature. Higher temperature super-linearly increases the cooling power, hence the allowed power consumption of CMOS electronics for controlling the qubits. For future integration of large number of qubits and CMOS controller, considering the heat flux from wires connecting between quantum dots and controllers, higher operation temperature of the qubits is strongly desired.

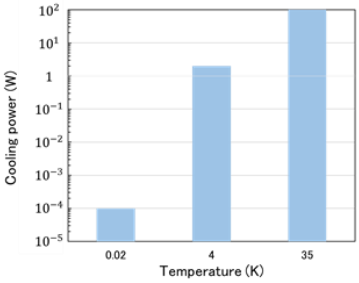

Fig. 1 Cooling power of the state-of-the-art dilution refrigerators with pulsed tubes.

In this work, we fabricated physically defined p-channel silicon quantum dots on a silicon-on-insulator (SOI) substrate (Fig. 2(a)) [2] and studied temperature dependence of the hole transport properties. Figure 2(b) shows the Coulomb diamonds in few-hole region measured at 4.2 K. The large addition energy (≈ 30 meV) was obtained in Coulomb diamond as surrounded by red dotted lines. We also observed Coulomb diamonds at 25 K in the same range as shown in Figure 2(c). The operation temperature is much higher than those of gate defined quantum dots. Change in number of holes in the double quantum dots was also detected with charge sensing technique. Those results suggest possibility for realizing quantum computing chip of qubits integrated with CMOS electronics operating with higher temperature and power consumption in future.

Part of this work is financially supported by JSPS KAKENHI (Nos. 26249048 and 26709023) and CREST-JST. The devices were fabricated using the facilities of the Nanotechnology Platform at QNERC.

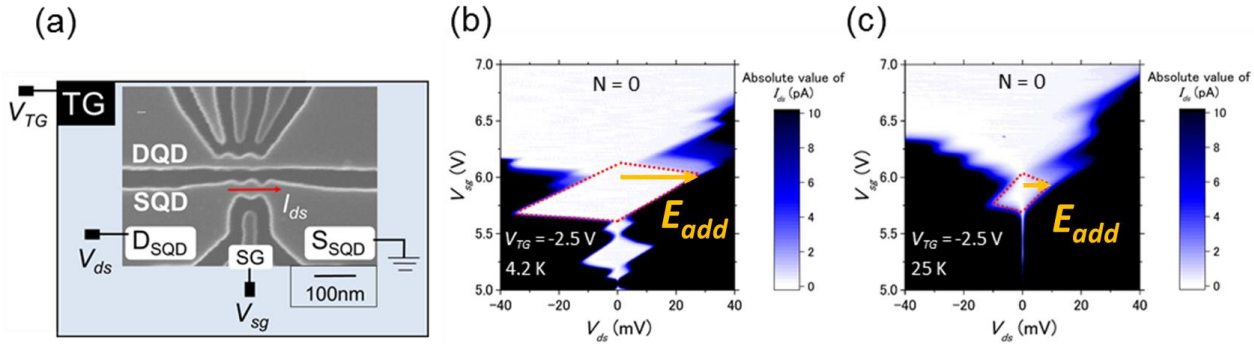

Fig. 2 (a) SEM image of the device and measurement setups. Double quantum dot (DQD) and single quantum dot (SQD) are fabricated. Global top gate (TG) is formed. (b) Coulomb diamonds measured at 4.2 K. E_{add} and N indicate addition energy and the number of holes in the SQD, respectively. (c) Coulomb diamonds measured at 25 K.

References

[1] J. J. Pla, et al., Nature 489, 541-545 (2012). [2] Y. Yamaoka, et al., Jpn. J. Appl. Phys. in press.

Transient regime of single-molecule magnets

B. Tanatar[1], V. Moldoveanu[2] and I. V. Dinu[2]
[1]*Department of Physics, Bilkent University, Bilkent, 06800 Ankara, Turkey*
[2]*National Institute of Materials Physics, PO Box MG-7, Bucharest-Magurele, Romania*
tanatar@fen.bilkent.edu.tr

Single-molecule magnets (SMM) coupled to ferromagnetic leads are promising candidates for solid state implementation of quantum information protocols [1]. The exchange coupling between electrons tunneling through unoccupied molecular orbitals and the localized molecular spin ${¥bf S}$ allows the electrical switching of the latter. A key ingredient here is the magnetic anisotropy characterized by two parameters D and E controlling the uniaxial anisotropy term DS_z^2 and the transverse anisotropy effects $E(S_x^2-S_y^2)$. We present a theoretical description of the time-dependent transport through SMM in the framework of the Generalized Master Equation (GME) method [2].

We analyze the effects of the transversal anisotropy on the transient currents and molecular spin dynamics, generalizing some previous results [3]. The possibility to read the dynamics of the molecular spin from transient current measurements and the effect of a perpendicular magnetic field are discussed.

Finally we investigate the effect of time-dependent signals applied at the contacts between the molecule and particle reservoirs, particular attention being paid to the quantum turnstile setting [4,5] which we propose as a new way to manipulate molecular spins. In particular, we show that for ferromagnetic leads with antiparallel spin polarizations the turnstile protocol allows the stepwise writing and reading of molecular states with well defined spin S_z. The efficiency of this operation depends crucially on the ratio E/D.

References

[1]. L. Bogani and W. Wernsdorfer, Nature Mater. {¥bf 7}, 179 (2008).
[2]. V. Moldoveanu, A. Manolescu, C-S Tang, and V. Gudmundsson, Phys. Rev. B {¥bf 81}, 155442 (2010).
[3]. F. Elste and C. Timm, Phys. Rev. B {¥bf 71}, 155403 (2005).
[4]. T. Fujisawa, T. Hayashi, S. Sasaki, Reports on Progress in Physics {¥bf 69}, 759 (2006).
[5]. W-T Lai, D. M. T. Kuo, P-W Li, Physica E {¥bf 41}, 886 (2009).

Transport far from equilibrium as a ground state problem

Lev Vidmar and Marcos Rigol
Physics Department, Penn State University, University Park, PA 16803, USA
luv2@psu.edu

The far-from-equilibrium dynamics of quantum many-body systems has become an active research area in recent years. Remarkable experimental and theoretical breakthroughs in different fields, such as and condensed matter, ultracold atoms and photonic systems, have demonstrated, among other things, that it is possible to dynamically create novel quantum states of matter that do not exist in equilibrium. We will introduce a new paradigm for quantum systems far from equilibrium: the generation of time-evolving states that are eigenstates of emergent local Hamiltonians [1]. The term 'emergent' is used in the sense that the Hamiltonian is not trivially related to the one driving the dynamics. Hence, this paradigm provides a means for realizing novel quantum states.

As an example, we will focus on transport in one-dimensional chains. We will consider a closed quantum system of spinless fermions with initial particle imbalance. Remarkably, the time-evolving current-carrying state exhibits power-law correlations with ground-state character. We will construct the emergent local Hamiltonian for this setup and show that the time-evolving state is the ground state of the latter Hamiltonian.

References

[1] L. Vidmar, D. Iyer, and M. Rigol, arXiv:1512.05373.

Electronic structure, optical and photoelectrical properties of Si_2Te_3 crystal

D.I. Bletskan, I.P. Studenyak, V.V. Vakulchak, M.M. Bletskan
Department of Physics, Uzhhorod National University,
54 Voloshyn Str., Uzhhorod, Ukraine
crystal_lab457@yahoo.com

Silicon sesquitelluride Si_2Te_3 crystallizes in the trigonal structure which symmetry is described by the space group $P\bar{3}1c$, and it belongs to the binary compounds, which specific characteristic is the presence of natural defects caused by the features of their crystal chemistry. The layered structure character and the presence of a large number of natural cation vacancies in Si_2Te_3 crystals favorably contribute to the intercalation them by Li^+ and Mg^{2+} ions, which opens the possibility of using them as energy storage materials [1].

This paper presents results of calculations of electronic structure, total and partial densities of states, valence charge density distribution as well as studies of intrinsic absorption edge and photoconductivity spectra of Si_2Te_3 crystals grown by a static sublimation method.

First principle calculations of Si_2Te_3 electronic structure performed within the density functional theory in the LDA+*U* approximation showed that the valence complex with a total width 13.41 eV consists of three separate bunches of bands separated by the forbidden energy intervals. The analysis of partial contributions into the density of electronic states allowed to identify the genetic origin of different subbands in the valence band. The lowest bunch of 12 occupied bands is created mainly by Te 5*s*-states with the impurity of Si 3*s*-, 3*p*-states. The middle bunch of 8 bands has the hybridized character with the participation of Te 5*s*-, 5*p*- and Si 3*s*-, 3*p*-states. The upper bunch of 32 valence bands is most complicated and it can be divided into two parts by the formation character: the lower part formed by p-states of tellurium and silicon, and the upper one formed mainly by tellurium 5*p*-states with the insignificant impurity of silicon *p*-, *d*-states. The low-energy structure of unoccupied electronic states of Si_2Te_3 is formed mainly by the "mixing" of free Te *p*-, *d*- and Si s-, *p*-, *d*-states with the predominant contribution of *p*-states of both atoms. According to performed calculations, Si_2Te_3 is the indirect-gap semiconductor with the calculated band gap width E_{gi} = 1.96 eV in the LDA+*U* approximation.

Edge absorption and photoconductivity spectra of Si_2Te_3 crystal were measured in the 80–293 K temperature range. It is shown that the dependence of absorption coefficient from photon energy is described by Urbach rule. The parameter σ_0 associated with a constant of electron-phonon interaction and the effective phonon energies $\hbar\omega_{ph}$ participating in the formation of absorption edge of Si_2Te_3 crystal were determined by the temperature dependence of absorption edge steepness parameter.

Layered Si_2Te_3 crystals are *p*-type conductivity and characterized by the strong electrical conductivity anisotropy. The room temperature conductivity measured along the layers is equal to $\sigma_{\parallel} = 10^{-4}$–$10^{-5}$ $Ohm^{-1}\cdot cm^{-1}$ as well as in the direction perpendicular to the layers is equal to $\sigma_{\perp} = 10^{-6}$–10^{-7} $Ohm^{-1}\cdot cm^{-1}$. Si_2Te_3 crystals exhibit the photosensitivity in the wide spectral range from 1.0 to 2.5 eV. The photoconductivity spectrum is complicated and it contains the strongly pronounced intensive intrinsic peak at 2.02 eV, one feature in the influx form at 2.12 eV on the high-energy decline of the main peak and two features at 1.7 and 1.32 eV on the long-wave decline.

References

[1] S. Keuletan, M. Wang, F. Chung *et al.*, Nano.Lett. **15**, 2285 (2015).

Ultrafast Phonon-assisted Exciton Transfer in Carbon Nanotube Films

A. H. Davoody and I. Knezevic
Department of Electrical and Computer Engineering
University of Wisconsin-Madison, Madison, WI 53705, USA
davoody@wisc.edu and iknezevic@wisc.edu

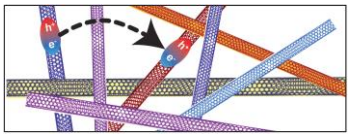

Carbon nanotubes (CNTs) are quasi-one-dimensional materials with a very unique set of optical, electronic, and mechanical properties. Their tunable optical bandgap and high optical density have drawn the attention of researchers for energy-harvesting applications. While a majority of research efforts have focused on understanding the physics of excitons in isolated CNTs, in most practical situations CNTs show a strong Coulomb interaction with the surrounding environment and other nearby CNTs. This interaction results in new dynamical processes for excitons in CNT films. Understanding these intertube dynamical processes is important for many applications, such as CNT-based photovoltaics [1].

Several groups have measured the intertube exciton transfer (ET) rate in CNT films [1]. The reported time constants range from tens of femtoseconds to tens of picoseconds. Our recent theoretical study of the first-order Coulomb-mediated ET process has shown that the wide range of measured ET rates could be explained by considering exciton confinement in local quantum wells that stem from sample disorder and from exciton thermalization between bright and dark excitonic states [2]. The physical process behind this type of exciton hopping is elastic: exciton hopping happens through Coulomb coupling between initial and final states with equal energies. The phonon baths act as scattering sources for excitons within each CNT and help relax exciton population toward thermal equilibrium. However, several studies have shown that more efficient ET between molecules and quantum dots can be facilitated by higher-order processes, which include exciton-phonon interactions, where sequential exciton-phonon and Coulomb-mediated scatterings happen in the hopping process.

In this work, we present a calculation of the intertube phonon-assisted ET rates between CNTs using second-order Fermi's golden rule. This transfer process consists of two successive scattering events: intratube scattering of excitons via their interaction with phonons, followed by intertube scattering of excitons due to Coulomb coupling between the two CNTs (Figure 1). Our results show that the second-order phonon-assisted ET process between CNTs has a rate of about 1 ps^{-1}, which is the same order of magnitude as the first-order ET process. We also find that, for optically inactive *E*-type excitons, the phonon-assisted transfer rate (~ 1 ps^{-1}) is at least two orders of magnitude higher than the rate of the first-order transfer process (~ 0.01 ps^{-1}). These results are important from an experimental point of view, as optically inactive excitons are invisible in the most common measurement methods, so one needs to complement measurements with theoretical calculations in order to get a correct picture of exciton dynamics in these types of nanostructures.

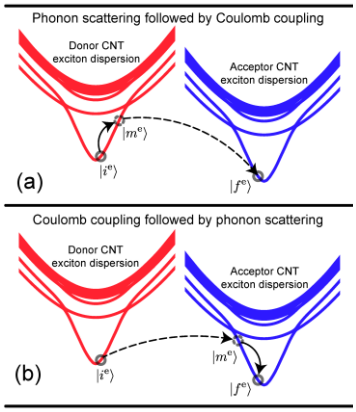

Figure 1. Schematic of phonon-assisted exciton hopping.

References

[1] M. S. Arnold, J. L. Blackburn, J. J. Crochet, S. K. Doorn, J. G. Duque, A. Mohite, and H. Telg, Phys. Chem. Chem. Phys. **15**, 14896, (2015).

[2] A. H. Davoody, F. Karimi, M. S. Arnold, and I. Knezevic, J. Phys. Chem. C **120**, 16354 (2016).

Photophysics of Single Nano-scale Metal-halide Cluster: an Optical Indicator for Molecular Oxygen

Ruby N. Ghosh and Reza Loloee
Physics Department, Michigan State University,
East Lansing, MI 48814, USA, PA 16803, USA
ghosh@pa.msu.edu

Measurements of the phosphorescent emission from a single metal-halide cluster provides a window into the photo-physics of these unique nano-scale optical indicators. Absorption of a UV photon by the family of molybdenum chloride clusters results in the emission of bright red emission with a long phosphorescent lifetime (~180us).[1] As the phosphorescent emission arises from spin forbidden transitions between the excited triplet and singlet ground state of the Mo-cluster, collisions with ground state molecular oxygen, $^3O_2$, provides an efficient pathway to quench both the intensity and lifetime of the phosphorescence.[2] Photo-bleaching, following repeated excitation of the metal-halide indicator is not observed. These optical properties are specific to *single* isolated Mo-clusters, in the as synthesized crystalline material there are strong interactions between the Mo-clusters which significantly alter their optical characteristics.[1]

We report on lifetime measurements from isolated $K_2Mo_6Cl_{14}$ clusters as a function of oxygen quencher concentration. A linear fit to the Stern-Volmer equation with an intercept of one, demonstrates that the observed phosphorescence quenching is due to bi-molecular collisional quenching between isolated Mo-clusters and molecular oxygen. The quenching of the emission from a luminnophore by simple bi-molecular collisional processes can be modeled with the Stern-Volmer equation:

$$\tau_o/\tau = 1 + K_{SV}\,[\text{quencher}]$$

where τ_o and τ are the emission lifetimes in the absence and presence of quencher respectively and K_{SV} is the overall dynamic quenching constant. The figure shows the least squares fit (solid lines) to the lifetime data (markers) at three different temperatures.

We discuss how our data demonstrates that the measured phosphorescence emission arises from single, isolated nano-scale Mo-clusters in the absence of cluster-cluster interactions that would be observed in a crystalline solid material.

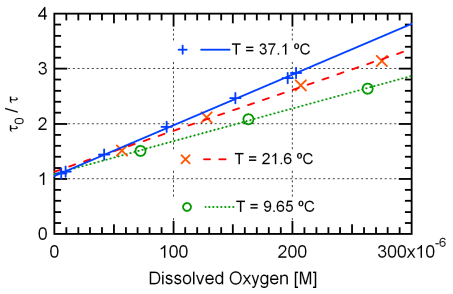

Fig.1 Normalized phosphorescence lifetime (τ_0/τ) as a function of quencher concentration, demonstrating that the emission arises from bio-molecular interactions between of an isolated nano-scale cluster and $^3O_2$.

References

[1] T. C. Zietelow, M. D. Hopkins, H. D. Gray, *J. Sol. St. Chem*. **57**, p. 112 (1985).
[2] R.N. Ghosh, P.A. Askeland, S. Kramer, R. Loloee, *Appl. Phys. Lett*. **98**, 221103 (2011).

Improved Characteristics of InP-based Nanowire Light-Emitting Diodes

Hiroki Kameda, Katsuhiro Tomioka, Fumiya Ishizaka, Masahiro Sasaki, and Junichi Motohisa
Graduate School of Information Science and Technology, and Research Center for Integrated Quantum Electronics, Hokkaido University
motohisa@ist.hokudai.ac.jp

Semiconductor nanowires (NWs) have attracted increasing attention due to their unique electrical and optical properties. In particular, InP-based NWs are promising for the application of photonic devices, because they have a direct band gap compatible with optical fiber telecommunication bands. We have reported single photon emission from a single InAsP QD in a density-controlled InP NWs[1], which can be used for on-demand single photon sources by combining with light-emitting diode (LED) structure. However, characteristics of the NW LEDs still need to be improved; for instance, anomalous large ideality factor *n* [2] is thought to be a problem for efficient emission of single photons. Here, we report on an improvement of performance of InP NW LEDs by optimization of their fabrication process.

Figure 1 shows a schematic illustration of a NW LED. InP NWs with axial pin structure were grown by selective-area metalorganic vapor-phase epitaxy (SA-MOVPE) on a p-InP (111)A substrate partially covered with a SiO_2 mask [2]. After the NW growth, the space between NWs was filled with polymer resin (benzocyclobutene, BCB) by spin coating to obtain an electrical separation layer. The top of the resin was removed by reactive ion etching. Next, a transparent indium tin oxide (ITO) film electrode was deposited on NWs by plasma sputtering and patterned by using photolithography and wet chemical etching by HCl. Finally, an Au-Zn electrode was formed on the back side of the substrate by vacuum evaporation and alloying for 15min at 400°.

Figure 2 shows typical *I-V* characteristics of fabricated NW pin diodes. The height, diameter, and pitch of InP NWs were 1.6 μm, 150 nm, and 800 nm, respectively. Good rectifying characteristics were confirmed. Notably, analysis of *I-V* characteristics of this device revealed ideality factor *n* of the diode to be about 1.9, which is reasonable in InP-based LEDs [3] and is thought to be an important improvement compared with our previous report [2]. A key to this improvement is considered to be in the contacting process between ITO and n-InP NWs. Figure 3 shows *I-L* characteristics of the same device. Nonlinearity in the *I-L* characteristics is presumably due to nonradiative recombination at the NW sidewalls, and is a room for a further improvement by introduction of core-shell structures.

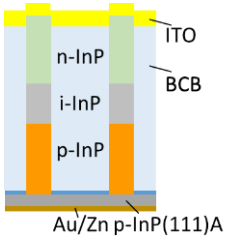

Fig.1 Schematics of a pin-InP NW LED.

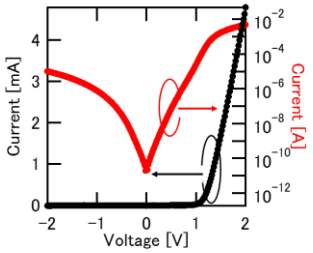

Fig.2 *I-V* characteristics of a pin-InP NW LED.

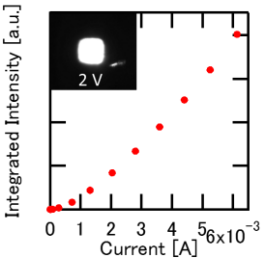

Fig. 3 *I-L* characteristics and emission image of a pin-InP NW LED

References

[1] S. Yanase *et al.*, Jpn. J. Appl. Phys **56** 04CP04 (2017). [2] S. Maeda *et al.*, Jpn. J. Appl. Phys. **51** 02BN03 (2012). [3] E. F. Shubert, Light-Emitting Diodes (Cambridge University Press, Cambridge, U. K. 2006), 2nd ed. Chap 4.

Spin-Valley Resolved Photon-Assisted Tunneling in Carbon Nanotube Double Quantum Dots

E. N. Osika and B. Szafran
AGH University of Science and Technology,
Faculty of Physics and Applied Computer Science,
al. Mickiewicza 30, 30-059 Kraków, Poland
edyta.osika@fis.agh.edu.pl

Carbon nanotubes (CNTs) are an attractive material for usage in quantum information on carrier spins, in particular due to the absence of the hyperfine interaction – the main source of decoherence in III-V semiconductors. Numerous experiments have been carried out focused on spin-valley qubit formation within CNT double quantum dot. In particular, a purely electrical manipulation of the qubit has been investigated by means of either electric dipole spin resonance or photon-assisted tunneling (PAT) [1].

We report on simulations of PAT in carbon nanotube pp quantum dot [2] – a system in which the process has been recently observed in experiment [1]. We consider transition of a single hole from one dot to another as driven by the microwave electric field. Both spin-valley-conserving transition, as well as transitions accompanied by spin or valley flip are considered in the model. We indicate at appearance of separate transition lines for spin and valley conserving/flipping excitations and a possibility of changing their respective position by variating the external magnetic field or the frequency of the microwave electric field. We observe fractional resonances due to simultaneous absorption of multiple microwave field quanta by the system. We report on the Landau-Zener-Stueckelberg interference [3] which appears in the system for strong electric fields. Also a case of two electron nn quantum dot is considered, where the Pauli blockade prohibits electron to jump between the dots while conserving the spin-valley state of the system. Therefore, only charge tunneling events accompanied by spin or valley flip can be observed.

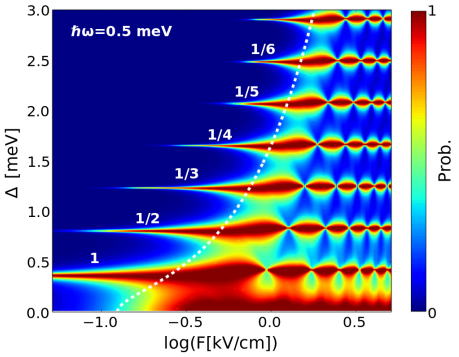

Fig.1 PAT spectrum – current through the pp double quantum dot as a function of potential difference between the dots Δ and log of the amplitude of microwave field F.

References

[1] A. Mavalankar, T. Pei, E.M. Gauger, J.H. Warner, G.A.D. Briggs, E.A. Laird, PRB **93**, 235428 (2016).
[2] E. N. Osika, and B. Szafran, arXiv:1702.08802
[3] S. N. Shevchenko, S. Ashhab, and Franco Nori, Phys. Rept. **492**, 1 (2010).

Observation of Joule Heating Induced Negative Differential Resistance in Mesoscopic Graphene Oxide

Servin Rathi[1], Inyeal Lee[1], Dongsuk Lim[1], Serhan Yamacli[2], Han-Ik Joh[3], Sukwon Choi[4] and Gil-Ho Kim[1*]

[1]*School of Electronic and Electrical Engineering, and Sungkyunkwan Advanced Institute of Nanotechnology (SAINT), Sungkyunkwan University, Suwon 16419, Korea*

[2]*Department of Electrical-Electronics Engineering, Nuh Naci Yazgan University, 38090 Kayseri, Turkey*

[3]*Institute of Advanced Composite Materials, Korea Institute of Science and Technology 864-9, Jeollabukdo 565-902, Korea*

[4]*Department of Mechanical and Nuclear Engineering, The Pennsylvania State University, University Park, PA 16802, USA*

ghkim@skku.edu

The alteration of electrical and chemical properties with reduction in graphene oxide (GO) is directly related to the ratio of various functional groups in the material. However, a method with sufficient controllability to regulate the reduction process has been missing.

In this this work, an accurate and progressive control on the ratio of various functional groups has been achieved in a precise and localized area, by using a hybrid method of thermal and joule heating processes. With such precise control over reduction process, a two-terminal device that exhibits negative differential resistance (NDR) is demonstrated. The subsequent study using X-ray photoelectron spectroscopy and Raman characterization along with *ab-initio* simulations provides a possible explanation of the NDR observation. It is concluded from the analysis that NDR is observed only at a particular carbon-oxygen ratio in the GO devices and the variation in transmission energies and localization degree with applied voltage results in the observation of NDR peak in I-V characteristics.

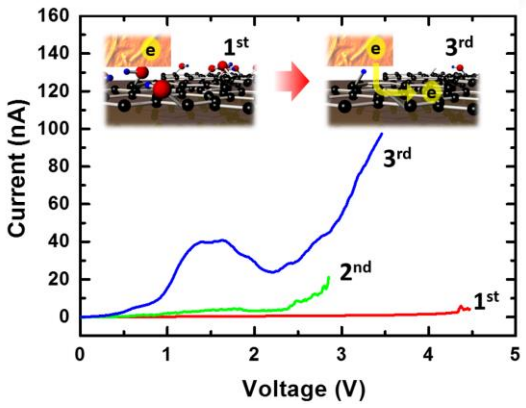

Fig.1 I-V curves for successive controlled sweeps, where an NDR peak is clearly visible in the 3rd sweep. Inset figure shows the efficient injection at the contacts after Joule-heating induced reduction of graphene oxide at the metal contacts.

References

[1] S. Yamacli, Nano-Micro Lett. 7, 42 (2014).

[2] K.P. Loh, Q. Bao, G. Eda, M. Chhowalla, Nat. Chem. 2, 1015 (2010).

Title: Fermi-edge singularity and related interaction induced phenomena in multilevel quantum dots

Anna Goremykina and Eugene Sukhorukov
Theoretical Physics Department, University of Geneva, Switzerland

The 22nd International We study the manifestation of the non-perturbative effects of interaction in sequential tunneling between a quasi-one dimensional system of chiral quantum Hall edge channels and a multilevel quantum dot (QD). We use the formal scattering theory approach to the bosonization technique to present an alternative derivation of the Fermi-edge singularity (FES) effect and demonstrate the origin of its universality. This approach allows us to address, within the same framework, plasmon assisted sequential tunneling to relatively large dots and investigate the interaction induced level broadening. The results are generalized by taking into account the dispersion in the spectrum of plasmons in the QD. We then discuss their modification in the presence of neutral modes, which can be realized either in a QD with two chiral strongly interacting edge channels or in a three dimensional QD in the Coulomb blockade regime. In the former case a universal behavior of the tunneling rate is discovered.

References

[1] Anna Goremykina and Eugene Sukhorukov, https://arxiv.org/abs/1611.02745

Transmission phase measurements of a large quantum dot

H. Edlbauer[1], S. Takada[1], G. Roussely[1], M. Yamamoto[2], S.Tarucha[2],
A. Ludwig[3], A. D. Wieck[3], T. Meunier[1], and C. Bäuerle[1]

[1]*CNRS, Institute Néel & Université Grenoble Alpes, 38042 Grenoble, France*
[2]*Department of Applied Physics, University of Tokyo, Bunkyo-ku, Tokyo, 113-8656, Japan*
[3]*Department of Applied Physics, University of Bochum, 44780 Bochum, Germany*
christopher.bauerle@neel.cnrs.fr

The electron wave function experiences a phase modification at coherent transmission through a quantum dot. This transmission phase undergoes a characteristic shift of π when scanning through a Coulomb-blockade resonance [1, 2]. Between successive resonances either a transmission phase lapse of π or a phase plateau is theoretically expected to occur depending on the parity of the corresponding quantum dot states. Despite important experimental effort, this transmission phase behavior has remained elusive for a large quantum dot. Here we report on transmission phase measurements across such a large quantum dot hosting hundreds of electrons. Using a novel electron two-path interferometer, we observe the theoretically predicted transmission phase behavior. We underpin our observation by demonstrating that quantum dot deformation alters the sequence of transmission phase lapses and plateaus via parity modifications of the involved quantum dot states. Our findings set a milestone towards a comprehensive understanding of the transmission phase of quantum dots.

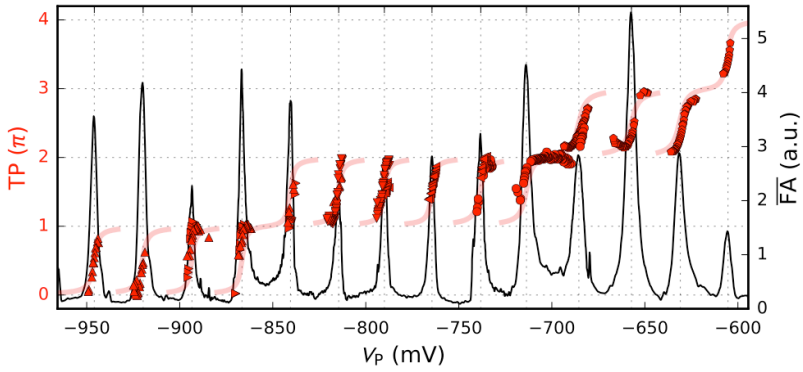

Fig. 1: Transmission phase along fourteen Coulomb peaks through a quantum dot containing several hundred electrons showing phase lapses of π as well as phase plateaus.

References

[1] R. Schuster et al., Nature **385**, 417- 420 (1997).
[2] S. Takada et al., Appl. Phys. Lett. **107**, 63101 (2015).
[3] H. Edlbauer et al. submitted.

Charge Reconfigurations in Quantum Dot Arrays

Johannes C. Bayer, Timo Wagner, Eddy P. Rugeramigabo and Rolf J. Haug
Institute for Solid State Physics, Leibniz Universität Hannover
Appelstraße 2, 30167 Hannover, Germany
bayer@nano.uni-hannover.de

The investigation of coupled quantum dot arrays is of great importance towards the implementation of multiple qubit architectures [1-3]. Our device is a serial configuration of four laterally coupled quantum dots. The device is based on a two-dimensional electron gas formed in a GaAs/AlGaAs heterostructure at 110nm beneath the surface with an electron density of $2.4 \cdot 10^{11}\,\mathrm{cm}^{-2}$ and an electron mobility of $5.1 \cdot 10^{5}\,\mathrm{cm}^{2}/\mathrm{Vs}$. Two quantum point contacts (QPCs) are attached to the system and work as sensitive charge detectors allowing the real-time detection of electrons tunneling through the system [4].

Isolating a double quantum dot has already been demonstrated to bring several advantages, most notably the possibility to control the tunnel coupling strength between the dots over orders of magnitude without detuning the dot potentials [5]. While transport vanishes when decoupling a quantum dot array form the reservoirs, charge reconfigurations are still observable in the detector signal. The high tunability of our device allowed the investigation of these reconfigurations in isolated double, triple and quadruple quantum dot configurations and over a wide range of parameters. Complementary simulations were performed, allowing detailed analysis of the charge reconfigurations and resonances in isolated quantum dot arrays and the identification of co-tunneling transitions between distant quantum dots.

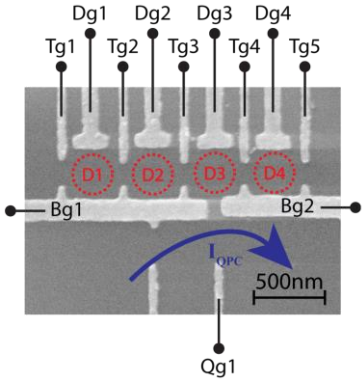

Fig.1 SEM image of our quadruple quantum dot device, the charge detector is indicated by the arrow. The dots are depicted by circles.

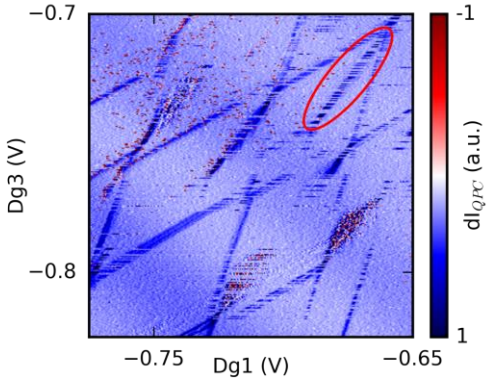

Fig.2 Stability diagram of an isolated triple quantum dot. Sequential as well as co-tunneling transitions (red ellipse) are observed.

References

[1] J. M. Taylor, H. A. Engel, W. Dür, *et. al.*, Nat. Phys. **1**, 177-183 (2005).

[2] A. Bogan, L. Bergeron, A. Kam, *et. al.*, Appl. Phys. Lett. **109**, 173108 (2016).

[3] T. Otsuka, T. Nakajima, M. R. Delbecq, *et. al.*, Sci. Rep. **6**, 31820 (2016).

[4] T. Wagner, P. Strasberg, J. C. Bayer, *et. al.*, Nat. Nanotech. DOI:10.1038/nnano.2016.225 (2016).

[5] B. Bertrand, H. Flentje, S. Takada, *et. al.*, Phys. Rev. Lett. **115,** 096801 (2015).

Energy Relaxation of Non-equilibrium Electrons in Quantum Hall Edge Channels

L. Freise, T. Gerster, D. Reifert, T. Weimann, K. Pierz, F. Hohls and N. Ubbelohde
Physikalisch-Technische Bundesanstalt (PTB),
Bundesallee 100, 38116 Braunschweig, Germany
Lars.Freise@ptb.de

Ballistic electrons propagating in Quantum Hall edge channels are one of the possible systems for realization of an electronic analog to quantum optics, often referred to as ‘electron quantum optics’. Single electrons can be generated and emitted on-demand at tunable excess energies far above the Fermi level by single electron pumps (SEPs) and will traverse an edge channel as a wave guide [1-4]. The development of complex single electron circuitry relies on the identification and the subsequent ability to manipulate the relaxation mechanisms, with additional applications such as quantized current sources for metrology.

We investigate the relaxation of non-equilibrium electrons over a wide range of emission energies and for different sample geometries. Dynamic quantum dots (SEPs) are used to generate single electrons with an accessible energy range limited to only a few meV. Therefore, a stochastic source (‘hot electrons’ driven over a static barrier) is additionally used to extend the covered range to several hundred meV. The electrons are emitted in high magnetic fields into edge channels in a GaAs heterostructure and are detected at various distances at an energy selective detection barrier. We measure the transmission probability and perform an energy-dependent spectroscopy of the scattered electrons by the use of the adjustable detection barrier.

Our data shows a clear signatures of different scattering processes, which are dominated by electron-electron scattering and the emission of longitudinal-optical phonons (the latter clearly visible in a strong periodicity [4-6]) and which strongly depend on device properties.

References

[1] J. D. Fletcher et al., Phys. Rev. Lett. **111**, 216807 (2013)
[2] J. Waldie et al., Phys Rev. B **92**, 125305 (2015)
[3] N. Ubbelohde et al., Nature Nanotechnology **10**, 46 – 49 (2015)
[4] M. Kataoka et al., Phys. Rev. Lett. **116**, 126803, (2016)
[5] D. Taubert et al., Phys. Rev. B **83**, 235404 (2011)
[6] C. Emary, A. Dyson, S. Ryu, H.-S. Sim and M. Kataoka, Phys. Rev. B **93**, 035436 (2016)

Accuracy and Robustness of Tunable-Barrier Single-Electron Pumps

F. Stein, H. Scherer, T. Gerster, R. Behr, M. Götz, E. Pesel, C. Leicht, N. Ubbelohde, T. Weimann, K. Pierz, H. W. Schumacher, and F. Hohls
Physikalisch-Technische Bundesanstalt (PTB), Bundesallee 100, 38116 Braunschweig, Germany
Frank.Hohls@ptb.de

Single-electron transport (SET) pumps are considered as promising candidates for future quantum current standards following the redefinition of the SI unit system [1]. The most advanced types of SET pumps, suitable for generating relatively high currents with reasonable accuracy, are based on 'dynamic' quantum dots (QD) that are defined by tunable energy barriers imposed by electrostatic gate electrodes [2,3]. Periodic modulation of these barriers causes a clocked transfer of electron, which results in a current $I = \langle n \rangle ef$. Here $\langle n \rangle$ is the average number of electrons transferred per transport cycle, e the electron charge and f the repetition rate of the transport cycles. The use of SET pumps for future metrological current standards, however, will only be possible, if a robust current quantization is given in the sense that $\langle n \rangle$ is sufficiently close to an integer for a sufficient range of working parameters.

We report on characterizations of single-electron pumps at highest accuracy level, enabled by improvements of the small-current measurement technique [4,5]. With these improvements a new accuracy record for high frequency single-electron pumps has been demonstrated: The pump current agrees with $I = ef$ within the relative combined uncertainty 0.16 µA/A which was reached within less than one day of measurement time [6].

Additionally, robustness tests of pump accuracy under variation of both gate voltages, source and drain voltage, frequency, and magnetic field at sub-ppm level revealed a good stability of tunable-barrier single-electron pumps against the variation of operating parameters [6]. Accurate pumping was found in several devices and multiple cooldowns.

The demonstrated accuracy is near the desired uncertainty of 0.1 µA/A to enable SET pumps to replace other realization of the ampere for the low current regime.

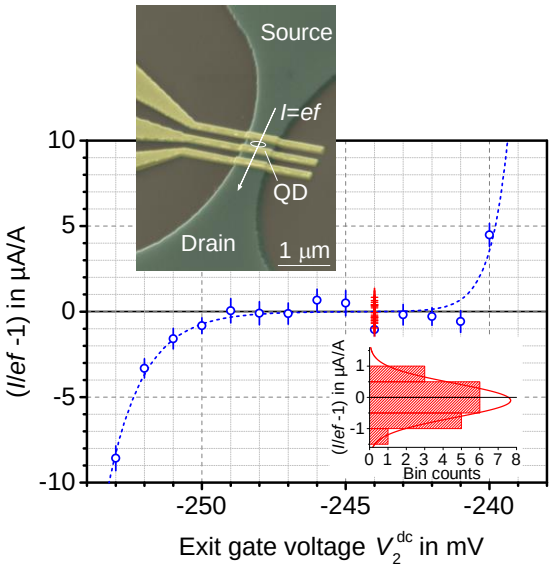

Fig.1: Colored SEM image of device. The QD is formed by two Schottky gates on a narrow quasi-1d channel shallow etched from a GaAs/AlGaAs herterotructure. Graph shows measured deviations of single-electron pump current I from ef as function of working point. Histogram shows 21 measurements of 1 hour duration at optimal gate voltage working point. (f = 0.6 GHz, ef = 96.130587 pA, B = 9.2 T, T = 0.1 K)

References

[1] J. P. Pekola *et al.*, Rev. Mod. Phys. 85 1421 (2013).
[2] B. Kaestner & V. Kashcheyevs, Reports Prog. Phys. **78**, 103901 (2015).
[3] L. Fricke *et al.*, Phys. Rev. Lett. **112**, 226803 (2014).
[4] D. Drung *et al.*, Rev. Sci. Instrum. **86** 024703 (2015); *ibid* IEEE Trans. Instrum. Meas **64** 3021 (2015)
[5] F. Stein *et al.*, Appl. Phys. Lett. **107**, 103501 (2015).
[6] F. Stein *et al.*, Metrologia **54**, S1 (2016).

Controlling the Error Mechanisms of Tunable-Barrier Single-Electron Pumps

F. Stein,[1] B. Kaestner, [2] V. Kashcheyevs,[3,4] T. Wenz, [1] C. Leicht, [1] K. Pierz, [1] H. W. Schumacher, [1] and F. Hohls[1]

[1]*Physikalisch-Technische Bundesanstalt (PTB), Bundesallee 100, 38116 Braunschweig, Germany*

[2]*Physikalisch-Technische Bundesanstalt (PTB), Abbestr. 2-12, 10587 Berlin, Germany*

[3]*Faculty of Computing, University of Latvia, Riga LV-1586, Latvia*

[4]*Faculty of Physics and Mathematics, University of Latvia, Riga LV-1002, Latvia*

Frank.Hohls@ptb.de

Recently the potential of tunable barrier single-electron pumps (SEPs) [1] as future current standard was demonstrated [2]. These SEPs are realized by semiconductor quantum dots with gate controllable barriers to source and drain (Fig.1a). Modulation of one or both barriers with high frequency f can generate a current $I = \langle n \rangle ef$ with $\langle n \rangle$ the average number of electrons transferred per transport cycle and e the electron charge. For a metrological current standard the deviation of $\langle n \rangle$ from an integer value due to erroneous pump events should be as small as possible for a sufficient range of working parameters. Therefor one aims to understand and control such errors. It was observed that in the single-parameter mode, where only one gate voltage is modulated, the SEPs are typically run in the so called decay cascade regime [3] where the so called plunger-to-barrier energy scale Δ_{ptb} dominates [4,5]. It was suggested [4,5] that reducing this energy scale could reduce associated errors due to unwanted loss of electrons during the pumping cycle until at sufficiently low Δ_{ptb} thermal effects will dominate.

Here we demonstrate that we can reduce decay cascade related errors by using a two-gate modulation scheme (Fig.1b). Compensating the plunger effect of the entry barrier gate used in single-gate mode by an opposite voltage (scaled by factor r) applied to the exit gate, Δ_{ptb} is reduced and the quantization quality is improved as the associated decay cascade errors are reduced (Fig.1c, no magnetic field applied, cryostat temperature 0.1 K). We present a systematic study of the transition from single-parameter driven SEPs to fully compensated two-gate operation and the associated change of the dominating error mechanism.

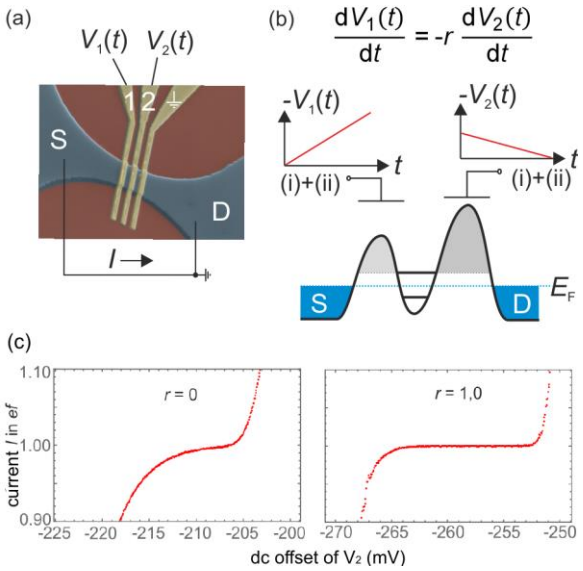

Fig.1: a) Colored SEM image of SEP device. b) Barrier gates forming the QD are operated with opposing voltage ramps with slope ratio r. c) Measured single-electron pump current I for single-gate operation (r = 0) and for equal reverse slope (r = 1).

References

[1] B. Kaestner & V. Kashcheyevs, Reports Prog. Phys. **78**, 103901 (2015).

[2] F. Stein *et al.*, Appl. Phys. Lett. **107**, 103501 (2015); *ibid.*, Metrologia **54**, S1 (2016).

[3] V. Kashcheyevs and B. Kaestner, Phys. Rev. Lett. **104**, 186805 (2010).

[4] V. Kashcheyevs and J. Timoshenko, Phys. Rev. Lett. **109**, 216801 (2012).

[5] L. Fricke *et al.*, Phys. Rev. Lett. **110**, 126803 (2013).

Coherent electron transport driven by surface acoustic wave

R. Ito, S.Takada, M. Yamamoto, C. Bauerle, A. D. Wieck and S. Tarucha
Department of Applied Physics, University of Tokyo, Bunko-ku,Tokyo, 113-8656, Japan
CNRS, Inst NEEL, F-38042 Grenoble, France
Angewandte Festk orperphysik, Ruhr-Universit¨at Bochum, D-44780 Bochum, Germany
ito@meso.t.u-tokyo.ac.jp

Recent development of the flying qubit architecture has enabled to control quantum states of propagating electrons in one-dimensional (1D) channels [1]. The main source of decoherence in such a structure is the electron-electron interaction, which limits the coherence length to the order of 10-100 μm at temperature of 100 mK. Existence of many transmitting channels also significantly affects visibility of interference for electrons transport through tunnel-coupled 1D channels to be less than 10%. A possible way to suppress the decoherence is to remove background conduction electrons in the transport channel. This is achieved simply by applying large negative gate voltages to deplete the channel. Then surface acoustic wave (SAW) can be used to transport electrons coherently through such depleted channels by confining isolated electrons in moving potential minima (moving quantum dots). In this work we study the interference effect of electrons transport in depleted but tunnel-coupled wires driven by SAW. We observe enhanced visibility of interference, probably due to the reduced number of transmitting channels in the strongly depleted coupled wires. In addition we assign the travelling electrons have high energy and are not bound by the SAW potential in the coupled wire region.

Here we demonstrate coherent electron transport driven by SAW travelling through depleted tunnel-coupled wires (Fig. 1). Each SAW potential minimum contains only one electron. Quantum interference leads to oscillation of single electrons tunneling between the two wires. We achieve interference visibility of ~60 % at 350 mK, which is significantly improved from the value (~8 %) previously observed for non-depleted channels [1]. The observed interference pattern as a function of the gate voltage V_T (tunnel coupling energy) and imbalance of V_{SU} and V_{SL} (inter-wire level detuning) is analyzed by numerical calculation of the inter-dot tunneling of travelling electrons. From this analysis we assume that the travelling electrons have sufficiently high energy that they are not bound by the SAW potential in the coupled wire region. Our work may pave a promising route for manipulating quantum interference of pure single flying electrons using a depleted interferometer, as a solid-state analogue of the ideal double-slit experiment in vacuum.

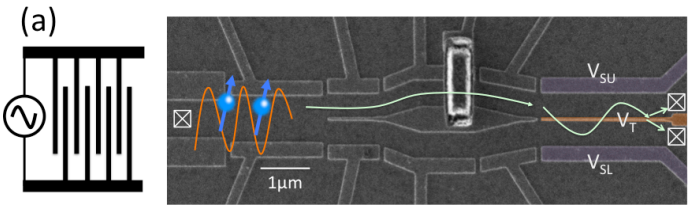

Fig.1 Device structure. An inter-digital transducer is placed about 1.2 mm to the left. SAW moving dots each carrying one electron travel through the upper channel of the coupled-wire and inject electrons one-by-one into the tunnel-coupled wire formed by the three colored gates on the right. We measure the output currents at the upper and lower channels simultaneously while injecting electrons from either of the upper or lower

References

[1] M.Yamamoto, S. Takada, C.Bauerle, K. Watanabe, A. D. Wieck and S.Tarucha, Nature Nano. **7**, 247 (2012).

On-Demand Emission and Detection of a Single-Electron Gaussian Wave Packet

Sungguen Ryu[†]*, M. Kataoka[‡], and H.-S. Sim[†]
[†] *Department of Physics, Korea Advanced Institute of Science and Technology, Daejeon 34141, Republic of Korea*
[‡] *National Physical Laboratory, Hampton Road, Teddington, Middlesex TW11 0LW, United Kingdom*
*sungguen@kaist.ac.kr

A tunable-barrier quantum-dot (QD) pump [1] is an on-demand single-electron source which has the unique property of emitting hot electrons of ~ 100 meV above Fermi energy. In order to utilize it for electron quantum optics and related quantum processing, it is crucial to realize a QD pump emitting a prescribed electron wave packet of a useful form. How to pump such states is a nontrivial question that requires understanding of the wave packet evolution during the emission process (see Fig. 1). Because the process is controlled by time-dependent QD barriers whose energy is changing by ~ eV with gigahertz frequency, it involves complications from nonadiabatic operations and tunneling through a QD barrier. How the shape of a wave packet changes by the tunneling is also a question that should be addressed.

We theoretically show that a prescribed wave packet (Gaussian or log-logistic) can be generated by a QD pump with realistic parameters. [2] With the help of a strong magnetic field, the electron occupies a coherent state as long as QD-confinement potential slowly changes in the length scale and time scale characterizing the magnetic confinement. The state changes during the emission from the pump, governed by competition between the Landauer-Buttiker traversal time for tunneling and the passage time [3] of the coherent state. The emitted wave function is a Gaussian (log-logistic) packet when the Landauer-Buttiker traversal time is smaller (larger) than the passage time. The emitted state and the competition between the time scales can be experimentally identified by a dynamical potential barrier, with resolution reaching the minimal value limited by Heisenberg uncertainty relation.

References

[1] B. Kaestner and V. Kashcheyevs, Rep. Prog. Phys. **78**, 103901 (2015)
[2] Sungguen Ryu, M. Kataoka, and H.-S. Sim, Phys. Rev. Lett. **117**, 146802 (2016)
[3] L. Mandelstam and I. G. Tamm, J. Phys. (Moscow) **9**, 249 (1945).

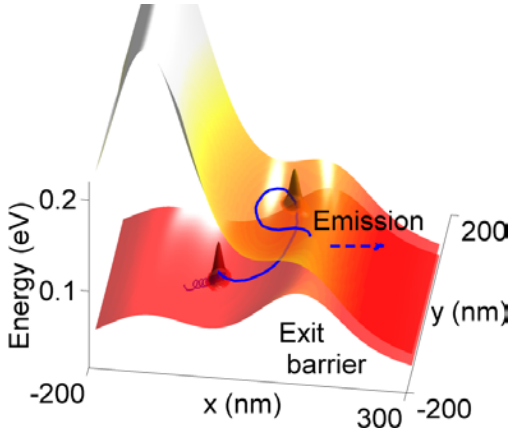

Fig.1 Numerical result of the time evolution of an electron wave packet in a QD pump with realistic parameters. The computed QD potential and the wave packet are shown at the initial time and a later time of the evolution. The state evolves in time into a coherent state (cone) moving along the E × B drift (curve) as the potential barriers rise.

Time dependence of electron capture in a dynamic quantum dot

N. Ubbelohde, D. Reifert, L. Freise, T. Gerster, F. Hohls, T. Weimann, K. Pierz and V. Kashcheyevs
Physikalisch-Technische Bundesanstalt (PTB),
Bundesallee 100, 38116 Braunschweig, Germany
Faculty of Physics and Mathematics, University of Latvia,
LV-1586, Riga, Latvia
niels.ubbelohde@ptb.de

Dynamic quantum dots and the clock-controlled single electron transfer are essential building blocks for the realization of on-chip sources for on-demand electrons or the direct conversion of frequency to current for the quantum ampere in the new SI [1]. The dynamics of the single electron capture process determines accuracy, error mechanisms and the possibility of high-frequency operation in such devices [2-4].

We present electron counting measurements of the frequency dependence of the capture probability for a tunable-barrier, semiconductor single-electron source by varying the effective rise time of the entrance barrier isolating the quantum dot from the lead during the capture process. The quantum dot is embedded in an array of interconnecting detector nodes to monitor the charge at the source and drain of the electron source. Reflectometry measurements of coupled charge detectors offer large bandwidth and sufficiently high fidelity to accurately measure the tails of the capture probability. Measuring the counting statistics of single shot charge capture enables to vary the equivalent frequency from kHz to GHz and to compare the results with the rise-time dependence of optimized excitation waveforms.

Using a non-Markovian single particle model [5] we analyze the non-adiabatic separation of a localized quantum state from the reservoir due to the closing barrier and identify the relevant energy scales from the frequency and temperature dependence of the capture statistics. These results are compared with a Markovian rate equation model at low frequency [6].

.

References

[1] B. Kaestner and V. Kashcheyevs , Rep. Prog. Phys. , **78**, 103901 (2015).
[2] A. Fujiwara, K. Nishiguchi and Y. Ono , Appl. Phys. Lett. , **92**, 042102 (2008).
[3] S. P. Giblin et al. , Applied Physics Letters , 108 (2016).
[4] G. Yamahata, K. Nishiguchi and A. Fujiwara , Phys. Rev. B , **89**, 165302 (2014).
[5] V. Kashcheyevs and J. Timoshenko , Phys. Rev. Lett. , **109**, 216801 (2012).
[6] V. Kashcheyevs and B. Kaestner , Phys. Rev. Lett. , **104**, 186805 (2010).

Energy Scales in Quantum Dots for Single Electron Pumps

Tobias Wenz, Friederike Stein, Frank Hohls, Hans W. Schuhmacher
Physikalisch-Technische Bundesanstalt (PTB), 38116 Braunschweig, Germany
Jevgeny Klochan, Vyacheslav Kashcheyevs
Faculty of Physics and Mathematics, University of Latvia, LV 1002 Riga, Latvia
Tobias.Wenz@ptb.de

Quantum dots based on GaAs/AlGaAs heterostructures with tunable barriers can be used as single electron pumps. By capturing a well-defined number of electrons n from source and emitting them to drain with a high frequency f a quantized current $I=nef$ is produced, where e is the electron charge [1]. This concept is useful for on-demand electron sources for electron quantum optics and for the redefinition of the ampere by fixing the value of e. For the latter case, robust pumping at sub-ppm accuracy levels has been demonstrated [2]. Several theoretical models, like the decay cascade model [3], describe the performance of tunable-barrier pumps in different regimes of operation. While they yield good fits, the respective energy scales cannot be obtained easily. Goal of this work is to determine these energy scales using multiple approaches. One approach is to investigate the performance of single electron pumps at different temperatures and observe the broadening of transition lines in different pumping regimes. Another method is to use custom-tailored waveforms to extract tunneling rates during the loading phase of the quantum dot (c.f. Fig. 1). Furthermore, this method can be used to study excited states of the quantum dot and their relaxation rates and reveal two-electron effects.

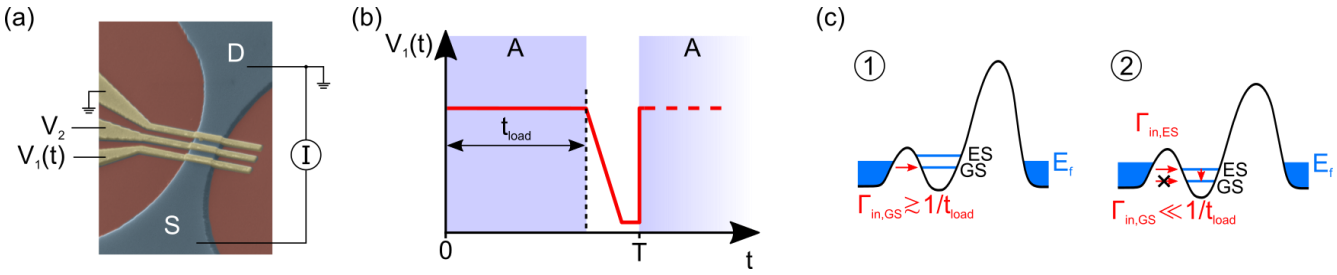

Fig.1 (a) A quantum dot is formed between gates 1 and 2. (b) RF modulation of the entry gate (typical frequency f=1/T=50 MHz). Loading of electrons into the dot occurs during phase A, when the entry barrier under gate 1 is low. (c) Sketch of band diagram during phase A for different settings of DC voltages. Depending on the alignment of ground and excited state and the respective tunnel barriers, tunneling can only occur into ground state (example 1) or excited state (example 2).

References

[1] B. Kaestner & V. Kashcheyevs, Rep. Prog. Phys. **78**, 103901 (2015)
[2] F. Stein *et al.*, Metrologia **54**, S1 (2017)
[3] V. Kashcheyevs & B. Kaestner, Phys. Rev. Lett. **104**, 186805 (2010)

Waiting times in feedback controlled and driven single-electron tunneling

T. Wagner, J. C. Bayer, E. P. Rugeramigabo and R. J. Haug
Institute for Solid State Physics, Leibniz Universität Hannover
Appelstraße 2, 30167 Hannover, Germany
wagner@nano.uni-hannover.de

Recently we reported the strong suppression of shot-noise in a closed-loop controlled single-electron transistor [1]. For the optimal feedback response the saturation value of second cumulant of the Full Counting Statistics is found to be given by the electron target number [2]. Here we compare the feedback control, with a periodically driven single-electron tunneling process by focusing on the waiting times between subsequent tunneling events [3,4]. Both techniques are capable of generating a highly accurate current [5], but achieve this in a very different way, as revealed by the extracted waiting time distributions (WTDs). The feedback optimizes the arrangement of the waiting times in such a way, that the random fluctuations of the tunneling process are fully suppressed on long time scales. In the driven case instead, the tunneling events become synchronized with the external signal, reducing the random fluctuations.

The waiting times are extracted from real-time charge detection measurements with an adjacent quantum point contact. By compensating the negative crosstalk with the detector, we are able to analyze both systems over a wide range of parameters.

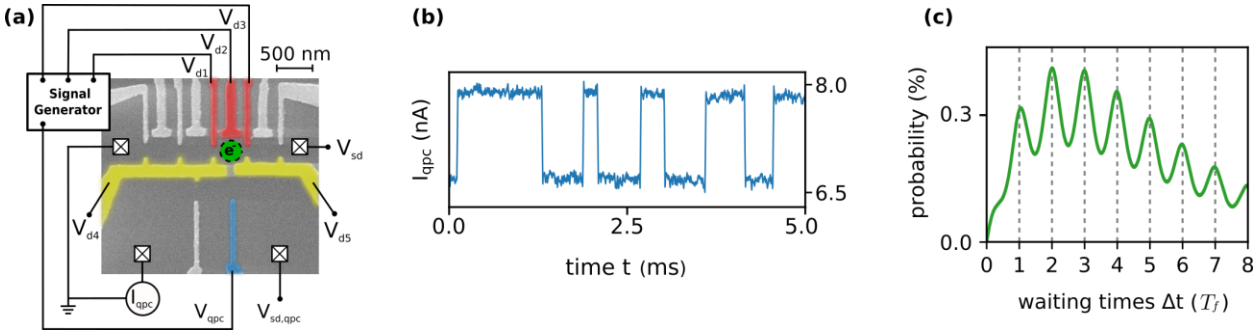

Fig. 1: a) SEM image of the quantum dot device for feedback controlled and driven single-electron tunneling. **b)** Snapshot of a time resolve QPC charge detector measurement. **c)** Waiting time distribution of the driven single-electron tunneling process.

References:

[1] T. Wagner, *et., al.*, Nature Nanotech., DOI:10.1038/nnano.2016.225 (2015)
[2] T. Wagner *et. al.*, Phys. Status Solidi B, DOI:10.1002/pssb.201600701 (2016)
[3] T. Brandes, *Ann. Phys.* **17**, 477 (2008)
[4] M. Albert, C. Flindt, and M. Büttiker, *Phys. Rev. Lett.* **107**, 086805 (2011)
[5] J. P. Pekola, *et. al.*, Rev. Mod. Phys. ***85***, *1421 (2013)*

Spin-orbit signatures in the dynamics of singlet-triplet qubits in double quantum dots

Juan E. Rolon
Department of Physics and Astronomy, University of North Carolina, Chapel Hill, North Carolina, 27599-3255, USA
Ernesto Cota
Centro de Nanociencias y Nanotecnologia, Universidad Nacional Autónoma de México, Apartado Postal 14, Ensenada, Baja California, 22800 México
Sergio E. Ulloa
Department of Physics and Astronomy, and Nanoscale and Quantum Phenomena Institute, Ohio University, Athens, Ohio, 45701-2979, USA
ernesto@cnyn.unam.mx

We characterize numerically and analytically the signatures of the spin-orbit interaction in a two-electron GaAs double quantum dot in the presence of an external magnetic field. In particular, we obtain the return probability of the singlet state by simulating Landau-Zener voltage detuning sweeps which traverse the singlet-triplet ($S - T_+$) resonance. Our results indicate that non-spin-conserving interdot tunneling processes arising from the spin-orbit interaction have well defined signatures. These allow direct access to the spin-orbit interaction scales and are characterized by a frequency shift and Fourier amplitude modulation of the Rabi flopping dynamics of the singlet-triplet qubits $S - T_0$ and $S - T_+$. By applying the Bloch-Feshbach projection formalism, we demonstrate analytically that the aforementioned effects originate from the interplay between spin-orbit interaction and processes driven by the hyperfine interaction between the electron spins and those of the GaAs nuclei.

Universal Modeling of Weak Localization-Antilocalization in Quasi-Two-Dimensional Electrons using Predetermined Return Trajectories

A. Sawada, K. Okamoto and T. Koga
Graduate School of Information Science and Technology, Hokkaido University
Kita 14, Nishi 9, Kita-ku, Sapporo, Hokkaido, 060-0814, Japan
koga@ist.hokudai.ac.jp

It is well-recognized that the weak localization-antilocalization (WL-WAL) effect provides a useful tool to study the phase relaxation time and the spin-orbit interaction (SOI) in quasi-two-dimensional electron systems (2DESs) [1]. To date, the most "useful" WL-WAL models use the "diffusion approximation", which both simplifies the theoretical procedures in k space and provides simple analytical formulas to fit the experimental data [2]. However, these formulas are valid only in small magnetic field ranges for B and B_{SO}, the external magnetic field perpendicular to the 2DES and the magnetic field relevant to the SOI, respectively. On the other hands, to compute the exact models for the WL-WAL effects numerically, such as the Golub model [3], is so cumbersome that many experimentalists tend to give up using the exact WL-WAL models in analyzing their experimental data, although they provide richer information than those with the "diffusion approximation".

In this work, we present a new method to calculate the WL-WAL corrections based on the real space simulation, using 147,885 predetermined return orbitals for a two-dimensional electron up to 5,000 scattering events [4]. As shown in Fig. 1, our model subsumes the results of the Golub model when the Rashba SOI is assumed. Our computation is very simple, fast, and versatile, where the numerical results, obtained all at once, cover wide ranges of the magnetic field under various one-electron interactions H' exactly. It has straightforward extensibility to incorporate interactions even other than the Rashba and Dresselhaus SOIs, such as the Zeeman effect, and interactions associated with the valley and pseudo spin degrees of freedom.

This work was supported by JSPS KAKENHI Grant Number 16H01045.

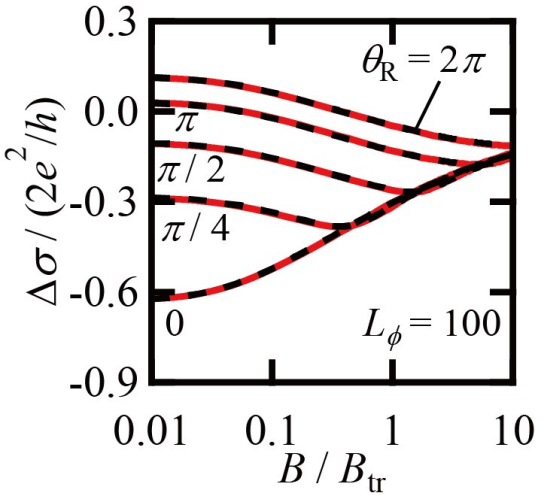

Fig.1 WL-WAL corrections to the magneto-conductivity $\Delta\sigma$ in the present model for various spin rotation angles θ_R per mean free path length ℓ by the Rashba SOI (red solid curves). Plotted together are the results obtained by the Golub model using the same θ_R's (black dashed curves). The phase coherence length of $L_\varphi = 100\ell$ was assumed. We also note $B_{tr}=\hbar/2e\ell^2$.

References

[1] S. Faniel, T. Matsuura, S. Mineshige, Y. Sekine, and T. Koga, Phys. Rev. B **83**, 115309 (2011).
[2] S. Hikami, A. I. Larkin, and Y. Nagaoka, Prog. Theor. Phys. **63**, 707 (1980).
[3] L. E. Golub, Phys. Rev. B **71**, 235310 (2005).
[4] A. Sawada and T. Koga, Phys. Rev. E **95**, 023309 (2017).

SU(2) Symmetric Spin-Orbit Coupling in 2D Electron System: the General Description for Quantum Wells with an Arbitrary Growth Direction

Alexander Kozulin, Alexander Malyshev, Vladimir Degtyarev, Sofia Khazanova,
Natalia Kirillova, and Anton Konakov
Faculty of Physics, Lobachevsky University,
23 Gagarin Avenue, 603950 Nizhniy Novgorod, Russia
anton.a.konakov@gmail.com

In this work we theoretically study realization of the “exact” SU(2) symmetry and formation of persistent spin helices [1] in two-dimensional electron systems with spin-orbit coupling. We consider a single-particle effective mass Hamiltonian with generalized linear in wave vector spin-orbit coupling term corresponding to a semiconductor quantum well grown in an arbitrary crystallographic direction [2], and derive the general condition for formation of the persistent spin helix [3]. Its application to the electron Hamiltonians in quantum wells with different growth directions indicates that persistent spin helices can manifest themselves in a wide class of 2D systems. In contrary to results obtained by Kammermeier *et al* [4], the proposed condition is formulated only in terms of the spin-orbit coupling parameters and does not prohibit the helices in zinc blende quantum wells with unequal in modulus growth-direction Miller indices. We also employ the translation operator formalism for analytical calculation of space-resolved spin density and visualization of the persistent spin helix patterns.

Then, using the envelope function approximation with the 8-band Kane Hamiltonian we numerically calculated parameters of the linear in wave vector spin-orbit coupling in the symmetric and asymmetric zinc blende quantum wells and find material parameters of the quantum wells (its width, chemical composition and external electric field) that leads to the realization of the SU(2) symmetry.

Finally, we consider the 1D waveguide formed in the 2D electron gas with the spin-orbit coupling. We calculated its spectral and transport properties and find their peculiarities in the system with “exact” SU(2) symmetry, including splitting of the transmitted wave packets and Fano resonances of the transparency in the waveguide with spin-dependent inhomogeneities similar to those investigated in [5].

References

[1] B. A. Bernevig, J. Orenstein, and S.-C. Zhang, Phys. Rev. Lett. **97**, 236601 (2006).
[2] S. D. Ganichev and L. E. Golub, Phys. Status Solidi B **251**, 1801 (2014).
[3] A. S. Kozulin, A. I. Malyshev, and A. A. Konakov, arXiv:1610.05251 (2016).
[4] M. Kammermeier, P. Wenk, and J. Schliemann, Phys. Rev. Lett. **117**, 236801 (2016).
[5] A. I. Malyshev, A. S. Kozulin, Journal of Experimental and Theoretical Physics **121**, 96 (2015).

Electric field induced enhancement of cubic Dresselhaus spin-orbit interaction in GaAs quantum well

Y. Kunihashi[1], H. Sanada[1], Y. Tanaka[1], H. Gotoh[1], K. Onomitsu[1], K. Nakagawara[2], M. Kohda[2], J. Nitta[2], and T. Sogawa[1]
[1]NTT Basic Research Laboratories, NTT Corporation, Atsugi, Japan
[2]Department of Materials Science, Tohoku University, Sendai, Japan
kunihashi.y@lab.ntt.co.jp

The electrical control of spin dynamics by using effective magnetic fields induced by spin-orbit interactions (SOI) is a key technology for realizing spin-based devices. In previous studies, it has been demonstrated that only the Rashba SOI-induced effective magnetic field is controlled by a gate electric field in III-V semiconductor heterostructures. In this report, we discuss the in-plane electric field dependence of the SOI for laterally drifting spins in a GaAs quantum well. The strengths of spin-orbit effective magnetic fields were quantitatively estimated from spin precession periods measured using spatially resolved Kerr rotation microscopy. The in-plane electric field dependence of the spin precession frequency for steadily drifting spins reveals that the strength of a cubic Dresselhaus SOI is varied by an in-plane electric field induced change in the momentum distribution in an electron system. Our achievement will provide a new way to control electron spins by using cubic Dresselhaus SOI and will be of great importance as regards a further understanding of spin transport dynamics.

The drift transport of electron spins optically injected into a GaAs quantum well was detected as spatially oscillating Kerr rotation signals θ_K at $T = 8$ K. The spatial frequency of the spin precession was extracted by fitting the experimental data to a model function $\theta_K = A\exp(-d/l_{SO})\cos(k_{SO}d)$, where d is the distance from the pump position, l_{SO} is the spin decay length and k_{SO} is the wavenumber that represents the spatial frequency of the spin precession. The drift velocity dependence of k_{SO} for spins drifting in the [1-10], [100], and [110] directions is shown in Fig. 1(a). The anisotropy of k_{SO} for the three directions is caused by the interplay between the Rashba and Dresselhaus SOIs. k_{SO} decreases monotonically with increases in drift velocity v_d for all crystallographic directions, indicating that the effective magnetic fields are weakened by applying in-plane electric fields. The experimentally observed drift velocity dependence of k_{SO} cannot be explained by the presence of a k-linear SOI, since the k_{SO} originating from the k-linear SOI is constant for the drift velocity [1]. A model developed for drifting spins with a heated electron distribution characterized by electron temperature T_e suggests that the in-plane electric field enhances the cubic Dresselhaus SOI, which cancels out the total effective magnetic fields and qualitatively explains the experimental result as shown in Fig. 1(b).

This work was supported by JSPS KAKENHI Grant Numbers JP15H05699 and JP16H03821.

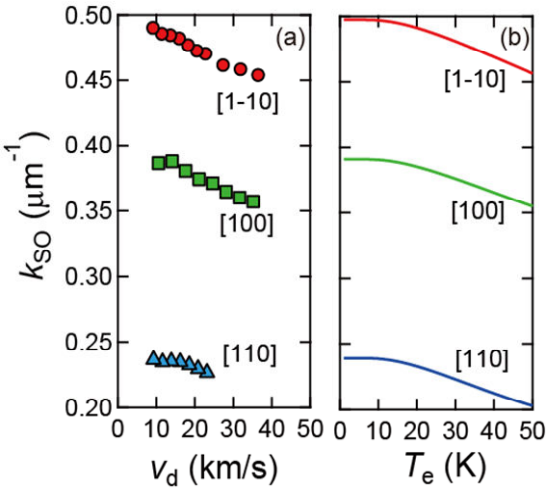

Fig. 1 (a) Drift velocity dependence of spin wavenumbers k_{SO} for the three drift directions. (b) Theoretically calculated k_{SO} as a function of electron temperature T_e.

References

[1] Y. Kunihashi et al., Nat. Comm. **7**, 10722 (2016).

Magnetoelectric coupling in GaMnAs /P(VDF-TrFE) and GaMnAs/Graphene/P(VDF-TrFE) hetero-structures

Shavkat U. Yuldashev, Ziyodbek A. Yunusov, Hee Chang Jeon, Gukhyung Ihm[+], Nojoon Myoung[++], Tae Won Kang, Seung Joo Lee*

Quantum-Functional Semiconductor Research Center, Dongguk University, Seoul 04620, Republic of Korea

[+]*Department of Physics, Chungnam National University, Daejeon, 34134, Republic of Korea*

[++]*Center for Theoretical Physics of Complex Systems, Institute for Basic Science, Daejeon 34051, Republic of Korea*

*leesj@dongguk.edu

The multiferroic materials possessing both ferroelectric and ferromagnetic orders attract high interest, driven by their potential for electronic and spintronic applications [1, 2]. The choice of materials for multiferroic heterostructure is mainly dictated by the processing compatibility between the ferroelectric and ferromagnetic components. The multifferoic heterostructures on the base of GaMnAs presents a major challenge due to very low temperature processing, below 250 ^{o}C. Recently, a multifferoic heterostructure on the base of GaMnAs and organic polyvinylidene fluoride with trifluoroethylene P(VDF-TrFE) layers has been demonstrated. This ferroelectric polymer does not react chemically with the semiconductor and offers very low processing temperature of 130-140 ^{o}C.

In this work, we present an experimental study of the electric field effect on the Curie temperature in GaMnAs/P(VDF-TrFE) (Fig. 1) and GaMnAs/Graphene/P(VDF-TrFE) multiferroic structures. The shift of the Curie temperature observed in GaMnAs thin layer demonstrates an effective and non-volatile electric-field control of ferromagnetism in the semiconductor layer using the ferroelectric P(VDF-TrFE) polymer as the gating material. The control of ferromagnetism using the ferroelectric gate relies on the mediation of the Mn-Mn exchange interaction by the strongly spin-orbit coupled valence band holes which control both the strength of the magnetic interactions and the magnetocrystalline anisotropies. This work has been supported by NRF Korea No NRF-2016R1D1A1B04935798

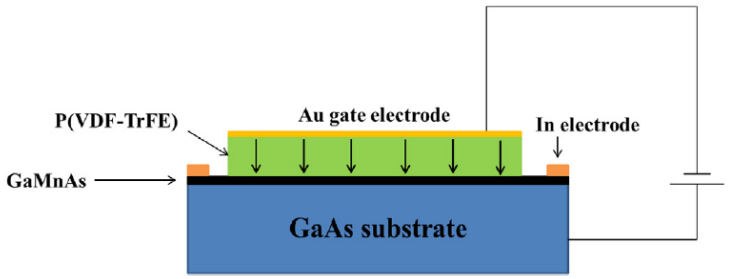

Fig. 1. Schematic cross section of GaMnAs/P(VDF-TrFe) composite multiferroic structure. The black arrows show the direction of polarization in the ferroelectric gate.

References

[1] W. Eerenstein, N. D. Mathur, J. F. Scott, Nature **442**, 759 (2006).

[2] H. Bea, M. Gajek, M. Bibes, A. Barthelemy, J. Phys. Condens. Matter **20**, 434221 (2008).

Time-Dependent Spin Precession Frequency in InGaAs/GaAs Quantum Wells with Mn Delta-Doped Heterostructures

F. C. D. Moraes[1], M. G. A. Balanta[2], F. Iikawa[2], Y. A. Danilov[3], M. V. Dorokhim[3], O. V. Vikhrova[3], B. N. Zvonkov[3] and F. G. G. Hernandez[1]

(1) Physics Institute, University of Sao Paulo ,Cidade Universitária, 05508-090 Sao Paulo, Brazil.

(2) Gleb Wataghin Physics Institute, UNICAMP, Barão Geraldo, 13083-970 Campinas, SP,Brazil.

(3) Physico-Technical Research Institute, Nizhny Novgorod State University, Russia.

fmoraes@if.usp.br

Semiconductor spintronics may have a giant impact on the market of storage and reading devices due to their possible enhanced velocity and storage capacity [1]. Nevertheless, the improvement of actual systems still requires spin injection and magnetic ordering at room temperatures. Heterostructures like (Ga,As)Mn, combining the Mn ferromagnetic properties with the well know technology of III-IV semiconductor structures, are being studied with the propose of increasing the number of spin carriers in semiconductors [2]. The initial problem of low critical temperature may have been solved with the demonstration of T_C = 250 K in GaAs by growing delta-Mn-layers [3]. Furthermore, the possibility of data memory was shown in InGaAs/GaAs quantum wells (QWs) adjacent to a delta-Mn-layer, due to the wavefunction overlap of spins carrier inside the quantum well and Mn atoms [4]. A more detailed study of the dynamical interaction between photoexcited spins in the quantum well and the Mn atoms is still necessary.

Here, we studied the spin dynamics in InGaAs QWs with Mn delta-doping in the barrier grown by MOCVD. Time-resolved Kerr rotation was performed using a tunable mode-locked Ti:sapphire laser with pulse duration of 1 ps and repetition rate of 76 MHz. The time delay (Δt) between pump and probe pulses was varied by a mechanical delay line. The pump beam was circularly polarized by means of a photo-elastic modulator and the probe was linearly polarized and modulated by a chopper. The polarization rotation of the reflected probe beam was detected with a balanced bridge using coupled photodiodes. The sample was immersed in the variable temperature insert of a split-coil superconductor magnet in the Voigt geometry. We observed a time-dependent spin precession frequency for the photo-excited electrons. We associated this effect to the dynamical alignment of the internal effective magnetic field produced by the Mn after optical excitation and successive relaxation. The strong dependence and control of the system magnetization with the experimental conditions will be presented.

References

[1] G. A. Prinz, Magnetoelectronics, Science 282, 1660 (1998).

[2] A. Haury, A. Wasiela, A. Arnoult, J. Cibert, S. Tatarenko, T. Dietl, and Y. Merle d'Aubigné. Phys. Rev. Lett. **79**, 511 (1997). K.W. Edmonds, P. Bogusławski, K. Y.Wang, R. P. Campion, S. N. Novikov, N. R. S. Farley, B. L. Gallagher, C. T. Foxon, M. Sawicki, T. Dietl, M. Buongiorno Nardelli, and J. Bernholc. Phys. Rev. Lett. **92,** 37201 (2004).

[3] A. M. Nazmul, T. Amemiya, Y. Shuto, S. Sugahara, and M. Tanaka, Phys. Rev. Lett. 95, 017201.

[4] V. Korenev, I. Akimov, S. Zaitsev, V. Sapega, L. Langer, D. Yakovlev, Y. A. Danilov, and M. Bayer. Nat Commun, **3,** 959 (2012). M. A. G. Balanta, M. J. S. P. Brasil, F. Iikawa, U. C. Mendes, J. A. Brum, Y. A. Danilov, M. V. Dorokhin, O. V. Vikhrova, and B. N. Zvonkov. Scientific Reports, **6**, 24537 (2016).

Spin Scattering from Dysprosium Atoms in Indium Tin Oxide Thin Films Produced by Sol-Gel Method

R. Ota[1], M. Nishioka[1], A. Fujimoto[1], Y. Kashiwagi[2], M. Saitoh[2], M. Nakamoto[2],
Y. K. Zhou[3], B. Liu[3], C. Xing-Heng [3], Y. Harada[1], T. Kamimura[1]
[1]*Osaka Institute of Technology, Osaka* 535-8585, *Japan*
[2]*Osaka Municipal Technical Research Institute, Osaka* 536-8553, *Japan*
[3]*Shanghai Normal University Shanghai* 200234, *China*
m1m16306@st.oit.ac.jp

Rare earth (RE) element doped diluted magnetic semiconductors have attracted much attention to their unique magnetic properties. For example, GaDyN single layer and GaDyN/AlGaN multi quantum well exhibit ferromagnetism (FM) [1]. Dy^{3+} ion shows the largest magnetic moment among RE elements. Moreover we have already reported some characteristic magneto-transport properties in the chemically synthesized indium tin oxide (ITO) nanoparticles thin films [2]. ITO achieves higher carrier concentration than that of other oxide semiconductors such as ZnO by means of Sn intentionally doping and double donors due to oxygen defects. Therefore Dy doped ITO (Dy-ITO) are expected to lead carrier-induced FM.

In this study we used sol-gel method to produce Dy-ITO thin films, which were chemically synthesized from the corresponding metal complexes, indium alkylcarboxylate, tin alkylcarboxylate, dysprosium acetylacetonate, and additional ligand, e.g. diethanolamine. They were put into toluene and heated at 120 ºC for 1 hour. The obtained sol materials were spin-coated on glass substrates and annealed at 500 ºC for 30 minutes. We prepared Dy-ITO thin films with different Dy concentration and examined Dy concentration dependence of quantum transport phenomena such as weak anti-localization (WAL). For a thin film with 4 mol % Dy and 8 mol % Sn, at low temperatures (T) an increase of resistivity with a log T dependence was found. Furthermore the sheet resistance is less than h/e^2, where h is Planck constant and e the elementary charge, showing that the electron system is in the state of weak localization (WL).

Figure 1 shows T dependence of magneto-resistance (MR) in perpendicular magnetic fields (B) for the above mentioned Dy-ITO thin film. Negative MR appeared at higher T, but positive MR in the region of weak B was observed at 4.7 K. This originates in WAL due to the spin scattering accompanied by Dy atoms. From the experimental results, the spin scattering time (τ_s) and an inelastic scattering one (τ_i) are extracted based on the WL theory, and we will discuss the important role of Dy atoms using τ_s and T dependence of τ_i in our presentation.

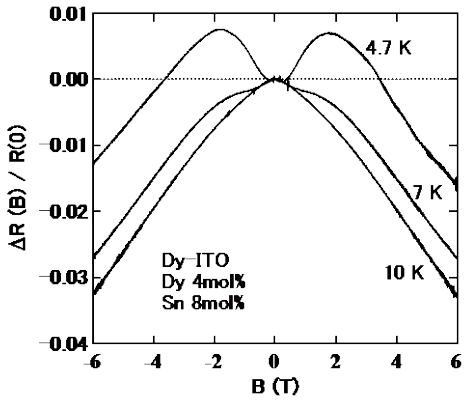

Fig.1 Temperature dependence of MR for Dy-ITO thin film (4 mol % Dy and 8 mol % Sn)

References

[1] Y. Nakatani, Y. K. Zhou, *et al*., e-Journal of Surf. Sci. and Nanotech. **10** 499-502 (2012).

[2] A. Fujimoto *et al*., J. Phys. Soc. Jpn. **82**, 024710 (2013).

Tailoring Quantum Wells for the Implementation of Two-Subband Persistent Spin Helices

A. S. L. Ribeiro[1], G. J. Ferreira[2], F. C. D. Moraes[1], G. M. Gusev[1], A. K. Bakarov[3], and F. G. G. Hernandez[1]

(1) Instituto de Física, Universidade de São Paulo, São Paulo, SP 05508-090, Brazil.

(2) Instituto de Física, Universidade Federal de Uberlândia, Uberlândia, MG 38400-902, Brazil.

(3) Institute of Semiconductor Physics and Novosibirsk State University, Novosibirsk 630090, Russia.

aminaslr@if.usp.br

Spin-electronics (spintronics) takes advantage of the quantum spin degree of freedom to create integrated devices with new functionalities [1]. Moreover, studies of electron transport by drift or diffusion in semiconductor nanostructures are still required for the implementation of practical technologies [2]. For two-dimensional electron gases (2DEGs) hosted in a semiconductor quantum well (QW), several reports explored the spin-orbit interaction tunability to produce a unidirectional spin-orbit field for the diffusive generation of a spin helix [3]. Very recently, the drift in those helical systems was also demonstrated showing remarkable properties [4]. For two-subband systems, the inter- and intra-subband spin-orbit constants (SOCs) were extensively studied, including a proposal for a crossed persistent spin helix (cPSH) and an intrinsic mechanism for edge spin accumulation [5].

Theoretically, the spin drift and diffusion in 2DEGs is developed here in terms of a random walk model incorporating Rashba, linear and cubic Dresselhaus, and intersubband spin-orbit couplings [2]. For two-subband systems, the additional subband degree of freedom introduces new characteristics to the persistent spin helix dynamics. We identified two possible scenarios regarding the intersubband scattering (ISS) rate.

Experimentally, we studied here a 2DEG confined in a symmetrically doped wide QW producing a two-subband electron system. The sample was characterized using magneto-transport and optical techniques. From the first, the electron mobility and total sheet and subband densities were obtained. All the relevant SOCs were calculated and the possibility of a two-subband spin helix was explored. For the later technique, time- and space-resolved Kerr rotation was performed using a pump-probe scheme. We determined the electron g-factor and spin relaxation time dependence on the experimental parameters and related both with the relaxation mechanisms.

References

[1] S. A. Wolf, D. D. Awschalom, R. A. Buhrman, J. M. Daughton, S. von Molnár, M. L. Roukes, A. Y. Chtchelkanova, D. M. Treger. Science 294, 1488 (2001).

[2] G. J. Ferreira, F. G. G. Hernandez, P. Altmann, G. Salis, arXiv: 1608.05437.

[3] M. P. Walser, C. Reichl, W. Wegscheider, and G. Salis, Nat. Phys. 8, 757 (2012). J. Ishihara, Y. Ohno, and H. Ohno, Appl. Phys. Exp. 7, 013001 (2014).

[4] Y. Kunihashi, H. Sanada, H. Gotoh, K. Onomitsu, M. Kohda, J. Nitta, and T. Sogawa, Nat. Commun. 7, 10722 (2016). P. Altmann, F. G. G. Hernandez, G. J. Ferreira, M. Kohda, C. Reichl, W. Wegscheider, and G. Salis, Phys. Rev. Lett. 116, 196802 (2016).

[5] E. Bernardes, J. Schliemann, M. Lee, J. C. Egues, and D. Loss, Phys. Rev. Lett. 99, 076603 (2007). R. S. Calsaverini, E. Bernardes, J. C. Egues, and D. Loss, Phys. Rev. B 78, 155313 (2008). J. Fu and J. C. Egues, Phys. Rev. B 91, 075408 (2015). J. Fu, P. H. Penteado, M. O. Hachiya, D. Loss, and J. C. Egues, Phys. Rev. Lett. 117, 226401 (2016). A. Khaetskii and J. C. Egues, arXiv:1602.00026.

Point defects and the electronic structure of the antiferromagnetic phases of CrN

Tomas Rojas and Sergio E. Ulloa
Department of Physics and Astronomy, and Nanoscale and Quantum Phenomena Institute, Ohio University, Athens, OH 45701 USA
tr074112@ohio.edu

Chromium nitride (CrN) is believed to be a small indirect gap semiconductor with unusual electronic and magnetic properties. It exhibits a phase transition at T_N~280K in which both the electronic and magnetic structures change from a paramagnetic cubic rock-salt at high temperature to an antiferromagnetic orthorhombic structure below T_N. However, the electronic transport properties of CrN thin films exhibit metallic and semiconducting behavior at low temperatures under different situations in experiments. In particular, the impact of nitrogen vacancies and other defects on the transport properties are yet to be analyzed in detail. Given the antiferromagnetic character of the structure at low temperature, the presence of such vacancies and other defects may also have important consequences on the magnetic behavior and the resistivity.

We have performed ab initio calculations using the LSDA+U method to examine the effect of N and Cr vacancies and antisites in bulk CrN. As antiferromagnetic models with different magnetic periodicities have been shown to be physically plausible in experiments [1], we also analyze the features of vacancies in different environments and compare their intrinsic features.

We study the effects of vacancy concentration by replacing or removing atoms in appropriate supercells of varying size, studying the accompanying deformations of the lattice structure as well as energetics and spatial distribution of the associated charge and spin distribution of the defect state, as seen in Fig 1. Correction of electrostatic artifacts originating from the periodic boundary conditions [2], are used to evaluate formation energies of different defects and compare with experiments. Our results indicate that a high percentage of N vacancies results in a transition towards a metallic phase, producing substantial defects on the local magnetic arrangements that may even create a small magnetization.

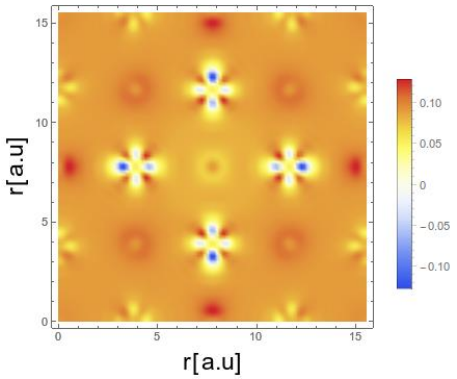

Fig 1. Spin density ρ(↑)-ρ(↓) near the N vacancy.

Other possible if less-likely defects such as N-N and Cr-N vacancies are also studied and shown to have unique spin and charge characteristics.

References

[1] L. Zhou *et al*., Phys. Rev. B **90**, 184102 (2014).
[2] C. Freysoldt, *et al*., Phys. St. Sol. (B) **248**, 1067 (2011).

Diffusion Dynamics of Long-lived Electron Spins in Undoped GaAs Quantum Wells

H. Sanada[1], Y. Kunihashi[1], Y. Tanaka[1], H. Gotoh[1], K. Onomitsu[1], M. Kohda[2], J. Nitta[2], and T. Sogawa[1]
[1]*NTT Basic Research Laboratories, NTT Corporation, Atsugi, Japan*
[2]*Department of Materials Science, Tohoku University, Sendai, Japan*
sanada.haruki@lab.ntt.co.jp

Finding a way to preserve spins in non-magnetic semiconductors is essential for future spin-based electronics. The spins of excitons have been widely studied because the polarization-dependent selection rule of the inter-band optical transition provides rich information about their spins [1]. However, the time scale on which we can measure the exciton spins is limited by the radiative lifetime, which is often less than 1 ns. In this report, we discuss the spin diffusion dynamics of electrons with unexpectedly long relaxation times (>10 ns) observed in an undoped GaAs quantum well (QW).

We grew an undoped 20-nm-thick GaAs/AlGaAs (001) QW by MBE, and carried out time and spatially resolved photoluminescence (PL) and Kerr rotation (KR) measurements at 8 K. The PL and PL excitation (PLE) peaks of the excitons had linewidths narrower than 0.7 meV, indicating that the crystal quality is sufficiently high for us to discuss the exciton behavior. The time-resolved KR in the absence of an external magnetic field shows that the photo-injected spins survived for 16 ns in a small area (FWHM ~6 μm) irradiated by circularly polarized pump laser. This decay time was one order of magnitude longer than the radiation lifetime and it decreased as we increased the temperature or the pump spot size.

To gain further insight into the spin dynamics, we investigated spin diffusion by measuring the probe-position dependence of the spin precession with the setup described in Fig. 1(a). Figure 1(b) shows the time-resolved KR for different probe positions (FWHM ~3 μm) on the X (|| [100]) and Y (|| [010]) axes under an external magnetic field B_{ext} = 49 mT applied in the X direction. The oscillations at the centers ($X = 0$ and $Y = 0$) correspond to the spin precession determined by $\mathbf{B}_{ext}$. For both scanning directions, the Gaussian envelopes of the spatial profiles do not expand clearly over time. However, the precession frequency Ω increases linearly in the X direction whereas it is constant in the Y direction. This behavior cannot be explained without spin diffusion, and its direction dependence is consistent with the symmetry of the k-linear Dresselhaus spin-orbit interaction [Fig. 1(c)]. A linear fit to Ω(X) provided $d\Omega/dX$ ~8 MHz/μm, from which a small diffusion coefficient D_s < 10 cm^2/s was obtained according to the theory [2]. These results suggest that the electron spins, which were prevented from radiative recombination, diffuse very slowly under the Dresselhaus spin-orbit field. The ability to access such long-lived spin dynamics might offer the possibility of memorizing quantum information in solid-state systems.

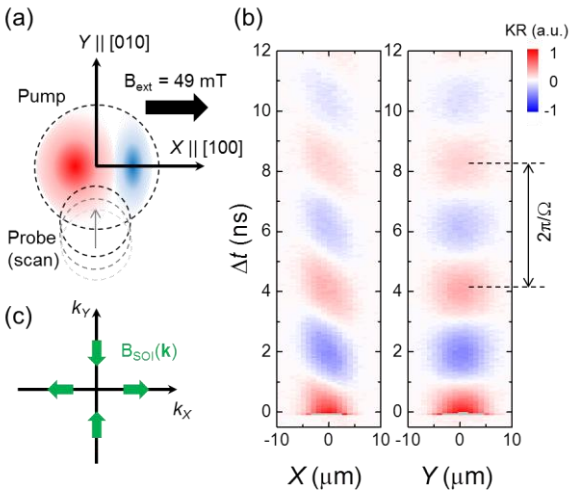

Fig.1 (a) Schematic configuration of the spin diffusion measurement. (b) KR signals plotted as a function of delay Δt and probe position (X and Y). (c) Dresselhaus effective magnetic fields in k-space.

This work was supported by JSPS KAKENHI Grant Numbers JP15H05699 and JP16H03821.

References

[1] A. Vinattieri *et al*., APL **63**, 3164 (1993), T. Amand *et al*., PRL **78**, 1355 (1997).
[2] M. Kohda *et al*., APL **107**, 172402 (2015).

Anomalous large apparent oscillation of effective g-factor in an InSb quantum well two-dimensional electron gas

G.V. Smith[1], P.D. Buckle[1], D.G. Hayes[1], C.P. Allford[1], E.M. Clarke[2] and S. Zhang[2]

1) School of Physics & Astronomy, Cardiff University, Cardiff, CF24 3AA, UK

2) EPSRC National Centre for III-V Technologies, North Campus, University of Sheffield, Sheffield, S3 7HQ, UK

smithg8@cardiff.ac.uk

Investigations into the effect of magnetic fields on the effective g-factor (g^*) for electrons in low dimensional heterostructures is an area of vigorous study due to its applications in spintronic devices and quantum computing. Indium antimonide (InSb) is an extremely attractive candidate for spin dependent field studies due to its small band gap, light electron effective mass and the largest intrinsic electron g-factor, which induces spin dependent effects at much lower magnetic fields when compared to other binary compounds like GaAs. In the presence of a quantizing magnetic field the 2D density of states separates into spin split Landau levels (LL's) due to Zeeman splitting of the spin states. Resolvable spin split LL's can be observed <1T in moderate mobility InSb QW samples, (Fig.1) and large net spin populations can be achieved at modest fields.

We report magnetotransport measurements for 30nm InSb/$Al_xIn_{1-x}Sb$ QW 2DEGs with mobility up to 200,000$cm^2V^{-1}s^{-1}$ processed into 6 contact Hall bar geometries. Values for g^* extracted from Shubnikov de-Haas (SdH) oscillations at fields up to 8T can appear on first analysis to show enhancement of g^* (Fig.2) of up to an order of magnitude above the bulk value and around 5 times larger than anything previously reported in the literature for this material system [2]. The sign of g^* in this analysis is also calculated to oscillate between successive LL occupation, a trend which has not previously been reported in III-V compounds. These anomalous results are extracted from analysis that is employed widely throughout the literature on other material systems. However we discuss the subtle problems with this method of analysis which become starkly apparent when working with very high g* materials such as InSb.

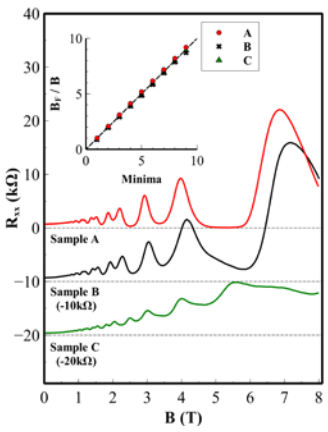

Fig.1 Longitudinal resistance (R_{xx}) as a function of B at 12mK. Samples B and C show non-ideal SdH through conduction via a parasitic conduction path. The inset shows the SdH minima positions with respect to the fundamental field (B_F).

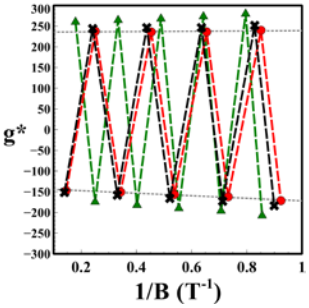

Fig.2 an apparent g* calculated for 3 samples using a non-parabolic approximation to the 2D density of states. The dotted grey lines guide the eye as to the minimum extent of the oscillation.

References

[1] Madelung O, Rössler U, and Schulz M, *Landolt and Bornstein—Group III Condensed Matter: Group IV Elements,(IV–IV) and (III–V) Compounds. Part b—Electronic, Transport, Optical and Other Properties.* (Springer, 2006).

[2] B. Nedniyom, R. J. Nicholas, M. T. Emeny, L. Buckle, A. M. Gilbertson, P. D. Buckle, and T. Ashley, Phys. Rev. B **80**, 125328 (2009).

Spatial-temporal analysis of diffusion-suppressed drift-spin dynamics

Yusuke Tanaka[1], Yoji Kunihashi[1], Haruki Sanada[1], Hideki Gotoh[1],
Koji Onomitsu[1], Keita Nakagawara[2], Makoto Kohda[2], Junsaku Nitta[2], and Tetsuomi Sogawa[1]
[1]*NTT Basic Research Laboratories, NTT Corporation, Atsugi, Japan*
[2]*Department of Materials Science, Tohoku University, Sendai, Japan*
tanaka.yu@lab.ntt.co.jp

The control of electron spin dynamics during drift transport is the key to developing spintronic devices. When two-dimensional electrons are exposed to an in-plane electric field, the spatial distributions of photo-injected spins change dynamically owing to the drift-diffusion equation [1, 2]. Diffusion reduces the spin densities over time, and so a small diffusion coefficient (D_s) is ideal for the efficient transfer of spins. Here, we report the results of our experimental spatial-temporal Kerr imaging of drifting electron spins with a suppressed D_s. We observed unexpected spin precession behaviors, which we explained using a drift-diffusion model involving the Dresselhaus spin-orbit interaction (SOI) and the Gaussian distribution of the initial spin polarization in a small D_s region.

We measured two-dimensional maps of the Kerr rotation angle $\theta_K(x, t)$ at 8 K for an *n*-doped GaAs quantum well, in which the photo-excited spins were transported with an in-plane electric field. Here, x and t are distance and delay time between the pump and probe, whose spots size were 7 and 2.5 μm, respectively. In general, a *k*-linear SOI induces velocity-independent spatial spin precessions, resulting in constant-phase lines that are parallel to the t axis in a $\theta_K(x, t)$ map. In actual systems, it has been reported that the slope of the constant-phase lines becomes positive because of the cubic Dresselhaus SOI [3]. However, our experimental data shows negative slopes, which cannot be understood with the previous interpretation. We discuss this unexpected phenomenon with a theoretical model. In the calculation, the spatial distribution of the electron spin was convoluted with the Gaussian profiles of the pump and probe lights. The oscillations in the simulated $\theta_K(x, t)$ shown in Fig. 1 represent the spin precession due to the SOI. The constant-phase lines have a positive slope for D_s = 0.015 m^2/s, whereas those for 0.003 cm^2/s have negative slopes, which are the same as we observed in the experiment. This negative slope appears only in systems with a sufficiently small D_s, thus we consider this to originate from the transient phenomenon of spin diffusion.

This work was supported by JSPS KAKENHI (JP15H05699 and JP16H03821).

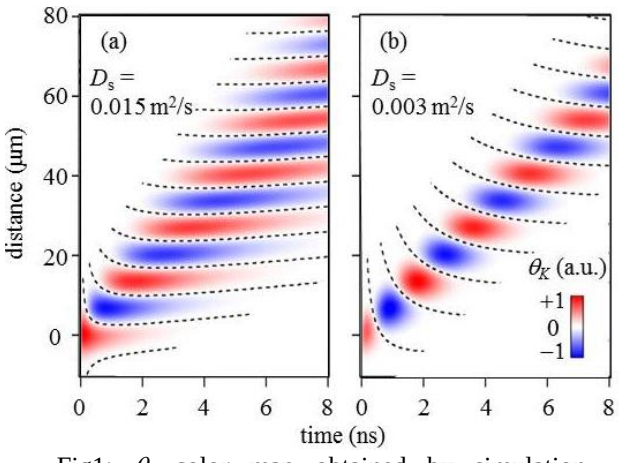

Fig1: θ_K color map obtained by simulation. Dashed lines show constant phase lines of θ_K = 0.

References

[1] M.P. Walser *et al*., Nat. Phys. **8**, 757 (2012).
[2] Y. Kunihashi *et al*., Nat. Comm. **7**, 10722 (2016).
[3] P. Altmann *et al*., PRL **116**, 196802 (2016).

Kondo Screening and Interference in a Dot-Cavity Geometry: Conductance Beyond Proportional Coupling

L. G. G. V. Dias da Silva[1], C. H. Lewenkopf[2], E. Vernek[3], G. J. Ferreira[3], and S. E. Ulloa[4]
[1]*Instituto de Física, Universidade de São Paulo, C.P. 66318, 05315–970 São Paulo, SP, Brazil*
[2]*Instituto de Física, Universidade Federal Fluminense, 24210-346 Niterói, Brazil*
[3]*Instituto de Física, Universidade Federal de Uberlândia, Minas Gerais 38400-902, Brazil.*
[4]*Department of Physics and Astronomy, and Nanoscale and Quantum Phenomena Institute, Ohio University, Athens, Ohio 45701-2979, USA*
ulloa@ohio.edu

The quantum coupling of spatially localized discrete levels onto cavity modes has emerged as a key tool for quantum information processing in cavity systems in atoms, as well as in semiconductor quantum dots and exciton-polariton condensates in optical systems. The coherent connection of such separate entities gives rise to interesting single-particle interference and may give rise to novel control of many-body states.

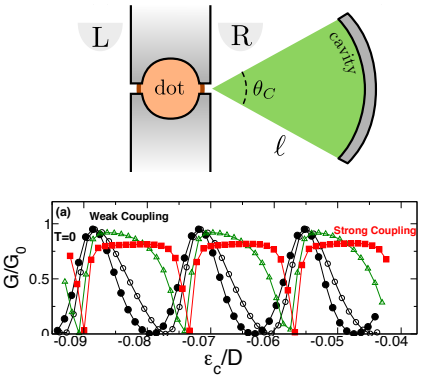

Such interference may be suitably explored through the electronic transport properties in nanostructured systems with complex geometry, as demonstrated in recent experiments [1,2]. As detailed measurements on interacting systems are possible, it is important to obtain a conductance expression for systems whose connectivities do not meet the proportional coupling condition of the well-known Meir-Wingreen formula. In this work, we present a generalization that allows for the analysis of more complex structures and sheds insights into the behavior of shared correlations and screening.

As an interesting use of this formalism, we study a quantum dot coherently connected to tunable electronic cavity modes (Fig. 1 top) [1]. The structure is shown to exhibit a well-defined Kondo effect over a wide range of coupling strengths between the subsystems. The calculated conductance curves exhibit strong modulations and asymmetric behavior as different cavity modes are swept through the Fermi level, as seen in experiments (Fig. 1 bottom). This occurs, however, while a robust Kondo singlet correlations of the dot with the electronic reservoir is maintained, a direct consequence of the complex geometry of the device.

References

[1] C. Rössler *et al.,* Phys. Rev. Lett. **115**, 166603 (2015).
[2] B. Brun *et al*., Phys. Rev. Lett. **116**, 136801 (2016).

Transport measurements in graphene/WSe_2 heterostructures

Tobias Völkl, Tobias Rockinger, Martin Drienovsky, Dieter Weiss, Jonathan Eroms
Institute of Experimental and Applied Physics, University of Regensburg,
Universitätsstraße 31, 93053 Regensburg, Germany
tobias.voelkl@physik.uni-r.de

Due to its low spin-orbit coupling (SOC) strength and therefore resulting low spin relaxation, graphene is a very interesting material for spintronic applications. However, for applications like the generation of pure spin currents through the spin-Hall-effect or the manipulation of spin currents through an electric field, high SOC is necessary. In recent years several methods to increase SOC in graphene have been proposed such as the application of hydrogen or heavy metals. These methods have the disadvantage of increasing the scattering rate in graphene and therefore lowering its mobility.

An alternative method that was recently proposed is to place graphene on a substrate with high SOC. The semiconducting two-dimensional transition metal dichalcogenides are ideal candidates due to their flat surface. Bandstructure calculations performed by Gmitra et al. on a WSe_2/graphene heterostructure showed that the position of the charge neutrality point of graphene lies well inside the bandgap of WSe_2, while a strong SOC is induced in graphene [1].

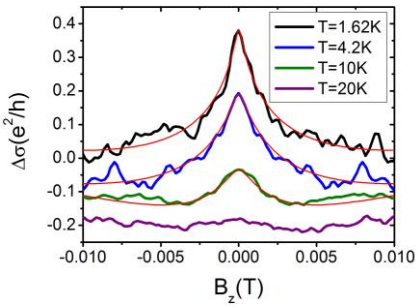

Fig.1 Temperature dependence of the conductivity of graphene/WSe_2. The sharp peak in the conductivity can be fitted with the theoretically predicted formula for the WAL effect (red lines).

In this work we employed a van-der-Waals pick-up technique to produce heterostructures consisting of graphene/WSe_2 and hBN/graphene/WSe_2. For the graphene/WSe_2 samples we could observe mobilities around 10000 cm^2/Vs. Magnetic field dependent resistance measurements on these samples showed a peak in the conductivity at low magnetic field. This dip is attributed to the weak antilocalization (WAL) effect, stemming from SOC. By comparing this feature with calculations of McCann and Falko [2] we estimate the spin diffusion length to be around 250 nm, i.e. much shorter than in pristine graphene (~1 µm). These results are in agreement with the findings of Wang et al. [3] and indicate the presence of strong SOC in these samples.

For hBN/graphene/WSe_2 we observe mobilities around 100000 cm^2/Vs. This confirms the suitability of WSe_2 as a substrate for high mobility graphene. However, in these samples no WAL peak can be observed. We attribute this to a transition from the diffusive to the quasiballistic regime. Also a feature dependent on a sample width emerges at low magnetic field. This we ascribe to a size effect, due to boundary scattering [4]. This feature further confirms the quasiballistic behavior of these samples.

References

[1] M. Gmitra et al., Phys. Rev. B 93, 155104 (2016)
[2] McCann and Falko, Phys. Rev. Lett. 108, 166606 (2012)
[3] Wang et al., Phys. Rev. X6, 041020 (2016)
[4] Thornton et al., Phys. Rev. Lett. 63, 2128 (1989)

Electrical control of large two-terminal spin-valve signals in 2DEG-based spin injection devices

F. Eberle, M. Oltscher, T. Kuczmik, A. Bayer, D. Schuh, D. Bougeard, M. Ciorga, and D. Weiss
Institute for Experimental and Applied Physics, University of Regensburg,
93040 Regensburg, Germany,
mariusz.ciorga@ur.de

A lateral channel with a spin-polarized current flowing between ferromagnetic source and drain contacts is a key ingredient in many spintronic device concepts. An essential prerequisite for a functional spintronic device is a high magnetoresistance ratio defined as $MR = (R_{AP} - R_P)/R_P$, where $R_{P(AP)}$ is the two-terminal resistance for parallel (antiparallel) magnetization orientation of source and drain contacts. Low MR ratios (<1%) observed so far for semiconducting channels [1] have been the main obstacle for realizing spin field effect transistor (sFET) proposals. The key functionality of sFET is electrical control of the resistance of the device, through acting on electron spins. In the seminal sFET proposal [2] the control mechanism is based on spin-orbit coupling (SOC). Realization of such devices requires materials with small enough SOC to guarantee efficient spin transport between source and drain and large enough SOC to enable efficient control of the travelling spins.

In this contribution we present the results of our experiments on lateral spin injection devices with a two-dimensional electron gas (2DEG) transport channel at an inverted GaAs/(Al,Ga)As interface and (Ga,Mn)As/GaAs spin Esaki diodes as spin aligning contacts [3]. We observe large, strongly bias-dependent, local spin valve signals in these two-terminal devices, with ΔR of order 1 kΩ and MR ratios reaching 80% in the nonlinear region of the Esaki diode.

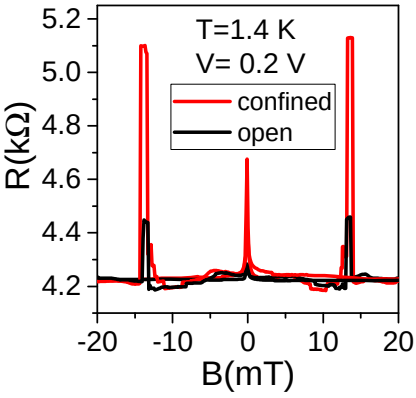

Fig.1. Local spin-valve signals in the open (black) and in the confined (red) configuration.

As an alternative way of tuning the resistance of the device, we propose electrical control via distribution of spins in the channel. Theory suggested [4] that confining spins in the small region between source and drain contacts results in larger spin valve signals, compared to a boundless geometry in which spins are free to diffuse in both directions away from the contacts. To switch controllably between open and confined geometry we employ gate electrodes, which deplete the 2DEG outside the current path, just behind injector and detector contact. Using this method, we can tune the resistance of the devices by up to 14% (see Fig. 1).

The work was supported by the German Science Foundation through the project SFB 689.

References

[1] A. Fert, J.-M. George, H. Jaffrès, and R. Mattana, IEEE Trans. El. Dev. **54**, 21 (2007)
[2] S. Datta and B. Das, Appl. Phys. Lett. **56**, 665 (1990)
[3] M. Oltscher *et al.*, Phys. Rev. Lett. **113**, 236602 (2014)
[4] H. Jaffrès, J.-M. George, and A. Fert, Phys. Rev. B **82**, 140408 (2010)

Coherent Dynamics of Magnetic Atoms in Spin-Polarized Environments

Lars-Hendrik Frahm and Daniela Pfannkuche
I. Institut für Theoretische Physik, Universität Hamburg,
Jungiusstraße 9, 25335 Hamburg, Germany
Lars-Hendrik.Frahm@physik.uni-hamburg.de

Atomic systems in interaction with the environment have gained wide attention in the electronic and spintronic community recently. The strong connection to fundamental physics, as well as its high potential for later use in computing devices made these systems attractive for many studies.

Here we investigate the dynamic and static transport properties of a single magnetic atom on a nonmagnetic surface. Resembling spin-polarized scanning tunneling microscopy (STM) setup the atom is exchange-coupled to a magnetic tip. We calculate the differential conductance of the tunneling current through the atom showing highly non-linear behavior depending on the magnetization direction of the tip.

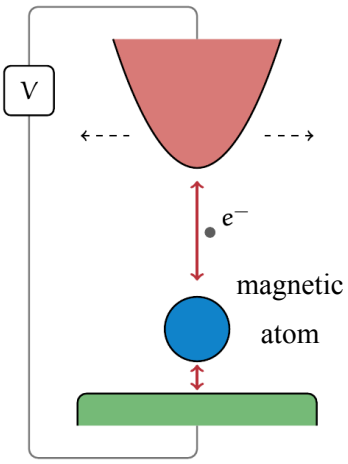

Using a description in the framework of open quantum systems, the atom evolves non-unitary dynamics, which we tackle by finding the Liouville operator of lowest order in atom-environment coupling. Additionally, an effective crystal field arises from the substrate the atom is living on, which gives the magnetic moment of the atom an easy axis for alignment. Further, the spin-polarized tip breaks the rotational symmetry around the spin quantization axis. A proper description of the dynamics of the magnetic atom requires to consider all elements of the reduced density operator, where its knowledge allows to calculate magnetization dynamics and transport properties on an equal footing.

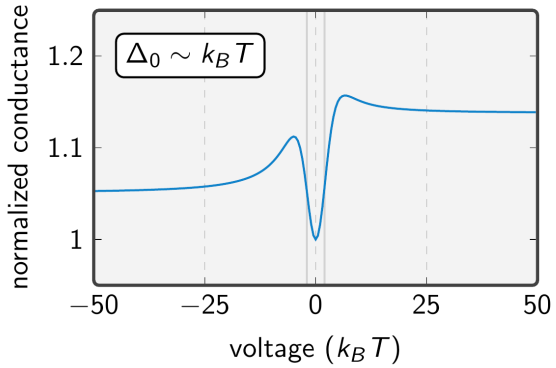

Treatment in same terms reveals the close interdependence between the atom's magnetization and the transport properties of the system. This allows to draw conclusions on the magnetic state from the conductance signal. Therefore, single magnetic atoms may be used as spintronic devices for both, classical and quantum computing

Spin Filtering Properties of Double Quantum Well System as an Enhancer of the Edelstein Effect Based on the Interband Rashba Effect

K. Okamoto,[1] A. Sawada, [1] J. C. Egues,[2] and T. Koga[1]
[1]*Graduate School of Information Science and Technology, Hokkaido University, Kita 14, Nishi 9, Kita-ku, Sapporo, Hokkaido, 060-0814, Japan*
[2]*Instituto de Física de São Carlos, Universidade de São Paulo, São Carlos, São Paulo, 13560-970, Brazil*
k-okamoto@nano.ist.hokudai.ac.jp

Edelstein predicted the current-induced spin polarization in the presence of the Rashba effect [1]. The number of accumulated spins per unit area is simply represented by the following equation:

$$\Sigma\langle\sigma_y\rangle/A = e\frac{m^*}{\pi\hbar^2}\frac{\alpha}{\hbar}\tau E_x \qquad (1)$$

where α is the Rashba coefficient. This is an as simple equation as the Drude conductivity $\sigma = e^2N_s\tau/m^*$ (N_s : sheet carrier density), whereas no experimental result directly confirming Eq. (1) has been reported yet. The value of $\Sigma\langle\sigma_y\rangle/A$ is predicted to be 0.87×10^8 cm^{-2} in $In_{0.53}Ga_{0.47}As/In_{0.52}Al_{0.48}As$ double hetero-structure, using $\alpha = 3.14\times10^{-12}$ eVm, $N_s = 1.8\times10^{16}$ m^{-2} and $j_x = 10$ Am^{-1} ($\Sigma\langle\sigma_y\rangle/V = 87$ μm^{-3} using $d_{QW} = 10$ nm, where V is the volume).

Recently, we have proposed that a double quantum well (DQW) system (Fig. 1) can be used as an enhancer of the Edelstein effect [2] based on the interband Rashba effect [3]. The present work considers the k_y dependence of the spin dependent electron transmittance $T_{\sigma'\sigma}$ and reflectance $R_{\sigma'\sigma}$ as shown in Fig. 2. We assume k_y conservation between incoming and outgoing electrons through the DQW stripe. We prospect that stripes of DQW modules properly engineered adjusting the length L (Fig. 2) should act as an effective enhancer of the Edelstein effect in the underlying quantum well (QW1 in Fig. 1).

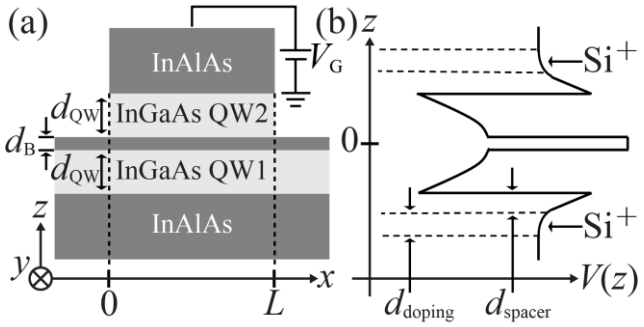

Fig. 1 (a) Structure of the proposed DQW system and (b) the potential profile ($V_G \equiv 0$V). $d_{QW} = 10$ nm, $d_B = 3$ nm, $d_{spacer} = d_{doping} = 6$ nm and n^+(Si) = 3×10^{24} m^{-3}. See Ref.[2].

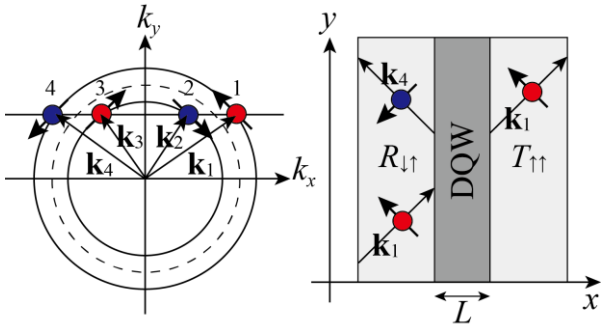

Fig. 2 Schematic diagrams of spin dependent electron transmittance and reflectance in k-space (left) and real space (right). In the left panel, solid circles represent the Fermi circles with the Rashba effect. In the right panel, we illustrate a real space electron with state 1 (see k-space) being scattered to states 1 and 4 with the probability $T_{\uparrow\uparrow}$ and $R_{\downarrow\uparrow}$.

The authors thank Prof. S. Datta and Dr. S. Sayed for informative discussions. This work was supported by JSPS KAKENHI Grant Number 16H01045.

Reference

[1] V. M. Edelstein, Solid State Commun. **73**, 233 (1990).
[2] S. Souma, A. Sawada, H. Chen, Y. Sekine, M. Eto, and T. Koga, Phys. Rev. Applied **4**, 034010 (2015).
[3] E. Bernardes, J. Schliemann, M. Lee, J. C. Egues, and D. Loss, Phys. Rev. Lett. **99**, 076603 (2007).

Non-collinear RKKY interaction in graphene with Rashba spin-orbit coupling

Diego Mastrogiuseppe[1] and Sergio E. Ulloa[2]
[1]*Instituto de Física Rosario (CONICET), 2000 Rosario, Argentina*
[2]*Department of Physics & Astronomy, and Nanoscale and Quantum Phenomena Institute, Ohio University, Athens, OH 45701, USA*
mastrogiuseppe@ifir-conicet.gov.ar

Spintronics is an active current area of research in condensed matter physics that has provided interesting insights on new phenomena, with strong impact on technological applications. It explores the possibility of transferring information via spin degrees of freedom, possibly manipulated by electrical means. As such, spin-orbit interaction (SOI) is an essential mechanism to provide the coupling between magnetic moments and electric fields. Two dimensional materials, such as graphene, are particularly suitable for this purpose. Their atomic layers can be manipulated in different ways, including local STM techniques, allowing the fabrication of novel efficient devices.

It is well known that the *intrinsic* SOI in graphene is negligible. However, an externally induced SOI with sizable strength, the *Rashba* SOI, can be effected on graphene. Strong Rashba couplings have been shown to be produced by external electric fields that break inversion symmetry, and/or by intercalation or deposition of certain atomic species [1]. This imparts an interesting character to the current carriers in graphene which may mediate the interaction between magnetic impurities (MIs) embedded in such material.

Here we study the RKKY interaction between MIs in graphene in the presence of Rashba SOI, using the Matsubara Green's function formalism. The RKKY interaction provides a way for magnetic moments to interact indirectly via the electrons in the host. We discuss results for varying SOI strength and graphene Fermi energy, at zero and finite temperatures. At charge neutrality, the interaction has a crossover from an R^{-3} decay with no SOI, to an R^{-2} decay for finite Rashba (see Fig. 1). The interaction is also shown to have anisotropic components, including in-plane (XY), out-of-plane (Ising), and a sizable twisted Dzyaloshinskii-Moriya (DM) term, which can be tailored by varying the electron concentration. We find that the amplitude of the interactions decreases slowly with temperature (up to ~100 K), which provides experimental significance. We calculate angular dependent factors that modulate the interaction, due to the existence of Dirac points at finite momenta. These factors induce rapid oscillations for different relative orientations of the impurities, including zigzag and armchair. We compare our results to those of bilayer graphene without SOC [3], which features similar band structure as in our system, but does not induce a DM term in the RKKY interaction.

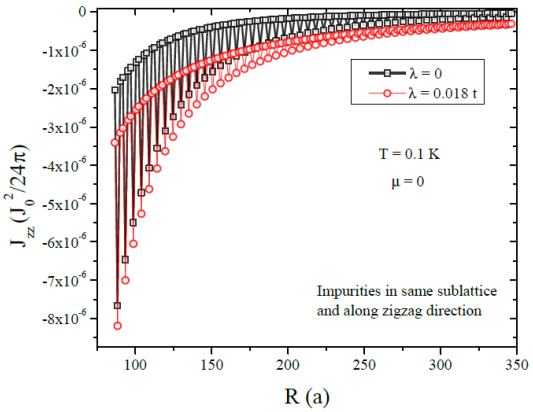

Fig.1 Ising component of the effective interaction between magnetic moments vs their separation, for graphene with and without Rashba (λ parameter), at T = 0.1 K and at charge neutrality. For λ=0 the interaction decays as R^{-3}, while for finite λ it decays more slowly, as R^{-2}. One can also observe a fast modulation introduced by the presence of Dirac K and K' points.

References

[1] D. Marchenko *et al.*, Nat. Commun. **3**, 1232 (2012); E. O'Farrell *et al.*, PRL **117**, 076603 (2016).

Weak anti-localization effects in $In_{0.75}Ga_{0.25}As$ two-dimensional electron gas bilayers

S. Hidaka, A. Fujimoto[A], S. Yamada[A]* and M. Akabori[B]
Nagaoka University of Technology
1603-1, Kamitomioka Nagaoka, Niigata, 940-2188, JAPAN
[A]*Osaka Institute of Technology*
5-16-1, Omiya, Asahi-ku Osaka, 535-8585 JAPAN
[B]*Japan Advanced Institute of Science and Technology*
1-1, Asahi-dai, Nomi, Ishikawa, 923-1292 JAPAN
*shoji.yamada@oit.ac.jp

In order to realize novel spin devices, we have proposed $In_{0.75}Ga_{0.25}As$ two-dimensional electron gas (2DEG) bilayer structures and studied their spin transport [1]. In the samples with much different sheet electron densities ($\mathbf{n_{s,\,upper}} : \mathbf{n_{s,\,lower}} \approx 1 : 3 - 4$), the separate estimation of spin-orbit interaction (SOI) coupling constant, $\boldsymbol{\alpha}$, is possible for the each 2DEG. But the estimation of $\boldsymbol{\alpha}$ by the standard magneto-resistance (MR) beat analysis becomes difficult due to the $\mathbf{n_s}$ peak superposition. Alternative method based on the weak-anti localization (WAL) effect is, however, not established in its theoretical aspect especially for the bilayer 2DEG system, since the interaction (including the cancellation [2] etc) between the SOIs of the bilayer 2DEG should be taken into account.

We report in this work the results of WAL measurements in the tightly coupled 2DEG bilayers, where the total width of $In_{0.75}Ga_{0.25}As$ well is t_{qw} = 20, 15 and 10 nm with the center $In_{0.75}Al_{0.25}As$ barrier of t_b = 4, 3 and 2 nm, respectively (see Fig. 1). From the MR Fourier analysis, the two (t_{qw}, t_b) = (20, 4) and (15, 3) nm samples seem to contain 2DEG bilayer at the upper and lower interfaces, whereas the 2DEG is likely monolayer in the (10, 2) nm sample. The WAL results against the top-gate voltage, $V_{g,top}$, are shown in Fig. 2. In the two bilayer samples, $\boldsymbol{\alpha}$ started from the small finite values $\leq 4\times10^{-12}$ eVm at $V_{g,top}$ = 0 and then gradually decreased to zero at $V_{g.top}$ ~ -1.2 V. In contrast, (10, 2) nm sample, $\boldsymbol{\alpha}$ initially takes a larger value of 6×10^{-12} eVm but quickly decreases to zero than in the other two samples. Since in the bilayer samples with different $\mathbf{n_s}$, the typical $\boldsymbol{\alpha}$ values were in the order of 10×10^{-12} eVm [1], the latter result of (10, 2) sample shows the dependency of $\boldsymbol{\alpha}$ on the electric field variation inside the well, whereas the former in the other two could be attributed to the cancellation effect, if we take aware of that almost equal $\mathbf{n_s}$ is attained also at $V_{g,top}$ ~ -1.2 V in the bilayers.

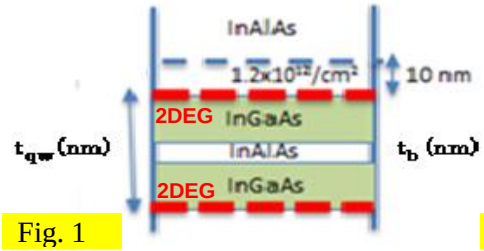

Fig. 1

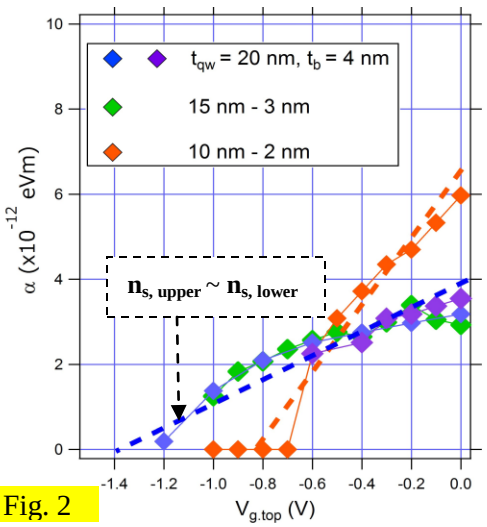

Fig. 2

Fig. 1 Sample structure: $In_{0.75}Ga_{0.25}As$ t_{qw} = 20, 15, 10 nm with $In_{0.75}A_{l0.25}As$ t_b = 4, 3, 2 nm.
Fig. 2 $\boldsymbol{\alpha}$ dependencies on $V_{g.top}$ in the three samples. $\mathbf{n_{s,\,upper}} \sim \mathbf{n_{s,\,lower}}$ is attained at $V_{g,top}$ ~ - 1.2 V in the (20, 4) and (15, 3) nm samples.

References

[1] M. Akabori et al, JAP.112, 113711 (2012).
[2] Ekenberg et al,APL., 48, 487(2007).

Poster Session 2

Tailoring supercurrent confinement in graphene bilayer weak links

R. Kraft[1], J. Mohrmann[1], R. Du[1], P.B. Selvasundaram[1,2], M. Irfan[3], U.N. Kanilmaz[1,4], F. Wu[1,5], D. Beckmann[1], H. von Löhneysen[1,6], R. Krupke[1,2], A.R. Akhmerov[3], I.V. Gornyi[1,4,7,] and R. Danneau[1,*]

[1]*Institute of Nanotechnology, Karlsruhe Institute of Technology, Germany*

[2]*Department of Materials and Earth Sciences, Technical University Darmstadt, Germany*

[3]*Kavli Institute of Nanoscience, Delft University of Technology, The Netherlands*

[4]*Institute for Condensed Matter Theory, Karlsruhe Institute of Technology, Germany*

[5]*College of Optoelectronic Science and Engineering, National University of Defense Technology, Changsha, China*

[6]*Institute for Solid State Physics and Institute of Physics, Karlsruhe Institute of Technology, Germany*

[7]*A.F. Ioffe Physico-Technical Institute, St. Petersburg, Russia*

romain.danneau@kit.edu

Graphene appears to be an ideal candidate for superconducting weak link [1-3] thanks to its low contact resistance, large mean free path and its two-dimensionality which allows device geometry flexibility. Designing nanostructures based on electrostatic gating has been at the heart of the research in mesoscopic physics for the last thirty years. While graphene undergoes Klein tunneling making it inappropriate for charge carrier confinement, it is possible to create nanostructures based on band gap engineering in bilayer graphene (BLG). By using edge connected hBN-BLG-hBN heterostructures, we have induced displacement fields between an overall back-gate and a local split-gate, *i.e.* in a quantum point contact-like structure, to confine the electrons and holes within a 1D constriction. Our superconducting leads allow measuring high supercurrent amplitudes and ballistic interferences. We have studied the confinement of the supercurrent by probing its magnitude and the variations of the magneto-interference patterns while the constriction is formed. We demonstrate that it is possible to fully gate-control both amplitude and density profile a supercurrent, making BLG a highly tunable superconducting weak link. Both analytical and numerical model support our findings. Our work opens up possibilities to create more complex circuits such as superconducting electronic interferometers or transition-edge sensors [3].

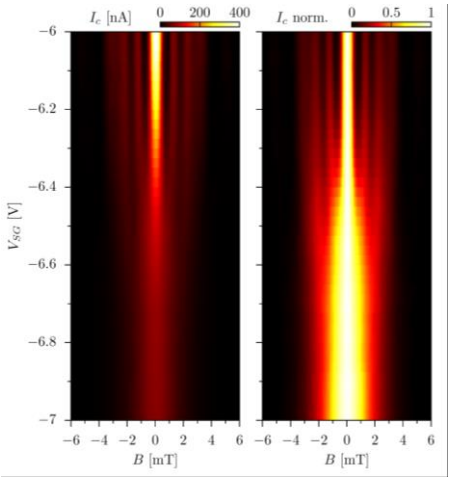

Fig.1 Critical current amplitude I_c (left panel) and normalized critical current amplitude $I_c^{norm.}$ (right panel) mapped as a function of magnetic field B and split-gate voltage V_{SG}. The transition from a beating pattern (Fraunhofer-like) to a monotonically decaying pattern is visible confirming the continuous change in the supercurrent confinement from 2D to 1D.

References

[1] V.E. Calado, *et al.*, Nat. Nanotech. 10, 761-764 (2015).
[2] M. Ben Shalom, *et al.*, Nat. Phys. 12, 318-322 (2016).
[3] R. Kraft, *et al.*, arXiv: 1702.08773 (2017).

Stabilizing metastable electron pairs in crystal through many-body effects due to electron-electron and electron-LO-phonon interactions

G.-Q. Hai[1] and L. Cândido[2]
[1]*Instituto de Física de São Carlos, Universidade de São Paulo, Brazil*
[2]*Instituto de Física, Universidade Federal de Goiás, Brazil*

We develop a theory for electron pairing in crystal. Our starting point is to consider both the single-electron states and electron-pair states (e.g., lone pairs) existing in atoms. The simplest model is a "hydrogen solid model" with including single-electron state of H atom and electron-pair state of H^- ion. In the periodic crystal potential, it is known that the single-electron states form energy bands. Our calculation for a 2D square lattice shows that the electron-pair states originating from individual atoms may survive forming a *metastable* electron-pair band. The bandwidth of this electron-pair band is one order of magnitude smaller than the corresponding single-electron band and is located a few effective Rydberg above it. This electron-pair band is result from interplay of the correlation energy of the two paired electrons, the local confinement in each unit cell and co-tunneling of the pair between neighbor cells. At this stage, we have obtained a two-band system with single electrons in a lower band and spin-singlet metastable electron pairs in a higher one.

We now show how to stabilize the electron pairs through band renormalization due to many-body effects. Although both bands are lowered by including many-particle exchange-correlation interactions, the correction to the electron-pair band is much larger due mainly to the pair being of double charge and mass of a single electron. If the bottom of the electron-pair band touches the Fermi surface of the single-electron band, the spin-singlet electron pairs (considered as bosons) at the bottom of the pair band cannot decay into two single electrons (considered as fermions) because of the Pauli exclusion principle. Consequently the electron pairs can be stabilized. The calculation is performed for the two-component system consisting of single electrons and electron pairs within the random phase approximation (RPA). The RPA is reasonably good for the band renormalization because we are interested in the energy difference between the two bands. The result shows that such a renormalization indeed reduces the gap between the two bands but is not sufficient to stabilize the electron pairs within reasonable single-electron and electron-pair densities introduced or doped into the system.

We further invoke the Fröhlich electron-LO-phonon interaction for the band renormalization. Including the electron-phonon (e-ph) coupling, the single electrons form polarons and the electron pairs become bipolarons. Howerver the bipolaron in the present context is different from the traditional bipolaron in the literature. In the formation of a traditional bipolaron, the e-ph attraction has to overcome the Coulomb repulsion requiring a minimum Fröhlich coupling constant α. In our theory, there is no restriction for the e-ph coupling strength because it involves only in renormalization of preformed electron pairs. The method of a Lee-Low-Pines (LLP) unitary transformation is used to calculate the polaron contributions to the band renormalization and the electronic screening is treated within the RPA. The LLP method is valid for weak and intermediate e-ph coupling strength. Our calculations show that the electron pairs can finally be stabilized within reasonable single-electron and electron-pair densities by including both the e-e and e-ph interactions for an e-ph coupling constant in the order of $\alpha \geq 1\sim2$ depending on the ratio of effective Rydberg to LO-phonon energy.

We also discuss the band-structure dependence of pair breaking anisotropy and possible hole doping mechanism for electron pairing.

This work was supported by FAPESP, FAPEG and CNPq.

Josephson radiation of InAs nanowire Josephson junctions

H. Kamata[1, 2], R. S. Deacon[1, 3], S. Matsuo[2], S. Baba[2], K. Li[4], H. Q. Xu[4, 5], K. Ishibashi[1, 3], and S. Tarucha[1, 2]
[1] *Center for Emergent Materials Science, RIKEN, Wako, Saitama, Japan*
[2] *Department of Applied Physics, University of Tokyo, Bunkyo, Tokyo, Japan*
[3] *Advanced Device Laboratory, RIKEN, Wako, Saitama, Japan*
[4] *Key Lab for the Physics and Chemistry of Nanodevices, Peking University, China*
[5] *Division of Solid State Physics, Lund University, Lund, Sweden*
hiroshi.kamata@riken.jp

InAs or InSb semiconductor nanowires (NWs), which exhibit a strong spin-orbit interaction and a large Landé g-factor, are good candidates for generating Majorana bound states (MBSs) in condensed matter when contacted to s-wave superconductors. Tunneling spectroscopy measurements on normal conductor/NW/superconductor junctions have often been used to reveal signatures of MBSs [1]. Observation of the 4π-periodic Josephson effect can be another strong evidence for MBSs, but still remains a challenge for NW-based topological systems because of the experimental difficulty. Here, we carry out direct measurement of rf emission spectra on NW-based Josephson junctions to investigate the 4π-periodic Josephson effect. In these junctions, emission spectra at half the Josephson frequency are predicted to appear in the topological regime.

Figure 1 shows a Josephson junction having an InAs NW transferred to a gate dielectric of hexagonal boron nitride (h-BN) contacted to NbTi/Al superconducting electrodes. The NW conductance is varied with gate voltage V_G applied to the local gate electrodes underneath the h-BN. Different NWs but prepared in the same way show ballistic transport. The junction is connected to a coaxial line and decoupled from the dc measurement line via a bias-T. The Josephson radiation emitted from the junction is amplified by cryogenic and room-temperature amplifiers and then measured with a spectrum analyzer. To enable a stable voltage bias to the junction, we employ an on-chip shunt resistance of ~ 50 Ω [2].

As shown in Fig.2, we observe the emission spectra at the fundamental Josephson frequency f_J but not the 4π-periodic Josephson effect in the bandwidth limited range of 6 to 8 GHz. We find that the observed spectra are tunable with gate voltage as well as magnetic field, and discuss the Majorana physics in our devices. Note in contrast to microwave spectroscopy measurements utilizing an on-chip detector, which is affected by the external magnetic field [3], our direct high frequency measurement will be more appropriate to investigate the excitation spectra in the high magnetic field regime or topological regime.

References

[1] M. T. Deng *et al*., Science **354**, 1557-1562 (2016); H. Zhang *et al*. arXiv:1603.04069 (2016). [2] R. S. Deacon *et al*., arXiv:1603.09611 (2016). [3] D. J. van Woerkom *et al*., arXiv:1702.02804 (2017).

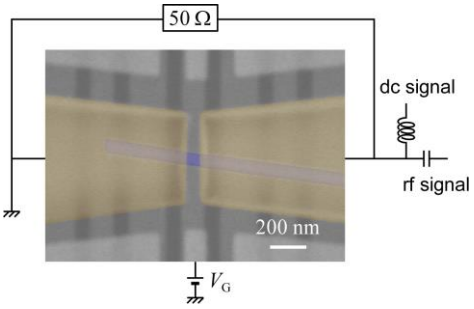

Fig.1 SEM image of a Josephson junction on h-BN and experimental setup for the emission measurement.

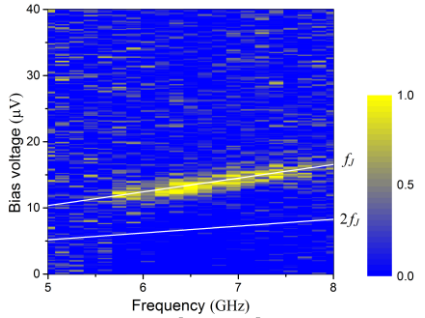

Fig.2 Emission spectra observed at zero magnetic field. The data is normalized to its maximum for each frequency.

Recurrence of multiple Andreev reflection versus magnetic field in InAs two-dimensional electrons

Makoto Onizaki, Taketomo Nakamura, Yoshiaki Hashimoto, and Shingo Katsumoto
Institute for Solid State Physics, The University of Tokyo,
5-1-5 Kashiwanoha, Kashiwa, Chiba 277-8581, Japan
m.onizaki@issp.u-tokyo.ac.jp

In spite of exhaustive fascinating ideas in superconductor (S) – two dimensional electron gas (2DEG) junction under magnetic field, experiments have been facing technical difficulties such as S-2DEG contacts or suppression of superconductivity with magnetic field and comparatively few have been reported. Here we report an experiment on an S-2DEG junction, in which magnetic suppression of superconductivity is moderated by adopting NbTi alloy for superconducting electrodes.

We fabricated NbTi/2DEG/NbTi junction from an InAs 2DEG with inverted modulation doping (mobility and concentration of 1.03×10^4 cm^2/Vs and 1.95×10^{12} cm^{-2}, respectively). The 2DEG was cut into a 4×7 μm^2 mesa as shown in the left inset of Fig.1. Then, after cleaning the surface with Ar ion beam, NbTi electrodes with 15 μm width were deposited with 1 μm overlapping on the mesa. The differential resistances dV/dI at 0 T and 0.24 T are shown as a function of bias voltage in Fig.1. The former has several dips, which almost disappear in the latter. From the position analysis shown in the right inset we attribute three outer peaks to multiple Andreev reflection (MAR) at NbTi-2DEG interface, while inner two are to MAR at the interfaces between superconductive proximity in InAs and normal 2DEG. The peaks are emphasized with subtracting background and exhibited as a color plot against the magnetic field B_z and the bias current I_{dc}. Surprisingly once suppressed MAR peaks reappear with further increase of B_z and such node-like behavior repeats up to around 2 T. From the fact that the squeezing of the peak position only occurs for the peaks of MAR at proximity super-normal interfaces, we infer that vortex superlattice in the 2DEG forms electron enery gaps which cause the repetitive peak suppression.

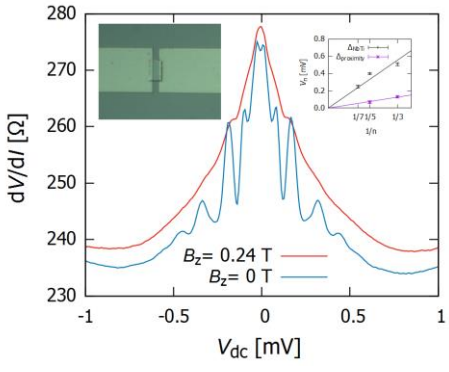

Fig.1 dV/dI-V characteristic of the junction at B = 0 T and 0.24 T. The left inset shows sample picture. The right inset shows n-th dV/dI dip position-1/n plot.

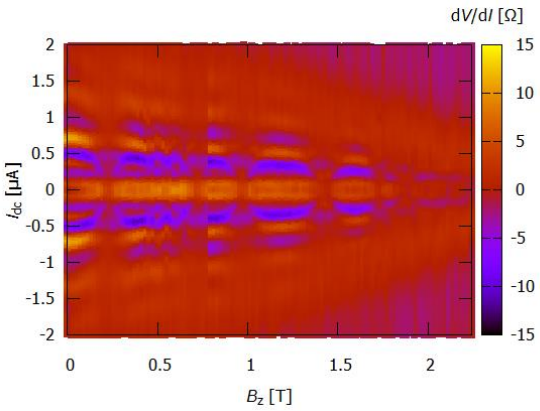

Fig.2 Peak-emphasized color plot of dV/dI

MBE Growth of Semiconductor-Superconductor Hybrid Structures for Topological Quantum Computing

T. Wang[1,2,*], A. T. Hatke[1,2], C. Thomas[1,2], G. C. Gardner[1,2,3] and M. J. Manfra[1,2,3,4]
[1]*Station Q Purdue and Department of Physics and Astronomy, Purdue University*
[2]*Birck Nanotechnology Center, Purdue University,*
[3]*School of Materials Engineering, Purdue University,*
[4]*School of Electrical and Computer Engineering*
West Lafayette, IN 47906, USA
**wang2444@purdue.edu*

Hybrid structures consisting of a two-dimensional electron gas (2DEG) in a quantum well proximitized with an epitaxially grown superconductor have become a prominent platform to explore topological quantum computing [1].

We report on the heterostructures design, MBE growth details and transport properties of the shallow 2DEGs situated in an InAs/InGaAs quantum well only 10 nm below the sample surface. The structure is grown on an InP (100) substrate. Due to the 3% lattice mismatch between InAs and InP, the growth of an $In_xAl_{1-x}As$ graded buffer with *x* varied from 0.52 to 0.84 then back to 0.81 has been added to the heterostructure (see Fig. 1(a)) to change the lattice constant and minimize the influence of dislocations. Defects in the graded buffer are known to generate excess charge carriers that can lead to parallel conducting channels and contribute to leakage within a device.

The InAs/InGaAs quantum well is made of a 5 nm InAs layer flanked by $In_{0.81}Ga_{0.19}As$ layers. The alloy content is chosen to minimize the strain energy between the quantum well and the Al superconducting layer. Magnetotransport characterization at 300 mK confirms a single carrier channel with mobility in excess of 50,000 cm^2/Vs (see Fig. 1(b)).

We then report the epitaxial growth of the Al superconducting layer. The in-situ epitaxial deposition can produce a flat, abrupt and low defect interface that does not degrade the 2DEG transport mobility. Samples generated with a 7 nm Al layer deposited at a low temperature (below -30°C) have demonstrated an upper critical field of 2.8 T with a hard superconducting gap. These results demonstrate the possibility to reach the topological superconducting regime.

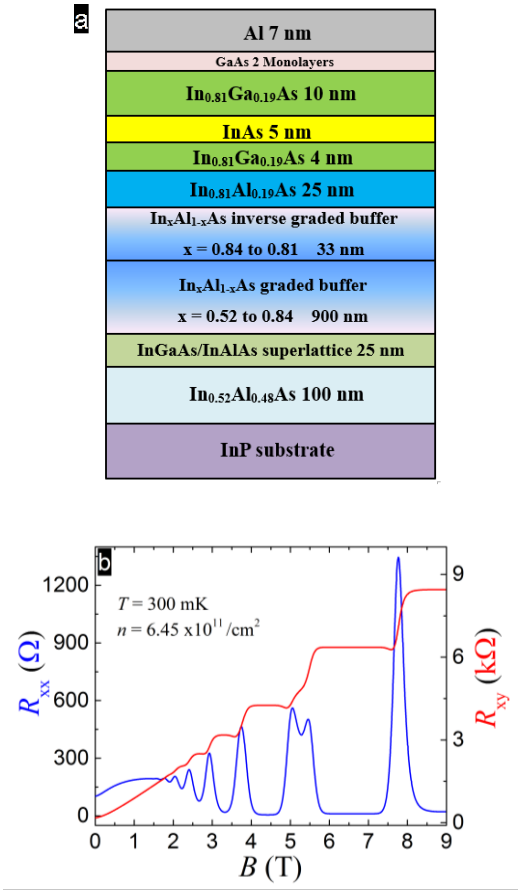

Figure 1: The hybrid heterostructure stack layer (a) and the associated magnetotransport measurement (b).

References

[1] J. Shabani, *et. al.*, Phys. Rev. B **93**, 155402 (2016).

Kitaev model with quantum dot chains in semiconductor nanowires

Z. Su[1], H. Wu[1*], M. Hocevar[2], D. Car[3], S.R. Plissard[4], E.P.A.M. Bakkers[3], D. Pekker[1] and S.M. Frolov[1]
[1]*Department of Physics and Astronomy, University of Pittsburgh, USA*
[2]*CNRS, Institut Neel, Grenoble, France*
[3]*Department of Applied Physics, Eindhoven University of Technology, The Netherlands*
[4]*LAAS CNRS, Universite de Toulouse, Toulouse, France*
haw74@pitt.edu

We experimentally explore whether chains of quantum dots in semiconductor nanowires can be used to emulate important one-dimensional Hamiltonians such as the topological p-wave superconductor [1-2]. First, we have realized a building block of the Kitaev model by establishing a double quantum dot with superconducting contacts in an InSb nanowire. We demonstrated that Andreev bound states in each dot hybridize to form the double-dot Andreev molecular states [3]. We showed the parity and the spin structure of Andreev molecular levels. Understanding Andreev molecules is a key step towards building longer chains which are predicted to generate Majorana bound states at the end sites.

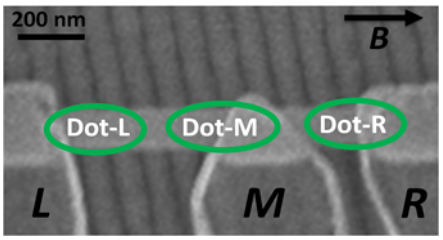

Fig.1 SEM of the triple dot device. Three superconducting leads are marked by L, M and R. Each dot is strongly coupled to its own lead. Between every two neighboring dots a gate is used to form a barrier and control the inter-dot coupling. Magnetic fields are parallel to the nanowire axis.

Next, we have implemented a triple quantum dot chain in an InSb nanowire where each dot is tuned to be strongly coupled to a separate NbTiN superconducting lead [Fig.1]. We have studied transport through Andreev bound states on individual dots, dot pairs and through the entire triple dot. We explore the influence of Coulomb energy on the Andreev spectra of the chain. We use magnetic fields parallel to the nanowire axis to study the field dependence of the triple dot Andreev bound states. We observe zero bias conductance peaks that appear at finite applied magnetic fields, as well as split peaks [Fig.2]. We explore these conductance resonances in the context of Majorana bound states, as well as considering supercurrents and trivial Andreev bound states.

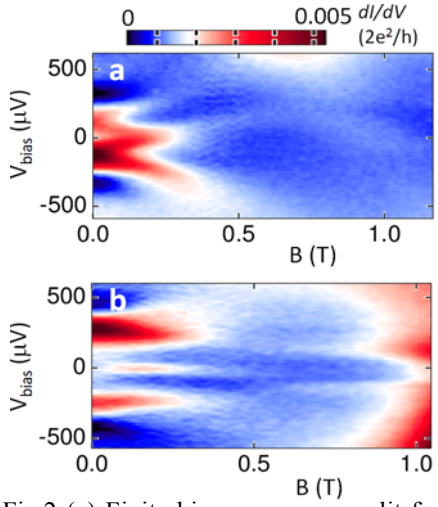

Fig.2 (a) Finite bias resonances split from zero field, cross at ~250mT and loop back to zero bias at high field. (b) For different gate settings, a zero bias peak emerges and sticks to zero bias for hundreds of mT.

References

[1] Sau, J. D. et al. Nat. Commun. 3, 964 (2012).
[2] Fulga, I. C. et al. New J. Phys. 15, 045020 (2012).
[3] Su, Z. et al. arXiv:1611.00727 (2016).

Phase Diagram of a Topological Superconductor in an InSb Nanowire

P. Yu,[1] J. Chen,[1] J. Stenger,[2] M. Hocevar,[3] D. Car,[4] S.R. Plissard,[5] E. Bakkers,[4] T.D. Stanescu,[2] S.M. Frolov[1]

[1]*Department of Physics and Astronomy, University of Pittsburgh, Pittsburgh, PA 15260, USA*

[2]*Department of Physics and Astronomy, West Virginia University, Morgantown, WV 26506, USA*

[3]*Institut Néel CNRS, 38042 Grenoble, France*

[4]*Eindhoven University of Technology, 5600 MB, Eindhoven, The Netherlands*

[5]*LAAS CNRS, 31031 Toulouse, France*

pey13@pitt.edu

Majorana bound states (MBS) are predicted to emerge in a nanowire with spin-orbit interaction, induced superconductivity and in external magnetic field. Following this prescription, we observe zero-bias peaks (ZBPs) in conductance in InSb nanowire devices with NbTiN superconductor electrodes. By tracing the onset points of ZBPs in magnetic field and gate potential, we have mapped out a topological phase diagram, which is in agreement with a numerical model for a finite size topological nanowire (Figure 1) [1]. At high magnetic fields, some devices exhibit split conductance peaks, which may originate from the overlap of two MBS. We are exploring the magnetic field orientation evolution of the phase diagram. Ongoing measurements in three-terminal devices are used to extract the topological segment length and demonstrate control over two Majorana bound states belonging to a single pair. Nero zero-bias resonances may also originate from trivial Andreev levels localized near the tunneling barrier. We are investigating methods to distinguish non-trivial MBS from trivial Andreev states by carefully mapping out magnetic field and gate dependence of the resonances.

[1] J. Chen, et al , arXiv:1610.04555 (2016).

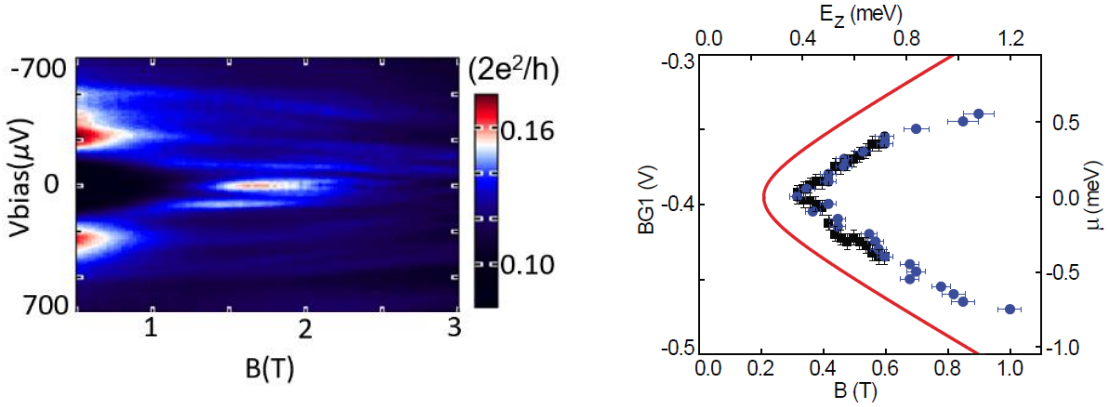

Fig.1 (Left) Zero bias peak appears at finite field and persist to over 2T where it splits in two finite bias peaks. (Right) Phase diagram of zero-bias peaks. The onset points of ZBPs extracted from our data. The red line is calculated from simple theory for an infinite-size topological superconductor. Data from Ref. [1]

Superconductivity in Atomically Thin Crystals

Brian M. Zakrzewski[1], Yixuan Chen[1], Azimkhan Kozhakhmetov[2], Joan M. Redwing[2], and Ying Liu[1]

[1]*Physics Department, Penn State University, University Park, PA 16803, USA*

[2]*Department of Materials Science and Engineering, Penn State University, University Park, PA 16803, USA*

bmz122@psu.edu

Superconductivity in the two-dimensional (2D) limit is defined by a nonlinear current-voltage characteristic resulting from the current driven vortex-antivortex unbinding below the Kosterlitz-Thouless transition, rather than zero resistance. We present the results of our low-temperature electrical transport measurements on atomically thin crystals of NbSe2, NbS2, and other materials, prepared by either mechanical exfoliation or chemical vapor deposition. These 2D crystals, weakly coupled to the substrate, may possess complex normal state and superconducting properties, including the interplay between the density waves and superconductivity, not found in disordered ultrathin superconducting films. We will also report results of our study of vortex motion in nanostructures prepared on 2D crystal superconductors, including vortex crossing and trapping, and examine their consequences in magnetoresistance behavior.

Topological Surface State, Size Quantization and Rashba Effect in PbSnSe Topological Crystalline Insulator Quantum Wells

R. Rechciński[1], M. Galicka[1], V.V. Volobuev[2], M. Simma[2], O. Caha[3], P.S. Mandal[4], E. Golikas[4], J. Sánchez-Barriga[4], A. Varykhalov[4], O. Rader[4], G. Bauer[2], G. Springholz[2], P. Kacman[1] and R. Buczko*[1]
[1]*Institute of Physics, Polish Academy of Sciences, Aleja Lotników 32/46, PL-02-668 Warszawa, Poland*
[2]*Institute for Semiconductor Physics, Johannes Kepler University, 4040 Linz, Austria*
[3]*Masaryk University, Kotlářská 2, 61137 Brno, Czech Republic*
[4]*Helmholtz-Zentrum Berlin für Materialien und Energie, 12489 Berlin, Germany*
buczko@ifpan.edu.pl

Topological crystalline insulator $Pb_{1-x}Sn_xSe$ surface quantum wells (QWs) on $Pb_{1-y}Eu_ySe$ barriers are studied experimentally and theoretically as a function of QW thickness in both the topological and trivial phases at different temperatures and Sn contents x. The theoretical tight-binding results are compared with experimental angle resolved photoemission (ARPES) investigations of epitaxial heterostructures grown by molecular beam epitaxy [1]. It is shown that for thin QWs, the interactions between the surface and interface states of the QW layer opens an energy gap in the topological surface states and therefore the Dirac points in the topological phase appear only for QWs with thicknesses exceeding ~24nm. Upon in situ submonolayer Sn deposition on the surface a strong Rashba effect appears in the conduction band which is modelled using the tight-binding approach and recursive Green's function method to derive the surface spectral density of states of the material. In our calculations we take into account the possibility that Sn covers only partially the surface of the QW. The strong Rashba effect observed in the conduction band was simulated by applying a potential described by Thomas-Fermi screening model, similarly as it was shown for PbSnTe films doped with Bi atoms [2]. Here we find, however, that even without screening potential, a Rashba splitting can be obtained in both valence and conduction bands due to the lack of inversion symmetry.

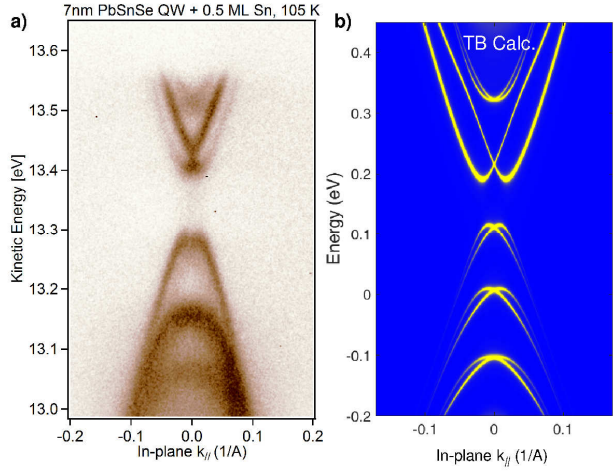

Fig.1 a) ARPES map of 7nm thick $Pb_{0.75}Sn_{0.25}Se$ QW on $Pb_{0.9}Eu_{0.1}Se$ barrier after deposition of 0.5 ML of Sn measured with a photon energy of 18 eV around the Γ point of the surface Brillouin zone; b) tight-binding spectral density of states calculated for a surface potential $V(z)=V_0e^{-z/\lambda}$ with V_0=-1.2 eV and λ=1.5nm.

References

[1] M Simma et al., Appl. Phys. Lett. **101**, 172106 (2012).
[2] V. Volobuev et al., Adv. Mater. **29**, 1604185 (2017).

Robust helical edge transport at ν=0 quantum Hall state in a single valley Dirac cone system

G. M. Gusev[1*], D. A. Kozlov[2], A. D. Levin[1], Z. D. Kvon[2,3], N. N. Mikhailov[2], and S. A. Dvoretsky[2,3]
[1]*Instituto de Física da Universidade de São Paulo, 135960-170, São Paulo, SP, Brazil*
[2]*Institute of Semiconductor Physics, Novosibirsk 630090, Russia*
[3]*Novosibirsk State University, Novosibirsk 630090, Russia*
*gusev@if.usp.br

Two dimensional massless Dirac fermions in the presence of a strong perpendicular magnetic field show several remarkable features that sharply diverge from conventional behaviour. The energy spectrum is organized in Landau levels (LL) with square root versus linear dependence on the magnetic field and square root dependence on the Landau index n versus n+1/2, in comparison with the parabolic dispersion at the zero field. The most remarkable consequence of this last property is the existence of a zero-energy Landau level (ν = 0). This is not due to the linear spectrum, but is related to the π Berry phase carried by each Dirac point. Therefore, the ν = 0 LL has a magnetic field independent energy, which is quite different from a quantized cyclotron orbit in the conventional quantum Hall effect. The existence of the zeroth Landau level has been examined by measurements of the integer quantum Hall effect (QHE) in graphene with two-valley degenerate spectrum [1]. Application of other materials that posses a single Dirac cone is of particular interest.

Recently a two-dimensional system with a single Dirac cone spectrum, based on HgTe quantum wells, has been discovered. The single spin degenerate Dirac valley allows unambiguous identification of the features resulting from the bulk zeroth Landau level. In addition, the high mobility and giant Lande g-factor favor formation of spin-polarized counter propagating states. In the present paper, we studied the nonlocal transport in 10-probe devices fabricated from HgTe zero-gap quantum structures. We observe a magnetic field induced, giant, nonlocal resistance peak near the CNP in different configurations of current and voltage probes. The nonlocal response is comparable with local resistance and increases rapidly with B. Simple Kirchhoff based estimations and more complicated model calculations clearly confirm the existence of helical edge states originating from the bulk zeroth LL.

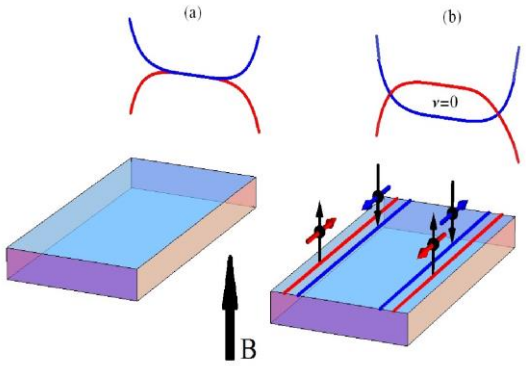

Schematics of band structure (energy spectrum) in low (a) and high (b) magnetic field, showing the zero LL in the middle of the sample and at the sample edge, and counter propagating spin polarized edge states in a slab-shaped sample for the ν=0 LL state.

References

[1] K. S. Novoselov, A. K. Geim, S. V. Morozov, D. Jiang, M. I. Katsnelson, I. V. Grigorieva, S. V. Dubonos and A. A. Firsov, Nature, 438, 197 (2005)

Electronic thermal transport in two-dimensional topological insulator

G. M. Gusev[1*], O. E. Raichev[2] , A. D. Levin[1], E.B.Olshanetsky[3], Z. D. Kvon[3,4], N. N. Mikhailov[3], and S. A. Dvoretsky[3]

[1]*Instituto de Física da Universidade de São Paulo, 135960-170, São Paulo, SP, Brazil*

[2]*Institute of Semiconductor Physics, NAS of Ukraine, Prospekt Nauki 41, 03028 Kyiv, Ukraine*

[3]*Institute of Semiconductor Physics, Novosibirsk 630090, Russia*

[4]*Novosibirsk State University, Novosibirsk 630090, Russia*

*gusev@if.usp.br

The thermal conductivity measurements in metals and semiconductors have been often used as a powerful tool for probing transport mechanisms. Within the Fermi liquid theory, electrons carry both charge and heat, and the relationship between the thermal κ and the electrical σ conductivities is given by the Wiedemann-Franz (WF) law, $\kappa/\sigma=LT$. The Lorentz number L takes the universal value $(\pi^2/3)(k_B/e)^2$, where k_B is the Boltzmann's constant and e the electron charge. The WF law is expected to be valid for one-dimensional electron transport in quantum wires and edge channels even if the transport is ballistic or quasi-ballistic.

The HgTe-based quantum well with inverted subband order are known to be in the state of 2D topological insulator (TI), characterized by a pair of gapless edge modes that are responsible for electron transport in such systems. Direct experimental measurement of thermal transport in 2D TI is a challenging task because isolating and quantifying heat flow in edge channels is extremely difficult.

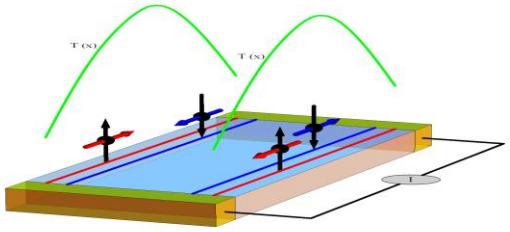

Schematic of the slab shape sample with counter propagating spin polarized edge states and electron temperature profile near the edge for diffusive transport.

We study the electronic thermal transport in the band-inverted HgTe-based quantum wells by measuring non-linear voltage-current characteristics at finite temperatures and extract the electron temperature generated by Joule heating by using the temperature-dependent resistance of 2D TI as its own thermometer. Theoretically, the inelastic electron-electron scattering within a single edge channel is much stronger than the scattering between counterpropagating edge states. This property leads to quasi-Fermi electron distributions, when each of the channels is characterized by its own local chemical potential and temperature [1]. A finite backscattering probability leads to electron transfer between the channels, which results in electron heating in both channels, with temperature distribution (see the figure) determined by the electric current, mean free path, distance between the contacts, and the Lorentz number. We calculate the temperature profile in our samples, assuming that the contacts are completely absorbing and thermalizing, and compare the dependence of the average electronic temperature on the current with our experimental data for the resistance. We find a good agreement between experiment and theory near the charge neutrality point, suggesting that the edge states in 2D TI can be described by the Fermi liquid theory.

References

[1] Marcelo A. Kuroda and Jean-Pierre Leburton, Phys. Rev. Lett. 101, 256805 (2008).

Bulk-Induced Correlated Mobility-Number Density Fluctuations in Molecular Beam Epitaxy Grown Topological Insulators

Saurav Islam[1], Semonti Bhattacharyya[1], Abhinav Kandala[2,3],
Anthony Richardella[2], Nitin Samarth[2] and Arindam Ghosh[1]
[1]*Department of Physics, Indian Institute of Science, Bangalore: 560012.*
[2]*Department of Physics, The Pennsylvania State University,*
University Park, Pennsylvania 16802-6300, USA.
[3]*IBM T.J. Watson Research Center, Yorktown Heights, New York 10598, USA.*
saurav@physics.iisc.ernet.in

Topological insulators (TI) are a new class of materials exhibiting gapless linear surface states in the bulk band gap. These materials are promising candidates for various electronic and spintronic applications due to topological protection of surface states against back scattering from non-magnetic impurities. Though there have been extensive transport and spectroscopic studies in TI systems, investigation of 1/*f* noise remains limited [1, 2]. Here, we report the first detailed study of noise in large-area molecular-beam epitaxy grown thin (~10 nm) films of topological insulator $(Bi,Sb)_2Te_3$ on strontium titanate (STO) substrate as a function of temperature, gate voltage and magnetic field. The temperature dependence of 1/*f* noise displays a sharp peak at $T = 50$ K which can be attributed to generation-recombination processes in the impurity band in the bulk gap. The gate-voltage dependence of noise reveals that both bulk and surface states are affected by correlated mobility-number density fluctuations caused by the defects present in the bulk with a density $D_{it} = 3.2\times10^{17}$ $cm^{-2}eV^{-1}$. In the presence of magnetic field, the 1/*f* noise follows a parabolic dependence which is qualitatively similar to mobility and charge density fluctuation noise in nondegenerate semiconductors. Our studies reveal that even in thin films of $(Bi,Sb)_2Te_3$ with thickness as low as 10 nm, the bulk defects are the dominant source of noise.

References

[1] S. Bhattacharyya, M. Banerjee, H. Nhalil, S. Islam, C. Dasgupta, S. Elizabeth, and A. Ghosh, ACS Nano **9**, 12529 (2015).
[2] S. Bhattacharyya, A. Kandala, A. Richardella, S. Islam, N. Samarth, and A. Ghosh, Appl. Phys. Lett. **108**, 082101 (2016).

Interacting two-channel helical liquids in a bilayer graphene

Chao-xing Liu
Physics Department, Penn State University,
University Park, PA 16803, USA
cxl56@psu.edu

A grand challenge in the field of topological physics is to understand the role of interaction and to realize interacting topological phases in realistic materials. In this talk, I will discuss the possible realization of interacting topological phases in a bilayer graphene under strong magnetic fields. We start from a fermionic two-channel quantum spin Hall state with two copies of helical edge states, which have been demonstrated experimentally in a bilayer graphene under a strong tilted external magnetic field when the Fermi energy is tuned into the gap of zero Landau levels. By introducing interaction into two-channel helical liquids, we demonstrate that all the fermion degrees are gapped out and only one bosonic mode remains, thus yielding a bosonic version of topological insulator, dubbed “bosonic symmetry protected topological state”. Physically, the two dual boson fields of this bosonic mode carry charge-2e and spin-1, respectively, due to the helical nature. Thus, we dubbed them “bosonic helical liquids”. We further study the transport of a quantum point contact for bosonic helical liquids and compare them to fermionic two-channel helical liquids. With the realistic interaction parameters, we find a novel charge insulator/spin conductor phase for bosonic helical liquids and charge insulator/spin insulator or charge conductor/spin conductor phase for fermionic two-channel helical liquids. Thus, a quantum point contact experiment will provide a “smoking-gun” transport signature for bosonic symmetry protected topological states in a bilayer graphene unambiguously. Similar physics can also emerge in topological mirror Kondo insulators, such as SmB_6.

.

References

[1] Bilayer Graphene as a platform for Bosonic Symmetry Protected Topological States, Zhen Bi, Ruixing Zhang, Yi-Zhuang You, Andrea Young, Leon Balents, Chao-Xing Liu, Cenke Xu, arXiv:1602.03190v1, 2016

[2] Interacting topological phases in thin films of topological mirror Kondo insulators, Rui-Xing Zhang, Cenke Xu, Chao-Xing Liu, arXiv: 1607.06073, 2016

[3] Fingerprints of bosonic symmetry protected topological state in a quantum point contact, Rui-xing Zhang, Chao-xing Liu, arxiv: 1610.01236, 2016

Geometric resonances in the 3D topological insulator HgTe

Hubert Maier, Johannes Ziegler, Ralf Fischer, Dieter Weiss
Institute of Experimental and Applied Physics, University of Regensburg,
Universitätstr. 31, 93053 Regensburg, Germany
Dmitriy Kozlov, Ze Don Kvon, Nikolay Mikhailov, Sergey A. Dvoretsky
A.V. Rzhanov Institute of Semiconductor Physics, Novosibirsk,
pr. Lavrentieva 13, Novosibirsk, Russia
Hubert.Maier@ur.de

Strained HgTe is a strong topological insulator [1] featuring Dirac surface charge carriers with elastic mean free path of typically 1-5µm, thus enabling to explore ballistic transport effects. The 3D HgTe surface states are expected to be helical, including that a particular k-state is only singly occupied, so that $k_F = \sqrt{4\pi n_s}$ holds. Geometric resonances, occurring in magnetotransport if the mean free path exceeds the period a of the antidot lattice, are a measure of the Fermi wave vector k_F and reflect the commensurability between the cyclotron orbit diameter $R_C = \hbar k_F / eB = a/2$ and the superlattice period a [2]. Here, we investigate square antidot arrays with periods a between 400nm and 800nm. The holes were etched wet chemically through the 40nm CdTe and 20nm HgCdTe cap layers and stop at the top surface of the 80nm thick HgTe layer (see Fig. 1). The longitudinal magnetoresistance R_{xx} displays clear commensurability features with the fundamental peak emerging at $R_C = a/2$, shown in Fig.1. Using the carrier density n_S of the top surface obtained from quantum capacitance oscillations [3] we prove that the Fermi wave vector, measured by the fundamental antidot peak is given by $k_F = \sqrt{4\pi n_s}$, in contrast to a conventional 2DES for which $k_F = \sqrt{2\pi n_s}$ holds.

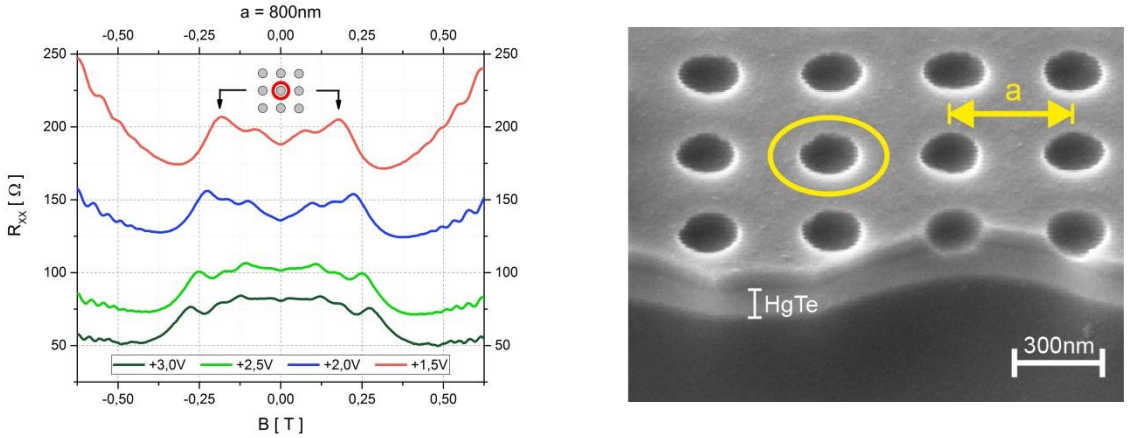

Fig.1 Left: Longitudinal resistance of a sample with $a = 800\ nm$ at different gate voltages. Arrows highlight the position of the fundamental antidot peak corresponding to a cyclotron orbit around one antidot. Right: SEM picture of an antidot lattice with $a = 400\ nm$ etched to the top surface of the 3D topological insulator (50° tilted).

References

[1] L. Fu and C.K. Kane, PRB **76**, 045302 (2007)
[2] D. Weiss et al., PRL **66**, 2790 (1991)
[3] D. Kozlov et al., PRL **116**, 166802 (2016)

Length Dependence of Edge Channel Resistance in Microstructures of HgTe/(Hg,Cd)Te Quantum Wells

M. Majewicz[1], G. Grabecki[1,2], P. Nowicki[1], Ł. Szyller[3], J. Wróbel[1,3], M. Zholudev[4], V. Gavrilenko[4], N. N. Mikhailov[5], S. A. Dvoretskii[5], W. Knap[6], F. Teppe[6] and T. Dietl[1,7,8]

1. Institute of Physics, Polish Academy of Sciences, PL 02-668 Warszawa, Poland
2. Department of Mathematics and Natural Sciences, College of Sciences, Cardinal Wyszyński University, PL 01-938 Warszawa, Poland
3. Faculty of Mathematics and Natural Sciences, Rzeszów University, PL 35-959 Rzeszów, Poland
4. Institute for Physics of Microstructures, Nizhny Novgorod, 603950, Russia
5. Institute of Semiconductor Physics, Siberian Branch, Russian Academy of Sciences, Novosibirsk, 630090, Russia
6. Laboratoire Charles Coulomb (L2C), University of Montpellier &CNRS, UMR 5221, F-34095 Montpellier, France
7. International Research Centre MagTop, PL 02-668 Warszawa, Poland
8. WPI-Advanced Institute for Materials Research (WPI-AIMR), Tohoku University, Sendai 980-8577, Japan
majewicz@ifpan.edu.pl

Since the breakthrough report that indicated the existence of quantized spin Hall resistance in HgTe quantum wells [1], it has been unclear which mechanism accounts for a relatively short topological protection length in two dimensional topological insulators. It was argued that backscattering in these systems originates from either disorder-induced charge puddles [2] or intrinsic edge reconstruction [3]. Our results obtained for HgTe/(Hg,Cd)Te:In quantum wells reveal a large dispersion in resistance values at a given channel length, which points out to an extrinsic origin of topological protection breaking.

We have drawn the above conclusion by studying two types of microstructures shown in Fig. 1 in the regime in which negative gate voltage deplete the quantum well from electrons. In this range, non-local resistance vanishes at about 4 T, in agreement with theoretical expectations [4]. We employ both quantum simulations (Kwant package) and a classical approach (a finite element method for a non-uniform current distribution) in order to evaluate channel resistance for various 4 probe configurations and channel lengths from 2 to 20 μm at 1.8 K. While for the channel length of L_{ch} = 2 μm, the resistances R is close to the expected value $R_K = h/e^2$, at L_{ch} = 10-20 μm, R varies between 10 and $28R_K$.

The research was partially supported by National Center of Science in Poland (Decision No. 2015/17/N/ST3/02314), by grants RBFR "15-52-16017 NTSL_a" and 15 -52-16008 NTSIL_a". Partial support by LIA TERAMIR is appreciated.

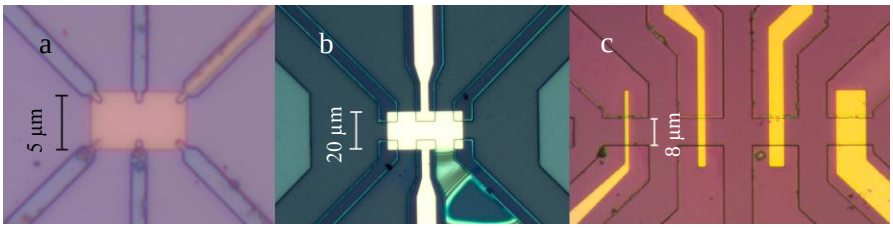

Fig. 1. Optical images of studied samples (preparation in ref. [5]). Bright area shows gate covering whole structure of dimension LxW = 4×4 (a) and 20×10 μm (b), and part of it (c).

References

[1] M. König et al., *Science* **318**, 766 (2007); [2] J. Väyrynen *et al.*, *Phys. Rev. B* **90**, 115309 (2014); [3] Jianhui Wang et al., *Phys. Rev. Lett.* **118**, 046801 (2017); [4] S. Krishtopenko *et al.*, *Phys. Rev. B* **94**, 245402 (2016); [5] M. Majewicz *et al.*, *Acta Phys. Pol. A* **126**, 1174 (2014).

A 3D strained HgTe topological *p-n* junction

C. Thomas[1,*,¥], O. Crauste[2], C. Bäuerle[2], P. Ballet[1], T. Meunier[2]
[1] *Univ. Grenoble Alpes, CEA, LETI, MINATEC campus, F38054 Grenoble, France.*
[2] *Institut Néel, C.N.R.S. Université Joseph Fourier, BP 166, 38042 Grenoble Cedex 9, France*
*thoma686@purdue.edu
[¥]*Present address: Department of Physics and Astronomy and Station Q Purdue, Purdue University, West Lafayette, IN 47907, USA*

Conducting surfaces with a massless and chiral Dirac band structure are expected to govern the transport properties of topological insulators (TI). Thanks to their true spin-momentum locking, novel circuit functionalities are predicted to emerge in the fields of quantum nanoelectronics and spintronics, but require the electronic transport to be solely mediated by topological surface charge carriers.

Constant efforts to improve the existing growth process [1] of our strained three-dimensional (3D) HgTe/CdTe TI lead to the realization of structures with sharp interfaces and very high mobility (up to 600,000 $cm^2/(V.s)$). Moreover, shrinking HgTe thickness down to the 2D to 3D crossover enables to limit bulk and side surface parasitic transport contributions leading to the first demonstration of the quantum Hall regime where plateaus of the Hall resistance are associated to vanishing longitudinal resistances. Consequently, a surface-restricted transport carried by Dirac fermions has been evidenced [2], offering a promising platform for applications.

We will present the first magneto-resistance investigation of a HgTe *p-n* junction fabricated with two independent top gates. The realization of such junction and the understanding of the underlying physics is essential for potential device application. Individual filling of Landau levels by each gate is demonstrated at high magnetic fields. Moreover, resistance quantization provides evidence of the chiral network created by the topological states in such junction. This whole experimental study will be reported in details, giving insights about the relevance of HgTe TI for the design of future quantum circuit.

References

[1] P. Ballet, C. Thomas, X. Baudry, C. Bouvier, O. Crauste, T. Meunier, G. Badano, M. Veillerot, J.P. Barnes, P.H. Jouneau and L.P. Lévy, *Journ. of Elec. Mat.*, 43, 2955-2962, (2014).
[2] C. Thomas, O. Crauste, B. Haas, P.-H. Jouneau, C. Bäuerle, L.P. Lévy, E. Orignac, D. Carpentier, P. Ballet, and T. Meunier, Revealing topological Dirac fermions at the surface of strained HgTe via Quantum Hall transport spectroscopy, *in preparation*

Quantum capacitance anomalies of two-dimensional non-equilibrium states under microwave irradiation

Jian Mi,[1] Jianli Wang,[1] Saeed Fallahi,[2, 3] Geoffrey C. Gardner,[2, 3, 4] M. J. Manfra,[2, 3, 4], Chi Zhang[1, 5,]

1, International Center for Quantum Materials, Peking University, Beijing, 100871, China

2, Department of Physics and Astronomy,and Station Q Purdue, Purdue University, West Lafayette, Indiana 47907, USA

3, Birck Nanotechnology Center, Purdue University, West Lafayette, Indiana 47907, USA

4, School of Electrical and Computer Engineering, and School of Materials Engineering, Purdue University, Indiana 47907, USA

5, Collaborative Innovation Center of Quantum Matter, Beijing, 100871, China

gwlzhangchi@pku.edu.cn

The microwave-induced resistance oscillations (MIRO) [1, 2] and the related zero-resistance states (ZRS) [3, 4] are novel phenomena in ultraclean two-dimensional electron system (2DES). In fact, there are still important puzzles in this research area.

We report our direct study of the compressibility on ultrahigh mobility two-dimensional electron system ($\mu \sim 1 \times 10^7$ cm^2/V sec) in GaAs/AlGaAs quantum wells under microwave (MW) irradiation. The field penetration current results show that the quantum capacitance oscillates with microwave induced resistance oscillations (MIRO), however, the trend is opposite with respect to the compressibility for usual equilibrium states in previous theoretical explanations. The anomalous phenomena provide a platform for study on the non-equilibrium system under microwave, and point to the current domains [5] and inhomogeneity induced by radiation. Moreover, the quantum capacitance indication for multi-photon process around $j = 1/2$ is detected under intensive microwave below 30 GHz.

References

[1] M. A. Zudov, R. R. Du, J. A. Simmons, and J. L. Reno, Phys. Rev. B **64**, 201311(R) (2001).
[2] P. D. Ye, L. W. Engel, D. C. Tsui, J. A. Simmons, J. R. Wendt, G. A. Vawter, and J. L. Reno, Appl. Phys. Lett. **79**, 2193 (2001).
[3] R. G. Mani, Jurgen H. Smet, Klaus von Klitzing, Venkatesh Narayanamurti, William B. Johnson, and Vladimir Umansky, Nature **420**, 646 (2002).
[4] M. A. Zudov, R. R. Du, L. N. Pfeiffer, and K. W. West, Phys. Rev. Lett. **90**, 046807 (2003).
[5] A. V. Andreev, I. L. Aleiner, and A. J. Millis, Phys. Rev. Lett. **91**, 056803 (2003).

Shot Noise in a Fractional Quantum Hall System with Multiple Quantum Point Contacts

Byeongmok Lee†, Cheolhee Han†, and H.-S. Sim†
†*Department of Physics, Korea Advanced Institute of Science and Technology, Daejeon 34141, Korea*
Qudahr1222@kaist.ac.kr

Fractional charge and fractional statistics of anyonic quasiparticles are the distinctive features of fractional quantum hall (FQH) systems. Experimental verification of fractional charge has been accomplished by measuring fano factor, the ratio of shot noise to current, in a tunneling experiment utilizing a quantum point contact (QPC) between two FQH edges. [1] The fano factor equals to the fractional charge in a weak-tunneling and shot-noise regime. On the other hand, for fractional statistics, intermediate between fermionic and bosonic statistics, unequivocal evidence has not been reported.

We study tunneling current and shot noise in an abelian fractional quantum hall system with two QPCs (see Fig. 1). We find that in a shot noise regime, the fano factor is the fractional charge multiplied by a function of anyon exchange-statistics phase, contrary to the case of the conventional system with a single QPC. We attribute the anomalous shot noise to a transport process involving 'topological vacuum bubbles' [2] which represent virtually excited anyons that wind around real anyonic excitations. Since the bubble process stems from the fractional exchange statistics, we suggest that the anomalous fano factor provides a way of experimentally detecting fractional statistics.

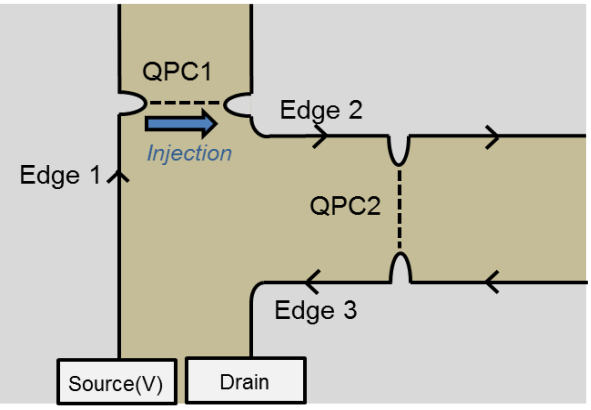

Fig.1 Fractional quantum hall system with two QPCs. The solid lines represent chiral FQH edge states and the dashed lines describe anyon tunneling at QPCs. Edge 1 is biased by voltage V so that anyons are dilutely injected from Edge 1 to Edge 2 at QPC1. The fano factor is obtained by measuring current and shot noise at the drain of Edge 3.

References

[1] R. de-Picciotto, M. Reznikov, M. Heiblum, V. Umansky, G. Bunin, and D. Mahalu, Nature **389,** 162 (1997).
[2] C. Han, J. Park, Y. Gefen, and H.-S. Sim, Nat. Commun. **7,** 11131 (2016).

Topological Insulator State and Beatings in Shubnikov – de Haas Oscillations in a Wide HgTe Quantum Well

A.A. Dobretsova, Z.D. Kvon, N.N. Mikhailov
Novosibirsk State University, 630090, Novosibirsk, Russia
Rzhanov Institute of Semiconductor Physics, 630090, Novosibirsk, Russia
DobretsovaAA@gmail.com

At the present time HgTe quantum well is one of the most intensively investigated subject of two-dimensional electron system physics. Due to the strong relativistic effects, and particularly spin-orbit interaction, different electron systems can be realized in these wells: ordinary insulator, 2D massless Dirac Fermions, 2D and 3D topological insulator, 2D semimetal.

This work is devoted to the investigation of a wide (~20 nm) HgTe quantum well. Together with being semimetallic in recent work [1] this well was shown to be an analog of 3D topological insulator with a quantum well instead of 3D crystal. The point was that electrons in the conduction band at large energies transform from “volume” ones, localized in the center of the well, to the surface ones, localized near two well surfaces. In this work manifestation of these surface states in magnetotransport was studied. Shubnikov – de Haas (ShdH) oscillations in 18-22 nm HgTe quantum wells with orientations (001) and (013) versus magnetic field and gate voltage were measured. As expected, due to different concentration of surface electrons at surfaces closer and farther from the gate, beatings occur in ShdH oscillations with gate voltage increase (see Fig. 1). The data obtained versus magnetic field can be well described by the suggested model of surface electrons. ShdH oscillations versus gate voltage were found to have more complicated behavior (see Fig. 1, b). In particular together with the appearance of the expected beatings in oscillations the equidistance between oscillation extrema becomes broken with gate voltage increase, what can be attributed to the spectrum characteristics.

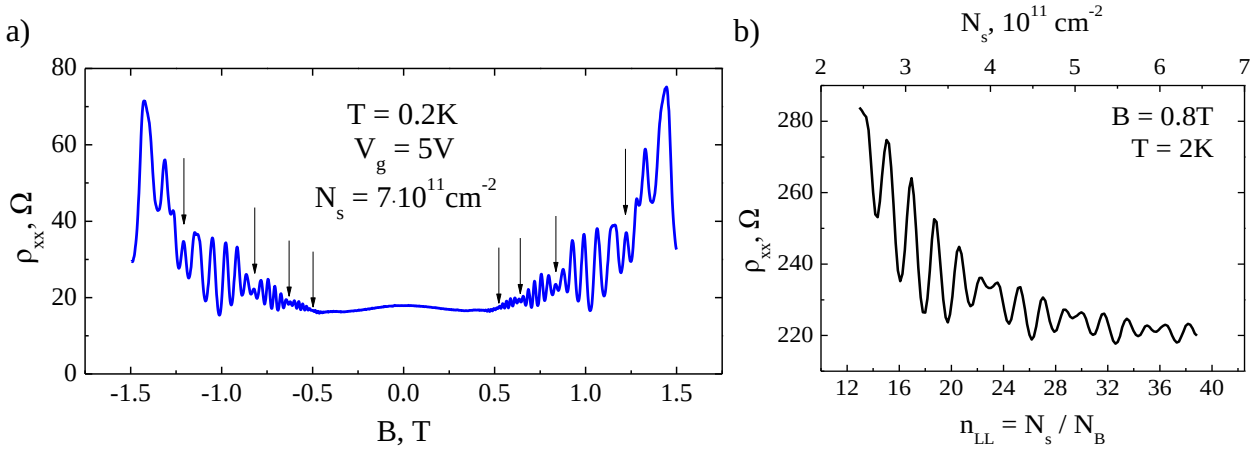

Fig. 1. Shubnikov – de Haas oscillations versus magnetic field (a), versus Landau level number ($N_B = eB/hc$ – Landau level degeneracy) and electron concentration (b) in a wide HgTe quantum well.

References

[1] A.A. Dobretsova, L.S. Braginskii, M.V. Entin, Z.D. Kvon, N.N. Mikhailov, S.A. Dvoretsky, *JETP Letters* **101**, 330 (2015).

Steady states and edge state transport in topological Floquet-Bloch systems

Iliya Esin* and Netanel H. Lindner
Physics Department, Technion, 320003 Haifa, Israel
Mark S. Rudner
Center for Quantum Devices and Niels Bohr International Academy,
Niels Bohr Institute, University of Copenhagen, 2100 Copenhagen, Denmark
Gil Refael
Institute for Quantum Information and Matter, Caltech, Pasadena, CA 91125, USA
*iliyaesin@campus.technion.ac.il

External driving is emerging as a promising tool for exploring new phases in quantum systems. We study the steady states of two dimensional Floquet topological insulators: systems in which a topological Floquet-Bloch spectrum is induced by an external periodic drive. We consider energy and momentum relaxation through radiative recombination and electron-phonon interactions, as well as coupling to an external fermionic reservoir. We show that the resulting steady state resembles a topological insulator in the Floquet basis. The particle distribution in the Floquet edge modes exhibits a sharp feature akin to the Fermi level in equilibrium systems, while the bulk hosts a small density of excitations. We discuss transport signatures and describe the regimes where edge-state transport can be observed. Our results give promise for realizing and probing Floquet topological insulators.

Quasiparticle tunneling in the lowest Landau level

S. Hennel, M. Kellermeier, P. Scheidegger, P. Caspar, C. Reichl, W. Wegscheider, T. Ihn and K. Ensslin
Solid State Physics Laboratory, ETH Zürich - 8093 Zürich Switzerland
hennels@phys.ethz.ch

We study the temperature- and dc-bias-dependence of the quasiparticle tunneling conductance across a top-gate-defined quantum point contact (QPC) in a GaAs/AlGaAs heterostructure, in the fractional quantum Hall states at filling $\nu = 1/3$ and $\nu = 4/3$. In the limit of high transmission, we observe a minimum in the differential tunneling conductance at zero bias [1], in disagreement with the zero-bias peak predicted by Wen for weak backscattering within Luttinger liquid theory [2]. As the transmission is lowered, a maximum progressively emerges at zero dc bias. We generically observe an intermediate regime where the processes responsible for the maximum and the minimum coexist. A fit to Wen's model in the low-transmisson regime yields a quasiparticle charge in agreement with $e^*/e = 1/3$ within experimental accuracy. The measured scaling parameter g is however nonuniversal and transmission-dependent. Furthermore, we investigate the influence of a biased edge channel on quasiparticle tunneling in a neighboring QPC with independent source and drain contacts. Our work is motivated by the puzzling results obtained in studies of the topological order in the second Landau level [3, 4, 5, 6], and in a wider picture by the search for the elusive signatures of coherent transport in quasiparticle interferometers designed to operate in the Aharonov-Bohm regime. In light of our results, one might in particular reconsider the interpretation of tunneling conductance experiments in the $\nu = 5/2$ state.

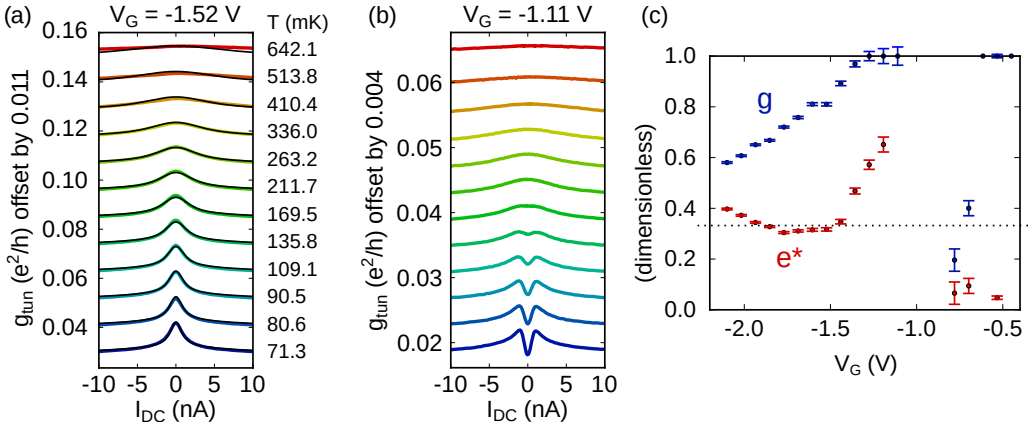

Fig. 1. **(a)** Temperature- and dc-bias-dependence of the differential tunneling conductance of the $\nu = 1/3$ state across a constriction in the low-transmission regime. The black line is a fit to Wen's model. **(b)** Intermediate regime, the gate voltage is slighly less negative, resulting in a wider constriction. **(c)** Best fit parameters g and e^* in a gate voltage range covering the low, intermediate and high transmission regimes.

References

[1] S. Roddaro, V. Pellegrini, F. Beltram, G. Biasol and L. Sorba, Phys. Rev. Lett. **93**, 046801 (2004).
[2] X.G. Wen, Phys. Rev. B **44**, 5708 (1991).
[3] I. P. Radu, J. B. Miller, C. M. Marcus, M. A. Kastner, L. N. Pfeiffer, and K. W. West, Science **320**, 899 (2008).
[4] X. Lin, C. Dillard, M. A. Kastner, L. N. Pfeiffer, and K. W. West, Phys. Rev. B **85**, 165321 (2012).
[5] S. Baer, C. Rössler, T. Ihn, K. Ensslin, C. Reichl and W. Wegscheider, Phys. Rev. B **90**, 075403 (2014).
[6] H. Fu, P. Wang, P. Shan, L. Xiong, L. N. Pfeiffer, K. West, M. A. Kastner, and X Lin, Proc. Natl. Acad. Sci. U.S.A. **133**, 12386 (2016).

Electronic Transport and Quantum Hall Effect in p–n junctions in InAs/GaSb Coupled Quantum Wells

M. Karalic, C. Mittag, T. Tschirky, W. Wegscheider, K. Ensslin and T. Ihn
Solid State Physics Laboratory, ETH Zurich
8093 Zurich, Switzerland
makarali@phys.ethz.ch

We have studied the formation of a p–n junction using local top gating in an inverted InAs/GaSb coupled quantum well heterostructure. A pair of overlapping top gates enables us to independently control carrier type and density in two adjacent regions in the device, allowing us to map out the phase diagram of the system, Fig. 1, consisting of *pp*, *np*, *pn* and *nn* regimes. In the *np* and *pn* regimes, the electrons and holes situated in their respective quantum wells are separated by the same hybridization gap responsible for the topological insulator properties of these quantum wells [1, 2].

In the quantum Hall state, we observe full equilibration along the 25 µm p–n junction between counterpropagating spin-polarized electron and hole edge states in the *pn* and *np* regimes. Fractional plateaus occurring due to equilibration are observed in the junction resistance over many filling factors, resulting in the pattern in Fig. 2, and their values are in agrement with theory [3]. Unlike in graphene, scattering between edge states with different spin polarization seems to be allowed [4, 5]. In the *pp* and *nn* regimes, we see expected edge state reflection and transmission according to the filling factors in the two regions. Our first results pave the way towards more complex experiments concerning edge dynamics and realizations of electronic beam splitters and interferometers in a system with a rich band structure (broken particle–hole symmetry, strong spin–orbit coupling, topological insulator properties, etc.).

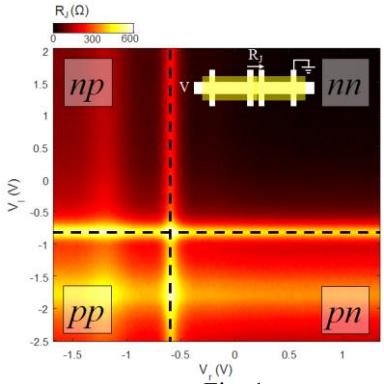

Fig. 1

Phase diagram at zero magnetic field. R_J is the junction resistance and V_r and V_l are the top gate voltages applied to the two parts of the junction. Inset shows device geometry.

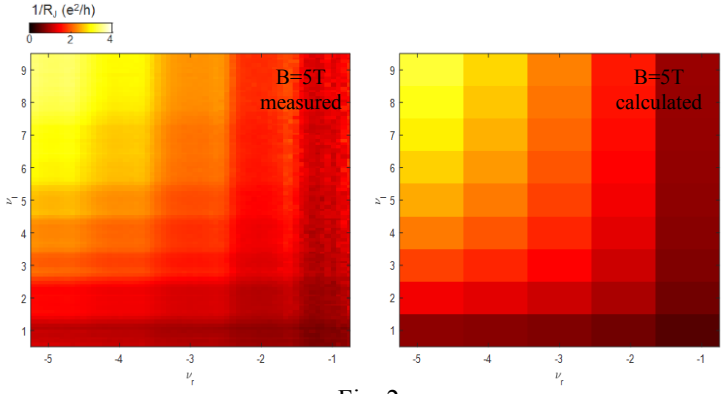

Fig. 2

Part of the phase diagram at a perpendicular magnetic field of 5T showing the quantized resistance, or equivalently, conductance, over the junction, as a function of filling factors in the two parts of the junction. The left map shows measured data, the right a calculation with the same color scale assuming complete edge state equilibration [3].

References

[1] Liu, C., Hughes, T. L., Qi, X. L., Wang, K., & Zhang, S. C. (2008), *Phys. Rev. Lett. 100*(23), 236601.
[2] Du, L., Knez, I., Sullivan, G., & Du, R. R. (2015), *Phys. Rev. Lett.*, *114*(9), 096802.
[3] Abanin, D. A., & Levitov, L. S. (2007), *Science*, *317*(5838), 641-643.
[4] Williams, J. R., DiCarlo, L., & Marcus, C. M. (2007), *Science*, *317*(5838), 638-641.
[5] Amet, F., Williams, J. R., Watanabe, K., Taniguchi, T., & Goldhaber-Gordon, D. (2014), *Phys. Rev. Lett.*, *112*(19), 196601.

Impact of thermodynamics on the Berry phase extracted from magnetooscillations.

A.Yu. Kuntsevich[1,2] (alexkun@lebedev.ru) and G.M. Minkov[3]

[1]*National Research University Higher School of Economics, Moscow, 101000, Russia*

[2]*P.N. Lebedev Physical institute of the RAS, Moscow, 119991, Russia*

[3]*Institute of Natural Sciences, Ural Federal University, 620002 Ekaterinburg,Russia*

Materials with Dirac spectrum of carriers are in the focus of modern condensed matter physics. The phase of the quantum oscillations (Shubnikov-de Haas, de Haas - van Alphen) is often associated with the Berry phase and is widely used to argue in favor of the presence of the Dirac-like carriers. We show that besides Diracness this phase is affected by thermodynamical constrains, i.e. by what is fixed in magnrtic field: chemical potential μ or carrier density n.

For all known 2D systems (e.g. graphene, quantum wells) with high precision the density remains fixed throughout the magnetic field sweep. The conductivity minima are observed when integer number N of Landau levels (LL) is filled. Each LL has a degeneracy eB/h. The condition for the mimima thus reads $1/B_N = Ne/h/n$. Nontrivial $N(1/B_N)$ dependence in graphene originates from 0th LL, that has 2 times lower degeneracy ($N/4+0.5\sim1/B_N$).

There is an opposite limit (3D topological insulators, like $(Bi,Sb)_2(Se,Te)_3$ with Fermi level in the bulk conduction band). Flakes and films of these materials have high-mobility surface electrons, those demonstrate magnetooscillations and low-mobility bulk with large density of states. The latter electrons maintain chemical potential fixed $\mu=const$ during the field sweep. For strictly linear spectrum of the surface states the phase of the oscillations appears to be non-trivial, while being affected by Zeeman splitting and nonlinearity of the spectrum[1,2].

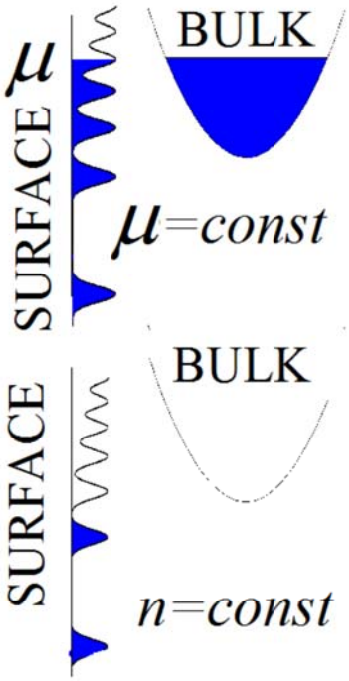

Fig.1 Two limiting cases $\mu=const$ and $n=const$ in 3D TI

In the intermediate case, when there are few subbands filled $n_{Total}=const,$, and if only one of these subbands oscillates, so neither μ nor n_{2D} is constant for the oscillating carriers. We determine the positions of conductivity minima from the condition $n_{Total}=const$ and show that the phase of the oscillations might become unusual, e.g nontrivial phase might be observed in topologically trivial system, and vice versa.

Our reasonings point that Diracness can not be not proven by nontrivial phase of magnetooscillations, we also explain unusual Berry phase observed in several experiments.

References

[1] A.R. Wright, R.H. McKenzie, PRB **87**, 085411 (2013) [2]A. Taskin, Y. Ando, PRB **84**, 035301 (2011)

Edge Photogalvanic Effect in a 2D Topological Insulator

M.V. Entin [+*] and L.I. Magarill [+*]
[+] *Rzhanov Institute of Semiconductor Physics, Siberian Branch of the Russian Academy of Sciences, Novosibirsk, 630090, Russia;*
[*] *Novosibirsk State University, Novosibirsk, 630090, Russia*
levm@isp.nsc.ru

2D topological insulator (TI) is actively developing area of the solid state physics. One of the most known 2D TI is the 2D CdTe/HgTe/CdTe quantum well with central layer width d > 6.3 nm. It attracts attention due to the gapless linear energy spectrum of the edge states and the absence of backscattering.

The purpose of the present report is the study of the mechanisms of optical transitions and photocurrent in the intrinsic 2D TI below the threshold of 2D absorption. In such a case the phototransitions occur within the edge states or between the edge and 2D states. The spin pumping by the polarized light leads (due to rigid link of spin and the velocity direction) to decompensation of the numbers of right- and left-moving electrons resulting in the residual current (photogalvanic effect (PGE)). The weakness of the backscattering in the edge states potentially provides large photoexcited current along the edges.

However, although the energy-momentum conservation permits the elastic optical transitions at small frequency between edge states of TI, the topological protection forbids these transitions. Here we report the possible way to overcome this difficulty.

The proposed mechanism of PGE is shown in Fig.1b (dotted arrows). Under circular-polarized light illumination electrons experience electrodipole indirect phototransitions between edge states via intermediate 2D states. The transition probability has a momentum asymmetry determined by the polarization direction. This gives rise to the edge photocurrent. Besides, direct transitions between the edge and 2D states are studied. In this case the edge current has a threshold behavior.

It was demonstrated, that the edge current in both cases is mostly determined by the carriers in the edge states owing to their topological protection.

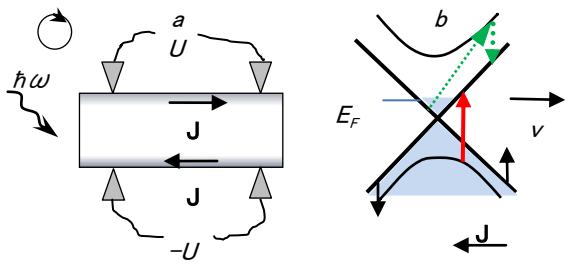

Fig.1 a) A sketch of the effect. The topological insulator is illuminated by the circular-polarized microwave. The photocurrent is concentrated near the edges. b) The band transitions picture. Solid arrow corresponds to the direct phototransitions preferably involving edge-states electrons with positive velocity v [1]. Dotted arrows show the indirect transitions between the edge states via the 2D states caused by the interaction with impurities [2].

References

[1] M.V. Entin and L.I. Magarill, JETP Lett. 103, 711 (2016).
[2] L.I. Magarill and M.V. Entin, JETP Lett. 104, 771 (2016).

Magnetoresistance response in the 3D topological insulator Bi_2Te_3 with indium superconducting electrodes

Zhuo Wang, Tianyu Ye and R. G. Mani
Dept. of Physics & Astronomy, Georgia State University, Atlanta, GA 30303
zwang16@student.gsu.edu

3D Topological insulators (TIs) are novel materials that insulate in the bulk but electrically conduct on their surfaces due to the strong spin-orbit interaction. The conducting surface states are manifested in the associated electronic structure as two crossed channels that connect the conduction- and valence-bands, and creates a single "Dirac cones" in the band gap. A profound significance of discovery of 3D TIs is their great potential ability to host the charge neutral particle, Majorana fermion, which was theoretically predicted to exist in a p-wave superconductor. In 2008, *Fu* and *Kane* suggested that with the help of superconducting proximity effect, the combination between a 3D TI with an s-wave superconductor can realize a p-wave superconducting state at the interface. [1] Thus, motivated by these ideas, we studied the magnetoresistance behavior in the 3D topological insulator Bi_2Te_3 in the presence of indium topside superconducting electrodes.[2] Remarkably, our experimental study showed two anomalous transitions in the magnetoresistance response below $T = 4.2$ K. The first transition is observed as a narrow and deep drop near the zero magnetic field below $T = 3.4$ K, while the second transition with another broader drop occurs at lower temperature.

These magneto-transport measurements were carried out on an exfoliated Bi_2Te_3 thin flake with six indium contacts in a Hall-measurement configuration. Magneto-transport measurements were performed via the standard four-terminal lock-in technique and temperature dependent measurements was carried out in a liquid helium cryostat in the range of $1.7\ K < T < 4.2\ K$.

Fig. 1 shows the normalized magnetoresistance response for specimen 1. Above $T = 3.4$ K, the magnetoresistance exhibits a weak positive magnetoresistance background. At $T = 3.4$ K, which is the critical temperature of indium superconductor, magnetoresistance exhibits an abrupt drop near the zero magnetic field. As the temperature is further decreased, this drop grows much more pronounced in depth. This narrow drop near the zero magnetic fields below $T = 3.4$ K is attributed to the superconducting effect in the indium superconducting electrodes. Further study at the lower temperatures reveals that a second broad drop shows up in the vicinity of B = 0, which is attributed to the proximity effect that occurs at the interface between a superconductor and TI.

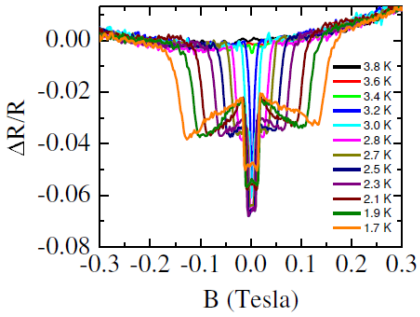

Fig.1 Temperature dependence of normalized magnetoresistance of Bi_2Te_3 flake contacted by indium superconducting electrodes.

References

[1] L. Fu and C. L. Kane, Phys. Rev. Lett. **100**, 096407 (2008).

[2] Zhuo Wang, Tianyu Ye, R. G. Mani, Appl. Phys. Lett. **107**, 172103 (2015).

Design rules for modulation doped AlAs quantum wells

Yoon Jang Chung, K.W. Baldwin, K.W. West, D. Kamburov, M. Shayegan, and L.N. Pfeiffer
Department of Electrical Engineering, Princeton University, Princeton, NJ, 08544, USA
edwinyc@princeton.edu

The fractional quantum Hall effect observed in clean 2D electron systems (2DES) is a remarkable consequence of electron-electron interaction. While GaAs has been the primary material of choice to examine such phenomena, AlAs has also proven to be an intriguing option as it differentiates itself from GaAs in its Landé g-factor, effective mass, valley degeneracy, and anisotropy in band structure. Studies have indeed reported the existence of valley susceptibility, valley Skyrmions, quantum Hall ferromagnetism, and anisotropy transference to composite fermions in AlAs 2DES [1-4].

However, despite the abundant literature on AlAs 2DES, a systematic sample design is still unexplored for AlAs quantum well (QW) structures. Most of the studies on AlAs 2DES use an $Al_xGa_{1-x}As$ barrier alloy fraction $x \approx 40\%$. Although this is the Al alloy fraction at which we expect maximum carrier density in a modulation doped AlAs QW, it may not be the point of highest sample quality, as is well known in GaAs QWs where interface quality and unwanted impurities in the $Al_xGa_{1-x}As$ also play important roles. Our goal is to grow AlAs QWs with various barrier alloy fractions and evaluate their electrical properties to provide a guideline for sample optimization in AlAs 2DES.

Fig. 1(a) shows the measured carrier densities in modulation-doped AlAs QWs over the barrier alloy fraction range of $0.2 < x < 0.8$, both in the dark and after light illumination. The spacer thickness (s) and well width (w) are 59 nm and 11 nm. Results are also shown for a series of GaAs QWs with s = 70 nm and w = 20 nm. From this data we can deduce all relevant energy levels for the modulation doping of the AlAs and GaAs QWs, and we find that there is good agreement between their values if we take the energy difference between the conduction band of GaAs(Γ) and AlAs(X) to be 114 meV. Once these values are established for all barrier alloy fractions, we can grow QWs with any density by varying the spacer thickness accordingly.

Fig. 1(a) implies that AlAs QWs with $x < 0.38$ barriers will behave similarly to GaAs QWs with $x < 0.38$ barriers. This hints that we can achieve high quality AlAs 2DES by using an $Al_xGa_{1-x}As$ barrier in this range. An example of a magneto-transport trace taken in such a sample is given in Fig. 1 (b). Even at the low density of 1.2×10^{11} cm^{-2}, fractional quantum Hall states at fillings $\nu = \frac{2}{3}, \frac{3}{5}, \frac{4}{7}, \frac{3}{7}$ and $\frac{2}{5}$ can clearly be seen, indicating the high quality of the sample.

The results presented here provide a basis to investigate quality improvement in AlAs 2DESs, which is essential if we are to more carefully study the physics of electrons in this system.

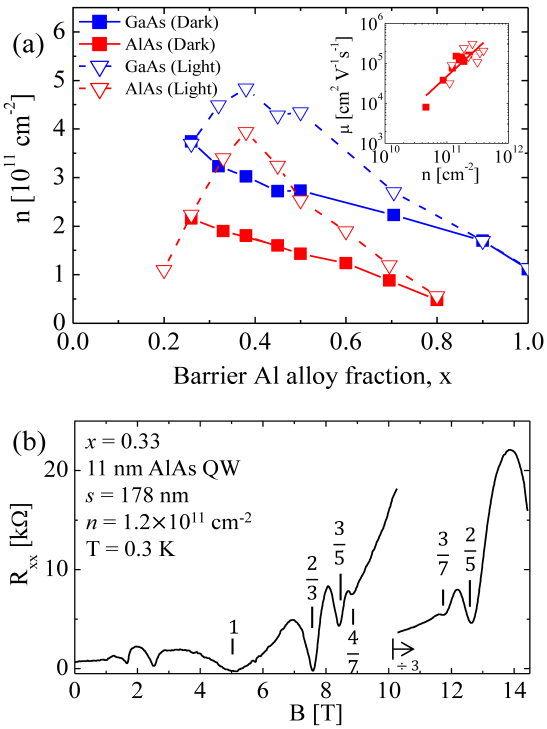

Fig. 1 (a) Measured carrier densities for AlAs and GaAs QWs vs barrier alloy fraction x, in the dark and after illumination. The inset shows the mobility vs carrier density for the AlAs QWs. (b) Magneto-transport data for an AlAs QW with $x = 0.33$ barrier measured after illumination.

[1] Y. P. Shkolnikov *et al.*, PRL **95**, 066809 (2005)
[2] O. Gunawan *et al.*, PRL **97**, 186404 (2006)
[3] E. De Poortere *et al.*, Science **290**, 1546 (2000)
[4] T. Gokmen *et al.*, Nat. Phys. **6**, 621 (2010)

Magnetorotons in the Excitation spectrum of the 2+1/3 FQHE State*

Lingjie Du[1], U. Wurstbauer[2,3], A. L. Levy[4], Y. Y. Kuznetsova[4], A. Pinczuk[1,4], K. W. West[5], L. N. Pfeiffer[5], M. J. Manfra[6], G. Gardner[6], and J. Watson[6]

[1]*Department of Applied Physics and Applied Mathematics, New York 10027, USA*

[2]*Walter Schottky Institut and Physik-Department, TU München, Garching 85748, Germany*

[3]*Nanosystems Initiative Munich (NIM), Munich 80799, Germany*

[4]*Department of Physics, Columbia University, Columbia University, New York 10027, USA*

[5]*Department of Electrical Engineering, Princeton University, Princeton, NJ 08544, USA*

[6]*Department of Physics, Purdue University, West Lafayette, IN 47907, USA*

ld2751@columbia.edu

Low-lying excitations in the second Landau level (SLL) are remarkably different from those in the lowest Landau level and offer crucial insights on the physics of quasi-particle interactions [1, 2, 3]. Our work explores the fascinating excitations in the SLL by measurements of low-lying neutral excitation modes from resonant inelastic light scattering (RILS) experiments.

RILS spectra identify several bands at ν=7/3 shown in Figs. 1(a) and 1(b) [3]. We focus here on the low energy spectra shown in the highlighted area in Fig. 1(a). The spectra are fundamentally different from those at ν=1/3. Remarkably, as shown in Fig. 1(b), our RILS experiments resolve two well defined low energy modes, E_{g1} and E_{g2}, which are centered at about 70μeV and 90μeV, respectively. By comparison with the calculation of magnetoroton modes, the E_{g1} and E_{g2} bands can be interpreted as collective charge excitations at finite wave vectors. As shown in Fig. 1(c), the measured peak energies are in a good agreement with pronounced roton minimum and other critical features in the calculated dispersion [2]. We will discuss these modes taking into account temperature and magnetic field dependent measurements.

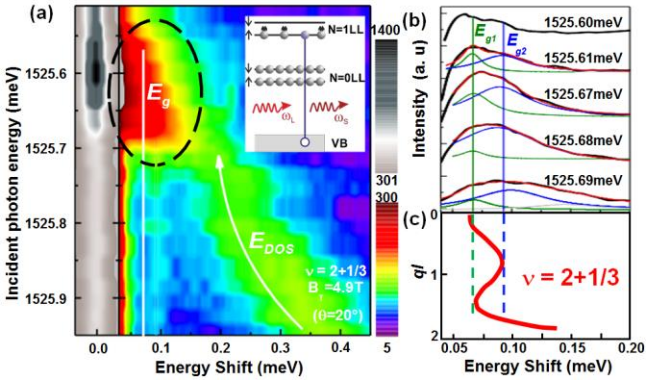

Figure 1: (a) Intensities for photon energies close to the optical emission from the N = 1 LL at ν=2+1/3 at T = 42 mK. Inset shows energy level scheme for incoming and outgoing photon energies. (b) RILS spectra shown in highlighted area of (a) after subtraction of resonant Rayleigh scattering intensities. Two resonantly enhanced low-energy modes are observed. (c) A calculated dispersion from Ref. [2] is in agreement with RILS results in (b).

*Supported by the U.S. National Science Foundation, Division of Materials Research under Award No. DMR-1306976.

References

[1] A. Balram, Y. Wu, G. J. Sreejith, A. Wójs, and J. K. Jain, Phys. Rev. Lett. 110, 186801 (2013)

[2] T. Jolicoeur, arXiv:1610.04477 (2016).

[3] U. Wurstbauer, A. L. Levy, A. Pinczuk, K.W. West, L. N. Pfeiffer, M. J. Manfra, G. C. Gardner, and J. D. Watson, Phys. Rev. B. 92, 241407(R) (2015).

Crystal Phases in Electron Bilayer Systems at High Magnetic Fields

W. Faugno[1], Y. Zhang[1], A. Duthie[2], D. Wales[2], and J. K. Jain[1]
[1]*Physics Department, Penn State University,*
University Park, PA 16803, USA
[2]*Department of Chemistry, University of Cambridge*
Cambridge, CB2 1TN, UK
wnf5015@psu.edu

Experimental results on bilayer fractional quantum hall (FQH) states have shown a long time ago that a strong insulating phase arises near ⅛ + ⅛ and ¼ +¼ filling factors when the layer separation increases past some critical value.[1, 2] This insulating phase persists even at relatively large interlayer separations. Theoretical work has been done to calculate the phase diagram for bilayer FQH states, but this original work did not consider the possibility of a crystalline phase.[3] It has been shown that the ⅛ and ¼ FQH states are very close in energy to that of composite Fermion Wigner crystals.[4] We propose that the insulating phase results from formation of a bilayer composite Fermion Wigner crystal. We present results of Monte-Carlo calculations for a new phase diagram of bilayer FQH system including liquid and crystal phases of composite fermions and show that the latter are stable for a wide range of parameters for total filling factor less than or equal to ½. Our calculations bring out the nature of the bilayer crystal phase.

The work at Penn State was supported in part by the US Department of Energy under Grant No. DE-SC0005042.

[1] H. C. Manoharan, Y. W. Suen, M. B. Santos, and M. Shayegan, Phys. Rev. Lett. **77** 9 (1996).
[2] J. P. Eisenstein, G. S. Boebinger, L. N. Pfeiffer, K. W. West, and Song He. Phys. Rev. Lett. **68** 9 (1992).
[3] V. W. Scarola, and J. K. Jain, Phys. Rev. B. **64** 085313 (2001).
[4] A. C. Archer, Kwon Park, and J. K. Jain, Phys. Rev. Lett. **111** 146804 (2013).

Microwave-induced Resistance Oscillations in a Backgated GaAs Quantum Well

X. Fu[1], Q. A. Ebner[1], Q. Shi[1], M. A. Zudov[1,*], Q. Qian[2], J. D. Watson[2], and M. J. Manfra[2,3]
[1]*School of Physics and Astronomy, University of Minnesota, Minneapolis, MN 55455, USA*
[2]*Department of Physics and Astronomy and Birck Nanotechnology Center, Purdue University, West Lafayette, Indiana 47907, USA*
[3]*Station Q Purdue, School of Materials Engineering, and School of Electrical and Computer Engineering, Purdue University, West Lafayette, Indiana 47907, USA*
[*]zudov@physics.umn.edu

One of the most popular methods to obtain the effective mass $m^\star$ of the charge carriers in a two-dimensional electron gas (2DEG) in GaAs heterostructures is based on the analysis of Shubnikov-de Haas oscillations (SdHO). Being a result of Landau quantization in a magnetic field B, SdHO are controlled by the filling factor, $\nu = 2\varepsilon_F/\hbar\omega_c$, where $\varepsilon_F = \pi\hbar^2 n_e/m^\star$ is the Fermi energy, n_e is the carrier density, and $\hbar\omega_c = eB/m^\star$ is the cyclotron energy. Since $m^\star$ does not enter ν, it cannot be obtained from the oscillation period but, instead, one has to analyze the temperature damping of the SdHO amplitude. Using this approach, a few studies reported significant variations of $m^\star$ with n_e [1, 2], which were taken as an evidence of electron-electron interactions. In particular, it was found that $m^\star$ exhibits a broad minimum at intermediate n_e (where it is lower than the band value of $m_b^\star = 0.067m_0$, m_0 is a free electron mass) but becomes significantly enhanced at low n_e. While the SdHO approach is employed widely, it suffers from a low accuracy [1, 2] and is time consuming as it calls for long B-sweeps at several different temperatures.

There exist other classes of magnetoresistance oscillations which can be used to obtain $m^\star$ more easily [3]. For example, unlike SdHO which are controlled by $m^\star$-independent ν, microwave-induced resistance oscillations (MIRO) [4] are governed by $\omega/\omega_c \propto m^\star$, where $\omega = 2\pi f$ is the microwave frequency. As a result, $m^\star$ is directly available from the MIRO frequency and thus can be obtained from a single B-sweep with high precision [5]. Here, we investigate the n_e-dependence of $m^\star$ obtained from MIRO measured in a 30-nm GaAs/AlGaAs quantum well which is top side-doped at a setback of 63 nm. An *in situ* gate, consisting of an n^+ GaAs layer at 850 nm below the quantum well, was used to tune n_e from 1.3 to 3.2×10^{11} cm^{-2}, at which the peak mobility of $\mu \approx 1 \times 10^7$ cm^2/Vs was reached. Measurements were performed in sweeping B using microwave frequency $f = 34$ GHz.

Despite relatively low f, which was chosen to avoid the regime of separated Landau levels, our sample produced well-developed MIRO showing at least four oscillations over the whole density range studied. At higher n_e, the analysis of the MIRO frequency revealed a considerably reduced $m^\star$, in agreement with Ref. 5, which investigated MIRO in fixed density samples with $n_e \approx 2.7 \times 10^{11}$ cm^{-2} and $n_e \approx 3.2 \times 10^{11}$ cm^{-2}. At lower n_e, however, our MIRO data clearly showed a significant enhancement of $m^\star$, in general agreement with earlier SdHO studies [1, 2]. These findings confirm that MIRO, like SdHO, are sensitive to electron-electron interactions but offer a much more convenient and accurate means to obtain $m^\star$.

References

[1] Y.-W. Tan, J. Zhu, H. L. Stormer, L. N. Pfeiffer, K. W. Baldwin, and K. W. West, Phys. Rev. Lett. **94**, 016405 (2005).
[2] P. Coleridge, M. Hayne, P. Zawadzki, and A. Sachrajda, Surf. Sci. **361**, 560 (1996).
[3] I. A. Dmitriev, A. D. Mirlin, D. G. Polyakov, and M. A. Zudov, *et al.*, Rev. Mod. Phys. **84**, 1709 (2012).
[4] M. A. Zudov, R. R. Du, J. A. Simmons, and J. L. Reno, Phys. Rev. B **64**, 201311(R) (2001).
[5] A. T. Hatke, M. A. Zudov, J. D. Watson, M. J. Manfra, L. N. Pfeiffer, and K. W. West, Phys. Rev. B **87**, 161307(R) (2013).

Giant Microwave Induced *B*-periodic Resistance Oscillations in a Two-Dimensional Electron Gas with a Quantum Point Contact

A.D.Levin,[1] S.A.Mikhailov,[2] G.M.Gusev,[1] Z.D.Kvon,[3,4] E.E.Rodyakina,[3,4] and A.V.Latyshev,[3,4]
[1]*Instituto de Fisica da Universidade de Sao Paulo, 135960-170, Sao Paulo, SP, Brazil*
[2]*Institute of Physics, University of Augsburg, D-86135 Augsburg, Germany*
[3]*Institute of Semiconductor Physics, Novosibirsk 630090, Russia*
[4]*Novosibirsk State University, Novosibirsk 630090, Russia*
gusev@if.usp.br

We study a magnetoresistance R_{xx} of a quantum point contact (QPC) fabricated in a high electron mobility two-dimensional electron gas (2DEG) and exposed to the microwave irradiation [1]. Instead of the conventional split-gate QPC we use a *bridged-gate* QPC which has recently demonstrated a giant microwave photoconductance in zero magnetic field B=0 [2]. In strong B (at $\omega_c>\omega$, ω_c and ω are the cyclotron and microwave frequencies) we observe giant B-periodic R_{xx} oscillations, Fig. 1(c), with the period $\Delta B \sim n_s/\omega L$ and the relative amplitude $\Delta R_{xx}/R_{xx}$ up to 700%, resulting from the interference of edge magnetoplasmons (EMPs) [3] excited by microwaves at different contacts to the 2DEG; here n_s is the electron density. Quantitatively comparing the data with the theory [3] we unambiguously identify the oscillation indexes and the interference length L, Fig. 2, which is shown to be determined not by the distance a-b between contact leads, Fig. 1(b), as was assumed in earlier works [4,5], but by the much larger distances c-d or c-g. The discovered very high sensitivity of the device and a better understanding of the nature of EMP-induced oscillations open new ways for the design and creation of highly sensitive detectors and spectrometers of microwave and terahertz radiation.

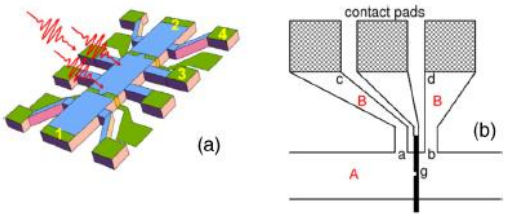

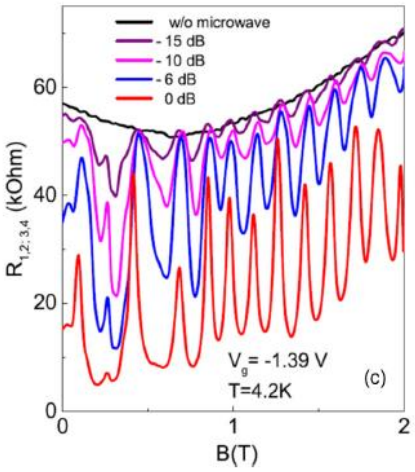

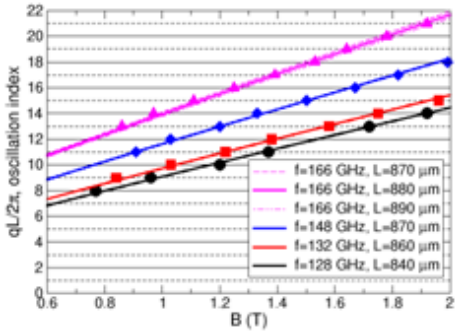

Fig. 1. (a) A schematic set-up of the bridged-gate sample. (b) Geometry of contact pads, contact leads (areas B) and of the 2DEG (area A). (c) The longitudinal resistance at f=156 GHz, T=4.2 K, gate voltage -1.39 V, at different values of the microwave power.

Fig. 2. The EMP interference parameter $qL/2\pi$ (q is the EMP wave-vector) and the oscillation indexes extracted by comparing the theory [3] with the experimental data.

References

[1] A. D. Levin *et al*., Phys. Rev. B **95**, 081408(R) (2017).
[2] A. D. Levin *et al*., Appl. Phys. Lett. **107**, 072112 (2015).
[3] V. A. Volkov and S. A. Mikhailov, Sov. Phys. JETP **67**, 1639 (1988).
[4] I.V. Kukushkin *et al.*, Phys. Rev. Lett. **92**, 236803 (2004).
[5] K.Stone et al., Phys. Rev. B **76**, 153306 (2007).

Topological Description of Tilted Dirac Fermions with/without Mass

T. Kawarabayashi[1], H. Aoki[2,3] and Y. Hatsugai[4]
[1]*Department of Physics, Toho University, Funabashi, 274-8510, Japan*
[2]*Department of Physics, University of Tokyo, Hongo, Tokyo 113-0033, Japan*
[3]*Electronics and Photonics Research Institute, Advanced Industrial Science and Technology, Tsukuba, Ibaraki 305-8568, Japan*
[4]*Division of Physics, University of Tsukuba, Tsukuba, 305-8571, Japan*
[1]tkawa@ph.sci.toho-u.ac.jp

Graphene as a prototype of massless Dirac fermion system in two dimensions has spin-off into variants with/without mass for topological properties such as valley/spin Hall effects. These include transition-metal dichalcogenides, organic compounds and optical lattices for cold atoms. We can attribute the origins of their topological behaviors to generic Dirac fermions, where the Dirac cones can in general be tilted. With these as a background, we have constructed a general description of tilted Dirac fermions with doubling (valley degeneracy) by extending the conventional chiral symmetry, which we call the "generalized chiral symmetry" [1,2], as a guiding principle. We have shown that by considering an algebraic and continuous deformation of lattice Hamiltonians having the generalized chiral symmetry, various series of lattice Hamiltonians with valley-degenerated tilted Dirac fermions can be generated systematically [3].

By applying the present deformation, which is not restricted to translationally invariant systems, to a fermion-vortex system [4,5], we show that the conventional zero modes associated with the vortex can be generalized to the tilted Dirac fermions, where the zero modes are given as the exact eigenstates of the generalized chiral operator [3]. The deformation can also be applied to models with different numbers of sub-lattice sites, such as the Lieb lattice having a flat band (Fig.1). Moreover, the symmetry breaking by the mass term, which is essential to the valley Hall effect, can also be treated in the present scheme, where the quasi-zero modes are shown to be topologically stable [3].

Since the present deformation generates tilted Dirac fermions without changing the topological property of the zero modes, it is expected to be useful in discussing the generality of the topological phenomena associated with the zero modes of tilted Dirac fermions in two dimensions, as in the organic material.

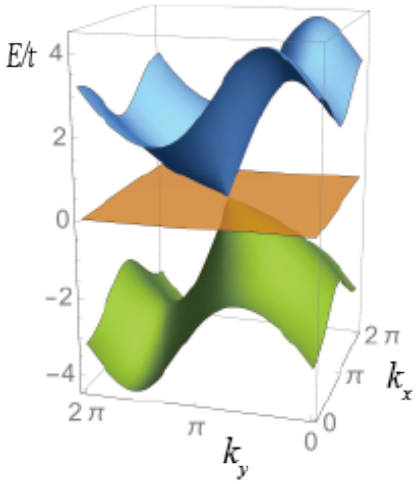

Fig.1 Energy dispersion of the deformed Lieb lattice [3].

References

[1] T. Kawarabayashi, Y. Hatsugai, T. Morimoto, and H. Aoki, Phys. Rev. B **83**, 153414 (2011).
[2] Y. Hatsugai, T. Kawarabayashi, and H. Aoki, Phys. Rev. B **91**, 085112 (2015).
[3] T. Kawarabayashi, H. Aoki, and Y. Hatsugai, Phys. Rev. B **94**, 235307 (2016).
[4] R. Jackiw and P. Rossi, Nucl. Phys. B **190**, 681 (1981).
[5] C. Chamon et al., Phys. Rev. Lett. **100**, 110405 (2008).

The ν=3+1/3 Fractional Quantum Hall State: a Ground State in the Second Landau Level with Puzzling Properties

Ethan Kleinbaum[1], Ashwani Kumar[2], Ken West[3], Loren Pfeiffer[3] and Gabor Csathy[1]
[1]*Department of Physics and Astronomy, Purdue University, West Lafayette, In, 47906, USA*
[2]*Department of Physics, Monmouth College, Monmouth, IL, 61462, USA*
[3]*Department of Electrical Engineering, Princeton, NJ, 08544, USA*
eik@princeton.edu

The two-dimensional electron gas exhibits a large number of fractional quantum Hall states. The vast majority of these can be understood remarkably well with the model of non-interacting composite fermions. Yet several fractional quantum Hall states appear to require exotic descriptions beyond this well-established conventional model.

In high quality two-dimensional electron gases confined to Gas/AlGaAs quantum wells, most exotic fractional quantum Hall states are thought to reside in the second Landau level. In order to gain a more detailed understanding of this intriguing region, we have used ultra-low temperature techniques to search for new ground states. These measurements reveal a previously not seen fractional quantum Hall state in the upper spin branch of the second Landau level at filling factor ν=3+1/3 [1].

This new fractional quantum Hall state exhibits unusual properties: the particle-hole conjugate state at ν=3+2/3 does not develop and the energy gap of the ν=3+1/3 state is about a factor of 3 less than that of the ν=3+1/5 state. This latter relationship means that the relative magnitudes of the energy gaps of the 3+1/3 and 3+1/5 states is reversed as compared to that of the 1/3 and 1/5 states. This anomalous gap reversal raises the possibility that at least one of these fractional quantum Hall states is of unconventional origin. We acknowledge funding from the NSF grants DMR-1207375 and 1505866, the Gordon and Betty Moore Foundation grant GBMF 4420, and the NSF MRSEC at the Princeton.

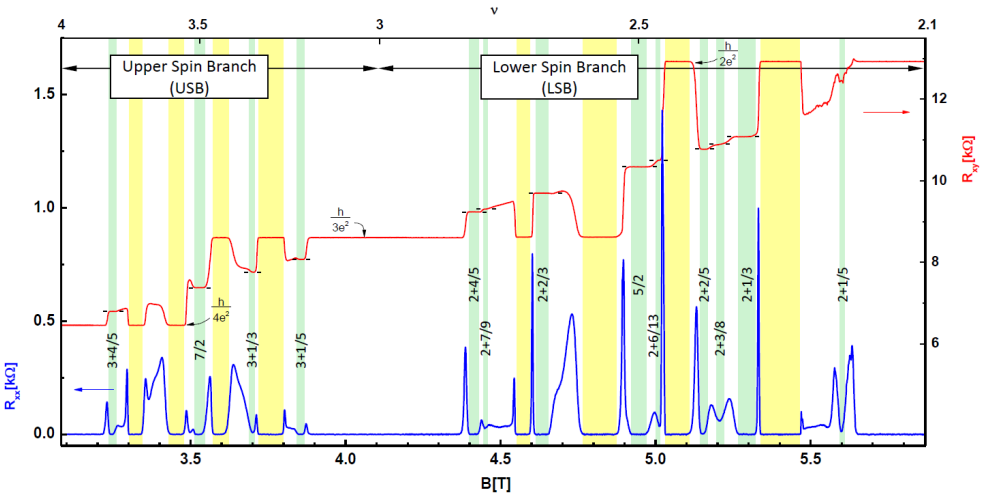

Fig.1 The magnetoresistance measured at ~6.9 mK of a high quality two-dimensional electron gas in the second Landau level. Green and yellow represent fractional quantum Hall states and bubble phases, respectively.

References

[1] E. Kleinbaum, A. Kumar, L.N. Pfeiffer, K. West, G.A. Csathy, Phys. Rev. Lett. **114**, 076801 (2015).

Many-Body States of a Projected Landau-Hofstadter Band on Various Lattices

Koji Kudo[1], Toshikaze Kariyado[2], Yasuhiro Hatsugai[1]
[1]*Graduate School of Pure and Applied Science, University of Tsukuba, Tsukuba 305-8577, Japan*
[2]*International Center for Materials Nanoarchitectonics (WPI-MANA), National Institute for Materials Science, Tsukuba 305-0047, Japan*
Kudo@rhodia.ph.tsukuba.ac.jp

The fractional quantum Hall (FQH) state is a quantum liquid, which does not accompany any symmetry breaking. The Hall conductance in the FQH system is given by the Chern number associated with the Berry connection as in the case of integer quantum Hall system, but is corrected by the topological degeneracy [1]. Here, we construct analogues of the Laughlin state on various lattice models and evaluate the Chern number explicitly. Specifically, our model is a two-dimensional lattice model with nearest-neighbor interaction subjected to external magnetic field. We consider six types of lattice structures, square, Lieb, square-octagon, triangular, honeycomb, and kagome, where the first three have the square Bravais lattice while the last three have the hexagonal one. The electron-electron interaction is taken into account by a pseudopotential, which is constructed by the following two steps: (i) one-body part of the tight-binding Hamiltonian with magnetic field is diagonalized to obtain the wave functions for the Landau-Hofstadter bands, and then (ii) interaction term is projected to the lowest band [2].

Our main focus is on the case with Landau level filling factor $\nu = 1/3$. Figure 1 shows the results for the square lattice system implying that the energy gap is finite in the large N_ϕ limit, where N_ϕ is the Landau degeneracy. This feature is consistent with the Laughlin state. Numerically obtained energy gaps for different lattices share essentially the same dependence on $1/N_\phi$ after a suitable rescaling *as long as the underlying Bravais lattice is the same*. We construct the Berry connection using the ground state multiplet and evaluate the Chern number numerically [4]. We also discuss the many-body states at $\nu = 1/2$, which are consistent with the presence of the Fermi surface of composite fermions [5].

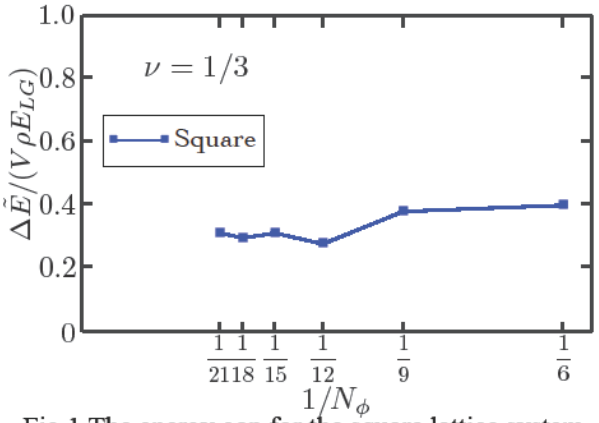

Fig.1 The energy gap for the square lattice system where N_ϕ is the Landau degeneracy, V is the strength of the nearest-neighbor interaction, ρ is the number of the particles per site, and E_{LG} is the lowest energy gap of the one-particle spectrum [3].

References

[1] Q. Niu, D. J. Thouless and Y.-S. Wu, Phys. Rev. B **31**, 3372 (1985).
[2] Y. Hamamoto, H. Aoki and Y. Hatsugai, Phys. Rev. B **86**, 205424 (2012).
[3] K. Kudo, T. Kariyado, and Y. Hatsugai, in preparation
[4] T. Fukui, Y. Hatsugai and H. Suzuki, J. Phys. Soc. Jpn. **74**, 1674 (2005).
[5] B. I. Halperin, P. A. Lee, and N. Read, Phys. Rev. B **47**, 7312 (1993).

Thermopower and Nernst measurements in a half-filled lowest Landau level

Xiaoxue Liu[1], Tingxin Li[2], Po Zhang[1], Loren Pfeiffer[3],
Ken West[3] and Rui-Rui Du[2,1]
[1]Peking University [2]Rice University [3]Princeton University

Recently Son presented a particle-hole symmetric (PHS) fermionic quasiparticle theory for half-filled lowest Landau level - massless Dirac composite fermions (DCF) [1]，which is different from the PHS broken HLR theory [2]. Subsequently, thermoelectric transport experiments were proposed to differentiate the DCF and HLR [3]. Motivated by this, we systematically study the electric and thermoelectric properties of v = 1/2 and 3/2 in high-mobility GaAs/AlGaAs 2DEGs. In this poster，preliminary results will be presented.

[1] Dam Thanh Son, Phys. Rev. X 5, 031027 (2015).
[2] B. I. Halperin, P. A. Lee, and N. Read, Phys. Rev. B 47, 7312 (1993).
[3] Andrew C. Potter, Maksym Serbyn, and Ashvin Vishwanath, Phys. Rev. X 6, 031026 (2016).

Quantum Statistics and Many-Body Correlations in the Lowest Landau Level

P. Łydżba and J. Jacak
Department of Fundamental Problems of Technology,
Wrocław University of Science and Technology,
Wyb. Wyspiańskiego 27, 50-370 Wrocław, Poland,
patrycja.lydzba@pwr.edu.pl

Most of interesting effects are manifested in many-body systems, especially those with strong correlations between particles. Therefore, it should come as no surprise that quantum Hall devices – with an incomparable hierarchy of incompressible states – continue to serve as a source of new, intriguing observations.

We demonstrate that the uniqueness of fractional quantum Hall phases is revealed, inter alia, in the exchange symmetry of many-body wave functions, Ψ_N. We recall that the statistics of particles – which follows from the quantum indistinguishability – determines the phase acquired by Ψ_N after its arguments complete an exchange trajectory in the configuration space, Ω. Furthermore, the statistics of particles is defined as a one-dimensional unitary representation (1DUR) of the full braid group ($\pi_1(\Omega)$). As a result, any modification of $\pi_1(\Omega)$ is simultaneously reflected in the exchange symmetry of many-body wave functions [1].

It can be shown that the quantizing magnetic field in 2D manifolds restricts $\pi_1(\Omega)$, since not all equivalence classes are accessible. Particles can develop a collective state in this system only if remaining braids can be organized into a new braid group (Ω stays connected). Using this assumption we can establish the hierarchy of collective states, which nicely agrees with the observed hierarchy of quantum Hall states.

What is by far more interesting, the mentioned alteration of $\pi_1(\Omega)$ instantly modifies the quantum statistics, and for non-Laughlin fillings weakens the anti-symmetry requirement typically imposed on fermionic wave functions. We put forward Ψ_N that transform in agreement with these unusual 1DURs [2]. We compare them with Laughlin wave functions (and point out differences in particle correlations).

The support from two NCN Projects UMO-2011/02/A/ST3/00116 and 2016/21/D/ST3/00958 is acknowledged.

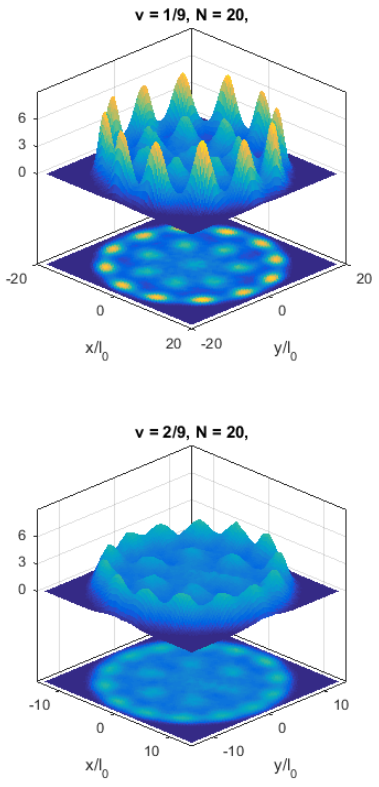

Fig.1 Correlations between 20 particles for ν=1/9 (top) and ν=2/9 (bottom). We consider a disc geometry.

References

[1] T. Einarsson, Phys. Rev. Lett. **64**, 17 (1995),
[2] P. Łydżba, J. Jacak, Proc. R. Soc. A **473**, 2197 (2017).

Unconventional Fractional Quantum Hall Effect in Bilayer Graphene

P. Łydżba and J. Jacak
Department of Fundamental Problems of Technology,
Wrocław University of Science and Technology,
Wyb. Wyspiańskiego 27, 50-370 Wrocław, Poland,
patrycja.lydzba@pwr.edu.pl

Recent progress in Hall measurements employing boron nitride encapsulated bilayer graphene samples [1], together with the former technique utilizing suspended bilayer graphene samples [2] allowed for an observation of the fractional quantum Hall effect (FQHE) in all four subbands of the lowest Landau level (with n=0 and n=1), and in several succeeding subbands (with n=2). Many observed features go beyond local quantum mechanics in an unusual manner, different than described by models implemented earlier to monolayer graphene [3]. We are able to explain this uniqueness of correlated multi-particle states in bilayer systems in the framework of the topological approach, which comprises both the composite fermion model, and its generalization.

We identify topological features which are different in bilayer systems when compared to monolayer graphene, or conventional 2DEG. The analysis of these differences allowed us to develop the dedicated nonlocal approach to bilayer graphene, which predicts the hierarchy of correlated multi-particle states in consistence with the experimentally observed FQHE fractions in all Landau subbands (up to n=2), including those believed to be controversial. In particular, we have explained an interesting experimental observation that the Hall state at half-filling, $\nu=-1/2$, manifested by suspended samples [2], disappears in samples supported by a boron nitride substrate [1]. The origin of this behavior can be identified with the manner in which 2xSU(4) degeneracy is lifted within the lowest Landau level (connected with the filling order of n=0 and n=1 subbands). The latter is, inter alia, influenced by the substrate of a Hall device.

The support from two NCN Projects UMO-2011/02/A/ST3/00116 and 2016/21/D/ST3/00958 is acknowledged.

References

[1] D. K. Ki, V. I. Falko, D. A. Abanin,& A. Morpurgo, Nano Lett. **14**, 2135 (2014),
[2] F. Amet et al., Nature Comm. **7**, 13908 (2016),
[3] P. Łydżba, L. Jacak, & J. Jacak, Sci. Rep. **5**, 14287 (2015).

Wigner Crystal of AlAs 2D Electrons near ν = 1/3

Meng K. Ma, Md. Shafayat Hossain, L. N. Pfeiffer, K. W. West, K. W. Baldwin & M. Shayegan
Department of Electrical Engineering, Princeton University, Princeton, NJ, 08544, USA
mengm@princeton.edu

We report the observation of a correlated phase of 2D electrons confined to an AlAs quantum well (QW), manifested by an insulating behavior at low temperatures near filling factor $\nu = 1/3$.

Our magnetotransport experiments are performed on an 11.3-nm-wide AlAs QW, containing 2D electrons with density, $n = 2.8\times10^{11}$ cm^{-2} and $\mu = 17$ m^2/Vs. In the absence of strain, 2D electrons in such a QW occupy two in-plane valleys. However, because of large residual strain during sample cool-down, only one of the in-plane valleys is occupied in our measurements.

As demonstrated in Fig. 1, this single-valley AlAs 2D electron system (2DES) exhibits an insulating phase between $\nu = 2/5$ and 1/3. The presence of the many-body fractional quantum Hall (FQH) states at $\nu = 2/5$ and 1/3 suggest that the insulating phase in between is a manifestation of a correlated phase of electrons, likely a Wigner crystal (WC) which is pinned by the ubiquitous disorder potential. This is similar to the WC reported in the case of GaAs 2DES, except that the insulating phase for the latter is observed near $\nu = 1/5$ [1-3] rather than $\nu = 1/3$. In a single-valley AlAs 2DES, thanks to the larger effective mass ($m^* = 0.45m_e$), the Landau level (LL) separation [$\hbar\omega_c = \hbar eB/m^* = (2\pi\hbar^2/m^*)n/\nu$] is small compared to the Coulomb energy $E_C = [e^2\sqrt{\pi n}/(4\pi\epsilon\epsilon_0)]$, leading to substantial LL mixing. In our AlAs 2DES, $E_C/\hbar\omega_c$ is indeed very large ($\approx$ 9). Such a significant LL mixing can favor the WC state over the FQH liquid, thus shifting the onset of the WC formation to the relatively large filling factor $\nu = 1/3$ (compared to $\nu = 1/5$ for GaAs 2D electrons). This observation is similar to the WC phases reported for low-density GaAs 2D *hole* systems of similar $E_C/\hbar\omega_c$ [4-5].

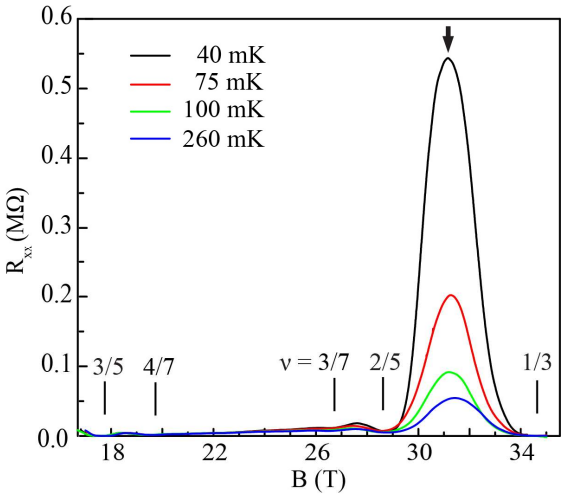

Fig. 1 Magnetoresistance trace for a single-valley 2DES with $n = 2.8 \times 10^{11}$ cm^{-2} confined to an 11.3-nm-wide AlAs QW. Between $\nu = 2/5$ and 1/3, an insulating phase (marked with an arrow)

References

[1] E. Y. Andrei *et al.*, Phys. Rev. Lett. **60**, 2765 (1988).
[2] H. W. Jiang *et al.*, Phys. Rev. Lett. **65**, 633 (1990).
[3] V. J. Goldman *et al.*, Phys. Rev. Lett. **65**, 2189 (1990).
[4] M. B. Santos *et al.*, Phys. Rev. Lett. **68**, 1188 (1992).
[5] M. B. Santos *et al.*, Phys. Rev. B **46**, 13639 (1992).

Photoluminescence Investigation of a Quantum Hall Skyrmion Transition

J. N. Moore[1], J. Hayakawa[1], H. Iwata[1], T. Mano[2], T. Noda[2], G. Yusa[1,*]
[1]*Department of Physics, Tohoku University, Sendai 980-8578, Japan*
[2]*National Institute for Materials Science, Tsukuba, Ibaraki 305-0047, Japan*
*yusa@m.tohoku.ac.jp

In the quantum Hall regime of 2D electrons, when the number of fully occupied Landau levels ν is slightly greater than or slightly less than unity, there exist topologically nontrivial spin textures called skyrmions [1]. Strong early evidence for skyrmions came from the observation of rapid nuclear spin depolarization [2] above and below $\nu = 1$ in agreement with predictions based on the Nambu-Goldstone mode of spin waves [3]. Theoretical treatments of skyrmions identify no major differences between the behaviors of skyrmions of opposite sides of $\nu = 1$; yet, experimentally skyrmion physics shows signs of asymmetry across $\nu = 1$ in, for example, the nuclear spin relaxation time [4] T_1.

Here we present further evidence of skyrmion asymmetry observed in the photoluminescence (PL) spectrum of GaAs quantum wells using a previously reported microscopy technique [5]. The onset of skyrmions coincides with an increase in the intensity of PL produced by singlet spin state trions (Fig.1), which we believe is due to the decreased degree of electron polarization. As skyrmions emerge, the PL intensity changes significantly more sharply for $\nu > 1$ than for $\nu < 1$ over a wide range of magnetic field. To confirm that skyrmions are the cause of the sharp change in PL intensity, we optically performed local measurements of T_1 on both sides of the PL transition (Fig.1 inset). We also performed spatial mapping of the PL intensity across $\nu = 1$, which which reveals asymmetry in the width of the PL intensity distribution and suggests non-uniformity in the concentration of skyrmions.

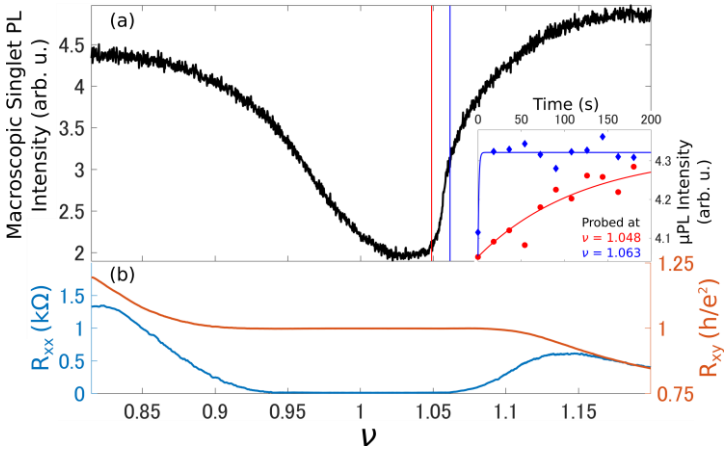

Fig.1 (a) Integrated intensity of the singlet PL peak as a function of the Landau-level filling factor at temperature ~50 mK, magnetic field 7 T. Inset: Singlet micro PL intensity measured as a function of the time of relaxation slightly above $\nu = 1$ fitted to $-0.27\exp(-t/T_1) + 4.3216$, where $T_1 = 120$ s and 1 s for $\nu = 1.048$ and 1.063 respectively. (b) Longitudinal and Hall resistance over the same filling factor range.

References

[1] S. L. Sondhi, A. Karlhede, and S. A. Kivelson, Phys. Rev. B **47**, 16419 (1993).

[2] K. Hashimoto, K. Muraki, T. Saku, and Y. Hirayama, Phys. Rev. Lett. **88**, 176601 (2002).

[3] R. Côté et al., Phys. Rev. Lett. **78**, 4825 (1997).

[4] T. Guan et al., Chin. Phys. B **24**, 067302 (2015).

[5] J. N. Moore, J. Hayakawa, T. Mano, T. Noda, and G. Yusa, Phys. Rev. Lett. **118,** 076802 (2017).

Composite Fermions on Torus

Songyang Pu and J. K. Jain
Physics Department, Penn State University, University Park, PA 16803, USA
sjp5650@psu.edu

The fractional quantum hall effect has been well explained in terms of composite fermions. In particular, the composite fermion theory gives wave functions that allow detailed calculations of various experimentally relevant quantities. While wave functions of composite fermions at filling factors of the form $\frac{n}{2pn\pm1}$ have been constructed in the disk and spherical geometries, it has not been possible to construct them, so far, on the torus geometry. We show how these wave functions can be constructed on torus, with lowest Landau level projection accomplished through the Jain-Kamilla trick. To demonstrate the validity of our construction, we explicitly evaluate the pair correlation function and the Coulomb energy for the 2/5 state.

This work is supported in part by the US National Science Foundation Grant no. DMR-1401636.

Metrics of 2DEG Quality at T=0.3K Useful to Predict the Strength of the ν=5/2 Fractional Quantum Hall State

Q. Qian[1], J. Nakamura[1], S. Fallahi[1,3], G. Gardner[2,3,4], G. A. Csáthy[1], and M. J. Manfra[1,2,3,4,5]

[1]*Department of Physics and Astronomy, Purdue University, West Lafayette, IN 47907, USA*

[2]*Station Q Purdue, Purdue University, West Lafayette, IN 47907, USA*

[3]*Birck Nanotechnology Center, Purdue University, West Lafayette, IN, 47907 USA*

[4]*School of Materials Engineering, Purdue University, West Lafayette, IN, 47907 USA*

[5] *School of Electrical and Computer Engineering, Purdue University, West Lafayette, IN 47907 USA*

qianq@purdue.edu

Recently effort has been put toward the study of the fractional quantum Hall state (FQHS) at filling factor ν = 5/2. This state is proposed to support non-Abelian excitations, which could be used to realize topological quantum computing [1]. However, this state is fragile and only exists in the highest quality two-dimensional electron gases (2DEGs). Traditionally, low temperature mobility has been used as the primary metric of 2DEG quality, but a large body of experimental evidence has shown that mobility does not encode all information needed to predict high-field behavior of FQHSs at low temperatures, including the energy gap at ν = 5/2, $\Delta_{5/2}$ [2].

We define, analyze and discuss the utility of a different metric, the resistivity $\rho_{5/2}$ at ν = 5/2, as a high temperature (T = 0.3K) predictor of $\Delta_{5/2}$. We assumed that at T = 0.3K, a Fermi sea of composite fermions forms at ν = 5/2, and measured this high field resistivity analogously to the zero field resistivity. In Fig. 1(a) we present the dependence of $\rho_{5/2}$ (left axis) and $\Delta_{5/2}$ (right axis) versus *n* of an *in situ* back gated GaAs 2DEG. As *n* increases, $\Delta_{5/2}$ increases and $\rho_{5/2}$ decreases. We observe a correlation between $\rho_{5/2}$ and $\Delta_{5/2}$ in this density tunable device.

In Fig. 1(b) we present $\Delta_{5/2}$ versus $1/\rho_{5/2}$ for a series of samples with the same heterostructure design: a symmetrically doped GaAs quantum well with density *n* = 3.0 x 10^{11} cm^{-2}. Here we also observe that $\Delta_{5/2}$ increases as $\rho_{5/2}$ decreases. Our results suggest a strong correlation between $\rho_{5/2}$ and $\Delta_{5/2}$. Therefore, we propose to use $\rho_{5/2}$ to assess 2DEG quality at T = 0.3K. The physical basis for this correlation will be discussed.

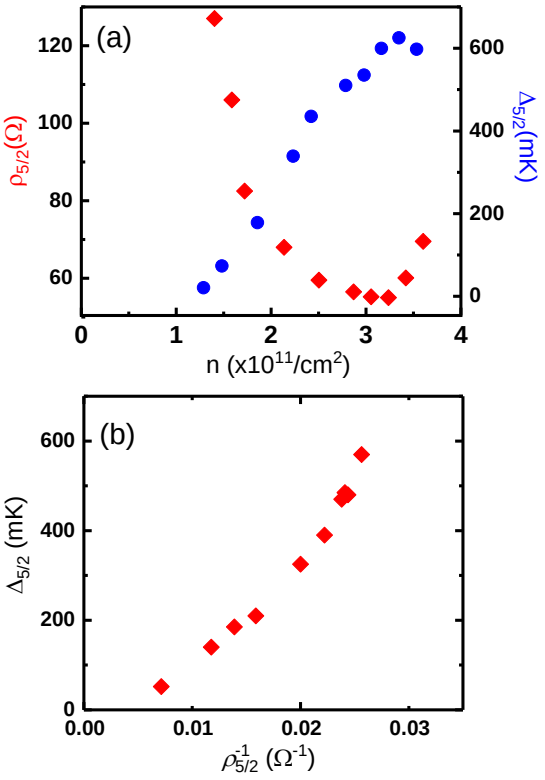

Fig. 1: (a) $\rho_{5/2}$ (left axis) and $\Delta_{5/2}$ (right axis) vs *n* of an *in situ* back gated sample. (b) $\Delta_{5/2}$ vs $1/\rho_{5/2}$ for samples with same heterostructure.

References

[1] S. D. Sarma *et al*., Phys. Rev. Lett. **94**, 166802 (2005).

[2] NP Deng *et al*., Phys. Rev. Lett. **112**, 116804 (2014).

Effect of density on quantum Hall stripe orientation in tilted magnetic fields

Q. Shi[1], M. A. Zudov[1,*], Q. Qian[2], J. D. Watson[2], and M. J. Manfra[2,3]
[1]*School of Physics and Astronomy, University of Minnesota, Minneapolis, MN 55455, USA*
[2]*Department of Physics and Astronomy and Birck Nanotechnology Center, Purdue University, West Lafayette, Indiana 47907, USA*
[3]*Station Q Purdue, School of Materials Engineering, and School of Electrical and Computer Engineering, Purdue University, West Lafayette, Indiana 47907, USA*
*zudov@physics.umn.edu

Quantum Hall stripes represent one class of exotic states that appear in high Landau levels of a two-dimensional electron gas (2DEG) at low temperatures [1]. An in-plane magnetic field $B_{||}$ can modify their orientation and, according to a "standard picture", stripes perpendicular to $B_{||}$ are favored in single-subband systems [2]. However, a few experiments revealed limitations of this "standard picture" and found that $B_{||}$ can render stripes parallel to it [3]. To shed light onto the nature of this parallel stripe alignment, it is desirable to identify a tuning parameter that would enable one to control stripe orientation under $B_{||}$.

Here, we investigate quantum Hall stripes under $B_{||}$ in a variable-density 2DEG. At filling factor $\nu = 9/2$, we observe one, two, and zero $B_{||}$-induced reorientations at low, intermediate, and high densities n_e, respectively (see Fig. 1). Appearance of these distinct regimes owes to a strong density dependence of the $B_{||}$-induced orienting mechanism which triggers the second reorientation, rendering stripes parallel to $B_{||}$. In contrast, $B_{||}$ needed to reorient stripes perpendicular to it showed no noticeable dependence on n_e. Measurements at $\nu = 9/2$ and 11/2 at the same, tilted magnetic field, allows us to rule out density dependence of the native symmetry-breaking field as a dominant factor. Our further analysis suggests that screening might play an important role in determining stripe orientation and provide guidance to future studies.

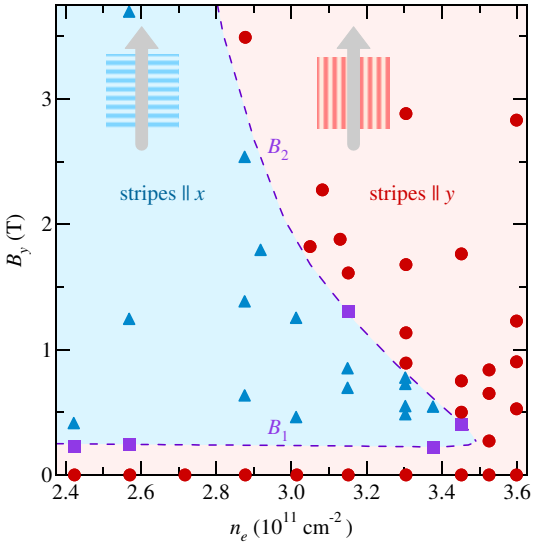

Fig. 1. Orientation of stripes vs n_e and B_y at $\nu = 9/2$. Triangles (circles) mark stripe orientation perpendicular (parallel) to $B_{||} = B_y$. Squares mark isotropic states. The phase boundary (dashed line) is a guide to eyes.

References

[1] A. A. Koulakov, M. M. Fogler, and B. I. Shklovskii, Phys. Rev. Lett. **76**, 499 (1996); M. P. Lilly, K. B. Cooper, J. P. Eisenstein, L. N. Pfeiffer, and K. W. West, Phys. Rev. Lett. **82**, 394 (1999); R. R. Du, D. C. Tsui, H. L. Stormer, L. N. Pfeiffer, K. W. Baldwin, and K. W. West, Solid State Commun. **109**, 389 (1999).

[2] W. Pan, R. R. Du, H. L. Stormer, D. C. Tsui, L. N. Pfeiffer, K. W. Baldwin, and K. W. West, Phys. Rev. Lett. **83**, 820 (1999); M. P. Lilly, K. B. Cooper, J. P. Eisenstein, L. N. Pfeiffer, and K. W. West, Phys. Rev. Lett. **83**, 824 (1999); T. Jungwirth, A. H. MacDonald, L. Smrcka, and S. M. Girvin, Phys. Rev. B **60**, 15574 (1999).

[3] J. Zhu, W. Pan, H. L. Stormer, L. N. Pfeiffer, and K. W. West, Phys. Rev. Lett. **88**, 116803 (2002); H. Zhu, G. Sambandamurthy, L. W. Engel, D. C. Tsui, L. N. Pfeiffer, and K. W. West, Phys. Rev. Lett. **102**, 136804 (2009); Q. Shi, M. A. Zudov, J. D. Watson, G. C. Gardner, and M. J. Manfra, Phys. Rev. B **93**, 121411(R) (2016).

Transference of Fermi contour anisotropy to composite fermions

K. A. Villegas Rosales[1], I. Jo[1], M. A. Mueed[1], L. N. Pfeiffer[1], K. W. West[1], K. W. Baldwin[1], R. Winkler[2], Medini Padmanabhan[3], and M. Shayegan[1]
[1]*Department of Electrical Engineering, Princeton University, Princeton, NJ 08544, USA*
[2]*Department of Physics, Northern Illinois University, DeKalb, IL 60115, USA*
[3]*Physical Sciences Department, Rhode Island College, Providence, RI 02908, USA*
kavr@princeton.edu

There has been a surge of recent interest in the role of anisotropy in interaction-induced phenomena in a two-dimensional (2D) charged carrier system, such as the fractional quantum Hall effect (FQHE) and composite fermions (CFs) [1-5]. The fundamental question we address here is how the anisotropy of the band structure of the low-field carriers transfers to the interacting particles at high magnetic fields, particularly to CFs. We present a study of tunable Fermi contour anisotropy in GaAs 2D hole system via the application of in-plane strain. We experimentally measure the anisotropy for both low-field holes (fermions) and hole-flux CFs at high fields and find a simple quantitative relation for how the anisotropy is transferred to the CFs.

Figure 1(a) shows the calculated Fermi contours at a density of 1.8×10^{11} cm^{-2} under various strain values applied along the $[\bar{1}10]$ direction. Without strain ($\epsilon = 0$) the spin-split Fermi contours show a four-fold symmetry and thus the Fermi wavevectors along $[110]$ and $[\bar{1}10]$ are the same. For tensile ($\epsilon > 0$) strain, the Fermi contours become elongated along the $[\bar{1}10]$ direction while they contract along $[110]$. Compressive strain ($\epsilon < 0$) results in the opposite effect.

We investigate the strain-induced Fermi contour anisotropy with the experimental set-up of Fig. 1(b). A thinned GaAs sample etched into an L-shaped Hall bar is glued on a cryogenic piezo-actuator, which serves to apply strain to the sample. The periodic grating of a negative e-beam resist patterned on the surface leads to a small potential modulation of the 2D holes via the piezoelectric effect. Because of the potential modulation, commensurability oscillations appear in the magnetoresistance from which the Fermi wavevectors are determined.

Our data reveal that the Fermi wave vector anisotropy of CFs equals *square-root* of the anisotropy for the zero-field holes [4]. This finding is in excellent agreement with the results of very recent numerical calculations [5]. We also measure the energy gap of the ν=2/3 state at various anisotropy values. The results reveal that the FQHE gap is essentially unaffected by the large anisotropy, up to 3.3, equivalent to a mass anisotropy of 11 in a parabolic band, suggesting that the FQHE is robust against the anisotropy.

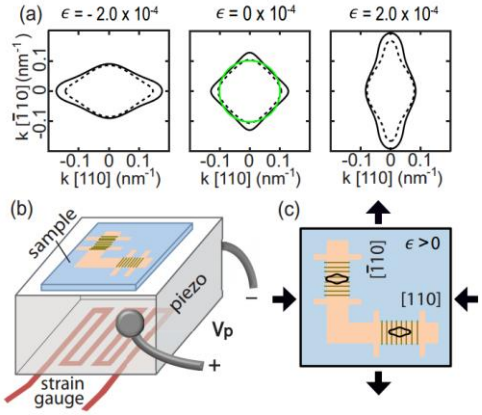

Fig. 1 (a) Calculated Fermi contours of GaAs 2D holes as a function of strain (ϵ) along the $[\bar{1}10]$ direction. (b) Experimental schematic showing the GaAs sample glued to a piezo-actuator. (c) The shapes of the real-space cyclotron orbits are depicted by black curves for $\epsilon > 0$. Periodic gratings patterned on the surface yield commensurability oscillations, providing the Fermi wavevectors along two perpendicular directions.

[1] T. Gokmen, Medini Pagmanabhan, and M. Shayegan, Nat. Phys. **6**, 621-624 (2010).
[2] F. D. M. Haldane, Phys. Rev. Lett. **107**, 116801 (2011).
[3] A. C. Balram and J. K. Jain, Phys. Rev. B **93**, 075121 (2016).
[4] I. Jo *et al.*, arXiv.1701.06684 (2017).
[5] M. Ippoliti, S. Geraedts, and R. N. Bhatt, arXiv.1701.07832 (2017).

Exact diagonalization quest for Jack ground states in fractional quantum Hall effect

Bartosz Kuśmierz, Paweł Potasz, and Arkadiusz Wójs
Department of Theoretical Physics, Wrocław University of Science and Technology
Wybrzeże Wyspiańskiego 27, 50-370 Wrocław, Poland

The Coulomb interaction among quasi-two-dimensional (2D) electrons in a strong perpendicular magnetic field induces various, sometimes complicated correlations, depending primarily on Landau level (LL) filling factor ν (dimensionless ratio of electron and magnetic flux densities), but also on the details of the Coulomb interaction pseudopotential, depending on the material (e.g., GaAs vs graphene) and the LL index, and tunable by the width of the 2D layer. These correlations can be accurately and elegantly described in terms of different variants of composite fermions (CFs), which are topological bound states of the electrons and vortices of the complex polynomial many electron wave function. For example, the $\nu = 1/3$ Laughlin liquid corresponds to a completely filled LL of identical and essentially noninteracting CFs. Remarkably, some of the correlated CF phases can also be generated by the appropriate simple multi-particle (i.e., more than two-body) interactions. For example, the $\nu = 5/2$ "Pfaffian" state, which can be viewed as either Bose condensate of identical *p*-wave paired CFs in effectively vanishing magnetic field or a dual partition of noninteracting CFs completely filling a LL, is an exact eigenstate of the three-body contact repulsion.

Emergence of the relevant (i.e., Coulomb) many-electron ground states from particularly simple many-body interactions (very different from the pair Coulomb repulsion) is essential for the relevance of the so-called Jack symmetric polynomials in analytical construction of those states and their elementary excitations [1].

In this work we use configuration interaction method to numerically generate Coulomb ground states of fairly large N-electron systems in Haldane spherical geometry, representing filling factors $\nu = K/(K+2)$ (i.e., $\nu = 1/3, 2/4, 3/5, \ldots$, for $K = 1, 2, 3, \ldots$), compare them with exact ground states of the relevant model interaction (i.e., the $(K+1)$-particle contact repulsion) which is generated analytically from the Jack polynomials, and present their interpretation in terms of multi-flavored CFs (i.e., divided into K distinct partitions) [2]. We also discuss the relevance for the fractional quantum Hall state at $\nu = 12/5$ (particle-hole conjugate of the $K=3$ state in the first excited LL) which supports nonabelian "Fibonacci anyon" quasiholes obeying sufficiently complex braiding rules to (hypothetically) allow topological quantum computation.

In particular, we present a simple formula for an approximate two-body repulsion pseudopotential generating the near exact Jack state at $\nu = K/(K+2)$, i.e., an exact ground state of a contact $(K+1)$-body repulsion. Interestingly, the range of the approximate pair pseudopotential increases regularly with K of the many-body interaction is it mimicking.

We also generated detailed maps of ground states of arbitrary short-range pair pseudopotentials at various filling factors corresponding to several principal Jack ground states, and thus showed which of these Jacks can emerge as electronic Coulomb ground states in GaAs or graphene, in various LLs, also as a function of the GaAs layer width.

References

[1] B. A. Bernevig and F. D. M. Haldane, Phys. Rev. Lett. **100**, 246802 (2008).
[2] G. J. Sreejith, C. Tőke, A. Wójs, and J. K. Jain, Phys. Rev. Lett. **107**, 086806 (2011).

Quantum Hall Nematics on the Surface of Bismuth

Fengcheng Wu[1,*] and Allan H. MacDonald[2]
1. Materials Science Division, Argonne National Laboratory, Argonne, IL 60439, USA
2. Department of Physics, University of Texas at Austin, Austin, TX 78712, USA
* wufcheng@gmail.com

Electronic surface states on bismuth (111) surface host six anisotropic hole pockets that are related by three-fold rotational symmetry. In a strong magnetic field, various types of quantum Hall ferromagnetism can occur when multiplets of Landau levels associated with the hole pockets are partially filled. A quantum Hall nematic state, which spontaneously breaks the lattice discrete rotational symmetry, has recently been observed using scanning tunneling microscope spectroscopy[1]. Motivated by the experiment, we will present a theory of quantum Hall ferromagnetism on the surface of bismuth. We will highlight the importance of the spin structure of Landau level wave functions due to strong spin-orbit coupling, and show that the spin structure can enable the observation of a valley-coherent quantum Hall state. Finally we will discuss prospects for observing similar physics in other multi-valley low-dimensional electron systems.

References

[1] Benjamin E. Feldman, Mallika T. Randeria, Andras Gyenis, Fengcheng Wu, Huiwen Ji, R. J. Cava, Allan H. MacDonald, Ali Yazdani, Science **354**, 6310 (2016).

Liquid crystal phase diagram in high magnetic fields: Effect of Landau level mixing

Jianyun Zhao, Yuhe Zhang, and Jainendra K. Jain,
Physics Department, Penn State University,
University Park, PA 16803, USA
jxz233@psu.edu

The 2D crystal phase of electrons in high magnetic fields has been of longstanding interest. There is experimental evidence that the phase boundary separating it from the fractional quantum Hall liquid is sensitive to Landau level mixing. We investigate this issue using the diffusion Monte Carlo (DMC) method, which treats Landau-level mixing in a nonperturbative manner and has proved quantitatively accurate in the determination of the spin phase transition [2]. Specifically, we predict the Landau level mixing parameter where the crystal phase is stabilized at 1/3, 2/5, 1/5 and 2/9. We find that the crystals of composite fermions [1] are favored in the vicinity of filling factor 1/5. We compare our results to experimental studies.

References

[1] A. Archer, K. Park, J. Jain, PRL 111, 146804 (2013).
[2] Y. Zhang, A. Wojs, J. Jain, PRL 117, 116803 (2016).

Numerical investigation on ground states of the ν=2/3 bilayer fractional quantum Hall systems

Y. D. Zheng [1, 2], A. Sawada [2], Z. F. Ezawa [2], J. Hirotsuji [1], T. Sorita [1]

[1]*Research and Development Department, Mitsubishi Electric (China) Company Limited, Shanghai 200336, P. R. C.*

[2]*Research Center for Low Temperature and Materials Sciences, Kyoto University, Kyoto 606-8501, Japan*

Email: zhengyd09@163.com

In the bilayer Quantum Hall (QH) systems with both spin and layer (pseudospin) degrees of freedom, four sub-energy levels are formed in the lowest Landau level (LLL), and the ground states are to be determined by various factors such as interlayer/intralayer Coulomb energies (Δ_C), Zeeman energy (Δ_Z), interlayer tunneling energy (Δ_{SAS}) and bias energy (Δ_{bias}), etc. The bilayer QH systems with filling factor $\nu=2/m$ should be of the same type for any odd integer m. Up to now, most of theoretical studies have focused on the $\nu=2$ bilayer integer QH systems [1]. While the $\nu=2/3$ bilayer QH system is a typical fractional QH system of this type, and can be regarded as a best example of the strongly correlated 2D electron system for investigating the interplay of those entangled energy factors indicated above. However, even the basic problems, the ground states and the basic phase diagram of the $\nu=2/3$ system are almost left uninvestigated from the theoretical viewpoint [2].

We report on some basic features of the ground states in the $\nu=2/3$ bilayer QH systems at the layer balanced point ($\Delta_{bias}=0$) and provide evidential quantitative results from exact-diagonalization (ED) [3] numerical calculations and an exactly solvable model carried out at $\nu=2/3$ [4]. We choose a finite size system (4 electrons) with rectangular geometry for ED calculations. Within the LLL, the Hamiltonian is described by $H=H_t+H_Z+H_{int}$, where H_t, H_Z, and H_{int} represent the interlayer tunneling energy, Zeeman energy and two-body Coulomb interaction energy terms, respectively. In the numerical results, the length unit is the magnetic length l_B and the energy unit is Coulomb energy scale $E_C=e^2/4\pi\varepsilon l_B$. Fig.1 illustrates the low-lying energy spectrum of finite size $\nu=2/3$ systems for Δ_{SAS} = 0.006, Δ_Z=0.05 at the fixed layer separation $d = l_B$. The degeneracy of the ground states occurs depending on the difference between intralayer and interlayer Coulomb energies, when Δ_{SAS} gets close to zero. Fig.2 shows image plot of energy gaps E_{gap} between the lowest first and second eigenstates of the $\nu=2/3$ systems. This is also regarded as the phase diagram in the Δ_{SAS}-Δ_Z plane, symbols SP, SU and CR denote the spin polarized, unpolarized phases and the crossover region, respectively. The transitions between SP and SU phases are mainly determined by the competition between Δ_Z and Δ_C. We also compare the numerical results with the experimental data (points A, B) and acquire a good agreement [5,6].

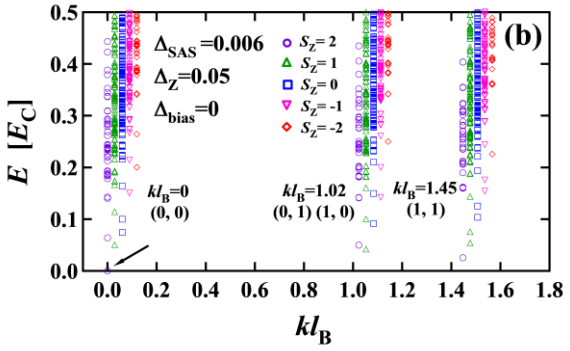

Fig.1 Energy spectrum of finite size $\nu=2/3$ bilayer QH systems (4 electrons) for Δ_{SAS} = 0.006, Δ_Z=0.05 at $d = l_B$.

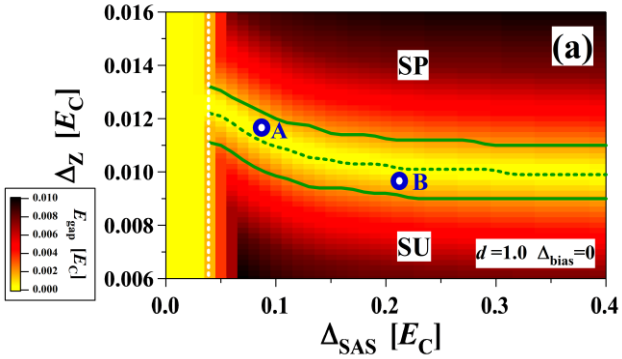

Fig.2 Image plot of energy gaps E_{gap} between the lowest first and second eigenstates in Δ_{SAS}-Δ_Z plane (phase diagram).

References

[1] S. Das Sarma *et al*., Phys. Rev. **B 58**, 4672 (1998).

[2] I. A. McDonald *et al*., *Phys. Rev.* **B 53**, 15845 (1996).

[3] D. Yoshioka *et al*., *Phys. Rev. Lett.* **50**, 1219 (1983).

[4] Y. D. Zheng *et al*., Solid State Commun. **155**, 82-87 (2013).

[5] N. Kumada *et al*., *Phys. Rev. Lett.* **89**, 116802 (2002).

[6] Y. D. Zheng *et al*., Phys. Rev. **B 83**, 235330 (2011).

Quantum Hall Effect in Bilayer Graphene

Jing Li and Jun Zhu
Physics Department, Penn State University,
University Park, PA 16802, USA
jxz26@psu.edu

The integer quantum Hall effect of bilayer graphene proves to be a fertile playground to explore the phenomena of quantum Hall ferromagnetism. The physics of the N=0 and 1 Landau levels (LLs) is particularly rich, owing to the eight-fold degeneracy resulting from the spin, orbital isopin and valley degrees of freedom in bilayer graphene. External knobs, such as a perpendicular electric field and a tilted magnetic field, can break the symmetry of the system in a controlled fashion and consequently a rich variety of many-body ground states including a putative canted anti-ferromagnet, and a quantum spin Hall liquid have been observed. Despite many efforts, a general LL diagram of this system is notably missing. Here, we have constructed an empirical LL diagram of bilayer graphene in the presence of an electric field. Interaction effects are parameterized to yield an effective single-particle diagram. It captures the collapse of the ν=0 and 1 gaps at all magnetic fields and provides a rational framework to interpret a diverse body of experiments in the literature. It could serve as a starting point to explore the more nuanced effects of electron-electron interactions. In a separate project, we demonstrate controlled tunneling of quantum Hall edge states in bilayer graphene between two lateral quantum Hall systems. A dual split gated structure enables us to independently control the filling factors of the quantum Hall systems, as well as the potential of the line junction separating them. We observe sequential pinch-off of individual edge states, which manifests as plateaus in the tunneling resistance measured across the line junction. The gate-controlled transmission of edge states is a first step towards realizing more sophisticated nanostructures that allow further explorations of the fascinating fractional quantum Hall states in bilayer graphene.

Microwave Absorption at the Edge of the Quantum Hall Systems

Akira Endo, Keita Koike, Shingo Katsumoto, and Yasuhiro Iye
Institute for Solid State Physics, The University of Tokyo
Kashiwanoha, Kashiwa, Chiba 277-8581, Japan
akrendo@issp.u-tokyo.ac.jp

Microwave transmission through a coplanar waveguide (CPW) placed on the surface of a two-dimensional electron gas (2DEG) wafer has been employed to investigate various properties of the underlying 2DEG. The conductivity of the 2DEG beneath the slots of the CPW can be deduced from the transmission, since the microwave absorption increases with the 2DEG conductivity. This is applied, for instance, to observe commensurability oscillations in the conductivity for a 2DEG subjected to a periodic modulation [1]. Microwave can also excite collective states, e.g., pinning modes of a Wigner crystal, which manifest themselves as resonant peaks in the microwave absorption [2]. In the present study, we explore microwave absorption at the edge of the quantum Hall states.

Edges were introduced to the slot regions by depleting the 2DEG below the central electrode of the CPW, applying a negative bias V_g via a bias-Tee coupling (Fig. 1). We measured microwave absorption of a 2DEG in the integer quantum Hall states as a function of the frequency f and V_g. An example for $\nu = 3$ is shown in Fig. 2. Sharp resonances, attributable to edge magnetoplasmons (EMP), emerge when the electrostatically defined edges are formed at $V_g \sim -0.4$ V (indicated by an arrow in Fig. 2). The resonance appears at a fundamental frequency f_0 and at its higher harmonics nf_0 (n: integer). With further decrease in V_g, the resonance frequencies increase, owing to the increase in the propagation velocity of the EMP following the increase in the steepness of the confining potential. Microwave resonances thus allow us to probe the potential landscape at the edges. In addition, small features are also observed, as marked by arrowheads in Fig. 2, when the upper Landau levels are emptied below the central electrode.

[1] A. Endo, T. Kajioka, and Y. Iye, J. Phys. Soc. Jpn. **82**, 054710 (2013).
[2] L. W. Engel, D. Shahar, C. Kurdak, and D. C. Tsui, Phys. Rev. Lett. **71**, 2638 (1993).

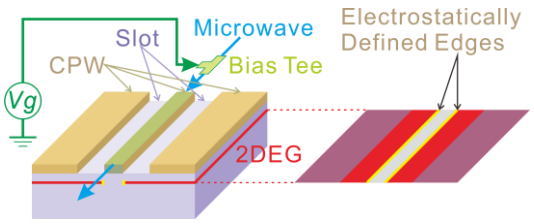

Fig.1 Schematic illustration of the measurement device. A negative bias V_g is applied to the central electrode to introduce edges to the slot regions.

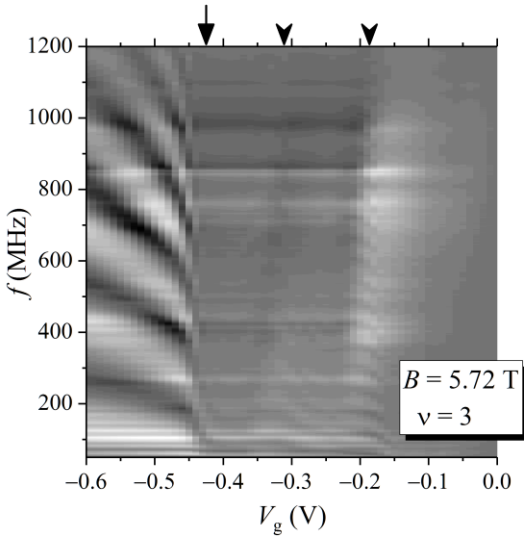

Fig. 2 Microwave absorption at $\nu = 3$ quantum Hall state, plotted in the V_g-frequency plane.

Lineshape of radiation-induced magnetoresistance oscillations under bichromatic photo-excitation in the GaAs/AlGaAs 2D electron system

B. Gunawardana,[1] H-C. Liu, [1] R.L. Samaraweera, [1] M.S. Heimbeck, [2] H.O. Everitt,[2,3] J. Iñarrea, [4] C. Reichl, [6] W. Wegscheider, [6] and R.G. Mani[1]

[1]*Department of Physics and Astronomy, Georgia State University, Atlanta, GA 30303, USA*

[2]*Army Aviation & Missile RD&E Center, Redstone Arsenal, Huntsville, AL 35898, USA*

[3]*Dept. of Physics, Duke University, Surham, NC 27708, USA*

[4]*Escuela Politécnica Superior, Universidad Carlos III, Leganes, Madrid, 28911, Spain*

[5]*Laboratorium für Festkörperphysik, ETH Zürich, CH-8093 Zürich, Switzerland*

kgunawardana1@student.gsu.edu

Photo-excited transport at large filling factors has been a topic of interest in the 2D electron system due in part to the microwave radiation-induced zero-resistance states and the associated 1/4-cycle phase shifted radiation-induced magnetoresistance oscillations observed under photoexcitation in a transverse magnetic field, B.[1] A subject in this area is the oscillatory photoresponse under bichromatic excitation. Previous work has suggested that the photo induced oscillatory response under bichromatic photo-excitation is approximately an average superposition of two monochromatic photo response.[2] In order to obtain a better understanding of such photo-excited transport, millimeter wave radiation-induced magneto-resistance oscillations are examined here under bichromatic excitation.

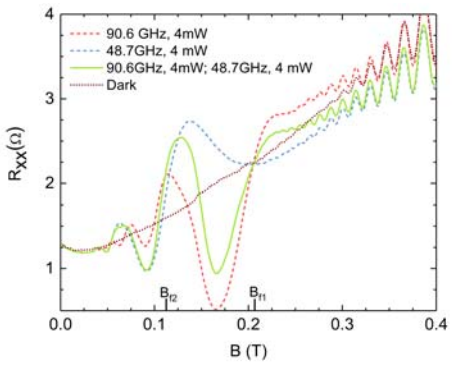

Fig. 1) Diagonal resistance, R_{xx} vs. the magnetic field, B, at f_1=90.6 GHz, f_2 = 48.7 GHz, f_1 AND f , and under dark conditions.

A GaAs/AlGaAs heterostructure device was illuminated by two different millimeter-wave sources simultaneously to compare the monochromatic and bichromatic response of the 2DES at liquid helium temperatures with frequencies f_1 AND f_2 showing ratios f_1/f_2 ranging from $1.84 \leq f_1/f_2 \leq 3.4$, such that the frequency ratios span both the situations where the two frequencies, and hence the associated oscillations, are close together and also when they are further apart on the B-scale. Fig. 1 exhibits typical data with $f_1 = 90.6$ GHz and $f_2 = 48.7$ GHz. Here, the monochromatic responses at both f_1 and f_2 are exhibited along with the bichromatic response at f_1 AND f_2, and the dark response. The results indicate that, generally, at low B, the bichromatic response is determined by the low frequency f_2 and the response shifts to the high frequency f_1 for $B > B_{f2}$, unlike expectations based on superposition. In this presentation, we report such results along with modeling for the observations.

[1] R.G. Mani, J.H. Smet, K. von Klitzing, V. Narayanamurti, W.B. Johnson and V. Umansky, Nature (London) **420**, 646 (2002); Phys. Rev. Lett. **92**, 146801 (2004).

[2] M. A. Zudov et al., Phys. Rev. Lett. **96**, 236804 (2006).

Study of Electron Heating via the Shubnikov-de Haas effect under a Current-bias in the High Mobility GaAs/AlGaAs Two Dimensional Electron System

C. Rasadi Munasinghe,[1] R. L. Samaraweera,[1] B. Gunawardana,[1] Zhuo Wang,[1] C. Reichl,[2]
W. Wegscheider,[2] and R. G. Mani,[1]
[1] *Department of Physics and Astronomy, Georgia State University, Atlanta, GA 30303, USA*
[2] *Laboratorium für Festkörperphysik, ETH Zürich, CH-8093 Zürich, Switzerland*
cmunasinghe1@student.gsu.edu

The high mobility GaAs/AlGaAs 2D electron system exhibits a fascinating Giant Magneto-resistance (GMR) effect at low magnetic fields, $B \leq 0.3$ T, and liquid helium temperatures.[1,2] For example, there is a device-size dependence for this GMR effect whereby smaller *mm*-scale devices exhibited a broader and deeper GMR at the lowest temperatures.[1] Most recently, it was shown that a supplemental current through the 2DES serves to provide an in-situ tunability of the magnitude of the GMR effect at a fixed temperature.[2] This feature has suggested that the GMR effect could be responsive to the heating of carriers. In order to investigate this possibility, we have studied the Shubnikov-de Haas effect in the ultra-high mobility (~ 10^7 cm^2/Vs) GaAs/AlGaAs 2DES as a function of both the bath temperature and the applied ac-current bias, I_{ac}. The SdH effect is well known for its utility in revealing the carrier mass, the Dingle temperature or single particle lifetime, and the shape of the Fermi surface.[3] Here, we utilize the SdH effect to extract the increase of the electron temperature above the bath temperature by following the variation in the SdH parameters with the I_{ac}.

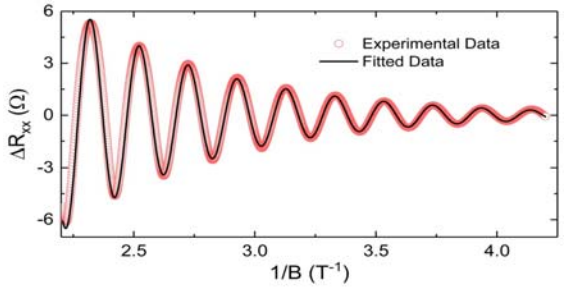

Fig.1: SdH oscillations in ΔR_{xx} at $I_{ac} = 2\mu A$ bias current and T = 1.673K vs. the inverse magnetic field, 1/B, and the numerical fit.

Thus, the background-subtracted longitudinal magnetoresistance (ΔR_{xx}) was obtained at different I_{ac} for $1.6K \leq T \leq 4.2K$, with the specimen immersed in pumped liquid Helium. I_{ac}-induced carrier-heating was investigated by fitting the SdH lineshape to the Lifshitz-Kosevich theory[4] as shown in Fig. 1. By observing the alteration in the amplitude of the SdH oscillations with I_{ac} at a constant temperature, we determine the elevated temperature of the carriers due to the increment of the current bias. Hence, the variation of the carrier temperature with the current bias was obtained.

References

[1] R. G. Mani, A. Kriisa, and W. Wegscheider, Sci. Rep. 3, 2747 (2013).
[2] Z. Wang, R. L. Samaraweera, C. Reichl, W. Wegscheider, and R. G. Mani, Sci. Rep. 6, 38516 (2016).
[3] A. N. Ramanayaka and R. G. Mani, Phys. Rev. B 83, 165303 (2011)
[4] H. Cao, J. Tian, I. Miotkowski, T. Shen, J. Hu, S. Qiao and Y. P. Chen, Phys. Rev. Lett. 108, 216803 (2012)

Possibility of Electron Heating Induced by Microwave Photo-excitation in the GaAs/AlGaAs 2D Electron System

Tharanga Nanayakkara, Rasanga Samaraweera, Zhuo Wang, Binuka Gunawardana, Rasadi Munasinghe, and Ramesh G. Mani
Department of Physics and Astronomy, Georgia State University, Atlanta, GA 30303

Christian Reichl and Werner Wegscheider
Laboratorium für Festkörperphysik, ETH-Zürich, 8093 Zürich, Switzerland

tnanayakkara1@student.gsu.edu

Theory has examined the possibility of electron heating by microwave photo-excitation in the large filling factor, low magnetic field limit in a balance-equation scheme that takes into account photon-assisted electron transitions as well as radiation-induced change of the electron distribution for high-mobility two-dimensional systems.[1] The results suggest that the electron temperature is a function of the magnetic field, the microwave intensity, and frequency, and it is determined by the balance between the energy absorption from the radiation field and the energy dissipation to the lattice through electron-phonon couplings. Such heating is thought to be manifested by microwave modulations of the Shubnikov–de Haas oscillation amplitude along with microwave-induced magnetoresistance oscillations.[1]

Experimentally, it is known that the Shubnikov de Haas (SdH) oscillation amplitude is sensitive to the electron temperature (T_e). An early study indicated the decay of SdH amplitude under the microwave radiation in the regime of the of the radiation-induced zero-resistance states in GaAs/AlGaAs devices, such that the SdH amplitude disappeared in proportion to the background resistance at the centers of the radiation-induced zero-resistance states [2]. However, the role of heating in that experimental result was not known.

Thus, we examined the influence of microwave radiation on the amplitude of Shubnikov-de Haas (SdH) oscillations at low temperatures, $T < 4.2$ K, in GaAs/AlGaAs Hall bar devices over the parameter space given by $1.7 < \omega_c/\omega \leq 3.3$, where $\omega_c = eB/m^*$, $\omega = 2\pi f$, B is the magnetic field, m* is the effective mass and f is the microwave frequency. Microwave radiation over the frequency range $30 \leq f \leq 110$ GHz with peak source power $1 \leq P_{peak} \leq 10$ mW served to photo-excite a high mobility ($\sim 10^7$ cm^2/Vs) 2DES as magnetoresistance traces were obtained as a function of the microwave power P and T. Then, fits of the SdH lineshape served to determine the electron temperature as a function of P and T over the above mentioned parameter window.

Theory has proposed that, in the $\omega_c/\omega \geq 1$ regime,[1,3] both the electron temperature T_e and radiation energy absorption rate (S_p) exhibit relatively constant response, while in $\omega_c/\omega \leq 1$ regime, both T_e and S_p exhibit oscillatory behavior. We compare the results of this experimental study with these theoretical predictions, and comment upon relative role of electron heating in the microwave photo-excited high mobility 2DES.

[1] X. L. Lei and S. Y. Liu, Phys. Rev. B 72, 075345 (2005)

[2] R. G. Mani, Appl. Phys. Lett. 91, 132103 (2007)

[3] X. L. Lei and S. Y. Liu, Appl. Phys. Lett. 94, 232107 (2009)

Separation and Study of Overlapping Current-induced Giant Magnetoresistance and Radiation-induced Magnetoresistance Oscillations in the GaAs/AlGaAs 2DES

R. L. Samaraweera, H. C.-Liu, Z. Wang, R. G. Mani
Dept. of Physics and Astronomy, Georgia State University, Atlanta, GA 30303
C. Reichl and W. Wegscheider
Laboratorium für Festkörperphysik, ETH-Zürich, 8093 Zürich, Switzerland
mani.rg.gsu@gmail.com

Interest in the GaAs/AlGaAs heterostructure two-dimensional electron systems (2DES) continues due to the enhanced physical and electrical properties of this system, including 2D electron mobilities well above 10^7 cm^2 /Vs. This 2DES showed unexpected physical phenomena such as novel microwave induced zero-resistance states and associated radiation- induced magnetoresistance oscillations, [1,2] and size dependent Giant Magnetoresistance (GMR) at low magnetic fields[3,4]. Here, we examine the overlap of radiation-induced magnetoresistance oscillations with a novel, recently observed current-induced GMR in GaAs/AlGaAs 2DES. To examine the mutual influence between these phenomena, we attempted to separate and extract the radiation-induced magnetoresistance oscillations from the current-induced bell-shape negative GMR using a two term Drude multi-conduction model [4]. Subtracting the multi-conduction Drude fit results from the experimental data served to isolate the microwave induced magnetoresistance oscillations. The aims of the study are to extract and characterize the overlapping microwave-induced magnetoresistance oscillations and current-induced GMR over a wider experimental parameter space, and understand the physical correlation and mutual influence between them. The results of the study are reported.[5]

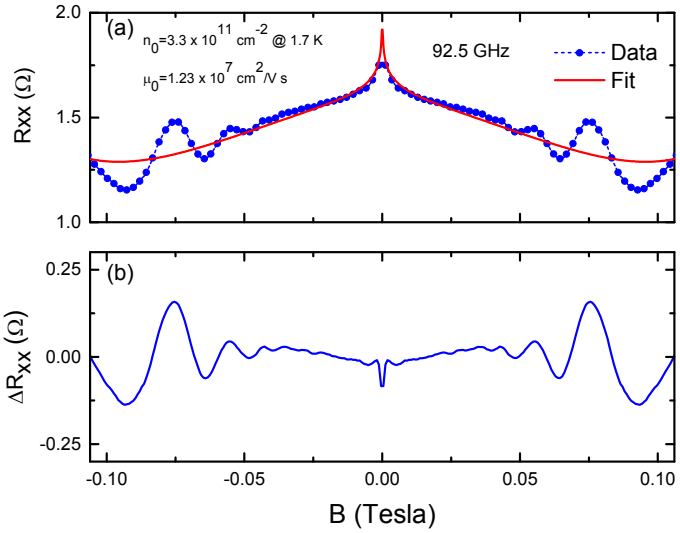

Fig.1 Extraction of microwave induced magnetoresistance oscillations from GMR using multi-conduction model. (a) Magnetotransport data exhibiting the microwave induced magnetoresistance oscillations at 92.5 GHz excitation (dot – dashed) and the associated fit using multi-conduction model (red-solid). (b) Extracted microwave induced magnetoresistance oscillations after subtracting the GMR effect.

References

[1] R.G. Mani, J.H. Smet, K. von Klitzing, V. Narayanamurti, W.B. Johnson and V. Umansky, Nature. **420**, 646 (2002).
[2] A. C. Durst, S. Sachdev, N. Read, and S. M. Girvin, Phys. Rev. lett. 91, 086803 (2003); J. Inarrea and G. Platero, Phys. Rev. Lett. 94, 016806 (2005); O. V. Zhirov et al., Phys. Rev. B 88, 035410 (2013); Y. M. Beltukov and M. I. Dyakonov, Phys. Rev. Lett. 116, 176801 (2016).
[3] M.A. Paalanen, D.C. Tsui and J.C.M. Hwang, Phys. Rev. Lett. **51,** 2226 (1983).
[4] R. G. Mani, A. Kriisa and W. Wegscheider, Nature – Scientific Reports **3,** 2747 (2013).
[5] R. L. Samaraweera et al., submitted for publication.

Current Tunable Giant Magnetoresistance in the High Mobility GaAs/AlGaAs 2D Electron System

Zhuo Wang[1], R. L. Samaraweera[1], C. Reichl[2], W. Wegscheider[2] and R. G. Mani[1]
[1]*Dept. of Physics & Astronomy, Georgia State University, Atlanta, GA 30303*
[2]*Laboratorium fur Festkorperphysik, ETH Zurich, Zurich, 8093, Switzerland*
zwang16@student.gsu.edu

Giant magnetoresistance (GMR), which is defined as a large change in the electrical resistance under the application of a magnetic field, has been widely used in many applications in the magnetic hard disk storage and memory industries. The most popular and useful GMR effect is the one that was observed in the magnetic-metallic-multilayer systems due to the relative re-alignment of the magnetic moments in successive ferromagnetic layers by a magnetic field.[1] Yet, it is known that the GMR effect is also observable in non-magnetic semiconductor systems, systems that are especially interesting for their compatibility with conventional semiconductor devices. Here, we examine a new mechanism for inducing- and controlling- GMR in a two-dimensional semiconductor system (2DES).[2] We demonstrate that a supplementary dc-current-bias in an ac- and dc- current biased high mobility 2DES results in a non-ohmic conductivity vs. the dc bias in the absence of a magnetic field, and this effect provides for enormous dc-current tunability in the GMR in the presence of 100's-of-millitesla-type magnetic fields. The effect is simply modeled using a two-term Drude model.[2]

The diagonal resistance $R_{xx} = V_{xx}/I_{ac}$ was measured in high mobility GaAs/AlGaAs Hall bar devices via standard low frequency lock-in techniques. The ac current (I_{ac}) and the dc-bias current (I_{dc}) were applied concurrently as shown in the inset of Fig.1. Temperature (T) dependent measurements were performed in a liquid helium cryostat in the range $1.7\ \text{K} \leq T \leq 4.2\ \text{K}$.

Fig.1 shows the I_{dc}-dependent magnetoresistance at T = 1.7 K, for $0 \leq I_{dc} \leq 19\ \mu\text{A}$. Here, the R_{xx} remains unchanged below $B = 0.05$ T for all I_{dc}. However, above $B = 0.05$ T, R_{xx} exhibits a positive magnetoresistance to B = 0.3 T at $I_{dc} = 0\ \mu\text{A}$ and that turns into a negative GMR at $I_{dc} = 19\ \mu\text{A}$. The data also exhibit well-known Shubnikov-de Haas and magneto-phonon oscillations. Increasing the temperature showed a smaller I_{dc}-induced change in the giant magnetoresistance. The non-oscillatory R_{xx} vs. B exhibiting GMR could be fit with a two-term Drude model at each I_{dc} and each T up to 4.2K.[2,3] The results suggest that I_{dc}-induced carrier heating could be responsible for the observed I_{dc} tunable GMR.[3]

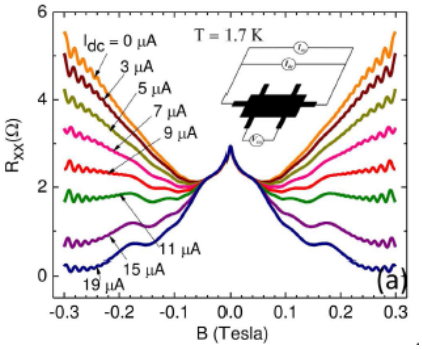

Fig.1 Tunable giant magnetoresistance induced by a dc current bias, I_{dc}, in a GaAs/AlGaAs heterostructure 2DES.

References

[1] M. N. Baibich, et al. Phys. Rev. Lett. **61** 24722475 (1988).

[2] R. G. Mani, A. Kriisa, and W. Wegscheider, Nature – Scientific Reports 3, 2747 (2013).

[2] Zhuo Wang, R. L. Samaraweera, C. Reichl, W. Wegscheider, and Ramesh Mani, Nature - Scientific Reports **6**, 38516 (2016).

Anomalies of the quantum Hall effect in the HgTe/CdHgTe double quantum well with the spectrum of bilayer graphene

M.V. Yakunin, S.M. Podgornykh, M.R. Popov, V.N. Neverov
M.N. Miheev Institute of Metal Physics, Ekaterinburg, 620990, Russia
S.S. Krishtopenko, *Institute for Physics of Microstructures, Nizhny Novgorod, 603087, Russia*
F. Teppe, B. Jouault, W. Desrat
Laboratoire Charles Coulomb (L2C), Universite Montpellier, 34095 Montpellier, France
N.N. Mikhailov, S.A. Dvoretsky, *Institute of Semiconductor Physics, Novosibirsk, 630090, Russia*
yakunin@imp.uran.ru

We report on observation of an unusual structure of the quantum Hall effect (QHE) in a double quantum well (DQW) formed by two layers of gapless material HgTe close to the critical thickness of 6.3–6.5 nm separated by the $Hg_{0.3}Cd_{0.7}Te$ barrier of ~3 nm [1]. In this case the DQW energy spectrum resembles that of bilayer graphene, although with its own specificity [2], which is radically different from the case for similar DQW with wider wells [3]. An anomalous peak is revealed at zero gate voltage V_g on the $i = 2$ QH plateau, $\rho_{xy} = h/ie^2$, which in fact is a manifestation of the reentrant $i = 2 – 1 – 2$ transition that separates two ranges of magnetic field B corresponding to substantially different densities of mobile holes p_s. A traditional structure of QHE is observed at weaker fields for $p_s = 0.4\times10^{15}$ m^{-2} stretched up to the lower field slope of the anomalous peak, while a stable plateau–plateau transition $i = 2 – 1$ is observed at much higher fields that yields $p_s = 1.6\times10^{15}$ m^{-2}. Two peaks in longitudinal magnetoresistance $\rho_{xx}(B)$ correspond to the left and right slopes of the anomalous peak in $\rho_{xy}(B)$. The left peak satisfies the traditional scheme of crossing the delocalized state between the $i = 2$ and $i = 1$ phases by the Fermi level E_F. Then the right peak should correspond to the reverse transition from the $i = 1$ to $i = 2$ phases that means a backward crossing of the delocalized state with the same sequential number.

We explain the observed phenomena on the basis of calculated pictures of magnetic levels as being due to (i) the existence of an electronic level superimposed upon the fan chart of hole levels and (ii) stabilization of $E_F(B)$ and localization of a part of holes in the heavy hole states of the lateral maximum in the valence subband. Evolution of the QHE with illumination, field tilt and V_g is at least with qualitative agreement with calculations. A notable feature in the QH conductivity is independence of its weak-field features on V_g within a considerable range of negative V_g (Fig. 1) in support of above-mentioned localization effects.

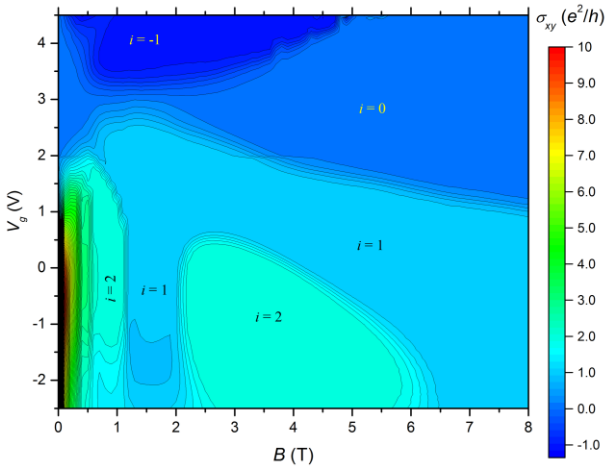

Fig.1. QH conductivity $\sigma_{xy}(B,V_g)$.

References

[1] M.V. Yakunin *et al.*, JETP Lett. **104**, 403 (2016).
[2] S.S. Krishtopenko *et al.*, Nature: Scientific Reports **6**, 30755 (2016).
[3] M.V. Yakunin *et al.*, Phys. Rev. B **93**, 085308 (2016).

Fractional quantum Hall effect and exotic phases in electrostatically defined Graphene structures

S. Chen[1,2]*, R. Ribeiro-Palau[1,3], T. Taniguchi[4], K. Watanabe[4], J. Hone[3] and C. R. Dean[1]

[1] *Department of Physics,* [2] *Department of Applied Physics and Applied Mathematics and* [3] *Department of Mechanical Engineering*

Columbia University, New York, NY 10027, USA

[4] *National Institute for Materials Science, 1-1 Namiki, Tsukuba 305-0047, Japan.*

* sc3724@columbia.edu

Even when the quality of graphene devices has improved greatly in the last five years, the study of its fractional quantum Hall (FQH) effect remains elusive. Current high quality devices still require high magnetic fields and sophisticated annealing processes [1,2] in order to observe the FQH effect. Here, we present a new approach where graphene structures are electrostatically defined, granting access to FQHE states at low magnetic fields (>5 T). Our devices take advantage of the fully-gapped, without edge states nature of the ν=0 Landau level at moderated magnetic field (>4 T) to electrostatically define the devices, see Fig. 1a. Our sample geometry allows us to check that the current flowing in the gapped regions is less than the 0.1 % of the total applied current, guaranteeing an efficient and tunable electronic confinement.

Beyond the remarkably well developed fractional quantum Hall states at moderated fields, our devices show as of yet unexplored features of the QHE of graphene, such as four-flux states (Fig. 1b), and reentrant integer quantum Hall effects (RIQHE, see Fig. 1c). The RIQHE is an exotic phase, observed only so far in conventional semiconductor heterostructures [3], which appears as a consequence of the competition between the electron-solid and electron-liquid phases.

The performance of our devices represents the first proof of principle that building complex structures based on controlled electrostatic confinement, such as quantum point contacts and edge states interferometers, is now possible in graphene.

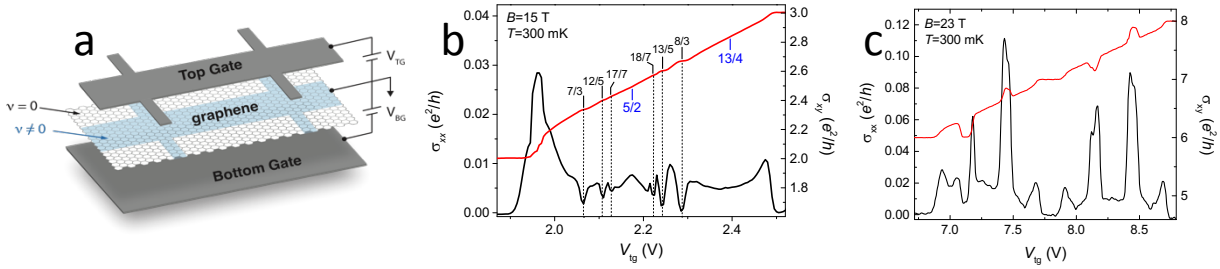

Fig.1 **a** Schematics of the device. **b** two and four-flux FQH sequence and **c** RIQH effects observed in the second Landau level.

References

[1] Dean, C. R., et al. Nat. Phys. **7**, 693 (2011).

[2] F. Amet. et al., Nat. Comm. **6**, 5838 (2015).

[3] Deng, N., et al. Phys. Rev. Lett. **108**, 086803 (2012).

Engineering charge noise reduction in modulation doped heterostructures

S. Fallahi[1,2], J. Nakamura[1,2], G. Gardner[1,2,4], M.Yannell[3], M. Manfra[1,2,3,4]
[1]*Department of Physics and Astronomy, Purdue University, West Lafayette, IN 47907, USA*
[2]*Birck Nanotechnology Center, Purdue University, West Lafayette, IN, 47907 USA*
[3]*School of Electrical Engineering, Purdue University, West Lafayette, IN, 47907 USA*
[4]*Station Q Purdue and School of Materials Engineering Purdue University, West Lafayette, IN 47907, USA*
sfallahi@purdue.edu

Electrostatically gated nanostructures such as quantum dots (QD) and quantum point contacts (QPC) fabricated on modulation doped GaAs/AlGaAs heterostructures are the essential building blocks in mesoscopic physics and are used to realize solid state qubits. These nanostructures may suffer from random telegraph noise and drift in operating voltage which cause instability in device performance. Although a few techniques [1, 2] are implemented to suppress charge noise, none of them address the root causes of noise and operating gate voltage drift in the heterostructures.

We present measurements of low frequency charge noise in modulation doped GaAs/AlGaAs heterostructures grown by molecular beam epitaxy in which the silicon doping density has been varied from $2.4\text{x}10^{18}$ cm^{-3} (critically doped) to $6.0\text{x}10^{18}$ cm^{-3} (overdoped). QPCs fabricated on these heterostructures are used to detect fluctuations in the vicinity of the QPC. We measured current noise through the QPCs on the riser of the first quantized conductance plateau at T = 4.2K. We quantify the noise level in terms of equivalent gate voltage noise, which is defined as the voltage noise level applied to the Schottky gates that would produce the same conductance fluctuations as caused by the charge fluctuations. We found a correlation between doping density and equivalent gate voltage noise (Fig.1) as well as operating voltage drift (Fig.2) in these heterostructures. By shifting the placement of the Si doping away from the Schottky contact, we obtained a further reduction in charge noise and voltage drift in these heterostructures. The underlying physical processes responsible for these observations will be discussed.

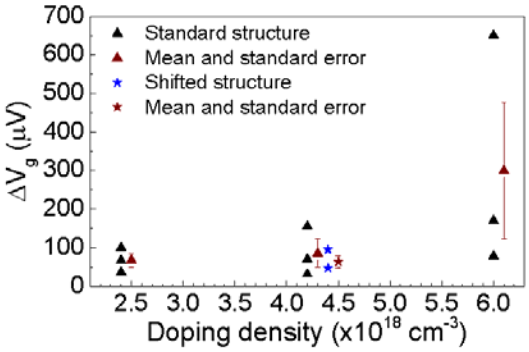

Figure 1. Equivalent gate voltage noise vs. doping density

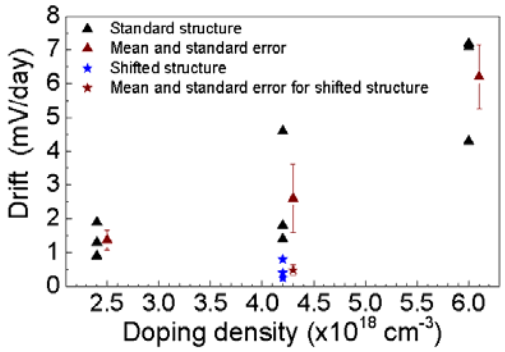

Figure 2. QPC Pinch off voltage drift vs. doping density

References

[1] M. Piore-Ladrie`re, et al., Phys. Rev. B **72,** 115331 (2005).

[2] C. Buizert, et al., Phys. Rev. Lett. **101**, 226603 (2008).

Four Single-spin Rabi Oscillations in a Quadruple Quantum Dot

T. Ito,[1, 2, †] T. Otsuka,[1, 2, †] T. Nakajima,[1, 2] M. R. Delbecq,[1, 2] S. Amaha,[1] J. Yoneda,[1, 2] K. Takeda,[1, 2]
A. Noiri,[1, 2] G. Allison,[1] A. Ludwig,[3] A. D. Wieck,[3] and S. Tarucha,[1, 2]
[1] *Center for Emergent Matter Science, RIKEN, 2-1 Hirosawa, Wako, Saitama 351-0198, Japan*
[2] *Department of Applied Physics, University of Tokyo, Bunkyo, Tokyo 113-8656, Japan*
[3] *Angewandte Festkörperphysik, Ruhr-Universität Bochum, D-44780 Bochum, Germany*
takumi.ito@riken.jp

Semiconductor quantum dots (QDs) are a promising candidate for application to quantum information processing [1]. By utilizing semiconductor micro fabrication techniques, QD systems are potentially scalable and meet the requirement of large-scaling necessary for practical quantum computing [2]. The required elementary operations in quantum computation are initialization, readout by Pauli spin blockade (PSB), single qubit manipulation by single electron spin resonance (ESR) and two-qubit operation by exchange control, and have all been demonstrated with single, double and triple QDs [3]. In addition quadruple and quintuple QDs have been studied so far [4], and especially in quadruple QD (QQD), c.w. ESR has recently been realized in each QD with micro-magnet mediated ESR (MM-ESR) [5].

In this work, we used a QQD to implement Rabi oscillation or coherent manipulation of single electron spins in the respective QDs. The QDs are coupled in series and connected to the reservoirs at both ends of the QD array. The charge state of the QQD is monitored by two nearby QD charge sensors with RF reflectometry and the spin state is converted into the charge signal utilizing PSB. First, we observed four individual ESR signals by applying a microwave (MW) to a gate electrode that runs parallel with the QQD array. The oscillating electric field in slanting magnetic field formed by MM is converted into the effective oscillating magnetic field that induces ESR. MM-ESR is useful for manipulating single electron spins in QDs because it can be designed to perform independent and fast manipulation of electron spin in each dot. Local Zeeman differences are induced between QDs by specially designed MM and this enables us to independently address ESR in the four QDs by choosing the MW frequency at a fixed magnetic field. Second, we change the MW burst time to observe Rabi oscillation for each ESR signal. Figures show the observed Rabi oscillations in each QD. The frequency of the observed Rabi oscillation ranges from 0.6 to 6 MHz. The frequency differences reflect the special variation of the slanting magnetic field over the four dots and can be used to estimate the positions of the QDs. These techniques of individual control of single electron spins in multiple QD will be important to scale up the QD systems in order to realize large scale quantum bit systems.

References

[1] D. Loss *et al.*, Phys. Rev. A **57**, 120 (1998).
[2] D. P. DiVincenzo *et al.*, Phys. Rev. Lett. **77**, 3260 (1996).
[3] A. Noiri *et al.*, Appl. Phys. Lett. **108**,153101 (2016).
[4] T. Ito *et al.*, Sci. Rep. **6**, 39113 (2016).
[5] T. Otsuka *et al.*, Sci. Rep. **6**, 31820 (2016).

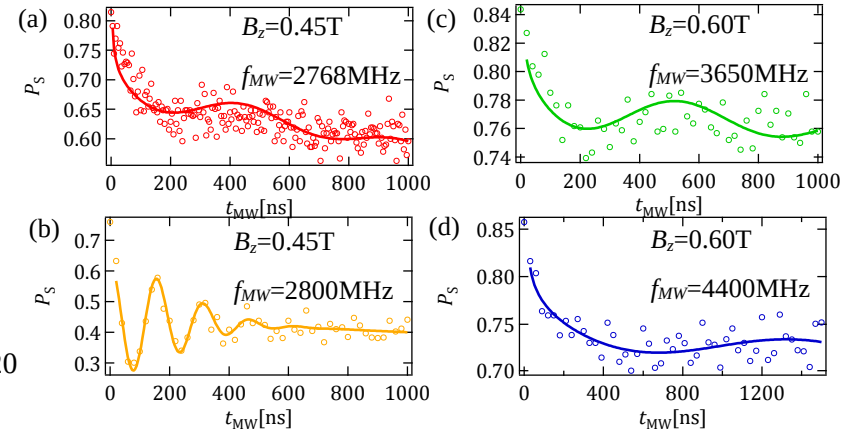

Fig. (a)-(d) Rabi oscillations observed in four QDs.

Hole Hybrid Qubit in a Gated Double Quantum Dot – Spin-Filp Tunneling, Anisotropic g-Factor, and Spin Coherence Time of a Single Hole

M. Korkusinski[1], A. Bogan[1], S. Studenikin[1], G. Aers[1], L. Gaudreau[1], P. Zawadzki[1], A. Sachrajda[1], L. Tracy[2], J. Reno[2], and T. Hargett[2]
[1]*Security and Disruptive Technologies, National Research Council, Ottawa, Canada*
[2]*Sandia National Laboratories, Albuquerque, New Mexico, USA*
Marek.Korkusinski@nrc-cnrc.gc.ca

Motivated by interest in quantum networks and long-distance quantum cryptography, there is currently a great deal of interest in interfacing the photonic and solid-state spin qubits in lateral gated quantum dot devices [1]. The transfer of the photon polarization state onto that of the confined spin is realized by generating an electron-hole pair and ejecting the extraneous carrier. Therefore, beside the long spin coherence time, the candidates for such interface are direct bandgap materials, with the effective g-factor engineered to a near-zero value to erase the which-path information in the coherent state transfer [1,2]. In spite of their ultra-long spin coherence times [3], the indirect bandgap excludes ^{28}Si devices. The GaAs electron-spin based devices, while more promising [1], still require g-factor engineering.

Here we put forward the heavy-hole (HH) spin in a gated GaAs double-dot device (DQD) as a good candidate for the spin qubit in the photon-to-spin interface. We describe theoretically and demonstrate experimentally its three relevant key properties: (i) fast coherent HH spin-flip transitions driven by gate voltage alone, (ii) the T1 spin-coherence time in tens of microseconds, measured by a novel single-shot method, and (iii) highly anisotropic HH g-factor, allowing to tune its effective value in situ, without complex sample engineering,

The characteristic HH properties stem from the p-type character of the valence band. As such, the HHs are expected to interact weaker than electrons with the nuclear spins, promising longer coherence times [4]. However, holes experience much stronger spin-orbit interactions (SOI), which brings new and nontrivial physics to the gated DQDs. We explore it by performing magneto-transport spectroscopy on p-GaAs DQD populated by one or two holes [5,6]. In the single-hole regime we map out the spin-conserving and spin-flipping tunneling (SFT) processes, of which the latter is due to the SOI. We find both processes to be of similar magnitude. This makes our single-hole DQD a hybrid spin-charge system, in which all degrees of freedom can be controlled electrically. Analysis of magneto-transport under microwave-frequency modulation of gate voltages gives the coherence and charge relaxation times for our device. Moreover, we describe a new, fast technique for single-shot projective measurement of a single spin state. The technique utilizes SFTs, as well as the latching of the charge state of the second quantum dot for enhanced sensitivity. It allows a direct measurement of the single spin relaxation time on time-scales set by physical device rather than the measurement circuit.

We also populate our DQD with two holes and study the transport in Pauli spin blockade regime [5,6]. The strong SFTs lift the blockade except for the regime of very small magnetic fields. While it complicates the spin-to-charge conversion, the SFT allows to measure directly the HH g-factor as a function of the magnetic field direction. As is typical for HHs, we find a strongly anisotropic g factor, nearly zero for the field oriented in the DQD plane.

[1] A. Oiwa et al., J. Phys. So.c Japan **86,** 011008 (2017); K. Morimoto et al., Phys. Rev. B **90,** 085306 (2014).
[2] E. Yablonovitch et al., Proc. IEEE **91,** 761 (2003); H. Kosaka, J. Appl. Phys. **109,** 102414 (2011).
[3] A. M. Tyryshkin et al.., Nature Materials **11,** 143 (2012).
[4] J. Fisher, W. A. Coish, D. V. Bulaev, and D. Loss, Phys. Rev. B **78,** 155329 (2008).
[5] L. A. Tracy, T. W. Hargett, and J. L. Reno, Appl. Phys. Lett. **104,** 123101 (2014).
[6] A. Bogan, S. Studenikin, M. Korkusinski G. Aers, L. Gaudreau, P. Zawadzki, A. Sachrajda, L. Tracy, J. Reno, and T. Hargett, Phys. Rev. Lett. (submitted).

Enhancing coherence of a single electron spin with adaptive control

T. Nakajima[1], K. Kawasaki[2], A. Noiri[1,2], J. Yoneda[1], P. Stano[1], T. Otsuka[1], K. Takeda[1], M. R. Delbecq[3], G. Allison[1], A. Ludwig[4], A. D. Wieck[4], D. Loss[1,5] and S. Tarucha[1,2]

[1]*Center for Emergent Matter Science, RIKEN, Wako, Saitama, Japan*

[2]*Department of Applied Physics, University of Tokyo, Bunkyo-ku, Tokyo, Japan*

[3]*Quantum Matter Group, Collège de France, Paris, France*

[4]*Lehrstuhl für Angewandte Festkörperphysik, Ruhr-Universität Bochum, Bochum, Germany*

[5]*Department of Physics, University of Basel, Klingelbergstrasse 82, 4056 Basel, Switzerland*

nakajima.physics@icloud.com

Gate-defined quantum dots in GaAs/AlGaAs heterostructures are a promising platform for quantum computation for their formidable electronic properties and reproducibility. Coherence of spin-based qubits in this architecture is, however, challenged by the magnetic fluctuation in the environment, mainly due to the nuclear spins in the host material. This fact motivated recent investigations of nuclear spin-free materials such as ^{28}Si, although they are technologically demanding. Instead of suppressing the magnetic fluctuation, it was recently shown that one could employ the adaptive control technique to suppress the qubit dephasing by rapidly probing and canceling out the magnetic fluctuations [1].

In this paper, we demonstrate enhancement of the ensemble coherence time of a single electron spin qubit in GaAs up to $T_2^* \approx 500$ ns by the open-loop adaptive control based on the real-time estimation of the nuclear spin fluctuations (Fig. 1). The instantaneous Overhauser field in a quantum dot is estimated from rapid single-shot measurements of the Ramsey oscillation and the microwave frequency for the qubit control is adjusted accordingly to maintain the desired qubit frequency in the rotating frame. When the update cycle of the estimation is reduced to a millisecond time scale, the effect of the slow nuclear spin diffusion on the spin coherence is significantly suppressed. This adaptive control scheme not only improves the ensemble coherence time but also compensates longer-term drift of the qubit frequency, which is typically more than 10MHz in GaAs. Combined with the fast spin manipulation by electric-dipole spin resonance [2], our scheme will enable high-fidelity control of a single spin even in GaAs quantum dots and possibly improve qubit fidelities in other materials on which slow magnetic fluctuation has an impact.

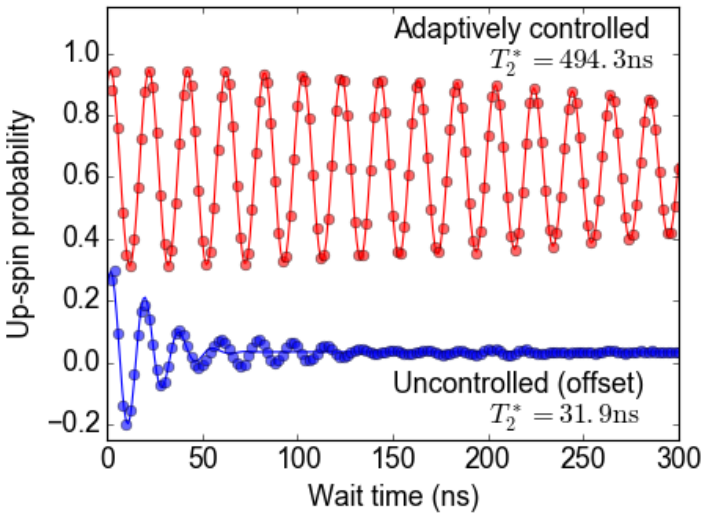

Fig. 1 Ramsey oscillations of a single electron spin with (upper) and without (lower) the adaptive control. The detuning frequency is targeted at 50MHz with the adaptive control.

References

[1] M. D. Shulman *et al*., Nature comm. **5** 5156 (2014).

[2] J. Yoneda *et al*., Phys. Rev. Lett. **113**, 267601 (2014).

Quantum non-demolition readout of a single spin in a quantum dot

A. Noiri[1,2], T. Nakajima[1], J. Yoneda[1], T. Otsuka[1], K. Takeda[1], M. R. Delbecq[3], K. Kawasaki[2], G. Allison[1], A. Ludwig[4], A. D. Wieck[4] and S. Tarucha[1,2]

[1]*Center for Emergent Matter Science, RIKEN, Wako, Saitama, Japan*

[2]*Department of Applied Physics, University of Tokyo, Bunkyo-ku, Tokyo, Japan*

[3]*Quantum Matter Group, Collège de France, Paris, France*

[4]*Lehrstuhl für Angewandte Festkörperphysik, Ruhr-Universität Bochum, Bochum, Germany*

akito.noiri@riken.jp

Readout of a single electron spin in a quantum dot (QD) is a key technology for realizing spin-based quantum computation as well as for studying spin-related phenomena. However, direct measurement of a single spin is challenging since the magnetic moment of a single electron spin is usually too small to detect. Therefore, spin readout has been performed by a combination of spin-to-charge conversion and a charge sensing technique. Conventionally, the spin-to-charge conversion relies on spin-dependent electron tunneling between a QD and an adjacent lead [1] or an adjacent QD [2], which is inherently destructive process. This hinders quantum non-demolition (QND) readout, which allows repetitive measurement of a qubit state and hence is regarded as an ideal readout scheme. Although QND readout is widely used in many different qubit systems to increase the readout fidelity, QND readout of a single electron spin in an electrically-controlled QD has never been realized.

In this presentation, we demonstrate QND readout of a single electron spin in a hybrid system of a single spin qubit and a singlet-triplet qubit, realized in a triple QD. A single spin in the left QD is read out using the exchange-coupled center-right DQD as a probe. When a singlet state is prepared in the DQD, it starts precessing between the singlet and triplet states with a precession frequency $f_{ST} = \Delta E_Z/h$ where ΔE_Z is the Zeeman energy difference between the center and the right QDs. When an exchange coupling J between the left and the center QDs is turned on, f_{ST} shifts by $J/2h$ depending on the projection of the left spin being either ↑ or ↓: $f_{ST,\uparrow(\downarrow)} = \Delta E_Z/h$ –(+) $J/2h$, as theoretically predicted [3]. This means that we can perform a projection measurement of the left spin by measuring f_{ST} while leaving the measured spin state to one of the eigenstates. This non-demolition property is verified experimentally by observing quantum jumps of a single spin with a jump time scale much longer than the measurement time resolution. We then rotate the single spin by electron spin resonance and obtain the Rabi oscillation both by standard energy-selective tunneling [1] and the QND readout schemes (Fig. 1). The QND readout gives better oscillation visibility, reflecting better readout fidelity. This is the first demonstration of QND readout of a single electron spin in an electrically-controlled QD, and may be an important step toward high-fidelity spin readout.

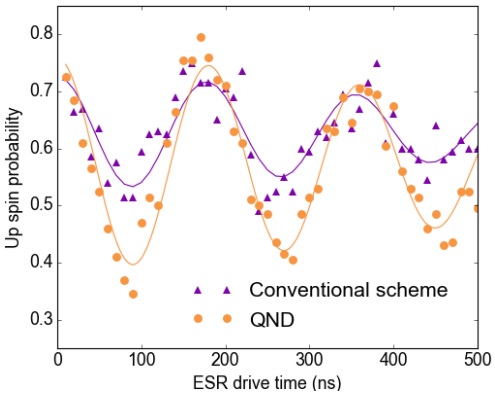

Fig.1 Rabi oscillation of a single spin obtained by the QND readout (yellow) and the energy-selective tunneling (purple).

References

[1] J. M. Elzerman *et al*., Nature, **430**, 431 (2004).
[2] K. Ono *et al*., Science, **297**, 1313 (2002).
[3] S. Mehl *et al*., Phys. Rev. B, **92**, 115448 (2015).

Spin and valley qubit in gated MoS_2 monolayer quantum dot

Jarosław Pawłowski
Department of Theoretical Physics, Faculty of Fundamental Problems of Technology,
Wrocław University of Science and Technology,
Wybrzeże Wyspiańskiego 27, 50-370 Wrocław, Poland
jaroslaw.pawlowski@pwr.edu.pl

The aim of presented research is to construct quantitative models describing quantum information carriers, single electrons confined in dwo-dimensional crystals of transition metal dichalcogenides (TMDC) [1]. Then design of nanodevices based on TMDC monolayer, performing operations on properly defined qubits. Such monolayers have a number of interesting properties. Unlike graphene, they have direct band gap and relatively high value of spin-orbit coupling. Moreover, they possess the ability of using valley pseudospin, in addition to spin, as quantum bit. Thus, they are important materials for spintronics and recently introduced valleytronics.

The proposed nanodevice consists of TMDC monolayer flake with nearby gates. Appropriate voltages applied to the gates crate electric fields within the monolayer. The electrostatic quantum dots within the flake, induced by the local gating, confines single electrons. Qubit is encoded in the valley or spin electron degree of freedom. In such a structure, spin transitions are induced by modulations of lateral electric field which in turn modulate the Rashba spin-orbit coupling. While the valley ones are induced by the confinement potential oscillatory modulations. Presented transitions mechanism allow to perform operations on spin or valley state of the electron confined in the nanodevice. The proposed electron spin and valley manipulation scheme is all-electrically controlled by voltages applied to the local gates.

We use the three-band tight-binding approach [2] to model TMDC monolayer flakes. We describe exact potential of the nanodevice taking into account proper boundary conditions on the electrodes by solving the Poisson equation. The time-evolution of the system is supported by realistic self consistent Poisson-Schrödinger tight-binding calculations. The tight-binding calculations are further confirmed by simulations within the continuum model [3]. We are developing previously used [4,5,6] precise realistic simulations of the time evolution of semiconductor nanodevices. Now introduced for new and attractive materials with the interesting properties.

References

[1] Q. H. Wang, K. Kalantar-Zadeh, A. Kis, J. N. Coleman and M. S. Strano, Nature Nanotechnology **7**, 699 (2012).
[2] Gui-Bin Liu, Wen-Yu Shan, Yugui Yao, Wang Yao, and Di Xiao, Phys. Rev. B **88**, 085433 (2013).
[3] A. Kormanyos, V. Zolyomi, N. D. Drummond, and G. Burkard, Phys. Rev. X **4**, 011034 (2014).
[4] J. Pawłowski, P. Szumniak, A. Skubis and S. Bednarek, J. Phys.: Condens. Matter **26**, 345302 (2014).
[5] J. Pawłowski, P. Szumniak, and S. Bednarek, Phys. Rev. B **93**, 045309 (2016).
[6] J. Pawłowski, P. Szumniak, and S. Bednarek, Phys. Rev. B **94**, 155407 (2016).

A SQUID-based Johnson Noise Thermometer for Quantum Resistors at Dilution Refrigerator Temperatures

Vidhi Shingla, Ethan Kleinbaum[a], and G.A. Csáthy
Department of Physics and Astronomy and the Birck Nanotechnology Center, Purdue University, West Lafayette, IN 47907, USA
vshingla@purdue.edu

Current fluctuations in topological electron fluids reveal valuable information about these fluids. For example, shot noise probes the charge of the quasiparticles. Furthermore, Johnson noise is commonly used to determine the electronic temperature. Johnson noise thermometry is an especially valuable tool at temperatures below 100 mK since in this temperature regime electrons often decouple thermally from the phonon bath and therefore have a larger temperature than that of the bath.

Numerous phenomena of current interest, such as the integer and the fractional quantum Hall effect, the quantum spin Hall effect, and charge flow in quantum point contacts, occur in samples with resistance of the order of the von Klitzing constant $h/e^2 \sim 25.8$ kΩ. Noise measurement at dilution refrigerator temperatures in such samples are most commonly performed using High Electron Mobility Transistor (HEMT) based circuits [1]. Low noise in such samples may also be achieved in SQUID circuits interfaced with Cryogenic Current Comparators routinely used in quantum metrology [2]. However, Cryogenic Current Comparators have an intricate construction, are bulky, and for noise measurement one has employ a cumbersome feedback circuit [2]. As a result, SQUIDs interfaced with Cryogenic Current Comparators have not been adapted for use in dilution refrigerators.

We present a SQUID-based circuit useful for Johnson noise measurements of quantum resistors at milliKelvin temperatures. Impedance matching in this circuit is achieved using a coreless cryogenic transformer. We demonstrate that when used with a resistor of 3.25 kΩ, this circuit does not add any appreciable noise to the Johnson noise of the resistor down to 16 mK. Our circuit is therefore a useful alternative to HEMT-based noise measurement setups, but in contrast to the latter, it can be used at arbitrarily low frequencies. This work was supported by the NSF grant DMR 1505866.

References

[1] R. de-Picciotto, M. Reznikov, M. Heiblum, V. Umansky, G. Bunin, and D. Mahalu, Nature **389**, 162 (1997).
[2] F. Gay, F. Piquemal, and G. Geneves, Rev. Sci. Instrum. **71**, 4592 (2000).

a now at Princeton University

The Coherence of a Photo-Generated Electron Spin in a Electrostatically-Confined Quantum Dot

Yasuhiro Tokura
Faculty of Pure and applied Sciences, University of Tsukuba,
1-1-1 Tennodai, Tsukuba, Ibaraki 305-8571, Japan
tokura.yasuhiro.ft@u.tsukuba.ac.jp

Maintaining the electron spin coherence is the most important factor when one transfers the quantum information of a photon state into that of an electron spin. In principle, this can be accomplished by using the optical selection rule of semiconductors with detailed *g*-factor engineering [1]. Recently, the transfer of classical bit information of a single photon to a single electron spin had been experimentally demonstrated [2]. For a more quantitative study of the transfer of *quantum* bit information, we need to study in more detail the process after the electron-hole pair generation by the photon. Rikitake and co-worker had studied the effect of exchange interaction between the electron and hole spins in a quantum dot (QD) made of type-I confinement potential, where the hole is resonantly extracted to the reservoir. However, it is probably more preferable to use electrostatically confined QD (type-II confinement, Fig. 1) since the hole escapes much faster from the QD area. Therefore, here we report the quantitative estimation of the effect of the exchange interaction on the coherence of the photo-generated electron spin in the system, Fig. 1.

For a very short time scale just after the electron–hole pair generation (t=0), the effect of phonons can be neglected and the dynamics is dominated by the quantum diffusion [4] of the hole. For the first approximation, we can assume the effective (Hartree) potential for the hole as a flat band, and we obtain the analytical expression of the exchange energy $J(t)$ as a function of time t. The time integral of $J(t)$ is the mixing angle θ, which is given by the ratio of the Coulomb interaction energy and the hole's kinetic energy at t=0. The factor $\sin^2\theta$ characterizes the infidelity of the quantum transfer. For more accurate study, we employed Suzuki-Trotter's formula [5] and numerically solved the time-dependent Schroedinger equation for a realistic confinement potential. We also discuss the effect of the hole-phonon coupling for a more effective decoupling.

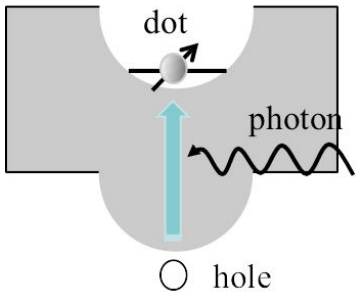

Fig.1 Schematic diagram of electron-hole pair generation by a photon in the electrostatically confined quantum dot.

This work was supported by CREST, JST.

References

[1] R. Vrijen and E. Yablonovich, Physica E **10**, 569 (2001).
[2] A. Oiwa, *et al*., J. Phys. Soc. Jpn. **86**, 011008 (2017).
[3] Y. Rikitake and H. Imamura, Phys. Rev. B **74**, 081307 (2006).
[4] D. Morita, T. Kubo, Y. Tokura, and M. Yamashita, Phys. Rev. A **93**, 063625 (2016).
[5] O. Halfpap, T. Kawarabayashi, and B. Kramer, Ann. Phys. (Leipzig) **7**, 483 (1998).

Quantum Dot Rapid Adiabatic Passage by Ultrafast Stark Tuning

A. Widhalm[1], A. Mukherjee[1,2], N. Sharma[1], A. Thiede[2], J. Förstner[2], D. Reuter[1] and A. Zrenner[1]
[1]*Physics Department and Center for Optoelectronics and Photonics Paderborn (CeOPP), University of Paderborn, Warburger Straße 100, Paderborn 33098, Germany*
[2]*Department of Electrical Engeneering and Center for Optoelectronics and Photonics Paderborn (CeOPP), University of Paderborn, Warburger Straße 100, Paderborn 33098, Germany*
alex.widhalm@upb.de

The excellent optical properties of single InGaAs QDs embedded in electric field tunable structures allow for the realization of new coherent optoelectronic functionalities. The well-controlled state preparation plays thereby a major role in the development of quantum functional devices. It is well known, that a selective population transfer from a ground quantum state into a desired target state requires specifically controlled pulses of radiation [1]. A robust state preparation can be achieved by using polarization tailored pulses [2] or frequency chirped pulses for the realization of a rapid adiabatic passage (RAP) [3, 4]. In alternative to chirped optical pulses, a hybrid approach using the combination of transform-limited optical pulses and fast electrically induced chirp by transient Stark shift looks very promising in respect to applications.

In this work, we use fast electric transients in combination with transform limited ps optical pulses (15 ps) to achieve a RAP. Our system is based on self-assembled InGaAs QDs embedded in a low capacitance Schottky-photodiode. The photodiode is closely connected to a He-temperature pulse generator based on pseudomorphic HEMT transistors, which deliver transients down to 10 mV/ps. The electric pulse source is synchronized with the pulsed laser source. The delay between electrical and optical pulses is controlled by an electric delay line. The occupancy of the QD can be read out by photocurrent detection.

By varying the delay between the optical ps pulses and the electric transient (fig. 1a,b) we can control the effective chirp on the QD. If the excitation occurs during the electric transient, the QD two-level system performs a RAP. In power dependent measurements (see fig.1c) we can demonstrate the transition from an un-chirped Rabi scenario (black) to a clear RAP signature (red) for conditions of applied electric chirp.

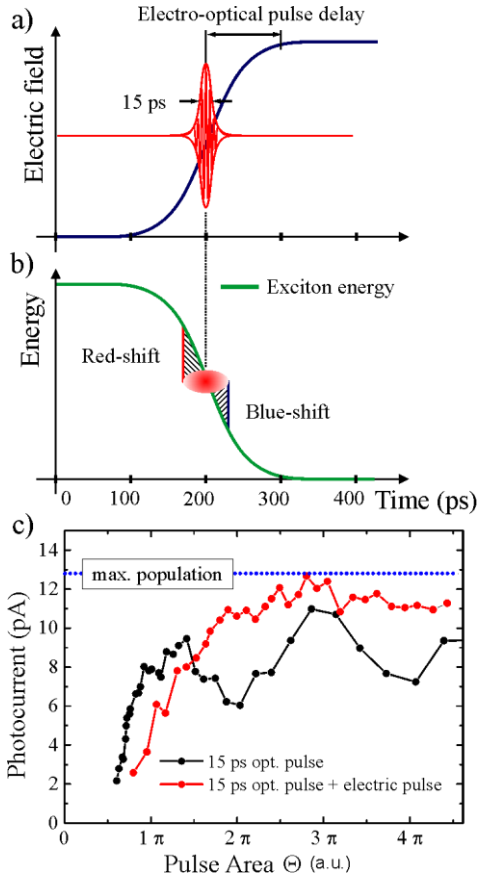

Fig.1 a,b) Schematic representation of electro-optical pulse delay. c) Photocurrent of QD in dependency of excitation power

References

[1] A. Zrenner et al., Nature **418**, 612 (2002).
[2] D. Mantei et al., Sci. Rep. **5**, S. 10313 (2015),
[3] Yanwen Wu et al., PRL **106**, 067401 (2011),
[4] C.M. Simon et al., PRL **106**, 166801 (2011).

Quantum Oscillation of Anomalous Hall Conductivity Induced by Magnetic Skyrmions on Topological Insulator Surfaces

Yasufumi Araki[1,2] and Kentaro Nomura[1]
[1] *Institute for Materials Research, Tohoku University, Sendai 980-8577, Japan*
[2] *Frontier Research Institute for Interdisciplinary Sciences, Tohoku University, Sendai 980-8578, Japan*
araki@imr.tohoku.ac.jp

Magnetic skyrmions, namely particlelike magnetic excitations with swirling magnetic texture at the boundary, are observed in non-centrosymmetric magnetic materials. They give rise to the so-called topological Hall effect (THE), which is the unconventional Hall effect of the conduction electrons caused by the emergent magnetic field, corresponding to the real-space Berry curvature at the skyrmion [1,2].

Surface states of topological insulators (TIs), on the other hand, host gapless Dirac electrons, whose properties are fairly sensitive to magnetic textures, such as domain walls and vortices [3], compared with the conventional electrons, due to the spin-momentum locking feature. Recent theoretical studies have shown a number of electron states localized at a skyrmion attached on the TI surface, which may lead to electric charging of the skyrmion [4].

In this work, we theoretically investigate the effect of magnetic skyrmions on the electron transport on TI surfaces [5]. We focus on the interface between a TI and a ferromagnetic insulator (FMI) with skyrmions, and take into account the exchange interaction between the electron spin on the TI and the local magnetization in the FMI. The system reveals a finite anomalous Hall conductivity due to the scattering skewness by a skyrmion, arising from the geometric phase acquired through the electron transmission process at the skyrmion boundary, which is distinct from the mechanism of the THE. We find quantum oscillations in both the longitudinal and Hall conductivities under the variation of the skrymion size or the electron chemical potential, as shown in Fig. 1, which are related to the electron resonance states formed inside the skyrmions. We expect such quantum oscillations to be signals of the emergence of skyrmions on TIs, and that they can help one estimate the size of the skyrmions.

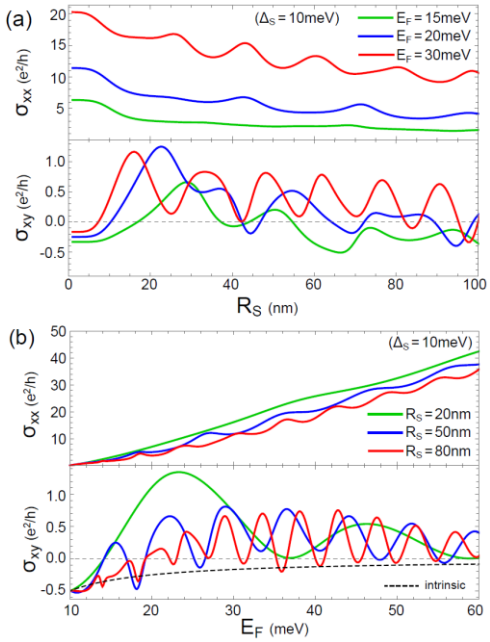

Fig.1: The longitudinal conductivity σ_{xx} and the Hall conductivity σ_{xy}, (a) with the Fermi energy E_F fixed and the skyrmion radius R_S varied, and (b) with R_S fixed and E_F varied.

References

[1] M. Lee, W. Kang, Y. Onose, Y. Tokura, and N. P. Ong, Phys. Rev. Lett. **102**, 186601 (2009).
[2] A. Neubauer, C. Pfleiderer, B. Binz, A. Rosch, R. Ritz, P. G. Niklowitz, and P. Böni, Phys. Rev. Lett. **102**, 186602 (2009).
[3] K. Nomura and N. Nagaosa, Phys. Rev. Lett. **106**, 166802 (2011).
[4] H. M. Hurst, D. K. Efimkin, J. Zang, and V. Galitski, Phys. Rev. B **91**, 060401 (2015).
[5] Y. Araki and K. Nomura, unpublished (paper in preparation).

Bott Index in Finite Size Systems in and out of Equilibrium

Yang Ge and Marcos Rigol
Physics Department, Penn State University,
University Park, PA 16803, USA
yug124@psu.edu

The application of a periodic drive can induce topological band structures in otherwise trivial insulators. These so-called Floquet topological insulators have been proposed [1,2] and realized with ultracold atoms [3] and photonic systems [4]. The flexibility of a driven dynamical system allows the engineering of different Floquet Hamiltonians, giving access to a wide range of topological phases.

In 2D insulators, the Chern number is used to characterize the topology of energy bands for periodic boundary conditions [5]. It has recently been proved that the Chern number cannot change under unitary time evolution [6]. This suggests that driving isolated quantum systems cannot change their topological character. On the other hand, it has also been shown that in systems with open boundary conditions, which are characterized instead by the Bott index [7], a periodic drive can change the Bott index and produce large edge currents [6], as observed in experiments.

Here we prove that the Bott index and the Chern number are identical in infinite systems with periodic boundary conditions. In finite systems, the Bott index converges much faster to the thermodynamic limit result than the traditionally computed Chern number. The Bott index is also better suited for calculations in finite systems out of equilibrium. We show that, in finite driven systems with periodic boundary conditions and in the absence of a band touching, the Bott index can change if the drive is turned on adiabatically. Our results provide a bridge between the no-go theorem for periodic systems in the thermodynamic limit and findings in systems with open boundary conditions [8].

References

[1] T. Oka and H. Aoki, Phys. Rev. B. **79**, 081406 (2009)
[2] N. Linder, G. Refael, and V. Galitski, Nat. Phys. **7**, 490 (2011)
[3] G. Jotzu, et al., Nature **515**, 237 (2014)
[4] M. Rechtsman, et al., Nature **496**, 7444 (2013)
[5] D. Xiao, M. Chang, Q. Niu, Rev. Mod. Phys. **82**, 1959 (2010)
[6] L. D'Alessio, M. Rigol, Nat. Comm. **6**, 8336 (2015)
[7] T. A. Loring and M. B. Hastings, EPL **92**, 67004 (2010)
[8] Y. Ge and M. Rigol, in preparation.

Magnetic and transport properties of $(Sb_{1-x}Cr_x)_2Te_3$

Sachin Gupta[1], S. Kanai[2,3], F. Matsukura[1,2,3] and H. Ohno[1,2,3]

[1]*WPI-Advanced Institute for Materials Research (WPI-AIMR), Tohoku University, 2-1-1 Katahira, Aoba-ku, Sendai 980-8577, Japan*

[2]*Laboratory for Nanoelectronics and Spintronics, Research Institute of Electrical Communication, Tohoku University, 2-1-1 Katahira, Aoba-ku, Sendai 980-8577, Japan*

[3]*Center for Spintronics Integrated Systems, Tohoku University, 2-1-1 Katahira, Aoba-ku, Sendai 980-8577, Japan*

gupta@wpi-aimr.tohoku.ac.jp

Ferromagnetism in topological insulators (TIs) allows us to observe many intriguing phenomena such as emergent massive Dirac fermions and quantum anomalous Hall effect. Among the reported magnetic TIs, Cr doped Sb_2Te_3 was shown to possess relatively high Curie temperature T_C up to 190 K [1]. In this work, we study magnetic and transport properties of Cr doped Sb_2Te_3.

We grow ~30 nm thick $(Sb_{1-x}Cr_x)_2Te_3$ with x up to 0.16 on a semi-insulating GaAs (111)B substrate at 280 °C using molecular beam epitaxy. The Cr composition x is determined by inductively coupled plasma analysis. Reflection high-energy electron diffraction during growth indicates single crystal growth with *c*-axis along growth direction, which is also confirmed by x-ray diffraction measurement. The lattice distance along *c* axis decreases with increasing x.

Magnetic measurements show that $(Sb,Cr)_2Te_3$ is a ferromagnetic material with an easy-axis parallel to *c*-axis (perpendicular magnetic easy axis), whose T_C increases monotonically with increasing x. The T_C determined from the temperature dependence of the remanent magnetization is found to be 187 K for $(Sb,Cr)_2Te_3$ with $x = 0.16$.

We measure transport properties of $(Sb,Cr)_2Te_3$ in Van der Pauw geometry. The temperature dependence of the sheet resistance R_{sheet} shows metallic conductivity, a hump around T_C, and small increase below 20 K. The Hall resistance R_{Hall} below T_C shows a hysteresis in its perpendicular magnetic-field dependence, reflecting the presence of the anomalous Hall effect. The hysteresis is squarer than that observed from direct magnetization measurement. All the transport properties presented here are quite similar to those observed for (Ga,Mn)As [2,3], indicating that $(Sb,Cr)_2Te_3$ is a useful material to investigate the spin-orbit coupling related phenomena in magnetic materials.

The work was supported in part by a Grant-in-Aid from MEXT (#26103002).

[1] Z. Zhou, Y. J. Chien, and C. Uher, Phys. Rev. B **74**, 224418 (2006).

[2] F. Matsukura, H. Ohno, A. Shen, and Y. Sugawara, Phys. Rev. B **57**, R2037 (1998).

[3] Y. Pu, D. Chiba, F. Matsukura, H. Ohno, and J. Shi, Phys. Rev. Lett. **101**, 117208 (2008).

[4] T. Jungwirth *et al*., Rev. Mod. Phys. **86**, 855 (2014).

Low temperature magnetotransport in topological insulator-ferromagnetic insulator heterostructures

James Kally,[1] Tao Liu,[2] Hailong Wang,[1] Danielle Reifsnyder Hickey,[3] K. Andre Mkhoyan,[3] Mingzhong Wu,[2] Anthony Richardella,[1] and Nitin Samarth[1]

[1]Department of Physics, The Pennsylvania State University, University Park, Pennsylvania 16802, USA
[2]Department of Physics, Colorado State University, Fort Collins, Colorado 80523, USA
[3]Department of Chemical Engineering and Materials Science, University of Minnesota, Minneapolis, Minnesota 55455, USA
jck246@psu.edu

The spin polarized surface states of a topological insulator (TI) have potential for topological spintronics applications wherein the surface states are used for electrically detecting and manipulating the magnetization of a ferromagnetic (FM) material. Heterostructures that interface a TI with a FM insulator are ideal in this context since they isolate the charge current to the topological insulator, thus allowing a clean probe of any phenomena related to spin-charge conversion between the TI surface states and the FM material. We use molecular beam epitaxy to deposit crystalline Bi_2Se_3 and $(Bi, Sb)_2Te_3$ films on high-quality yttrium iron garnet (YIG) thin films [1] and report on the magneto-transport properties of these heterostructures at low temperature (400 mK < T < 4.2 K). Our measurements show evidence for a magnetic coupling between the FM insulator and the TI thin film.

This work is funded by C-SPIN, a funded center of STARnet, an SRC program sponsored by MARCO and DARPA.

References

[1] H. Wang *et al*., Phys. Rev. Lett. **117**, 076601 (2016).

Characteristic Transport Properties of InAs/GaSb QWs and InAs/GaInSb QWs in Different Regimes

Tingxin Li, Rui-Rui Du, *Rice University*
Gerard Sullivan, *Teledyne Scientific and Imaging*

Quantum spin Hall effect (QSHE) is a fundamental and spectacular phenomenon arising from topological protection. Inverted InAs/GaSb quantum wells (QWs) [1-2] and strained InAs/GaInSb QWs [2] have been proved to support QSH states. Moreover, their band structure hence the transport properties can be tuned by the QWs width, electric and magnetic fields, and the strain effect inside the QWs. Here we summarize the characteristic transport properties in three distinct regimes, which are topological trivial (semiconductor) regime, shallow inverted regime, and deeply inverted regime.

[1] Lingjie Du, Ivan Knez, Gerard Sullivan, and Rui-Rui Du, *PRL* **114**, 096802 (2015).
[1] Tingxin Li, Pengjie Wang, Hailong Fu et al, *PRL* **115**, 136804 (2015).
[2] Lingjie Du, Tingxin Li, Wenkai Lou et al, Arxiv 1608.06588.

Anomalous Phase Shift of Quantum Oscillations in Topological Semimetals

Hai-Zhou Lu
Institute for Quantum Science and Engineering and Department of Physics, South University of Science and Technology of China
Shenzhen 518055, China
luhz @sustc.edu.cn

Topological semimetal can be regarded as formed by stacking quantum anomalous/spin Hall insulators (see Fig. 1). Berry phase physics is closely related to a number of topological states of matter. Topological semimetals are believed to host a nontrivial π Berry phase to induce a phase shift in the quantum oscillation (1/8 for hole and -1/8 for electron carriers). We theoretically study the Shubnikov – de Haas oscillation of Weyl and Dirac semimetals. For a Weyl semimetal, the phase shift is found to change nonmonotonically and go beyond known values of 1/8 and 5/8, as a function of the Fermi energy. For a Dirac semimetal, time-reversal symmetry leads to a discrete phase shift of 1/8 or 5/8. The topological band inversion can lead to beating patterns. We clarify that the resistivity peaks should be assigned integers in the Landau index plot. Our findings may be helpful for exploring the Berry phase in recent experiments on Cd_2As_3 and various systems.

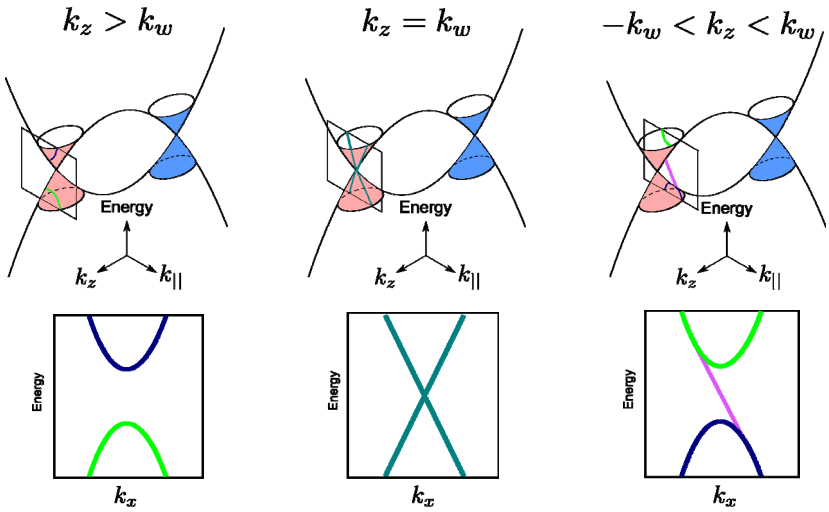

Fig.1 Band structure of a topological semimetal. It can be regarded as stacked quantum anomalous/spin Hall insulators, and there is a momentum-dependent topological phase transition and edge states (i.e., Fermi arcs).

References

[1] C. M. Wang, Hai-Zhou Lu*, Shun-Qing Shen, Phys. Rev. Lett. **117**, 077201 (2016).

Chiral topological superconductor from quantum anomalous Hall plateau transitions

Jing Wang
State Key Laboratory of Surface Physics and Department of Physics, Fudan University, Shanghai, 200433, China
wjing01@gmail.com

We propose to realize a two-dimensional chiral topological superconducting (TSC) state from the quantum anomalous Hall plateau transition in a magnetic topological insulator thin film through the proximity effect to a conventional *s*-wave superconductor. This state has a full pairing gap in the bulk and a single chiral Majorana mode at the edge, which is tunable by either external magnetic field [1] or electric field [2]. Several transport experiments have been proposed to detect the chiral TSC and the single chiral Majorana edge mode [1-3]. One unique signature is that the conductance will be quantized into a half-integer plateau at the coercive field in this hybrid system [1]. Remarkably, some of the theoretical predictions are already borne out in recent experiment [4].

References

[1] J. Wang, Q. Zhou, B. Lian, and S.-C. Zhang, Phys. Rev. B **92**, 064520 (2015).

[2] J. Wang, Phys. Rev. B **94**, 214502 (2016)

[3] B. Lian, J. Wang, and S.-C. Zhang, Phys. Rev. B **93**, 161401(R) (2016)

[4] Q. He, L. Pan, *et al*, arXiv: 1606.05712 (2016)

Author Index

Fu, Xiaojun	QH-5
Galicka, Marta	ES-1
Ge, Yang	TI-3
Ghosh, Ruby	MS-14
Ghosh, Ruby	2DT-19
Gunawardana, Binuka	QH-25
Gupta, Sachin	TI-4
Gusev, Gennady	ES-2
Gusev, Gennady	QH-6
Gusev, Gennady	ES-3
Hai, Guo-Qiang	2DS-2
Halbertal, Dorri	2DT-5
Hao, Jianhua	2DT-20
Hennel, Szymon	ES-13
Henriksen, Erik	2DO-5
Hohls, Frank	SE-3
Hohls, Frank	SE-4
Ihn, Thomas	2DT-6
Inarrea, Jesus	2DT-22
Inarrea, Jesus	2DT-21
Ishchenko, Denis	IH-15
Islam, Saurav	ES-4
Ito, Ryo	SE-5
Ito, Takumi	QI-3
Jacobs, Andrew	MS-2
Jaziri, Sihem	2DO-18
Johnston-Halperin, Ezekiel	2DO-19
Kally, James	TI-5
Kamata, Hiroshi	2DS-3
Kameda, Hiroki	MS-15
Karalic, Matija	ES-14
Karnatak, Paritosh	2DT-7
Katz, Benjamin	MS-3
Kawarabayashi, Tohru	QH-7
Khadka, Sudiksha	2DO-6
Khisameeva, Alina	2DO-7
Kim, Young Dong	2DO-8
Kiminori, Okamoto	ST-17
Kiyama, Haruki	MS-4
Kleinbaum, Ethan	QH-8

Koga, Takaaki	ST-2
Konakov, Anton	ST-3
Korkusinski, Marek	QI-4
Koski, Jonne	MS-5
Kriisa, Annika	2DT-23
Kudo, Koji	QH-9
Kunihashi, Yoji	ST-4
Kuntsevich, Aleksandr	ES-15
Kuntsevich, Aleksandr	IH-16
Lee, Seung Joo	ST-5
Li, Qi	IH-17
Li, Tingxin	TI-6
Lin, Kuan-Ting	2DO-9
Liu, Chaoxing	ES-5
Liu, Han-Chun	2DT-24
Liu, Xiaoxue	QH-10
Lu, Haizhou	TI-7
Lu, Zhengguang	2DO-10
Lv, Yawei	2DT-8
Lydzba, Patrycja	QH-12
Lydzba, Patrycja	QH-11
Ma, Meng	QH-13
Ma, Wenquan	IH-18
Magarill, Lev	ES-16
Maier, Hubert	ES-6
Majewicz, Magdalena	ES-7
Makarovsky, Oleg	2DT-25
Marcellina, Elizabeth	IH-3
Mastrogiuseppe, Diego	ST-18
Mehew, Jake	IH-19
Minami, Yusuke	MS-6
Mitioglu, Anatolie	2DO-20
Moore, John	QH-14
Moraes, Flavio	ST-6
Munasinghe, Rasadi	QH-26
Mun?oz, Karen	IH-20
Myers, David	IH-4
Nakajima, Takashi	QI-5
Nanayakkara, Tharanga	QH-27

Neupane, Tikaram	2DO-21
Neupane, Tikaram	2DO-22
Nilsson, Malin	MS-7
Noiri, Akito	QI-6
Nomura, Shintaro	2DO-12
Nomura, Shintaro	2DO-11
Onizaki, Makoto	2DS-4
Osika, Edyta	MS-17
Ota, Ryoya	ST-7
Ozden, Burcu	IH-5
Pawlowski, Jaroslaw	QI-7
Pennachio, Dan	IH-6
Pisoni, Riccardo	2DT-27
Pu, Songyang	QH-15
Qian, Qi	QH-16
Ramirez Ramos, Carlos	2DT-9
Rasanen, Esa	IH-7
Ribeiro, Amina	ST-8
Rode, Johannes	IH-8
Rojas, Tomas	ST-9
Ryu, Sungguen	SE-6
Sablon, Kimberly	2DO-23
Samaraweera, Rasanga	QH-28
Sanada, Haruki	ST-10
Sandler, Nancy	2DT-10
Sato, Yosuke	MS-8
Savchenko, Maxim	2DT-28
Servin, Rathi	MS-18
Sharma, Chithra	IH-21
Sharma, Girish	2DT-29
Shi, Qianhui	QH-17
Shimatani, Naoki	MS-9
Shingla, Vidhi	QI-8
Smith, George	ST-11
Suen, Yuen-Wuu	2DT-11
Sukhorukov, Evgeny	MS-19
Sun, Hui	IH-9
Sun, Hui	IH-10
Takada, Shintaro	MS-20

Tanaka, Yusuke	ST-12
Tanatar, Bilal	MS-10
Telesio, Francesca	2DT-30
Thalakulam, Madhu	2DT-31
Thomas, Candice	ES-8
Tiemann, Lars	2DT-12
Timo, Wagner	SE-9
Tito Patricio, Marco Antonio	IH-11
Tokura, Yasuhiro	QI-9
Toshihito, Osada	2DT-32
Ubbelohde, Niels	SE-7
Ullah, Farman	2DO-13
Ulloa, Sergio	ST-13
Valkovskii, Vitalii	2DO-14
Vidmar, Lev	MS-11
Villegas Rosales, Kevin	QH-18
Voelkl, Tobias	ST-14
Wang, Jing	TI-8
Wang, Tiantian	2DS-5
Wang, Yuanxi	IH-12
Wang, Zhuo	ES-18
Wang, Zhuo	QH-29
Weng, Qianchun	2DT-13
Wenz, Tobias	SE-8
Widhalm, Alex	QI-10
Wojs, Arkadiusz	QH-19
Wu, Fengcheng	QH-20
Wu, Hao	2DS-6
Yakunin, Mikhail	QH-30
Yamada, Syoji	ST-19
Yang, Ming	2DT-14
Yang, Ming	IH-13
Yu, Peng	2DS-7
Yu, Sheng	2DT-33
Yu, Sheng	2DT-34
Zabolotnykh, Andrey	2DO-15
Zakrzewski, Brian	2DS-8
Zhai, Dawei	2DT-15
Zhang, Chi	ES-9
Zhang, Ding	IH-22

Zhao, Jianyun	QH-21
Zheng, Boyang	2DT-16
Zheng, Yangdong	QH-22
Zhu, Jun	QH-23